AN INVESTIGATION OF THE CONDITIONS FOR THE OCCURRENCE OF FLUTTER IN AIRCRAFT AND THE DEVELOPMENT OF CRITERIA FOR THE PREDICTION AND ELIMINATION OF SUCH FLUTTER

Thesis by

Albert E. Lombard, Jr.

In Partial Fulfillment of the Requirements

for the

Degree of Doctor of Philosophy

California Institute of Technology

Pasadena

1939

ABSTRACT

A review is presented of the work done by other investigators on the effects of inertia couplings in producing flutter in control surfaces that are not mass balanced. The conclusion is reached that for the prevention of such flutter complete dynamic balance should always maintain.

Flexural-torsional flutter is investigated in considerable detail from the consideration of the dynamical equations for steady state forced oscillations of the two-dimensional case. A complete set of response curves for two typical cases are included to show the types of responses that should be observed in flight with vibration pick-up equipment. The important fact is brought out that the response and behavior of the wing at its natural bending frequency has little or no correlation with the behavior of the wing at the stability limit of flutter. Curves are presented to show that, for normal airplanes, the most important parameters which determine flutter in this mode are (a) the position of the inertia axis, (b) the torsional frequency, and (c) the radius of gyration of the wing mass about the inertia axis.

The dynamical equations are set up for the cases of flexural-aileron, torsional-aileron, and flexural-torsional-aileron flutter in the two-dimensional case and an example is given of the determination of the stability limit of a specific example of the first of these modes.

ABSTRACT (continued)

An extension of the two-dimensional case to the three-dimensional case is presented with particular reference to determining the flexural-torsional flutter speed of a tail surface with vertical surfaces on the tips of the horizontals. The method of attack is outlined for the calculation of natural frequencies at zero airspeed to use in determining the flutter speed.

Statistical data in a graphical form show the variations of natural frequencies of the various components of airplanes with the size of such airplanes.

The conclusion is reached that the speed of airplanes should be restricted to two-thirds of the critical speed for any mode of flutter, divergence, or aileron reversal.

ACKNOWLEDGMENT

The author has derived much of value from the published papers by others that are referred to throughout this thesis. In particular, he wishes to acknowledge his debt of gratitude to COX, DEN HARTOG, DUNCAN, FINGADO, FRAZER, GARRICK, KASSNER, KÜSSNER, PUGSLEY, and THEODORSEN, whose writings have been valuable sources of information.

Acknowledgment must be made to DR. THEODORE VON KÁRMÁN for his kindness in supervising this investigation and in giving many helpful suggestions and interpretations.

To LIEUTENANTS ELLIOTT W. PARISH, JR., and ANDREW McB. JACKSON, JR., of the U. S. Navy, must go the author's sincere thanks for their assistance in checking the equations, calculating responses, and plotting curves, as well as in collaborating in this investigation.

MESSRS. SCHUYLER KLEINHANS, CARLOS WOOD, and JEAN WYLIE, of the Douglas Aircraft Company, Inc., have continually supported the work of this thesis by discussing with the author the results of their investigations, both in flight and on the ground, and by supplying statistical data that formed the very cornerstone from which much of this thesis developed. Their assistance is gratefully acknowledged. Acknowledgment is also made of vibration data furnished by the LOCKHEED AIRCRAFT CORPORATION.

The author wishes to express his appreciation to MR. GEORGE A. PAGE, Chief Engineer of the St. Louis Airplane Division of the Curtiss-Wright Corporation, for his generous attitude toward the pursuit of research by the author at the time when he was regularly employed by that company as

well as when he was retained as a consultant. In particular, he wishes to acknowledge the permission granted to embody Curtiss-Wright Report No. 20-Y 10, by the author, as Chapter VII of this thesis in a modified form.

During the past ten years, the author has valued especially the friendship of MR. THEODORE P. WRIGHT, Director of Engineering of the Curtiss-Wright Corporation, whose consistently appreciative attitude toward research has supplied an immense stimulus to explore new fields and scale new heights. This intangible help and inspiration given by Mr. Wright has exceeded in many respects all other human aid on this thesis and for it the author is sincerely grateful.

Appreciation is gratefully extended to MRS. ALICE GAZIN for her diligence and care in typing this thesis.

TABLE OF CONTENTS

CHAPTER I. INTRODUCTION

1:01. The General Problem.

1:02. Flexural-Aileron Flutter.

1:03. Torsional-Aileron Flutter.

1:04. Küssner Formula for Critical Speed of Aileron Flutter.

1:05. Statistical Method for Determining the Critical Speed of Aileron Flutter.

1:06. Flexural-Torsional Flutter.

1:07. Wing Divergence.

1:08. Aileron Reversal Speed.

1:09. Servo-Tab Flutter.

CHAPTER II. FLEXURAL-TORSIONAL FLUTTER (TWO-DIMENSIONAL)

2:01. Aerodynamic Forces and Moments due to Apparent Mass of Fluid Adjacent to a Moving Plate.

2:02. Aerodynamic Forces in Quasi-Steady Motion.

2:03. Summary of Aerodynamic Forces and Moments arising from Apparent Mass and Quasi-Steady Motion.

2:04. Aerodynamic Forces and Moments for Steady State Oscillations by Method of von Kármán-Sears.

2:05. Summary of Aerodynamic Forces and Moments in Steady State Oscillations.

2:06. Dynamical Equations for Steady State Forced Oscillations.

TABLE OF CONTENTS (continued)

CHAPTER II. FLEXURAL-TORSIONAL FLUTTER (TWO-DIMENSIONAL) (continued)

2:07. Method of Solution of Dynamical Equations.

2:08. Critical Speed of Torsional Divergence.

2:09. Normal Modes of Vibration at Zero Velocity.

2:10. Responses in Steady State Forced Oscillations as Function of Airspeed.

2:11. Determination of Critical Speed for Flexural-Torsional Flutter.

2:12. The Treatment of Structural Damping.

CHAPTER III. FLEXURAL-AILERON FLUTTER (TWO-DIMENSIONAL)

3:01. Aerodynamic Forces and Moments in Steady State Oscillations.

3:02. Dynamical Equations for Steady State Forced Oscillations.

3:03. Example of Flexural-Aileron Flutter

CHAPTER IV. TORSIONAL-AILERON FLUTTER (TWO-DIMENSIONAL)

4:01. Aerodynamic Forces and Moments due to Steady State Oscillations.

4:02. Dynamical Equations for Steady State Forced Oscillations.

CHAPTER V. FLEXURAL-TORSIONAL-AILERON FLUTTER (TWO-DIMENSIONAL)

5:01. Dynamical Equations for Steady State Forced Oscillations.

5:02. Aileron Reversal Speed.

TABLE OF CONTENTS (continued)

CHAPTER VI. EXTENSION OF METHOD OF ANALYSIS TO THREE-DIMENSIONAL CASE OF FLEXURAL-TORSIONAL FLUTTER

6:01. Dynamical Equations for Free Oscillations at Stability Limit.

6:02. Special Case - Constant Chord-Constant Weight per Unit Span-Concentrated Tip Weight.

CHAPTER VII. PROCEDURE FOR THE PRELIMINARY PREDICTION OF FLUTTER SPEEDS

7:01. Introduction.

7:02. Method of Calculation of Primary Flexural Mode of Vibration of Wings and Tails.

7:03. Method of Calculation of Primary Torsional Mode of Wing or Tail.

7:04. Method of Calculation of Critical Speed of Torsional-Flexural Flutter.

7:05. Statistical Data of Vibration Frequencies.

CHAPTER VIII. CONCLUSIONS AND RECOMMENDATIONS

APPENDIX I. REFERENCES AND BIBLIOGRAPHY.

APPENDIX II. NOMENCLATURE.

APPENDIX III. VALUES OF R FUNCTIONS.

APPENDIX IV. TYPICAL CALCULATION OF RESPONSE IN STEADY STATE OSCILLATIONS.

APPENDIX V. SUMMARY OF CHARACTERISTICS OF SPECIFIC CASES INVESTIGATED.

FIGURES 1 to 66.

CHAPTER I. INTRODUCTION

1:01. The General Problem

This thesis is intended to cover the basic considerations of the types of flutter most likely to occur in airplane wings and tail surfaces by giving a brief analysis of the underlying cause of each type of flutter, a review of the criteria for the determination of the critical speed, and a discussion of the methods of remedy in each case. Other related problems dealing with aerodynamic-elastic-inertia couplings are similarly discussed.

Flutter may be defined as any oscillation of an airplane wing or control surface in which aerodynamic forces are acting in conjunction with elastic and inertia forces. It is essential to the existence of flutter as defined above that there be an aerodynamic force coupled to the elastic and inertia forces. It is the aerodynamic force that provides a source of additional energy for the system. This can be visualized by considering a simple pendulum as an oscillating system. If allowed to oscillate without external excitation, the pendulum swings with an almost constant amplitude which diminishes only according to the amount of internal friction in the system. In order to make the pendulum oscillate with a continually increasing amplitude, it is necessary to introduce an external exciting force that will act in the direction of motion of the pendulum, the exciting force being of sufficient magnitude to overcome the damping resistance. Such an exciting force in phase with the motion will increase the energy content of the system.

Thus, when considering types of flutter, it is important that the aerodynamic exciting force is in the direction of the relative oscillating motion of the section of wing on which the force acts, and in phase with the motion.

The types of "binary" flutter of a wing (flutter occurring in systems with two degrees of freedom) are:

(a) Flexural-Aileron Flutter, in which a wing of infinite torsional rigidity bends about a fore-and-aft axis at the same time that the aileron rotates about its hinge line;

(b) Torsional-Aileron Flutter, in which a wing of infinite bending rigidity twists about a spanwise axis at the same time that the aileron rotates about its hinge line;

(c) Flexural-Torsional Flutter, in which a wing oscillates in combined bending and twisting, without independent motion of the aileron.

Many cases of flutter involve all three of the above modes, but generally the mode associated with the least elastic stiffness or greatest inertia unbalance is the important one in any particular case. Cases of flutter of tail surfaces fall into the same classification as those given above and can be analyzed by the methods developed for wing flutter.

1:02. Flexural-Aileron Flutter

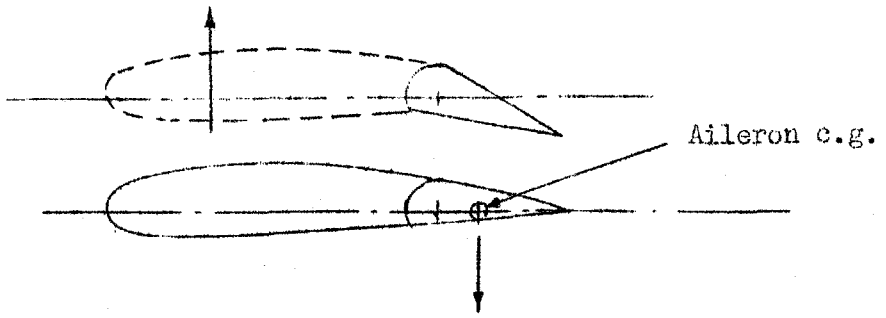

Figure A

Consider a section of wing of infinite torsional rigidity fitted with an aileron in which the aileron mass is concentrated back of the hinge line. If this wing is initially at rest relative to the complete airplane and is then suddenly deflected upward due to some disturbance, the aileron will tend to lag behind the motion of the wing to produce a section as shown dotted in Figure A.* The result of the aileron's being drooped is to increase the aerodynamic lift on this section, i.e., to introduce an aerodynamic force in the direction of the motion of the wing. As the wing starts downward from its maximum upward position, the aileron will continue to swing upward for a while so that, in the downward motion as well, the aerodynamic force due to the aileron will act in the direction of motion and tend to increase the amplitude. It should be noted

*Note: Figures lettered A, B, C, etc., are included in the body of the text. Figures numbered 1, 2, 3, etc., are at the end of the thesis, following the appendices.

parenthetically that aerodynamic damping forces are also present during this oscillation so that unstable flutter will occur only when the speed is sufficient to produce in-phase aerodynamic forces of sufficient magnitude to overcome the damping.

Obviously, this type of flutter is due to the mass unbalance of the aileron (or, more precisely, to the dynamic mass unbalance). The effects of mass unbalance were reported in the literature as early as 1923, when von Baumhauer and Koning[1] gave the results of wind tunnel tests in which flutter had been eliminated by adding weights to the paddle balances then used for aerodynamic balance.

Frazer and Duncan[14,15] recognized and commented on the importance of the product of inertia, but to the best of the author's knowledge, Roché[29], of the Materiel Division of the U. S. Army Air Corps, first introduced the conception of a dynamic mass balance coefficient. Consider an aileron, Figure B, mounted on a

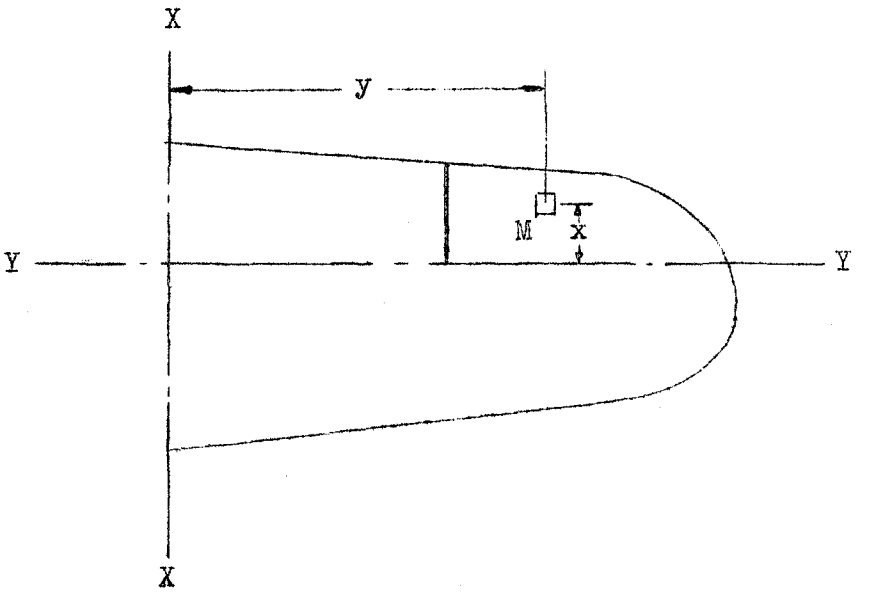

Figure B

hinge line Y-Y which in turn is mounted rigidly on a wing oscillating about an axis X-X. The inertia force acting on any element of this aileron is proportional to the maximum amplitude of the oscillation of the hinge line at that particular section. If the wing is assumed to oscillate as a rigid beam about X-X so that the hinge line remains straight at all times, the inertia force on any element will be proportional to the distance y, and the moment about the hinge line of any element will be proportional to Mxy in which M is the mass of the element. The total moment will be proportional to the product of inertia of the mass of the aileron:

$$J_{xy} = \sum Mxy \qquad (1:01)$$

If $J_{xy} = 0$, under the bending assumption as above, there is no inertia moment to cause the aileron to lag behind the wing in its oscillation and consequently no possibility of flexural-aileron flutter. However, in the types of aileron construction most commonly used, J_{xy} does not become zero generally without the addition of mass balancing weights. Therefore, in order to compare the relative values of the product of inertia for various sized airplanes, Roché introduced the non-dimensional "dynamic balance coefficient":

$$C_{db} = \frac{J_{xy}}{\text{Mass} \cdot \text{Area}} \qquad (1:02)$$

In Table I (page 6) are listed the values of C_{db} for all sorts of control surfaces of a number of airplanes, the data coming from Roché's paper. For C_{db} greater than 0.06, flutter has been observed in certain cases. It would appear that any value of C_{db} less than

TABLE I. COEFFICIENTS OF DYNAMIC BALANCE FOR VARIOUS CONTROL SURFACES

Data from Roché[29], rearranged.

Control Surface	Trailing Edge Covering	C_{db}	Remarks
Rudder	Metal	0.1958	Excessive tail vibration at various speeds.
Aileron	Metal	0.1521	Left aileron lost in flight.
Rudder	Metal	0.1160	Buckled fuselage members in coming out of dive at 240 m.p.h. with landing gear exposed.
Rudder	Metal	0.1032	Reported tail vibration at 160 m.p.h.
Elevator	Metal	0.1027	Complete disintegration of airplane at 350 m.p.h.
Rudder	Fabric	0.0953	Gave satisfactory results without perfect balance.
Rudder	Metal	0.0851	Unsatisfactory at 200 m.p.h.
Rudder	Fabric	0.0847	No trouble reported.
Aileron	Fabric	0.0719	Caused wing flutter through amplitude of 18 in. Two of crew jumped; airplane landed O.K.
Aileron	Metal	0.0611	No trouble reported.
Rudder	Metal	0.0317	O.K.
Rudder	Fabric	-0.0010	Satisfactory at all conditions.

0.06 is satisfactory for relatively slow airplanes. However, for fast airplanes, there should be complete dynamic balance, $C_{db} = 0$, to preclude the possibilities of flutter.

It should be noted that, in developing the idea of C_{db} above, it has been assumed that the wing remains absolutely rigid in the region of the aileron so that the hinge line remains straight. In practice this is not so, the wing will continue to bend through the region of the aileron so that the maximum amplitude of the oscillation of any point on the hinge line will be more nearly proportional to y^2 or y^3 than to y. Therefore, a more rigorous criterion might be

$$J'_{xy} = \sum Mxy^2 \leqslant 0 \qquad (1:03)$$

However, if an aileron is completely mass balanced about the hinge line at each section individually, both $J_{xy} = 0$ and $J'_{xy} = 0$. Furthermore, if dynamic balance is obtained by adding a balance mass forward of the hinge line near the tip of the aileron to the extent that $J_{xy} = 0$, then J'_{xy} becomes negative, indicating excessive mass balancing (but not in the least objectionable). Therefore, it appears that the general use of the coefficient C_{db} will be satisfactory--somewhat conservative.

Theodorsen and Garrick[35] have carried out an extensive investigation of this type of flutter both by wind tunnel tests and by calculations of two-dimensional examples. The results of Graphs II A, B, C, D, E of the Theodorsen-Garrick report seem particularly significant when interpreted in a manner modified from

that given. They define the amount of mass unbalance by

$$x_\beta = \frac{\text{Aileron mass} \cdot \text{Moment arm to c.g.}}{\text{Wing mass} \cdot \text{Semi-chord}} \qquad (1:04)$$

in which the aileron and wing masses are taken per unit span. This may be written

$$x_\beta = 2 \cdot \left[\frac{\text{Aileron wt. per sq.ft.}}{\text{Wing wt. per sq.ft.}}\right] \cdot \left[\frac{\text{Aileron ch.}}{\text{Wing ch.}}\right]^2 \cdot \left[\frac{\text{Mass ecc.}}{\text{Aileron ch.}}\right] \qquad (1:05)$$

In general the aileron weight per square foot is about one half that of the wing. If the aileron weight is taken as one half the wing weight, the following maintains:

$$\frac{\text{Mass eccentricity}}{\text{Aileron chord}} = x_\beta \left[\frac{\text{Wing chord}}{\text{Aileron chord}}\right]^2 \qquad (1:06)$$

The Theodorsen-Garrick curves show that flutter does not occur below a certain critical value of x_β, as follows:

$\frac{\text{Aileron chord}}{\text{Wing chord}}$	x_β	$\frac{\text{Mass eccentricity}}{\text{Aileron chord}}$**
0.167 (c = 2/3)*	0.0025	0.090
0.25 (c = 1/2)*	0.004	0.064
0.50 (c = 0)*	0.018	0.072

*c here is Theodorsen's notation, not wing chord as used in this thesis. For comparison of notations, see Appendix II.

**If aileron weight per sq.ft. = 0.5 wing weight per sq.ft.

If the problem is extended to the three-dimensional case in which the dynamic balance coefficient C_{db} has meaning, the value of C_{db} for a rectangular aileron of constant characteristics along the span is

$$C_{db} = \frac{1}{2} \frac{\text{Mass eccentricity}}{\text{Aileron chord}} \qquad (1:07)$$

The theoretical study indicates, therefore, that to preclude the possibility of this type of flutter, C_{db} should be less than 0.032. This is in agreement with conclusions reached from flight tests.

Theodorsen and Garrick's[35] curves show also that, if the natural frequency of the aileron oscillation at zero airspeed is over twice that of wing flexure, a substantial amount of mass unbalance can be tolerated.

However, it should be recognized that generally there are two possible modes of aileron flutter: "symmetrical," as when both ailerons move up together by stretching the control system; and "anti-symmetrical," as when one aileron moves up and the other down at the same time. With rigid control systems of low internal friction, the flutter will be anti-symmetrical; but with relatively flexible control systems, either mode may occur depending upon the circumstances.

One case of aileron flutter of a biplane of which the author has close personal knowledge was of the anti-symmetrical type in which the control stick moved from side to side in the cockpit. The pilot was able to damp out the flutter by holding the stick in

his hand. However, in a glide at about 200 m.p.h. with the stick free to move without restraint, the flutter became violent and the wings left the ship. The pilot landed safely with a parachute. The ailerons were not mass balanced in this case.

Unless a control surface has irreversible controls the situation always arises that the surface may have a natural frequency of zero with free controls in the anti-symmetrical mode, so that the only general expedient is mass balancing.

Smilg[32], in a wind tunnel investigation of tail flutter with particular attention to that of the rudder, found similar results, namely, that flutter occurs with mass unbalance and is prevented by complete dynamic balance. He observed flutter with a dynamic balance coefficient as low as $C_{db} = 0.002$. However, it should be noted that his model was heavy in relation to the enclosing air mass so that a small eccentricity would still produce a relatively large inertia moment of force. He also found that flutter could be prevented by restraining the rudder to provide a natural frequency equal to that of the fuselage in torsion in all cases in which $C_{db} < 0.05$.

In Chapter III, the equations are set up for steady state forced oscillations in the flexural-aileron mode of the two-dimensional case. These equations may be used to analyze the following types of flutter:

Wing flexure	vs.	aileron torsion
Stabilizer flexure	vs.	elevator torsion
Fuselage flexure	vs.	elevator torsion

Fuselage torsion	vs.	elevator torsion
Fin flexure	vs.	rudder torsion
Fuselage flexure	vs.	rudder torsion
Fuselage torsion	vs.	rudder torsion

1:03. Torsional-Aileron Flutter

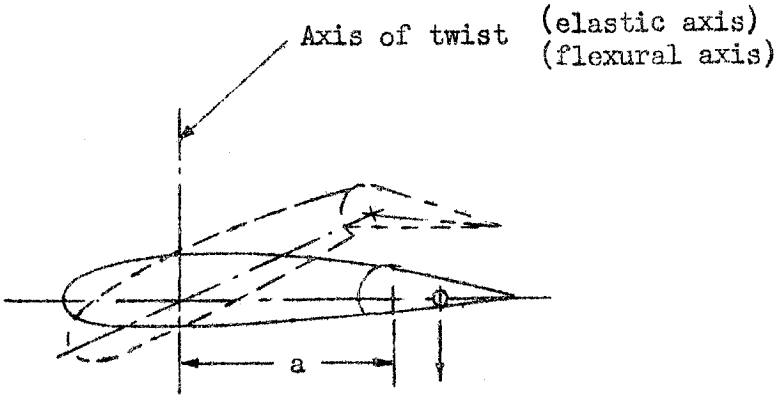

Figure C

The case will now be considered of a wing of infinite bending stiffness which may twist about a span-wise axis, Figure C. Again there exists a means of moving the aileron hinge line up and down and if the mass of the aileron is principally behind the hinge line, the aileron will tend to lag behind the motion of the wing just as in the case of the flexural-aileron flutter. The downwardly deflected aileron produces an aerodynamic twisting moment that acts in the direction of the rotational velocity of the wing and hence increases the energy and amplitude of oscillation at high airplane speeds. Dynamic balancing eliminates the possibilities of flutter in this case if the dynamic balance is based on a coefficient of the form involving:

$$J''_{xy} = \sum Mx(x + a) = 0 \qquad (1:08)$$

in which "a" is the distance from the hinge line to the flexural axis about which the wing twists. Rewriting equation (1:08),

$$\sum Mx(x + a) = \sum Mx^2 + a\sum Mx = 0 \qquad (1:09)$$

so that for complete dynamic balance,

$$\sum Mx = -\frac{\sum Mx^2}{a} \equiv \text{static balance} = -\frac{\text{moment of inertia}}{a} \qquad (1:10)$$

Therefore, some static overbalance is requisite to eliminate all mass coupling in torsional-aileron flutter at all speeds. However, Theodorsen and Garrick[35] have found that this mode of flutter is not critical if mass balancing is carried out to the extent needed for the prevention of flexural-aileron flutter. In general, the torsional frequency of the wing is substantially higher than the flexural. Furthermore, the friction of the control system has a definite damping effect to prevent flutter in this mode.

In Chapter IV, the equations are set up for steady state forced oscillations in this mode.

1:04. Küssner Formula for Critical Speed of Aileron Flutter

On the basis of a theoretical analysis originally conceived by Birnbaum[2,3], in Göttingen, and developed by Küssner[22], also in Göttingen, the critical speed at which any flutter will occur can be expressed by the formula

$$v_k = \frac{\nu l}{\omega} \tag{1:11}$$

in which:

v_k = critical speed in feet per second.

ν = natural frequency of the wing in the mode which will give aerodynamic couplings to the elastic forces, in radians per second.

l = semi-chord of the vibrating portion of the wing - feet.

ω = "reduced frequency," a non-dimensional parameter.

Equation (1:11) may be expressed in the alternate forms:

$$v_k = \frac{\pi n c_m}{\omega} \tag{1:12}$$

or

$$\omega = \frac{\pi n c_m}{v_k} \tag{1:13}$$

in which:

n = frequency in cycles per second.

c_m = mean chord of vibration portion of wing - feet.

Küssner[22] has analyzed the characteristics of several airplanes in which flutter has been observed, determining the natural frequencies of the wings in the critical modes by vibration tests on the ground, and found that, with mass unbalanced ailerons, the reduced frequency in all cases was very close to a constant value:

$$\omega = 0.9 \pm 0.12 \qquad (1:14)$$

Table II, page 16, gives the results from Küssner's paper, somewhat rearranged. It is noteworthy that in all cases with metal structure the flutter had a vicious aspect except in the one case of the M-28 which had very rigid aileron controls. The metal structure has much less internal damping friction than wood and is therefore much more susceptible to vicious flutter.

TABLE II. OBSERVED CASES OF WING-AILERON FLUTTER

Data from Küssner[22], rearranged.

Airplane Type	Chord t_m m	Crit. Freq. 1/min.	Speed V_k km/hr.	Reduced Freq. ω	Rigidity of Controls	Wing Structure	Aspect
He 60	2.2	780	350	0.93	-	metal	vicious
Do 10	1.6	1450	450	0.97	great	metal	vicious
L 102	1.56	835	290	0.85	small	metal	vicious
Do 12	1.3	580	180	0.79	small	metal	vicious
M 28	1.05	770	220	0.69	great	metal	mild
DP 9	1.5	520	180	0.82	small	wood	vicious
He 8	3.0	540	350	0.87	small	wood	vicious
KL 1a	1.3	675	145	1.14	small	wood	vicious
S 24	1.18	1215	280	0.97	small	wood	vicious
Ar 66c	1.65	790	340	0.72	small	wood	vicious
L 78	1.36	860	210	1.05	great	wood	mild
He 46c	1.4	845	268	0.87	small	wood	mild
AC 12e	1.4	805	220	0.98	small	wood	mild

1:05. Statistical Method for Determining the Critical Speed of Aileron Flutter

From the theoretical work of Frazer and Duncan[14,15], H. Roxbee Cox[5] deduced that the critical parameters for wing flutter in non-dimensional form are:

(A) $$\frac{m_\Theta}{\rho v^2 s c^2}$$

(B) $$\frac{l_\varphi}{\rho v^2 s^3}$$

(C) $$\frac{\delta}{\rho c}$$

in which:

m_Θ = torsional stiffness of wing = $\frac{\text{torque}}{\text{angle of twist of eff.tip}}$

l_φ = flexural stiffness of wing = $\frac{\text{max. bending moment} \cdot \text{semi-span}}{\text{lineal deflection of tip}}$

v = critical velocity

ρ = air density

c = wing chord

s = semi-span

δ = wing mass in lb./sq.ft.

By plotting the functions (A) and (B) against (C) for airplanes which have been known to flutter and for other airplanes in which flutter had not been observed, Cox obtained critical values at which flutter is likely to occur for airplanes with mass unbalanced ailerons as shown

in Figures 1 and 2* reproduced from his report.

It is interesting to note that these curves closely approximate a parabola as would be expected from Küssner's formula, equation (1:11), in which for constant chord, using the Cox notation:

$$\frac{1}{v} \backsim \frac{1}{n} \backsim \sqrt{\frac{\delta}{m_\Theta}} \tag{1:14}$$

or

$$\frac{m_\Theta}{v^2} \backsim \delta \tag{1:15}$$

In conclusion, it is believed that all binary flutter of the flexural-aileron and torsional-aileron types can be eliminated by complete dynamic mass balancing of the ailerons.

*Figures numbered 1, 2, 3, etc., are at the end of this thesis, following the appendices.

1:06. Flexural-Torsional Flutter

Even after ailerons are mass balanced as discussed above, there remains a possibility of another kind of flutter if the speed of airplanes is still further increased. This flutter, called "flexural-torsional flutter," arises in cases in which the center of mass of the wing and the flexural axis are aft of the aerodynamic center.

The fundamental cause of this type of flutter can be seen from reasoning along the same line as that above for the aileron flutter by considering a section of wing as shown in Figure D. If such a

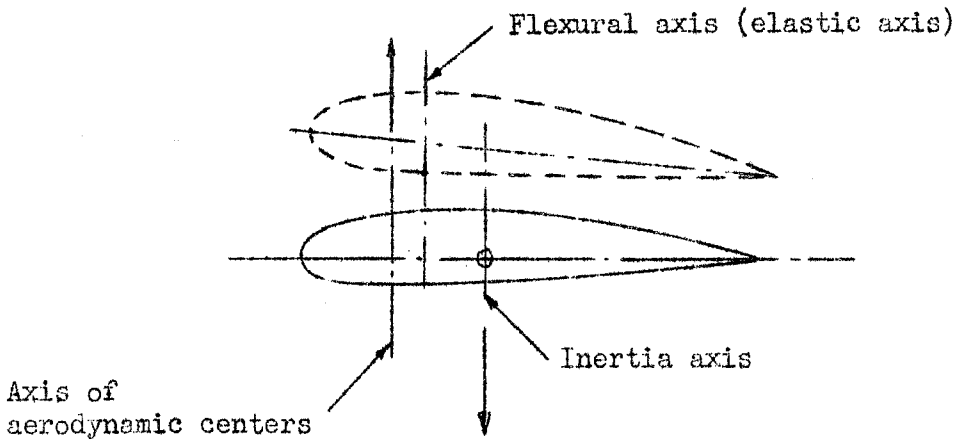

Figure D

wing is momentarily displaced upward by any cause whatsoever, it will tend to twist due to the inertia lag of the center of mass of the wing. This twist is in the direction to produce an increased lifting force as the wing moves upward, thereby introducing an in-phase coupling of the aerodynamic force with the motion of the wing.

It is apparent that important parameters are particularly: (a) the torsional stiffness, (b) the relation of torsional stiffness to flexural stiffness, and (c) the distances of the inertia axis and flexural axis aft of the quarter-chord axis.

In Chapter II of this thesis the whole subject of flexural-torsional flutter is dealt with in considerable detail in the two-dimensional problem. Experimental results reported by Voigt[37,38,39] and by Theodorsen and Garrick[35] indicate good agreement between the flutter speeds calculated by theoretical two-dimensional methods as here presented and flutter speeds as observed in the wind tunnel. This experimental check therefore forms the authority in justification of the subsequent theoretical work by the author.

Two cases are studied specifically in which this mode of flutter can occur. Case A is a case in which the elastic axis and inertia axis coincide at 50% chord. Case B is representative in general of present-day construction for which the torsional frequency has been chosen on the lower limit of that found in practice in order to reduce the flutter speeds. See Appendix V for a summary of the parameters of Cases A and B.

Figures 3 to 10* show the effects of varying the parameters of the wing of Case B, one at a time. The basic condition of Case B is represented by the circled point on each curve. The following conclusions can be drawn which may be considered to apply to the wings of present-day stressed skin construction:

---

*The author is indebted to Lt. Parish and Lt. Jackson[26] for their assistance in the preparation of these figures.

(a) Figure 3 shows that the effect on the flutter speed of moving the elastic axis fore and aft is relatively small in that a 5% rearward change in the position of this axis increases the flutter speed by 30 m.p.h. It is noteworthy that the rearward change of the elastic axis increases the flutter speed but decreases the divergence speed.

(b) Figure 4 shows that the effect on the flutter speed of moving the inertia axis fore and aft is substantial. With the inertia axis in the region of 40% of the chord, a 5% motion forward of that axis increases the flutter speed by 100 m.p.h.

(c) Figure 5 shows the result that is obtained under conditions in which the relative distance between the elastic and inertia axes are fixed. A 5% forward motion of both axes in this case increases the flutter speed by 80 m.p.h.

(d) Figure 6 shows the effect of varying the radius of gyration of the mass of the wing about the inertia axis while holding the torsional stiffness constant. An increase of the radius of gyration from 0.25c to 0.30c reduces the flutter speed by 30 m.p.h.

(e) Figures 7 and 8 show the effects of varying the torsional and bending frequencies independently. The flutter speed

is almost directly proportional to the torsional frequency, a most important parameter. The effect of the bending frequency is negligible.

(f) Figure 9 shows the effect of wing weight on the flutter speed if the stiffnesses are varied to hold frequencies constant. In the range of wing weights found in practice there is only a small effect due to wing weight. It is interesting to note that if wing weights might be reduced to below 1 lb./sq.ft. the flutter speed would increase substantially.

(g) Figure 10 shows that the true airspeed of flutter increases with altitude although the indicated airspeed decreases somewhat.

In summary, the parameters most directly affecting flexural-torsional flutter are:

(a) Position of inertia axis.

(b) Torsional frequency.

(c) Radius of gyration of mass of wing about inertia axis.

It should be noted, however, that the flexural stiffness of a wing is important for general considerations in order to eliminate large amplitude responses of the wing tips to gusts, etc., in flight, even though Figure 8 shows that flutter would not occur at low speeds even with zero bending stiffness.

Theodorsen and Garrick[35] state that when the bending frequency is low relative to the torsional frequency, the critical speed of flexural-torsional flutter can be predicted by the following equation in their notation:

$$\frac{v_f}{b\,\omega_\alpha} = \sqrt{\frac{r_\alpha^2}{k} \cdot \frac{(1/2)}{(1/2 + a + x_\alpha)}} \qquad (1:16)$$

Converted to the nomenclature of this thesis, the equation becomes:

$$v_{cr.} = \frac{\nu_t c}{2} \sqrt{\frac{(i_F^2 + \sigma_F^2)}{\varepsilon + \sigma_F}} \qquad (1:17)$$

in which:

$v_{cr.}$ = critical flutter speed (ft./sec.).

ν_t = natural torsional frequency (rad./sec.).

c = wing chord.

ε = distance of elastic axis back of 25% chord point, as fraction of chord.

σ_F = distance of inertia axis back of elastic axis, as fraction of chord.

i_F = radius of gyration of mass of wing about inertia axis, as fraction of chord.

μ = ratio of wing mass to air mass (see equation 7:27)

The Theodorsen-Garrick formula may be rearranged to show a relation to divergence speed as follows:

$$v_{cr} = v_d \sqrt{\frac{1 + (\sigma_F/i_F)^2}{(1 + \sigma_F/\varepsilon)}} \qquad (1:18)$$

Hence when $\sigma_F = 0$, the flutter speed equals the divergence speed by this formula. It should be emphasized that this formula is represented to be only approximate. Applying it to the two cases studied in Chapter II, the following results are obtained:

Case A. (Note: $\sigma_F = 0$)

$\frac{v_{cr.}}{c}$ = 31.6 rad./sec. (by Theodorsen-Garrick formula)

$\frac{v_{cr.}}{c}$ = 28.6 rad./sec. (by precise calculations). (Chapter II)

Case B.

$v_{cr.}$ = 366 m.p.h. (by Theodorsen-Garrick formula)

$v_{cr.}$ = 374 m.p.h. (by precise calculations). (Chapter II)

Based on average positions of the inertia and elastic axes, Pugsley[26] has given the requirement that at sea level maximum speed:

$$\frac{1}{v}\sqrt{\frac{m_0}{dc^2}} \geqslant 0.020\sqrt{\frac{\sigma}{0.20}} \qquad (1:19)$$

and

$$\frac{1}{v}\sqrt{\frac{I_\Phi}{d^3}} \geqslant 0.025\sqrt{\frac{\sigma}{0.20}} \qquad (1:20)$$

in which:

σ = wing density = δ/c (lb./sq.ft./ft.-chord).

d = semi-span from root to effective tip (ft.)

c = mean chord (ft.).

Chapter VI of this thesis gives a method by which the two-dimensional problem may be extended to take care of the three-dimensional problem, including the effects of vertical surfaces on the tips of the horizontal.

In Chapter VII the procedure is outlined for the calculation of the critical speed of flutter of wings and tails.

1:07. Wing Divergence

If a wing is considered in which the axis of the aerodynamic centers* is forward of the flexural axis, it is seen that the aerodynamic forces produce a moment about the flexural axis which twists the wing in the direction of increasing angle of attack whenever the wing is at a positive angle of attack. This aerodynamic twisting moment is of the form:

$$m \backsim \rho v^2 s c^2 \alpha \tag{1:21}$$

or, the "aerodynamic rigidity" is

$$m_\alpha \backsim \rho v^2 s c^2 \tag{1:22}$$

Inasmuch as the elastic rigidity of a given wing is a fixed quantity, independent of the conditions of flight, it follows that when some critical flight speed is exceeded,

$$m_\alpha \text{ (aerodynamic)} > m_\theta \text{ (elastic)} \tag{1:23}$$

Under this condition, when the aerodynamic moment is greater than the elastic restoring moment, the wing will diverge in torsion. This critical speed is called, therefore, the "divergence speed,"

---

*The aerodynamic center of a section is the point about which the pitching moment is constant and hence the point through which lift forces due to changes in angle of attack are taken to act. The flexural axis is defined as the axis along which loads can be applied without twisting the wing and, conversely, the axis about which the wing twists if pure torsion is applied.

which, from equations (1:17) and (1:18), can be written:

$$v_d = D\sqrt{\frac{m_\Theta}{\rho s c^2}} \tag{1:24}$$

Hanson[17], shows that the value of D in equation (1:24) will lie between 5 and 6 when the aerodynamic center is 5% of the wing chord forward of the flexural axis. The value of D varies inversely as the distance from the aerodynamic center to the flexural axis.

In Section 2:08 of this thesis, it is shown that the torsional divergence can be expressed in terms of the torsional frequency as follows:

$$v_d = \frac{\eta \nu_1 c}{2}\sqrt{\frac{\mu}{\epsilon}} \tag{1:25}$$

or

$$v_d = \frac{\nu_t i_r c}{2}\sqrt{\frac{\mu}{\epsilon}} \tag{1:26}$$

1:08. Aileron Reversal Speed

A phenomenon somewhat related to the wing divergence is that of the reversal of aileron control at very high speeds so that the ailerons produce rolling moments in the opposite direction from what would be normally expected. Considering a wing of a given elastic rigidity, the angular twist of the wing caused by the aerodynamic moment about the flexural axis for an angular deflection of the aileron β can be written:

$$\theta \backsim \frac{\rho v^2 c^2 d}{m_\theta} \beta \qquad (1:27)$$

from which the ratio of angle of twist to aileron angle is

$$\frac{\theta}{\beta} \backsim \frac{\rho v^2 c^2 d}{m_\theta} \qquad (1:28)$$

As the speed increases, this ratio increases, so that eventually a condition is reached in which the rolling moment due to θ is just equal to and in the opposite direction to that due to β, and consequently there is no net roll due to deflection the ailerons.

From equation (1:28), it follows that this speed of aileron reversal is of the form:

$$v_r = K\sqrt{\frac{m_\theta}{\rho c^2 d}} \qquad (1:29)$$

in which K is a non-dimensional constant dependent on the particular plan-form of the wing and the aileron shape. Hanson[17] indicates that the average value is about $K \doteq 2$ and gives curves showing

the effects of taper and wing characteristics.

In Section 5:02, it is shown that the reversal speed is related to the divergence speed by the equation (5:33).

$$v_r = v_d \sqrt{\frac{R_1 \varepsilon}{R_5}} \qquad (1:30)$$

The constants R_1 and R_5 are functions only of the ratio of aileron chord to wing chord, as tabulated in Appendix III, from which the table below was determined.

$\frac{\text{Aileron chord}}{\text{Wing chord}}$	$\sqrt{\frac{R_1}{R_5}}$
0.15	2.23
0.20	2.32
0.25	2.43
0.30	2.55

Using an average value of $\sqrt{R_1/R_5} = 2.4$, the effect of ε is shown.

ε	Elastic axis % chord	$\frac{v_r}{v_d}$
0.05	30	0.54
0.10	35	0.76
0.15	40	0.93
0.174	42.4	1.00

Hence, whenever the elastic axis is forward of the 42.4% chord point, aileron reversal is more critical than torsional divergence. However, this is due to the fact that the torsional divergence speed varies inversely with $\sqrt{\varepsilon}$, rather than because of effects of ε on reversal speed because the reversal speed explicitly is not a function of ε but is given by

$$v_r = \frac{\eta \nu_1 c}{2} \sqrt{\frac{R_1 \mu}{R_5}} \tag{1:31}$$

or

$$v_r = \frac{\nu_t i_F c}{2} \sqrt{\frac{R_1 \mu}{R_5}} \tag{1:32}$$

in which:

ν_t = natural torsional frequency (rad./sec.).

i_F = radius of gyration, as fraction of chord.

c = chord (ft.)

μ = ratio of wing mass to air mass (see equation 7:27).

The reader is referred to the papers by Cox and Pugsley[6], Duncan and McMillan[9], Pugsley[28], and Hirst[41] for further discussions of aileron reversal and the extension to three-dimensional cases.

1:09. Servo Tab Flutter

Another type of flutter is possible when servo tabs are incorporated in the control surfaces which closely resembles the fluttering of a flag. This case is quite analogous to the torsional-aileron case discussed above except that all motion is confined to movable surfaces.

Two expedients are available to prevent this type of flutter:

(a) Use a rigid irreversible tab control system.

(b) Static balance the tab about the hinge line to the extent indicated by equation (1:10).

The reader is referred to the paper by Dietze[8] should he be interested in the aerodynamic forces acting for the purposes of setting up the dynamical equations.

CHAPTER II. FLEXURAL-TORSIONAL FLUTTER (TWO-DIMENSIONAL)

It is essential to the development of the conditions of flutter in this category to first determine the aerodynamic forces and moments acting on an airfoil of infinite aspect ratio which is performing an oscillation vertically in combination with an oscillation in angle of attack. In all these studies it will be considered that the oscillations represent a steady state condition, i.e., they have existed with constant magnitude for a period of time sufficient for all transient phenomena to have vanished. Because of the importance of the aerodynamic forces and moments to this theory, they will be derived here by several methods in succession.

The dynamical equations will then be set up for the case of a steady state forced oscillation and methods shown for the determination of the amplitude of the responses to such forced vibrations as well as for the calculation of the stability limits.

2:01. Aerodynamic Forces and Moments due to Apparent Mass of Fluid Adjacent to a Moving Plate

It is a well known theorem of the aerodynamics of perfect fluids that the only forces acting on a body or a plate moving with constant velocity and at a constant angle of attack are those associated with the circulation of fluid around the body or plate. It is essential to recognize that this theorem is postulated on the basis of a constant flow of fluid at a constant angle of attack. In the case at hand, the plate is performing harmonic motions which produce changing accelerations and decelerations of the fluid so that the fluid exerts forces and moments on the plate, even in the absence of circulation. This section is devoted to determining these forces and moments by the classical method as outlined in Lamb[24], (page 83 et seq).

Consider first a plate which is moving in a fluid with an instantaneous velocity $\dot{x}$ in the direction of the chord and $\dot{y}$ perpendicular to the chord, together with an angular velocity $\dot{\varphi}$. The fluid is at rest at infinity.

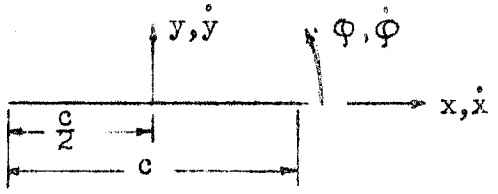

At any point on this plate, the velocity of the fluid in the y direction is

$$v_y = \dot{y} + x\dot{\varphi} \quad \text{(at boundary)} \tag{2:001}$$

and in the x direction

$$v_x = 0 \quad \text{(for the fluid, at boundary)} \tag{2:002}$$

The stream function Ψ is now introduced to describe the motion of the fluid by the following defining equation:

$$v_x = \frac{\partial \Psi}{\partial y} \tag{2:003}$$

$$v_y = -\frac{\partial \Psi}{\partial x} \tag{2:004}$$

It is seen, therefore, that the complete stream function which satisfies equations (2:001) and (2:002) is, at the boundary:

$$(\Psi)_{\text{bound.}} = x\dot{y} + \frac{x^2\dot{\varphi}}{2} + \text{const.} \tag{2:005}$$

The complex potential function is now introduced and defined by the equation

$$\Phi + i\Psi = i\left[C_1 e^{-(\xi + i\eta)} + C_2 e^{-2(\xi + i\eta)} \right] \tag{2:006}$$

in which:

$i = \sqrt{-1}$

C_1 and C_2 are constants to be evaluated

ξ and η are related to x and y by:

$$x + iy = \frac{c}{2} \cosh (\xi + i\eta) \qquad (2:007)$$

Equation (2:007) can be expanded to separate the real and imaginary parts, making use of the relations

$$\cosh iz = \cos z$$

$$\sinh iz = i \sin z$$

so that the equation becomes

$$x + iy = \frac{c}{2} \left[\cosh \xi \cos \eta + i \sinh \xi \sin \eta \right] \qquad (2:008)$$

where, equating the real and imaginary parts independently

$$\left.\begin{aligned} x &= \frac{c}{2} \cosh \xi \cos \eta \\ y &= \frac{c}{2} \sinh \xi \sin \eta \end{aligned}\right\} \qquad (2:009)$$

It is readily seen that $\xi = 0$, $\cosh \xi = 1$, $\sinh \xi = 0$, defines the boundary of the fluid adjacent to the plate, viz.:

$$\left.\begin{aligned} (x)_{\xi=0} &= \frac{c}{2} \cos \eta \\ (y)_{\xi=0} &= 0 \end{aligned}\right\} \qquad (2:010)$$

Substituting equations (2:010) into (2:005) gives:

$$(\Psi)_{\xi=0} = \frac{c}{2} \dot{y} \cos \eta + \frac{c^2}{8} \dot{\varphi} \cos^2 \eta + \text{const.} \qquad (2:011)$$

which can be altered slightly, using the relation $\cos^2 \eta = \frac{1 + \cos 2\eta}{2}$

to give:

$$(\Psi)_{\xi=o} = \frac{c}{2}\dot{y}\cos\eta + \frac{c^2}{16}\dot{\varphi}\cos 2\eta + \text{const.} \qquad (2:012)$$

Equation (2:006) can be evaluated on the boundary to be

$$(\Phi + i\Psi)_{\xi=o} = i\left[C_1 e^{-i\eta} + C_2 e^{-2i\eta}\right] \qquad (2:013)$$

Using the relation which is well-known in the theory of complex numbers that,

$$e^{iz} = \cos z + i \sin z$$

the equation (2:013) yields the stream function at the boundary

$$(\Psi)_{\xi=o} = C_1 \cos\eta + C_2 \cos 2\eta \qquad (2:014)$$

Comparing equations (2:012) and (2:014), the constants C_1 and C_2 can be evaluated as

$$C_1 = \frac{c}{2}\dot{y} \qquad (2:015)$$

$$C_2 = \frac{c^2}{16}\dot{\varphi} \qquad (2:016)$$

Substituting these values of C_1 and C_2 into equation (2:006) gives

$$\Phi + i\Psi = i\frac{c}{2}\dot{y}e^{-(\xi+i\eta)} + i\frac{c^2}{16}\dot{\varphi}e^{-2(\xi+i\eta)} \qquad (2:017)$$

or

$$\Phi = \dot{y}\frac{c}{2}e^{-\xi}\sin\eta + \dot{\phi}\frac{c^2}{16}e^{-2\xi}\sin 2\eta \qquad (2:018)$$

$$\Psi = \dot{y}\frac{c}{2}e^{-\xi}\cos\eta + \dot{\phi}\frac{c^2}{16}e^{-2\xi}\cos 2\eta \qquad (2:019)$$

It is shown by Millikan[25] (page 3.3 et seq.) that the potential function Φ bears the relation to the impulsive pressure p_i as follows:

$$p_i = \rho\Phi + \text{const.} \qquad (2:020)$$

The impulsive force acting on any area dS is then, disregarding the constant in equation (2:020),

$$df_i = \rho\Phi\, dS \qquad (2:021)$$

The velocity of flow normal to the surface S is given by

$$v_n = \frac{\partial\Phi}{\partial s_n} = \frac{\partial\Psi}{\partial s_t} \qquad (2:022)$$

The total kinetic energy imparted to the fluid must be equal to the work done by the external forces, hence

$$T = \frac{1}{2}\int_{\text{Boundary}} v_n\, df_i \qquad (2:023)$$

Or, the energy per unit depth of fluid in the two-dimensional case is:

$$T = \frac{\rho}{2}\int \Phi\, d\Psi \qquad (2:024)$$

in which the integral is performed over the entire boundary in a positive direction.

The functions Φ and Ψ of equations (2:018) and (2:019) approach zero as ξ approaches infinity so that the only integral that need be considered is that on the surface of the plate, namely,

$$T = -\frac{\rho}{2} \int_{\eta=0}^{2\pi} \Phi \, d\Psi \qquad (\text{at } \xi = 0) \tag{2:025}$$

On the surface $\xi = 0$

$$(\Psi)_{\xi=0} = \dot{y} \frac{c}{2} \cos\eta + \dot{\phi} \frac{c^2}{16} \cos 2\eta$$

$$(d\Psi)_{\xi=0} = -\left[\dot{y} \frac{c}{2} \sin\eta + \dot{\phi} \frac{c^2}{8} \sin 2\eta \, d\eta \right] \tag{2:026}$$

$$(\Phi)_{\xi=0} = \dot{y} \frac{c}{2} \sin\eta + \dot{\phi} \frac{c^2}{16} \sin 2\eta$$

Inasmuch as

$$\int_0^{2\pi} \sin^2\eta \, d\eta = \int_0^{2\pi} \sin^2 2\eta \, d\eta = \pi$$

and

$$\int_0^{2\pi} \sin\eta \sin 2\eta \, d\eta = 0$$

the total kinetic energy of the fluid is

$$T = \frac{1}{2}\left[\frac{\pi\rho c^2}{4}\dot{y}^2 + \frac{\pi\rho c^4}{128}\dot{\varphi}^2\right] \qquad (2:027)$$

For any body moving with a vertical velocity $\dot{y}$ and an angular velocity $\dot{\varphi}$, the kinetic energy may be written

$$T = \frac{1}{2}\left[M\dot{y}^2 + I\dot{\varphi}^2\right]$$

so that, by analogy, the fluid is said to have an "apparent mass" per unit span to resist motion in the y direction of

$$m_L = \frac{\pi\rho c^2}{4} \qquad (2:028)$$

This mass m_L is seen to be the mass of the cylinder of air enclosing the plate in such a way that the chord forms the diameter of the cylinder. This apparent mass is often called the "mass of enclosing air cylinder" in the literature on flutter, and must be added to the mass of the wing in order to obtain the true effective mass in the dynamical equations.

By analogy, that "apparent moment of inertia" per unit span is seen to be

$$I = \frac{\pi\rho c^4}{128} = m_L\left(\frac{c^2}{32}\right) \qquad (2:029)$$

It is a curious phenomena that, while the apparent mass equals the mass of the enclosing air cylinder, the apparent moment of inertia equals only one fourth of that of the enclosing air cylinder

if that cylinder were solid, for which

$$I = M\left(\frac{d^2}{8}\right)$$

In the analysis thus far, the axis x has been in the chordwise direction and the axis y in the direction normal to the chord. It is instructive now to consider the transformation to a new set of axes.

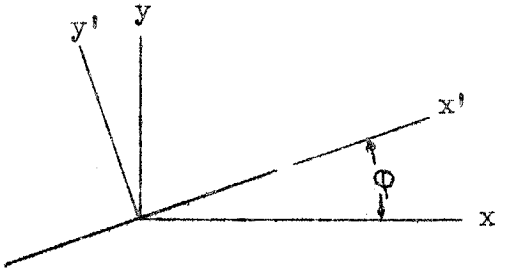

The velocities at the mid-point of the chord are transformed as follows, changing the notation to that of the figure:

$$\dot{x}' = \dot{x}\cos\varphi + \dot{y}\sin\varphi$$
$$\dot{y}' = -\dot{x}\sin\varphi + \dot{y}\cos\varphi \qquad (2:030)$$

Equation (2:027) in terms of the new notation becomes:

$$T = \frac{1}{2}\left[\frac{\pi\rho c^2}{4}(\dot{y}')^2 + \frac{\pi\rho c^4}{128}\dot{\varphi}^2\right] \qquad (2:031)$$

Hence, the kinetic energy per unit span becomes:

$$T = \frac{\pi\rho c^2}{8}\left[\dot{x}^2\sin^2\varphi + \dot{y}^2\cos^2\varphi - 2\dot{x}\dot{y}\sin\varphi\cos\varphi\right] + \frac{\pi\rho c^4}{256}\dot{\varphi}^2 \qquad (2:032)$$

It is convenient here to use Lagrange's Equation* to determine the forces acting, which, for generalized coordinates q_k, is

$$\frac{d}{dt}\left(\frac{\partial T}{\partial \dot{q}_k}\right) - \frac{\partial T}{\partial q_k} = Q_k \tag{2:033}$$

in which Q_k is the external generalized force acting in the directions of q_k. It is important to note that in applying equation (2:033) to the problem at hand, the force Q_k would represent the force of the plate on the air. The force of the air on the plate would be $-Q_k$.

Consequently, the vertical force of the air on the plate may be written:

$$Y = -\frac{d}{dt}\left(\frac{\partial T}{\partial \dot{y}}\right) + \frac{\partial T}{\partial y} \tag{2:034}$$

The moment of force of the air on the plate is

$$M = -\frac{d}{dt}\left(\frac{\partial T}{\partial \dot{\varphi}}\right) + \frac{\partial T}{\partial \varphi} \tag{2:035}$$

Substituting the value of T given in equation (2:033) into equations (2:034) and (2:035) leads to the following results, if we further require that

$$\dot{x} = v = \text{const.} \tag{2:036}$$

$$Y = -\frac{\pi \rho c^2}{4}\left[\ddot{y}\cos^2\varphi - v\dot{\varphi}\cos 2\varphi - 2\dot{y}\dot{\varphi}\sin\varphi\cos\varphi\right] \tag{2:037}$$

*For a derivation of Lagrange's Equation, see Byerly[4], Timoshenko[36], Webster[40], or any treatise on classical mechanics. The form used here is that in which there is no potential energy.

$$M = -\frac{\pi\rho c^4}{128}\ddot{\varphi} + \frac{\pi\rho c^2}{4}\left[+v^2\sin\varphi\cos\varphi - \dot{y}^2\sin\varphi\cos\varphi - v\dot{y}\cos 2\varphi\right] \quad (2{:}038)$$

It is now necessary to make the further assumption that must usually be made in studying vibrations, namely, that oscillations are small, i.e.,

$$\dot{y} \ll v$$

$$\varphi \ll \pi$$

Whence, for small oscillations

$$Y = -\frac{\pi\rho c^2}{4}\left[\ddot{y} - v\dot{\varphi}\right] \quad (2{:}039)$$

$$M = -\frac{\pi\rho c^4}{128}\ddot{\varphi} + \frac{\pi\rho c^2 v^2}{4}\left[\varphi - \frac{\dot{y}}{v}\right] \quad (2{:}040)$$

The moment is taken about the mid-point of the chord. It should be noted that the second term in equation (2:039) has the character of a "centripetal acceleration." In equation (2:040) only the first term involves a non-steady state acceleration. The second term, containing φ and $\dot{y}$, appears even in cases of steady motion. Consequently, the first term of equation (2:040) is taken as the apparent mass contribution to the moment and the second term as a steady motion contribution to the moment.

2:02. Aerodynamic Forces and Moments in Quasi-Steady Motion.

In this section of the analysis, the aerodynamic forces and moments are determined under conditions of steady motion, or in particular, on the assumption that there are no effects of vortices shed from the wing. The assumption is continued that the wing has infinite aspect ratio.

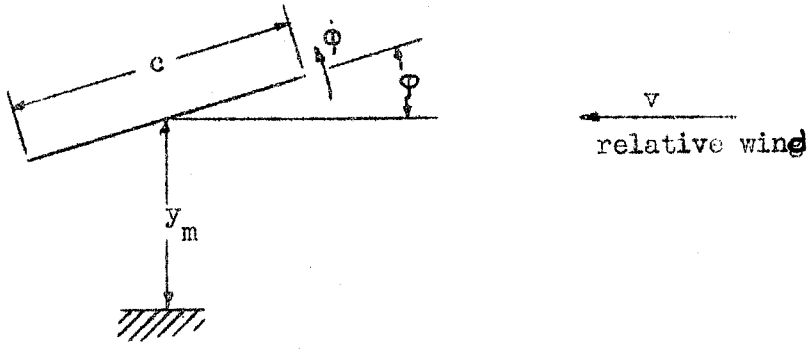

A plane airfoil, as shown, having a vertical velocity at its mid-point of $\dot{y}_m$ and an angular velocity $\dot{\phi}$ as well as an angular position φ to the free air stream can be replaced by a cambered airfoil of such camber that at each point, if φ is small:

$$\frac{d}{dx} y_c = - \frac{x \dot{\Phi}}{V} \qquad (2:041)$$

in which y_c is the vertical position of the camber line relative to the chord line through the leading and trailing edge.

Integrating equation (2:041),

$$y_c = - \frac{x^2 \dot{\Phi}}{2V} + C_1 \qquad (2:042)$$

Inasmuch as $y_c = 0$ at $x = \frac{+c}{2}$, the constant $C_1 = \frac{c^2\dot{\varphi}}{8v}$ and the equation for the camber line becomes

$$y_c = \frac{c^2\dot{\varphi}}{8v} \quad \frac{x^2\dot{\varphi}}{2v} \tag{2:043}$$

The plane airfoil, as shown above, can be replaced by the cambered airfoil below without affecting the aerodynamic forces and moments inasmuch as the velocities and inclinations of corresponding points on the two airfoils relative to the free stream velocity are identical.

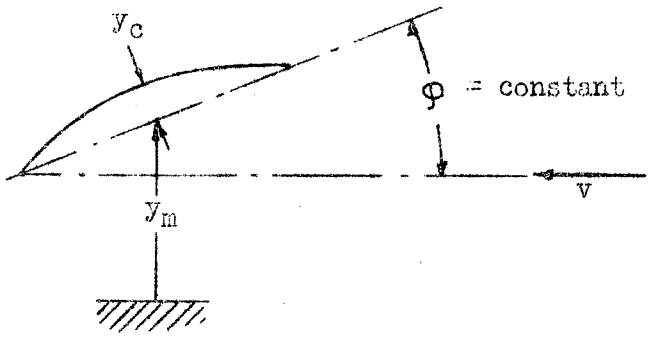

The lift forces on such an airfoil are given by Millikan[25], (page 15.6), and Kármán-Burgers[18], (page 49, section a). The aerodynamic forces and moments per unit span under this condition can be represented completely by two lift vectors, viz.:

$$L_a = \pi\rho cv^2\left(\varphi - \frac{\dot{y}_m}{v}\right) \quad \text{(acting through forward quarter-chord point)} \tag{2:044}$$

and

$$L_b = 2\pi \rho c v^2 \left(\frac{y_c}{c}\right) \qquad \text{(acting through mid-chord point)} \qquad (2:045)$$

Substituting that $y_c = \frac{c^2 \dot{\varphi}}{8v}$

$$L_b = \frac{\pi \rho c^2}{4} v \dot{\varphi} \qquad \text{(acting through mid-chord point)} \qquad (2:046)$$

It is important to note that the force L_a is taken to act through the quarter-chord point in all cases of steady motion. This is the result of a combination of circumstances, namely, that the following forces and moments are acting:

Lift due to circulation $= \pi \rho c v^2 \left(\varphi - \frac{\dot{y}_m}{v}\right)$ (acting at mid-chord)

Moment due to apparent mass $= \frac{\pi \rho c^2 v^2}{4} \left(\varphi - \frac{\dot{y}_m}{v}\right)$ (see eq. 2:040 and subsequent discussion)

The above combine to form the quasi-steady lift, L_a, which is taken to act at the forward quarter-chord point.

It is worthy of comment, further, that the lift L_b (equation 2:045) arises from the Kutta condition that the circulation about the airfoil must be sufficient that the flow is tangential at the trailing edge. The second term in equation (2:039) is identical in value to L_b and arises from apparent mass effects. The total lift must include both these terms.

2:03. Summary of Aerodynamic Forces and Moments arising from Apparent Mass and Quasi-Steady Motion

In this section all of the aerodynamic forces and moments are summarized for the conditions of quasi-steady motion including effects of accelerations but under the specific assumption that there are no effects of vortices shed from the wing, which is taken further to have infinite aspect ratio. The effects of the shed vortices will be considered later in Section 2:04.

At 25% chord

$$L = \pi \rho c v^2 (\varphi - \frac{\dot{y}_m}{v}) \qquad (2:047)$$

At 50% chord

$$L = \frac{\pi c^2}{4} (-\ddot{y}_m + 2v\dot{\varphi}) \qquad (2:048)$$

Moment

$$M = -\frac{\pi \rho c^4}{128} \ddot{\varphi} \qquad (2:049)$$

2:04. Aerodynamic Forces and Moments for Steady State Oscillations by Method of von Kármán and Sears[19].

In this method, the airfoil is replaced by a vortex sheet such that the vorticity is $\gamma(x) = \frac{d\Gamma}{dx}$ in which $d\Gamma$ is the circulation about any element dx. The strength of the vorticity in the wake is written as $\gamma(\xi)$

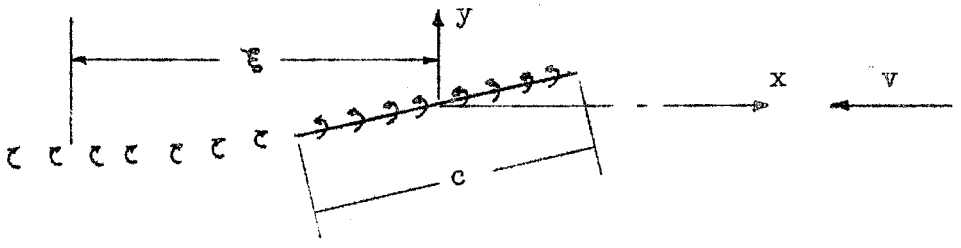

It is shown by Kármán-Sears[19] that the total lift can be written in the form, for an airfoil of chord c,

$$L = L_o + L_1 + L_2 \qquad (2:050)$$

in which*

$$L_o = \rho v \int_{-\frac{c}{2}}^{\frac{c}{2}} \gamma_o(x)\, dx \qquad \text{(quasi-steady lift)} \qquad (2:051)$$

*The notation and directions of positive axes of this thesis differ from those used by Kármán-Sears. The signs for the integrals are modified to apply to the notation used here.

$$L_1 = +\rho \frac{d}{dt} \left[\int_{-\frac{c}{2}}^{\frac{c}{2}} \gamma_o(x)\, x\, dx \right] \qquad \text{(apparent mass lift)} \qquad (2:052)$$

$$L_2 = \frac{\rho v c}{2} \int_{\frac{c}{2}}^{\infty} \frac{\gamma(\xi)\, d\xi}{\sqrt{\xi^2 - c^2/4}} \qquad \text{(lift due to wake effects)} \qquad (2:053)$$

Similarly, the moment of all aerodynamic forces about the mid-point of the airfoil may be written:

$$M = M_o + M_1 + M_2 \qquad (2:054)$$

in which:

$$M_o = \rho v \int_{-\frac{c}{2}}^{\frac{c}{2}} \gamma_o(x)\, x\, dx \qquad \text{(quasi-steady moment)} \qquad (2:055)$$

$$M_1 = +\frac{\rho}{2} \frac{d}{dt} \left[\int_{-\frac{c}{2}}^{\frac{c}{2}} \gamma_o(x)\left(x^2 - \frac{c^2}{8}\right) dx \right] \qquad \text{(moment due to apparent mass)} \qquad (2:056)$$

$$M_2 = +\frac{\rho v c^2}{8} \int_{\frac{c}{2}}^{\infty} \frac{\gamma(\xi)\, d\xi}{\sqrt{\xi^2 - c^2/4}} \qquad \text{(moment due to wake effects)} \qquad (2:057)$$

The lift and moment L_2 and M_2 shall be ignored for the instant except to note that $M_2 = L_2 \cdot (\frac{c}{4})$ and hence that the lift force L_2 may be taken to act through the forward quarter-chord point of the airfoil, in which case there is no added moment.

The distance x along the chord may be expressed as

$$x = (\frac{c}{2})\cos\theta \tag{2:058}$$

$$dx = -(\frac{c}{2})\sin\theta\, d\theta \tag{2:058a}$$

Substituting equations (2:058) and (2:058a) into those previously written yields:

$$L_o = \frac{\rho v c}{2} \int_o^{\pi} Y_o \sin\theta\, d\theta \tag{2:059}$$

$$L_1 = + \frac{\rho c^2}{4} \frac{d}{dt} \left[\int_o^{\pi} Y_o \sin\theta \cos\theta\, d\theta \right] \tag{2:060}$$

$$M_o = \frac{\rho v c^2}{4} \int_o^{\pi} Y_o \sin\theta \cos\theta\, d\theta \tag{2:061}$$

$$M_1 = + \frac{\rho c^3}{16} \frac{d}{dt} \left[\int_o^{\pi} Y_o \cos^2\theta \sin\theta\, d\theta - \frac{1}{2} \int_o^{\pi} Y_o \sin\theta\, d\theta \right] \tag{2:062}$$

To evaluate the quasi-steady and apparent mass terms above, it is necessary only to determine $\gamma_o(x)$, ignoring the effects of the wake. The quasi-steady conditions for the airfoil are the same as those of Section 2:03, namely, the vertical velocity of the mid-chord point is $\dot{y}_m$, the angle to the wind in free stream is φ, the angular velocity is $\dot{\varphi}$.

The flat airfoil with the angular velocity $\dot{\varphi}$ is replaced by a parabolically cambered airfoil at zero angular velocity with a maximum camber in the same manner as in Section 2:03,

$$y_c = \frac{c^2 \dot{\varphi}}{8v} \tag{2:063}$$

or

$$\frac{y_c}{c/2} = \frac{c \dot{\varphi}}{4v} \tag{2:064}$$

Kármán and Burgers[18] (equation 10.7, page 49) give the vorticity distribution due to camber at zero angle of attack

$$\gamma = 4v \left(\frac{y_c}{c/2}\right) \sin \theta \tag{2:065}$$

whence

$$\gamma = c \dot{\varphi} \sin \theta \qquad \text{(due to camber, } \varphi = \dot{y}_m = 0) \tag{2:066}$$

Karman and Burgers (equation 7.9, page 38) give the vorticity distribution for a flate plate at an angle of attack α to the relative wind*

*Note that the positive x direction of this thesis is opposite to that of Kármán and Burgers so that the signs of x are reversed.

$$\gamma = 2v \sin \alpha \sqrt{\frac{c/2 + x}{c/2 - x}} = 2v \sin \alpha \frac{1 + \cos \theta}{\sin \theta} \qquad (2:067)$$

In this analysis, it is assumed that α is small so that $\sin \alpha = \alpha$. The angle of attack to the relative wind is

$$\alpha = \varphi - \frac{\dot{y}_m}{v} \qquad (2:068)$$

Hence, the vorticity due to the angle φ and vertical velocity $\dot{y}_m$ is

$$\gamma = 2v \left(\varphi - \frac{\dot{y}_m}{v} \right) \left(\frac{1 + \cos \theta}{\sin \theta} \right) \qquad \text{(due to } \varphi \text{ and } \dot{y}_m \text{ with } \dot{\varphi} = 0) \qquad (2:069)$$

The complete vorticity for the quasi-steady condition is then the sum of the vorticities given by equations (2:066) and (2:069),

$$\gamma_o = c\dot{\varphi} \sin \theta + 2v \left(\varphi - \frac{\dot{y}_m}{v} \right) \left(\frac{1 + \cos \theta}{\sin \theta} \right) \qquad (2:070)$$

Before calculating the forces and moments, it is convenient first to evaluate the definite integrals which appear in equations (2:059) through (2:061), namely,

$$\int_0^{\pi} \gamma_o \sin \theta \, d\theta = \frac{\pi c \dot{\varphi}}{2} + 2\pi v \left(\varphi - \frac{\dot{y}_m}{v} \right) \qquad (2:071)$$

$$\int_0^{\pi} \gamma_o \sin \theta \cos \theta \, d\theta = + \pi v \left(\varphi - \frac{\dot{y}_m}{v} \right) \qquad (2:072)$$

$$\int_0^{\pi} \gamma_o \cos^2\theta \sin\theta \, d\theta = \frac{\pi c \dot{\varphi}}{8} + \pi v \left(\varphi - \frac{\dot{y}_m}{v}\right) \qquad (2:073)$$

Hence, the lift forces become:

$$L_o = \frac{\pi \rho c^2}{4} v\dot{\varphi} + \pi \rho c v^2 \left(\varphi - \frac{\dot{y}_m}{v}\right) \qquad (2:074)$$

$$L_1 = \frac{\pi \rho c^2}{4} \left(v\dot{\varphi} - \ddot{y}_m\right) \qquad (2:075)$$

The moments of the aerodynamic forces, about the mid-chord point, are:

$$M_o = \frac{\pi \rho c^2}{4} v^2 \left(\varphi - \frac{\dot{y}_m}{v}\right) \qquad (2:076)$$

$$M_1 = + \frac{\pi \rho c^4}{128}\ddot{\varphi} + \frac{\pi \rho c^3}{16}\left(v\dot{\varphi} - \ddot{y}_m\right) - \frac{\pi \rho c^4}{64}\ddot{\varphi} - \frac{\pi \rho c^3}{16}\left(v\dot{\varphi} - \ddot{y}_m\right)$$

or

$$M_1 = - \frac{\pi \rho c^4}{128}\ddot{\varphi} \qquad (2:077)$$

It is seen by inspection that the forces and moments, L_o, L_1, M_o, M_1, are identical to those listed in Section 2:03, equations (2:047) through (2:049).

The aerodynamic force L_2 as defined by equation (2:053) will now be determined, which force takes into account all the effects of the vorticity in the wake, under conditions of steady state oscillations, with a circular frequency ν radians per second,

in which case it is possible to write the instantaneous values of y and φ as

$$y = a_1 \cos \nu t + b_1 \sin \nu t \tag{2:078}$$

$$= a_2 \cos \nu t + b_2 \sin \nu t \tag{2:079}$$

However, it is more convenient to introduce a complex variable notation by writing:

$$y + iy' = \bar{y} = \bar{c}_1 e^{i\nu t} \tag{2:080}$$

$$\varphi + i\varphi' = \bar{\varphi} = \bar{c}_2 e^{i\nu t} \tag{2:081}$$

The variables $\bar{y}$ and $\bar{\varphi}$, written with the bars, are complex and such that the instantaneous values of y and φ are represented by the real parts of $\bar{y}$ and $\bar{\varphi}$ respectively. $\bar{c}_1$ and $\bar{c}_2$ are complex constants which determine the magnitude and phase of the steady-state oscillations.

Similarly, the vorticity in the wake may be represented by

$$\gamma(\xi) + i\gamma(\xi)' = \bar{\gamma}(\xi) = \bar{g} e^{i\nu\left[t-(\xi/v)\right]} \tag{2:082}$$

where $\bar{g}$ is a constant which may be complex and v is the constant mean horizontal velocity.

Substituting the value of equation (2:082) into equation (2:053) at the same time that the conception of the complex lift vector is introduced, namely,

$$L_2 + iL_2' = \bar{L}_2 = \frac{\rho v c}{2} \int_{\frac{c}{2}}^{\infty} \frac{\bar{\Gamma}(\xi)\, d\xi}{\sqrt{\xi^2 - c^2/4}} \tag{2:083}$$

yields:

$$\bar{L}_2 = \frac{\rho v c}{2} \bar{g} e^{i\nu t} \int_{\frac{c}{2}}^{\infty} \frac{e^{-\left(\frac{i\nu\xi}{V}\right)} d\xi}{\sqrt{\xi^2 - c^2/4}} \tag{2:084}$$

or, rearranging:

$$\bar{L}_2 = \frac{\rho v c \bar{g}}{2} e^{i\nu t} \int_{\left(\frac{2\xi}{c}\right)=1}^{\infty} \frac{e^{-\left(\frac{i\nu c}{2V}\right)\cdot\left(\frac{2\xi}{c}\right)} d\left(\frac{2\xi}{c}\right)}{\sqrt{\left(\frac{2\xi}{c}\right)^2 - 1}} \tag{2:085}$$

Kármán and Sears show that the integral above may be expressed as a modified Hankel function, namely,

$$K_o\left(\frac{i\nu c}{2v}\right) = \int_{\left(\frac{2\xi}{c}\right)=1}^{\infty} \frac{e^{-\left(\frac{i\nu c}{2V}\right)\cdot\left(\frac{2\xi}{c}\right)} d\left(\frac{2\xi}{c}\right)}{\sqrt{\left(\frac{2\xi}{c}\right)^2 - 1}} \tag{2:086}$$

whence:

$$\bar{L}_2 = \frac{vc}{2} \bar{g} K_o e^{i\nu t} \tag{2:087}$$

Kármán and Sears show further that in order to satisfy the conditions (a) that the vorticity in the wake must equal the vorticity shed from the wing, and (b) that the flow is tangential at the trailing edge, a definite relation must hold between the constant $\bar{g}$ defining the vorticity in the wake and the constant $\bar{G}_o$ defining the quasi-steady circulation. (See equation 25, reference 19.)

$$\frac{c\bar{g}}{2} = -\frac{\bar{G}_o}{K_o + K_1} \tag{2:088}$$

in which K_o and K_1 are modified Hankel functions, and the constant $\bar{G}_o$ is defined by

$$L_o + iL'_o = \bar{L}_o = \rho v \bar{\Gamma}_o = \rho v \bar{G}_o e^{i\nu t} \tag{2:089}$$

whence

$$\bar{L}_2 = -\bar{L}_o\left(\frac{K_o}{K_o + K_1}\right) \tag{2:090}$$

It must be noted that functions K_o and K_1 are complex in nature and hence that there is a phase difference between $\bar{L}_2$ and $\bar{L}_o$. As was shown by equations (2:053) and (2:057), $\bar{L}_2$ may be taken to act at the forward quarter-chord point.

Substituting the value of L_o from equation (2:074), the result is obtained that

$$\bar{L}_o + \bar{L}_2 = \pi\rho c v^2 \left[\varphi - \frac{\dot{\bar{y}}_m}{v} + \frac{\dot{\bar{\varphi}} c}{4v}\right]\left[1 - \frac{K_o}{K_o + K_1}\right] \tag{2:091}$$

Attention is directed to the relation:

$$\left[\bar{\varphi} - \frac{\dot{\bar{y}}_m}{v} + \frac{\dot{\bar{\varphi}}c}{4v}\right] = \bar{\alpha}_h \qquad (2:092)$$

in which α_h is the angle of attack of the 75% chord point (in German, the "hinterpunkt").

The factor $\left[1 - \frac{K_o}{K_o + K_1}\right] = \left[\frac{K_1}{K_o + K_1}\right]$ is called the "complex lift vector factor" and is written in the Kassner-Fingado[20] notation

$$\bar{P} = A - iB = \frac{K_1(\frac{i\nu c}{2v})}{K_o(\frac{i\nu c}{2v}) + K_1(\frac{i\nu c}{2v})} \qquad (2:093)$$

in which A and B are real, positive quantities which are functions of $(\frac{i\nu c}{2v})$. The original discovery of the fact that this vector is such a Hankel function is attributed to Theodorsen[34], who defines the non-dimensional parameter, "reduced frequency," k, as

$$k = \frac{\nu c}{2v} \qquad \text{(Theodorsen[34])} \qquad (2:094)$$

This is identical with the reduced frequency as sometimes used by Küssner[22], namely,

$$\omega = \frac{\nu c}{2v} \qquad \text{(Küssner[22])} \qquad (2:095)$$

However, on other occasions, Küssner[23] uses as the reduced frequency

$$\omega = \frac{i\nu c}{2v} \qquad \text{(Küssner[23])} \qquad (2:096)$$

Kassner and Fingado[20] have taken the reciprocal of this parameter, dropped the factor 2, and obtained what they call the "reduced velocity,"

$$V = \frac{v}{\sqrt{c}} \qquad (2:097)$$

The author feels that the reduced velocity V in the form as defined by equation (2:097) is more suited to engineering use and has therefore adopted its use in the remainder of this treatise.

The values of the components of the vector $\bar{P}$ are given graphically in Figures 11 to 13 for the complete range of V from zero to infinity.

2:05. Summary of Aerodynamic Forces and Moments in Steady State Oscillations (Two-Dimensional Case)

The forces and moments given by equations (2:074) through (2:077), and (2:091) may be combined to the following:

At 25% chord

$$\bar{L} = \pi\rho c v^2 \bar{\alpha}_h \bar{P} \quad * \tag{2:098}$$

At 50% chord

$$\bar{L} = -\frac{\pi\rho c^2}{4} \ddot{\bar{y}}_m \tag{2:099}$$

in which $\ddot{\bar{y}}_m$ is the vertical acceleration of mid-chord point.

At 75% chord

$$\bar{L} = \frac{\pi\rho c^2}{4} v \dot{\bar{\varphi}} \tag{2:100}$$

Moment

$$\bar{M} = -\frac{\pi\rho c^4}{128} \ddot{\bar{\varphi}} \tag{2:101}$$

In all the above equations the barred symbols, $\bar{L}$, $\bar{M}$, $\bar{\alpha}$, $\bar{y}$, $\bar{\varphi}$, $\dot{\bar{\varphi}}$, etc., indicate complex vectors of constant amplitude which rotate about the origin with an angular velocity (frequency) of ν rad./sec. The instantaneous value of any variable is the horizontal projection (the real part) of the corresponding complex variable.

---

* $\bar{\alpha}_h$ is the effective angle of attack at the three-quarter chord point.

The forces and moments given above are in exact agreement with those given by Theodorsen[34], Küssner[23], and Kassner and Fingado[20]. These same forces and moments reputedly agree with those used by Lyon and by Cicala, whose papers are listed in the Bibliography, although the author has not actually verified this agreement. However, it should be remarked that many flutter investigations, particularly those reported by British writers, have been made with only partially complete forces and moments. It has been a common assumption of many authors to neglect the effects of the reduced velocity or reduced frequency on the magnitude and phase of the lift acting at the 25% point, as shown in equation (2:098).

2:06. Dynamical Equations for Steady State Forced Oscillations.

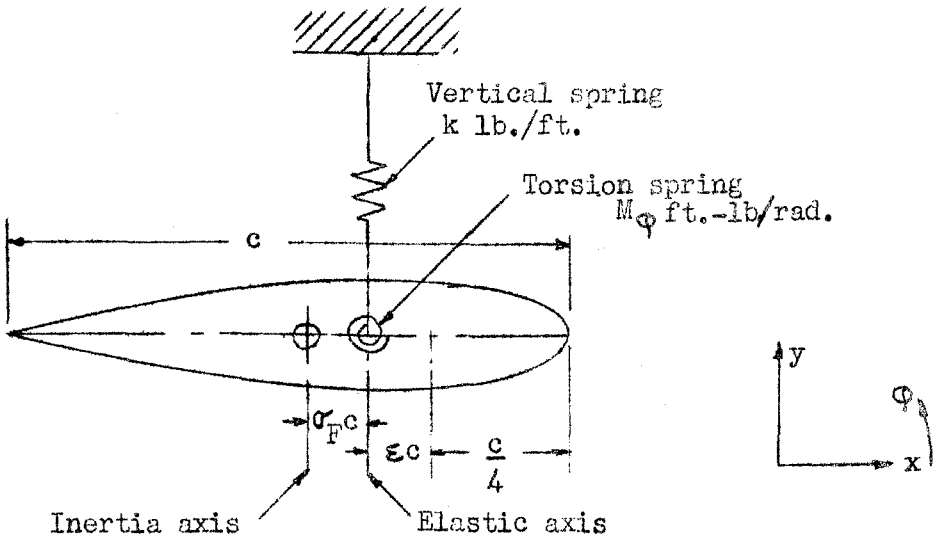

The airfoil is taken to be supported at the elastic axis by a flexural spring of constant k lb./ft. and a torsional spring of constant M_φ ft.-lb./radian. The mass of a unit length of wing is taken as m_F slugs, and the radius of gyration of the mass of the wing about its center of gravity (inertia axis) is given by $i_F c$.

There will be the following forces and moments acting in addition to the aerodynamic forces and moments which are summarized in Section 2:05:

Elastic Force (acting on elastic axis)

$$\bar{F} = -k\bar{y}_e \qquad (2:102)$$

in which $\bar{y}_e$ is vertical displacement of the elastic axis.

Elastic Moment

$$\bar{M}_{el} = -(M_\varphi)\bar{\varphi} \tag{2:103}$$

Kassner and Fingado[20] have found it convenient to introduce the conception of an "elastic radius of gyration" defined as

$$\eta^2 c^2 = \frac{M_\varphi}{k} \tag{2:104}$$

Using this, the elastic moment becomes

$$\bar{M}_{el} = -k\eta^2 c^2 \bar{\varphi} \tag{2:105}$$

Inertia Force of Wing (acting on inertia axis)

$$\bar{F}_i = -m_F \ddot{\bar{y}}_s \tag{2:106}$$

in which $\ddot{\bar{y}}_s$ is the vertical acceleration of the inertia axis.

Inertia Moment of Wing

$$\bar{M}_i = -m_F i_F^2 c^2 \ddot{\bar{\varphi}} \tag{2:107}$$

There is now a considerable latitude in the choice of co-ordinates for use in setting up the dynamical equation. For the present instant, it is convenient and instructive to use the vertical displacement of the elastic axis, $\bar{y}_e$, and the angle of the airfoil $\bar{\varphi}$. It is necessary, therefore, to transform all vertical displacements into terms of $\bar{y}_e$ and $\bar{\varphi}$.

$$\bar{\alpha}_h = \bar{\varphi} - \frac{\dot{\bar{y}}_h}{v} \tag{2:108}$$

Inasmuch as $\bar{y}_h = y_e - \bar{\varphi}c(\frac{1}{2} - \varepsilon)$

$$\bar{\alpha}_h = \bar{\varphi} - \frac{\dot{\bar{y}}_e}{v} + \frac{\dot{\bar{\varphi}}c}{v}(\frac{1}{2} - \varepsilon) \tag{2:109}$$

$$\ddot{\bar{y}}_m = \ddot{\bar{y}}_e - \ddot{\bar{\varphi}}c(\frac{1}{4} - \varepsilon) \tag{2:110}$$

$$\ddot{\bar{y}}_s = \ddot{\bar{y}}_e - \ddot{\bar{\varphi}}c\,\sigma_F \tag{2:111}$$

Inasmuch as all the forces and moments have been predicated on the basis of steady state oscillations, it was shown above that the displacements may be written (see equations 2:080 and 2:081)

$$\bar{y}_e = \bar{c}_1 e^{i\nu t} \tag{2:112}$$

$$\bar{\varphi} = \bar{c}_2 e^{i\nu t} \tag{2:113}$$

Differentiating (2:112) and (2:112) with respect to time:

$$\begin{aligned} \dot{\bar{y}}_e &= i\nu\bar{c}_1 e^{i\nu t} \\ \dot{\bar{\varphi}} &= i\nu\bar{c}_2 e^{i\nu t} \end{aligned} \tag{2:114}$$

and differentiating again:

$$\begin{aligned} \ddot{\bar{y}}_e &= -\nu^2\bar{c}_1 e^{i\nu t} \\ \ddot{\bar{\varphi}} &= -\nu^2\bar{c}_2 e^{i\nu t} \end{aligned} \tag{2:115}$$

Hence:

$$\dot{\bar{y}}_e = i\,\bar{y}_e$$

$$\ddot{\bar{y}}_e = -\nu^2 \bar{y}_e$$

$$\dot{\bar{\varphi}} = i\nu\bar{\varphi} \qquad (2:116)$$

$$\ddot{\bar{\varphi}} = -\nu^2\bar{\varphi}$$

Introducing $\bar{F}$ as the complex vector representing the external exciting force, the complete dynamical equation for the force becomes, if the relations (2:116) are used:

$$\sum F = 0 = \bar{F} + \bar{y}_e \left[-k + \nu^2(m_F + m_L) - 4i\nu\frac{v}{c} m_L \bar{P} \right]$$

$$+ \bar{\varphi} c \left[-m_F\nu^2\sigma_F + m_L \left\{ -\nu^2\left(\frac{1}{4} - \varepsilon\right) + 4\frac{v^2}{c^2}\bar{P} \right.\right.$$

$$\left.\left. + 4i\nu\frac{v}{c}\bar{P}\left(\frac{1}{2} - \varepsilon\right) + i\nu\frac{v}{c}\right\}\right] \qquad (2:117)$$

in which $m_L = \frac{\pi\rho c^2}{4}$ (see equation 2:028).

It is convenient to take moments about the elastic axis and to introduce $\bar{M}_e$ as the complex vector representing the external exciting moment. The dynamical equation for the moment becomes:

$$\sum M = 0 = \bar{M}_e + \bar{y}_e c \left[-4i\nu \frac{v}{c} m_L \bar{P}\epsilon - m_L \nu^2 (\tfrac{1}{4} - \epsilon) - m_F \nu^2 \sigma_F \right]$$

$$+ \bar{\varphi} c^2 \left[m_L \left\{ 4 \frac{v^2}{c^2} \bar{P}\epsilon + 4i\nu \frac{v}{c} \bar{P}(\tfrac{1}{2} - \epsilon)\epsilon - i\nu \frac{v}{c}(\tfrac{1}{2} - \epsilon) \right.\right.$$

$$\left.\left. + \frac{\nu^2}{32} + (\tfrac{1}{4} - \epsilon)^2 \nu^2 \right\} + m_F (i_F^2 + \sigma_F^2)\nu^2 - k\eta^2 \right] \quad (2{:}118)$$

Equations (2:117) and (2:118) can be simplified somewhat and reduced to a convenient form if the following parameters are introduced:

$$\mu = \frac{m_F}{m_L}$$

$$\nu_1^2 = \frac{k}{m_F}$$

whence:

$$\frac{\bar{F}}{m_F} = \bar{y}_e \left[\nu_1^2 + \frac{4i\nu v}{\mu c} \bar{P} - (1 + \tfrac{1}{\mu})\nu^2 \right]$$

$$+ \bar{\varphi} c \left[\left\{ \sigma_F + \tfrac{1}{\mu}(\tfrac{1}{4} - \epsilon) \right\} \nu^2 - \frac{4v^2 \bar{P}}{c^2 \mu} - \frac{4i\nu v}{\mu c} \bar{P}(\tfrac{1}{2} - \epsilon) - \frac{i\nu v}{\mu c} \right] \quad (2{:}119)$$

and

$$\frac{M_e}{c m_F} = \bar{y}_e \left[\left\{ \sigma_F + \tfrac{1}{\mu}(\tfrac{1}{4} - \epsilon) \right\} \nu^2 + \frac{4i\nu v}{\mu c} \bar{P}\epsilon \right]$$

$$+ \bar{\varphi} c \left[\eta^2 \nu_1^2 - (i_F^2 + \sigma_F^2)\nu^2 - \frac{\nu^2}{\mu} \left(\epsilon^2 - \frac{\epsilon}{2} + \frac{3}{32} \right) + \frac{i\nu v}{\mu c}(\tfrac{1}{2} - \epsilon) \right.$$

$$\left. + \frac{4i\nu v}{\mu c} \bar{P}(\epsilon^2 - \frac{\epsilon}{2}) - \frac{4v^2}{\mu c^2} \bar{P}\epsilon \right] \quad (2{:}120)$$

If the reduced velocity V is introduced, the equations can be put into a form with non-dimensional coefficients which is convenient for some cases:

$$V = \frac{v}{cv}$$

$$\frac{\bar{F}}{m_L v^2} = \bar{y}_e \left[\frac{\nu_1^2 \mu}{v^2} + 4iV\bar{P} - (1+\mu) \right]$$

$$+ \bar{c} \left[+\mu\sigma_F + \frac{1}{4} - \varepsilon - 4V^2\bar{P} - 4iV\bar{P}\left(\frac{1}{2} - \varepsilon\right) - iV \right] \qquad (2{:}121)$$

and

$$\frac{\bar{M}_e}{cm_L^2} = \bar{y}_e \left[+\mu\sigma_F + \frac{1}{4} - \varepsilon + 4iV\bar{P}\varepsilon \right]$$

$$+ \bar{c} \left[\frac{\eta^2 \nu_1^2 \mu}{v^2} - \left(\frac{1}{4} - \varepsilon\right)^2 - \frac{1}{32} - \mu(i_F^2 + \sigma_F^2) + iV\left(\frac{1}{2} - \varepsilon\right) \right.$$

$$\left. + 4iV\bar{P}\left(\varepsilon^2 - \frac{\varepsilon}{2}\right) - 4V^2\bar{P}\varepsilon \right] \qquad (2{:}122)$$

2:07. Method of Solution of Dynamical Equations

The general dynamical equations (2:119) and (2:120) for forced oscillations may be written as

$$\frac{\bar{F}}{m_F} = \bar{A}_{11}\bar{y} + \bar{A}_{12}\bar{\varphi}_c \tag{2:123}$$

$$\frac{\bar{M}}{cm_F} = \bar{A}_{21}\bar{y} + \bar{A}_{22}\bar{\varphi}_c \tag{2:124}$$

in which $\bar{A}_{11}$, $\bar{A}_{12}$, $\bar{A}_{21}$, and $\bar{A}_{22}$ are complex functions of the frequency of the oscillation ν and of the parameter $\frac{V}{c}$. These quantities, $\bar{A}_{11}$, $\bar{A}_{12}$, etc., are closely analogous to impedances that are found in the equations of electrical engineering, except that $\bar{A}_{12} \neq \bar{A}_{21}$, whereas in general the electrical cross impedances are equal, i.e., $Z_{12} = Z_{21}$.

The two equations above are linear equations in $\bar{y}_e$ and in $\bar{\varphi}_c$ and consequently can be solved by determinants in the usual way, making allowance for the fact that the constants are all complex.

$$\bar{y} = \frac{\begin{vmatrix} \frac{\bar{F}}{m_F} & \bar{A}_{12} \\ \frac{\bar{M}}{cm_F} & \bar{A}_{22} \end{vmatrix}}{\begin{vmatrix} \bar{A}_{11} & \bar{A}_{12} \\ \bar{A}_{21} & \bar{A}_{22} \end{vmatrix}} = \frac{\frac{\bar{F}}{m_F}\bar{A}_{22} - \frac{\bar{M}}{cm_F}\bar{A}_{12}}{\bar{A}_{11}\bar{A}_{22} - \bar{A}_{12}\bar{A}_{21}} \tag{2:125}$$

$$\bar{\varphi}c = \frac{\begin{vmatrix} A_{11} & \frac{\bar{F}}{m_F} \\ A_{21} & \frac{\bar{M}}{cm_F} \end{vmatrix}}{\begin{vmatrix} A_{11} & A_{12} \\ A_{12} & A_{22} \end{vmatrix}} = \frac{\frac{\bar{M}}{cm_F}\bar{A}_{11} - \frac{\bar{F}}{m_F}\bar{A}_{21}}{\bar{A}_{11}\bar{A}_{22} - \bar{A}_{21}\bar{A}_{12}} \qquad (2:126)$$

The denominator in the equations above, being the determinant of the coefficients, is often called the "stability determinant" in vibration problems because in general when this determinant vanishes, the values of $\bar{y}_e$ and $\bar{\varphi}c$ go to infinity. It is convenient to designate this determinant as $\bar{\Delta}$

$$\bar{\Delta} = \begin{vmatrix} \bar{A}_{11} & \bar{A}_{12} \\ \bar{A}_{21} & \bar{A}_{22} \end{vmatrix} \qquad (2:127)$$

Attention must be directed to the fact that $\bar{\Delta}$ is a complex quantity, so that for $\bar{\Delta} = 0$, both the real and imaginary parts must be zero.

Inasmuch as all the work involved in solving these equations deals with complex numbers, it is appropriate to summarize the methods used in performing the arithmetic operations of multiplication and division. Given two complex numbers, $\bar{z}_1$ and $\bar{z}_2$, defined as

$$\bar{z}_1 = a_1 + b_1 = r_1 e^{i\theta_1} \tag{2:128}$$

$$\bar{z}_2 = a_2 + ib_2 = r_2 e^{i\theta_2} \tag{2:129}$$

$$\bar{z}_1 \bar{z}_2 = (a_1 a_2 - b_1 b_2) + i(a_1 b_2 + a_2 b_1) \tag{2:130}$$

$$\frac{\bar{z}_1}{\bar{z}_2} = \left(\frac{r_1}{r_2}\right) e^{i(\theta_1 - \theta_2)} \tag{2:131}$$

in which:

$$r = \sqrt{a^2 + b^2}$$

$$\theta = \tan^{-1}\left(\frac{b}{a}\right)$$

Consider first the case where $\bar{F}$ has a definite value and $\bar{M} = 0$. Inasmuch as the vector $\bar{F}$ is a vector rotating in the complex field, with angular velocity ν, it is convenient to solve the equations at the instant of time when $\bar{F}$ lies along the positive real axis. Hence, it is convenient to let $\frac{F}{m_F} = +1$, whence, for $\bar{M} = 0$,

$$\left.\begin{aligned} \bar{y} &= \frac{\bar{A}_{22}}{\bar{\Delta}} \\ \bar{\varphi}_c &= \frac{-\bar{A}_{21}}{\bar{\Delta}} \end{aligned}\right\} \quad \text{for} \quad \frac{\bar{F}}{m_F} = 1, \quad \bar{M} = 0$$

The vector diagram can now be drawn to show the magnitude and phase relations between $\bar{y}$, $\bar{\varphi}$, and the exciting force $\bar{F}$.

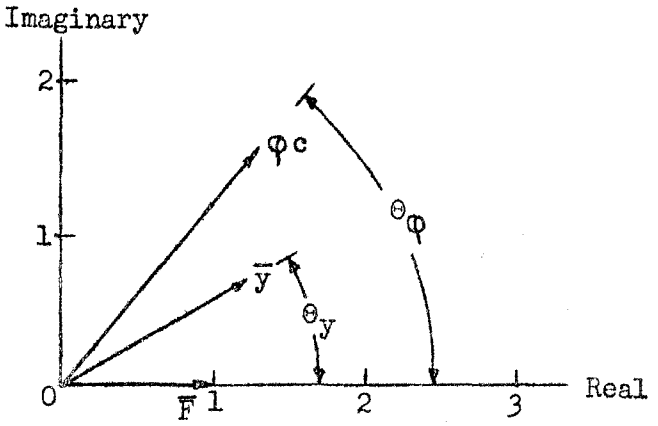

The maximum displacement of y is represented by the length of the vector $\bar{y}$. The phase angle Θ_y indicates that y reaches its maximum value at a phase Θ_y ahead of F.

The method when applied to moments is identical in procedure to that outlined above. The response due to the combination of a force and a moment is the sum of the individual responses, in which the complex nature of the responses is considered.

It was mentioned above that in general whenever $\bar{\Delta} = 0$, the responses become infinite. With the equations for flexural-torsional flutter as they appear here, there are four combinations of the frequency ν and the velocity-chord ratio $\frac{V}{c}$ such that $\bar{\Delta} = 0$, namely,

1. When $v = 0$, two frequencies exist, ν_b and ν_t, such that $\bar{\Delta} = 0$. These are called the "natural frequencies" at zero velocity.

2. When $\nu = 0$, there is a speed v_d such that $\bar{\Delta} = 0$. This is called the "divergence speed."

3. When $\nu = \nu_{cr.}$ and $v = v_{cr.}$, which have such a value that $\bar{\Delta} = 0$, the condition is termed "torsional-flexural flutter."

2:08. Critical Speed of Torsional Divergence

The critical speed of torsional divergence is easily obtained from equations (2:119) and (2:120), setting $\nu = 0$. For $\nu = 0$, $V = \infty$, $\bar{P} = 1$, the dynamical equations for forced oscillations become

$$\frac{\bar{F}}{m_F} = \bar{y}_e \left[\begin{matrix} \nu^2 \\ 1 \end{matrix} \right] + \bar{\varphi}_c \left[-\frac{4v^2}{\mu c^2} \right] \qquad (2:132)$$

$$\frac{\bar{M}_e}{cm_F} = \bar{y}_e \left[0 \right] + \bar{\varphi}_c \left[\eta^2 \nu_1^2 - \frac{4v^2}{\mu c^2} \varepsilon \right] \qquad (2:133)$$

Hence the torsional divergence speed occurs when

$$\eta^2 \nu_1^2 - \frac{4v^2}{\mu c^2} \varepsilon = 0 \qquad (2:134)$$

so that

$$v_{\text{divergence}} = \frac{\eta \nu_1 c}{2} \sqrt{\frac{\mu}{\varepsilon}} \qquad (2:135)$$

It should be noted that $\eta \nu_1$ is closely related to the torsional frequency at zero airspeed as given by equation (7:38) so that

$$v_d = \frac{\nu_t i_F c}{2} \sqrt{\frac{\mu}{\varepsilon}} \qquad (2:135a)$$

2:09. Normal Modes of Vibration at Zero Velocity

An important part of the present technique in vibration studies of airplanes is that of determining the natural frequencies of vibration on the ground at zero velocity. The technique is relatively straightforward and simple. Consequently it is enlightening to consider the dynamical equations developed in Section 2:06 with particular reference to the ground observations at zero airspeeds.

At v = 0, equations (2:119) and (2:120) become:

$$\frac{\bar{F}}{m_F} = \bar{y}_e \left[\nu_1^2 - (1 + \tfrac{1}{\mu})\nu^2 \right] + \bar{\varphi}c \left[\nu^2 \left\{ \sigma_F + \tfrac{1}{\mu}(\tfrac{1}{4} - \varepsilon) \right\} \right] \qquad (2:136)$$

$$\frac{\bar{M}e}{cm_F} = \bar{y}_e \left[\nu^2 \left\{ \sigma_F + \tfrac{1}{\mu}(\tfrac{1}{4} - \varepsilon) \right\} \right]$$

$$+ \bar{\varphi}c \left[\eta^2 \nu_1^2 - \nu^2 \left\{ i_F^2 + \sigma_F^2 + \tfrac{1}{\mu}(\varepsilon^2 - \tfrac{\varepsilon}{2} + \tfrac{3}{32}) \right\} \right] \qquad (2:137)$$

The normal modes and natural frequencies are obtained by setting the determinant of the above equations equal to zero and solving for the frequency ν.

$$\bar{\Delta} = 0 = \eta^2 \nu^4 - \nu_1^2 \nu^2 \left[\eta^2 (1 + \tfrac{1}{\mu}) + i_F^2 + \sigma_F^2 + \tfrac{1}{\mu}(\varepsilon^2 - \tfrac{\varepsilon}{2} + \tfrac{3}{32}) \right]$$

$$+ \nu^4 \left[(1 + \tfrac{1}{\mu}) \left\{ i_F^2 + \sigma_F^2 + \tfrac{1}{\mu}(\varepsilon^2 - \tfrac{\varepsilon}{2} + \tfrac{3}{32}) \right\} - \left\{ \sigma_F + \tfrac{1}{\mu}(\tfrac{1}{4} - \varepsilon) \right\}^2 \right]$$

(2:138)

This equation is of the form

$$a\nu^4 - b\nu^2 \nu_1^2 + \eta^2 \nu_1^4 = 0 \qquad (2:139)$$

so that

$$\nu^2 = \nu_1^2 \left[\frac{b \pm \sqrt{b^2 - 4a\eta^2}}{2a} \right] \qquad (2:140)$$

The above equations are somewhat meaningless because of the large number of parameters involved. It is therefore believed to be more appropriate to consider two specific examples, giving definite values to ε and σ_F and the other parameters as necessary.

Case A. $\varepsilon = 0.25$; $\sigma_F = 0$; $i_F^2 = 0.100$; $\eta = 1.00$; $\mu = 10.0$

This case represents the condition in which the elastic axis is located at the mid-chord point (i.e., 25% back of forward quarter-chord point) and the inertia axis coincides with the elastic axis. This case is unusual and not found in general practice, but it is significant in that it will be shown later that flexural-torsional flutter can occur even in this case without a coupling between the elastic and inertia forces.

The dynamical equations (2:136) and (2:137) become

$$\frac{\bar{F}}{m_F} = \bar{y}_e \left[\nu_1^2 - 1.10\nu^2 \right] + 0 \qquad (2:141$$

$$\frac{\bar{M}_e}{cm_F} = 0 + \bar{\varphi}_c \left[\nu_1^2 - 0.1030\nu^2 \right] \qquad (2:142$$

Obviously the determinant of the coefficient of $\bar{y}_e$ and $\bar{\varphi}_c$ vanishes when either

$$\nu = \frac{\nu_1}{\sqrt{1.10}} = 0.954\,\nu_1$$

or

$$\nu = \frac{\nu_1}{\sqrt{0.1031}} = 3.115\,\nu_1$$

Equations (2:141) and (2:142) are in such a form that the introduction of an exciting force $\bar{F}$ produces only a response in $\bar{y}_e$, and of a moment $\bar{M}_e$ only a response in $\bar{\varphi}_c$. Consequently, $\bar{y}_e$ and $\bar{\varphi}_c$ are the "normal coordinates" in this particular case and $\bar{F}$ and $\bar{M}/c$ are the corresponding "normal forces." However, in general it is not the case that $\bar{y}_e$ and $\bar{\varphi}_c$ are normal coordinates; it was because Case A was specifically chosen with $\varepsilon = 0.25$ and $\sigma_F = 0$ that this maintains. This statement can be generalized somewhat further, namely, that $\bar{y}_e$ and $\bar{\varphi}_c$ are normal coordinates only whenever:

$$\mu\sigma_F = \frac{1}{4} - \varepsilon \qquad (2:143)$$

Case B. $\varepsilon = 0.10;\ \sigma_F = 0.05;\ i_F^2 = 0.0625;\ \eta^2 = 0.50;\ \mu = 6.00$

This case has been chosen to be closely representative of the parameters of wings of present-day aircraft.

The dynamical equations (2:136) and (2:137) become

$$\frac{\bar{F}}{m_F} = \bar{y}_e \left[\nu_1^2 - 1.167\nu^2 \right] + \bar{\varphi}c \left[0.075\nu^2 \right] \qquad (2:144)$$

$$\frac{\bar{M}_e}{cm_F} = \bar{y}_e \left[0.075\nu^2 \right] + \bar{\varphi}c \left[0.50\,\nu_1^2 - 0.07363\nu^2 \right] \qquad (2:145)$$

Setting the determinant of the coefficients of $\bar{y}_e$ and $\bar{\varphi}c$ zero yields an equation in ν^2,

$$\Delta = 0.0803\nu^4 - 0.6569\nu^2\nu_1^2 + 0.50\nu_1^4 = 0 \qquad (2:146)$$

whence:

$$\nu^4 - 8.180\,\nu_1^2\nu^2 + 6.227\nu_1^4 = 0$$

$$\nu^2 = \nu_1^2 \left[4.090 \pm \sqrt{4.090^2 - 6.227} \right] = \nu_1^2 \left[4.090 \pm 3.240 \right]$$

The two values of ν fulfilling equation (2:146) are then

$$\nu^2 = 7.330\,\nu_1^2$$

and

$$\nu^2 = 0.850\,\nu_1^2$$

The normal coordinates are now obtained by substituting the values of ν above into equations (2:144) and (2:145), setting $\bar{F} = 0$ and $\bar{M} = 0$.

$\underline{\nu^2 = 7.330\,\nu_1^2}$ $\qquad (\nu = 2.71\,\nu_1)$

By (2:144) with $\bar{F} = 0$

$$\frac{\bar{y}_e}{\bar{\varphi}c} = -\frac{0.0750\nu^2}{\nu_1^2 - 1.167\nu^2} = +0.0728$$

By (2:145) with $\bar{M} = 0$

$$\frac{\bar{y}_e}{\bar{\varphi}c} = -\frac{0.50\,\nu_1^2 - 0.07363\nu^2}{0.0750\nu^2} = +0.0722$$

$$\text{Use } \frac{\bar{y}_e}{\bar{\varphi}c} = 0.072$$

Note, therefore, that vibrations in this mode are such that

$$y_e - 0.072\,\bar{\varphi}c = 0$$

so that the nodal point occurs at 7.2% of the chord aft of the elastic axis, i.e., the nodal point is at 42.2% chord.

$\underline{\nu^2 = 0.850\,\nu_1^2}$ $\qquad (\nu = 0.922\,\nu_1)$

By (2:144) with $\bar{F} = 0$

$$\frac{\bar{y}_e}{\bar{\varphi}c} = -\frac{0.0750\nu^2}{\nu_1^2 - 1.167\nu^2} = \text{(approx.)}\ -8$$

By (2:145) with $\bar{M} = 0$

$$\frac{\bar{y}_e}{\bar{\varphi}c} = -\frac{0.50\nu_1^2 - 0.0736\nu^2}{0.0750\nu^2} = -6.85 \quad \text{(Use)}$$

In vibrations in this mode, the nodal point is 6.5c ahead of the leading edge, (6.85c forward of the elastic axis), since:

$$\bar{y}_e + 6.85\bar{\varphi}c = 0$$

Therefore the normal coordinates for the configuration of Case B are, for zero velocity

$$\bar{y}_{.422c} = \bar{y}_e - 0.072\bar{\varphi}c \qquad \text{(Oscillates with natural frequency } \nu = 0.922\nu_1\text{)} \qquad (2:147)$$

and

$$\bar{y}_{-6.5c} = \bar{y}_e + 6.85\bar{\varphi}c \qquad \text{(Oscillates with natural frequency } \nu = 2.71\nu_1\text{)} \qquad (2:148)$$

To set up the equations in true normal coordinates, one should use the force and vertical displacement at the point 0.422c, and the force and vertical displacement at the point 6.5c ahead of the leading edge. If this set of coordinates is used, there would be no cross responses at any frequency at zero airspeed, i.e., a force at 0.422c would produce no displacement at -6.5c, and vice-versa. A force at 0.422c produces vibration in one normal mode, and a force at -6.5c in the other.

However, in observing vibration phenomena on the ground, it is easier to conceive of one mode of vibration as essentially vertical motion and the other as essentially angular. Therefore, although subsequent studies of forced vibrations for this case will be carried out using the forces to produce the normal modes, the responses will be determined for $\bar{y}_{.422c}$ and $\bar{\varphi}$. The advantage of using forces to produce normal modes is that each response curve at zero velocity has only one peak.

2:10. Responses in Steady State Forced Oscillations as Function of Airspeed

Von Schlippe[31] has shown that, for certain types of flutter, it is possible to determine the critical speed of flutter by observing the amplitudes and frequencies of forced oscillations in flight. Frazer and Jones[16] made a theoretical study of the method and concluded that "the critical speed for flutter cannot in general be estimated satisfactorily by von Schlippe's method unless some measurements of maximum forced amplitude corresponding to airspeeds close to the critical speed are included." Further objections were raised to carrying out forced oscillation tests in flight after the Junkers Ju 90 crashed, which crash was believed to have been caused by a failure in the electrical circuit controlling the eccentric vibrator, which permitted the vibrator to increase its speed indefinitely.

The work of this thesis indicates that it is unwise to attempt to produce forced oscillations in flight but that forced vibration tests in wind tunnels should provide an excellent method for determining aerodynamic forces.

It is the purpose of this section to determine, by direct computation, the variations of the responses with frequency and with airspeed in order to demonstrate certain fundamental characteristics of this type of flutter. It is expected that response curves of the type presented here should be of value in facilitating the interpretation of observations of amplitudes and frequencies of wing and tail

vibrations in flight without mechanical vibrators. It is believed that gusts are present in the air to produce momentarily forced oscillations at any frequency for which the wing has a susceptibility, so that flight test results should agree qualitatively with the results presented here.

The exciting forces applied will be those which produce normal modes at zero velocity, as was discussed in Section 2:09. The forced oscillations will be calculated for a number of airspeeds for the two cases A and B of Section 2:09.

Case A. $\varepsilon = 0.25;\ \sigma_F = 0;\ i_F^2 = 0.100;\ \eta = 1.00;\ \mu = 10.0$

The substitution of these quantities in equations (2:119) and (2:120) yields the following equations:

$$\frac{\bar{F}}{m_F} = \bar{y}_m \left[\nu_1^2 + 0.4i\nu \frac{V}{c} \bar{P} - 1.100\nu^2 \right] + \bar{\varphi}c \left[-0.1i\nu \frac{V}{c}(1 + \bar{P}) - 0.4 \frac{V^2}{c^2} \bar{P} - 0.1i\nu \frac{V}{c} \right] \qquad (2:149)$$

$$\frac{\bar{M}_m}{cm_F} = \bar{y}_m \left[+ 0.1i\nu \frac{V}{c} \bar{P} \right] + \bar{\varphi}c \left[\nu_1^2 + 0.025i\nu \frac{V}{c}(1 - \bar{P}) - 0.1 \frac{V^2}{c^2} \bar{P} - 0.1031\nu^2 \right] \qquad (2:150)$$

The subscript m as in $\bar{y}_m$ and $\bar{M}_m$ denotes the mid-chord point.

The two equations above are solved by the methods outlined in Section 2:07. A representative calculation for this case is given for $\frac{v}{c\nu_1} = 2.0$ in Appendix IV to show in detail the method followed. The results are plotted in Figures 14 to 30. In order to eliminate the effect of the magnitude of the force, all curves are plotted in terms of the static deflections which are designated by the subscript o.

Figures 14 and 15, which are presented first, show the responses and phases for the airfoil as a one degree of freedom system in the $\bar{y}$ coordinate with the torsional deflection prevented by restraint. The curves are characteristic of forced oscillations with damping, and show that at the critical flutter speed, $\frac{v}{c\nu_1} = 2.87$, the oscillation in this mode is almost critically damped. The frequency for maximum amplitude remains essentially constant at $\nu = 0.95\nu_1$.

Figures 16 and 17 show the corresponding curves for the response of $\bar{\varphi}$ to a moment in which the mid-chord point is prevented from moving by the addition of restraints. These curves show several features of note:

(a) The frequency of maximum amplitude decreases with airspeed. This is due directly to the fact that the second term of equation (2:150) contains the expression $(\nu_1^2 - 0.1\frac{v^2}{c^2}\bar{P})$, which is a determining factor in the frequency for maximum amplitude. It is significant that when this factor $(\nu_1^2 - 0.1\frac{v^2}{c^2}\bar{P}) = 0$ at $\nu = 0$; (i.e., $\bar{P} = 1.0$); torsional divergence occurs.

(b) The value of $\bar{\varphi}/\bar{\varphi}_o$ increases with airspeed at zero frequency and becomes infinite at divergence speed.

(c) The damping of the torsional oscillation by the air is much less than that of the vertical oscillation. This is believed to be an important and significant fact.

Figures 18 to 30 show the responses and phases for the coupled system with two degrees of freedom. It is significant to note in Figure 18 that the vibrations around $\nu/\nu_1 = 1$ are very highly damped and that at a frequency about $\nu/\nu_1 = 2.8$ a new hump has formed for the value of $v/c\nu_1 = 2.0$ which will increase at higher speeds to produce flutter. This is an indication that the original frequency in bending is of little significance in this type of flutter. Observations in flight intended to detect the incipient stages of flutter should be made at frequencies near the natural torsional frequency, but watching for increasing vertical amplitudes.

Figure 20 again shows the characteristics of the torsional oscillations (a) reduction of resonant frequency with airspeed, (b) the small amount of damping.

Figures 22 to 26 show the cross responses, which at zero airspeed are zero due to the fact that $\bar{y}$ and $\bar{\varphi}c$ are normal coordinates at zero airspeed. The response of $\bar{y}$ to a moment is much greater than that of $\bar{\varphi}c$ to a force.

In Figure 26 are replotted the curves for the restrained and coupled systems at $v/c\nu_1 = 2.0$ to show a particular point, namely, that the coupled system acts to increase the damping in vertical oscillations

at $\nu/\nu_1 = 1.0$, but to decrease the damping in torsion at $\nu/\nu_1 = 2.8$. Again this points to the significance of the torsional frequency and the relative unimportance of the bending frequency.

Figures 27 to 30 give the responses and phases of $\bar{y}$ to a motion of $\bar{\varphi}$, and vice-versa. These indicate what the $\bar{y}$ motion will be, for example, if the $\bar{\varphi}$ is given a steady state oscillation by any means. It is curious that the conditions for flutter instability are represented by points that are quite unspectacular in their positions. However, it is significant that at flutter the response of $\bar{y}$ to the motion of $\bar{\varphi}$ is the reciprocal of the response of $\bar{\varphi}$ to the motion of $\bar{y}$ and the phase angles are equal and opposite. This condition is only true at flutter.

In Figure 31 are plotted the values of the frequency for the maximum amplitude of response as a function of airspeed. The bending mode at a frequency in the neighborhood of $\nu = \nu_1$ is entirely damped out above $v/c\nu_1 = 2.0$. Above $v/c\nu_1 = 2.0$ the bending mode picks up a frequency which essentially coincides with that of the torsion. It is believed that these curves again point to the relative unimportance of the bending frequency in flexural-torsional flutter. Calculations by Theodorsen and Garrick[35] show that the critical frequency for flexural-torsional flutter usually is about two-thirds the natural torsional frequency at $v = 0$.

Case B. $\varepsilon = 0.10$; $\sigma_F = 0.05$; $i_F^2 = 0.0625$; $\eta^2 = 0.50$; $\mu = 6.00$; $\nu_1 = 10\pi$ rad./sec.; $c = 7.5$ ft.

The parameters chosen for this case are closely representative

of those which maintain for present day airplanes, as was noted in Section 2:09. The normal modes at zero velocity were found in Section 2:09 to be produced by (a) an oscillating vertical force at the 42.2% chord point, and (b) an oscillating vertical force at the point 6.5 chord lengths forward of the leading edge. It was also noted in Section 2:09 that the normal coordinates at zero velocity were the vertical displacements (a) of the 42.2% chord point, and (b) of the point 6.5 chord lengths forward of the leading edge. However, in this present section the responses shall be evaluated for (a) the vertical displacement of the 42.2% point, called $\bar{y}_{.422c}$, and (b) the angular displacement, $\bar{\varphi}$, because these coordinates have more tangible meaning in general.

The substitution of the parameters for this case into equations (2:119) and (2:120) yields:

$$\frac{\bar{F}}{m_F} = \bar{y}_e \left[987 + 0.667i\nu \frac{v}{c} \bar{P} - 1.167\nu^2 \right] + \bar{\varphi}c \left[-0.667 \frac{v^2}{c^2} \bar{P} - 0.2667i\nu \frac{v}{c} \bar{P} - 0.1667i\nu \frac{v}{c} + 0.075\nu^2 \right] \quad (2:151)$$

and

$$\frac{\bar{M}_e}{cm_F} = \bar{y}_e \left[0.075\nu^2 + 0.0667i\nu \frac{v}{c} \bar{P} \right] + \bar{\varphi}c \left[493 - 0.0667 \frac{v^2}{c^2} \bar{P} - 0.02667i\nu \frac{v}{c} \bar{P} + 0.0667i\nu \frac{v}{c} - 0.07363\nu^2 \right] \quad (2:152)$$

If the substitutions are now made that

$$\bar{y}_e = \bar{y}_{.422c} + 0.072\,\bar{\varphi}c$$

$$\frac{\bar{M}_{-6.5c}}{cm_F} = \frac{\bar{M}_e}{cm_F} - 6.85\,\frac{\bar{F}}{m_F}$$

$$\frac{\bar{M}_{.422c}}{cm_F} = \frac{\bar{M}_e}{cm_F} + 0.072\,\frac{\bar{F}}{m_F}$$

the equations become

$$\frac{\bar{F}}{m_F} = \bar{y}_{.422c}\left[987 + 0.667i\nu\frac{v}{c}\bar{P} - 1.167\nu^2\right]$$

$$+ \bar{\varphi}c\left[72 - 0.667\frac{v^2}{c^2}\bar{P} - 0.2187i\nu\frac{v}{c}\bar{P} - 0.1667i\nu\frac{v}{c} - 0.01\nu^2\right] \qquad (2{:}153)$$

$$\frac{\bar{M}_e}{cm_F} = \bar{y}_{.422c}\left[0.0667i\nu\frac{v}{c}\bar{P} + 0.075\nu^2\right]$$

$$+ \bar{\varphi}c\left[493 - 0.0667\frac{v^2}{c^2}\bar{P} - 0.0219i\nu\frac{v}{c}\bar{P} + 0.0667i\nu\frac{v}{c} - 0.06823\nu^2\right] \qquad (2{:}154)$$

$$\frac{\bar{M}_{-6.5c}}{cm_F} = \bar{y}_{.422c}\left[-6761 - 4.502i\nu\frac{v}{c}\bar{P} + 8.07\nu^2\right]$$

$$+ \bar{\varphi}c\left[+4.501\frac{v^2}{c^2}\bar{P} + 1.208i\nu\frac{v}{c} + 1.476i\nu\frac{v}{c}\bar{P}\right] \qquad (2{:}155)$$

$$\frac{\bar{M}_{.422c}}{cm_F} = \bar{y}_{.422c}\left[72 + 0.1147i\nu\frac{v}{c}\bar{P} - 0.010\nu^2\right]$$

$$+ \bar{\varphi}_c\left[498 - 0.1147\frac{v^2}{c^2}\bar{P} + 0.0547i\nu\frac{v}{c} - 0.0376i\nu\frac{v}{c}\bar{P} - 0.0690\nu^2\right] \qquad (2:156)$$

When a force $\bar{F}_{.422}$ is applied at the 42.2% chord point, it produces moments

$$\frac{\bar{M}_{-6.5c}}{cm_F} = -6.92\frac{\bar{F}_{.422c}}{m_F}$$

$$\bar{M}_{.422c} = 0 \cdot \bar{F}_{.422c}$$

When a force $\bar{F}_{-6.5c}$ is applied at the point 6.5 chord lengths forward of the leading edge, the following moments result:

$$\bar{M}_{-6.5c} = 0 \cdot \bar{F}_{-6.5c}$$

$$\frac{\bar{M}_{.422c}}{cm_F} = 6.92\frac{\bar{F}_{-6.5}}{m_F}$$

The dynamical equations can therefore be written in the following form, in which $\bar{F}_{.422c}$ indicates the application of a force at the 0.422c point and $\bar{M}_{.422c} = 0$:

$$\frac{\overline{F}_{.422c}}{m_F} = \overline{y}_{.422c}\left[+977 + 0.6501i\nu\frac{v}{c}\overline{P} - 1.166\nu^2\right]$$

$$+ \overline{\varphi}c\left[-0.650\frac{v^2}{c^2}\overline{P} - 0.2133i\nu\frac{v}{c}\overline{P} - 0.1745i\nu\frac{v}{c}\right] \qquad (2{:}157)$$

$$\frac{\overline{F}_{-6.5c}}{m_F} = \overline{y}_{.422c}\left[10 + 0.0166i\nu\frac{v}{c}\overline{P} - 0.0014\nu^2\right]$$

$$+ \overline{c}\left[72 - 0.0166\frac{v^2}{c^2}\overline{P} - 0.0054i\nu\frac{v}{c}\overline{P} + 0.0079i\nu\frac{v}{c}\right.$$

$$\left. - 0.00996\nu^2\right] \qquad (2{:}158)$$

Equations (2:157) and (2:158) are of the form

$$\frac{\overline{F}_{.422c}}{m_F} = \overline{A}_{11}\overline{y}_{.422c} + \overline{A}_{12}\overline{\varphi}c \qquad (2{:}159)$$

$$\frac{\overline{F}_{-6.5c}}{m_F} = \overline{A}_{21}\overline{y}_{.422c} + \overline{A}_{22}\overline{\varphi}c \qquad (2{:}160)$$

so that the responses are obtained by the determinants as explained in Section 2:07, viz.:

when $\frac{\overline{F}_{.422}}{m_F} = 1$; $\overline{F}_{-6.5c} = 0$

$$\overline{y} = \frac{\overline{A}_{22}}{\overline{\Delta}} \qquad (2{:}161)$$

$$\overline{\varphi}c = -\frac{\overline{A}_{21}}{\overline{\Delta}} \qquad (2{:}162)$$

when $\bar{F}_{.422c} = 0$; $\frac{F_{-6.5c}}{m_F} = 1$

$$\bar{y} = -\frac{\bar{A}_{12}}{\bar{\Delta}} \tag{2:163}$$

$$\bar{\varphi}_c = \frac{\bar{A}_{11}}{\bar{\Delta}} \tag{2:164}$$

when $\bar{y}_{.422c} = 0$ by restraint; $\frac{\bar{F}_{-6.5c}}{m_F} = 1$

$$\bar{\varphi}_c = \frac{1}{\bar{A}_{22}} \tag{2:165}$$

when $\bar{\varphi} = 0$ by restraint; total $\frac{\bar{F}}{m_F} = 1$; by equation (2:151)

$$\bar{y} = \frac{1}{(987 + 0.667i\frac{v}{c}P - 1.167v^2)} \tag{2:166}$$

The responses and phases for all the above are plotted in Figures 34 to 49*. For reference in studying the curves, note that

Critical Speed - Flexural-Torsional Flutter	549 ft./sec. (374 m.p.h.)
Critical Speed - Torsional Divergence	645 ft./sec. (440 m.p.h.)

Figures 34 and 35 for the one-degree-of-freedom cases exhibit many of the same characteristics as those discussed previously under Case A, namely,

---

*The author is indebted to Lt. Parish and Lt. Jackson[26] for their assistance in the preparation of these figures.

(a) Flexural oscillations have no change in resonant frequency with airspeed and are highly damped at airspeeds approaching that of flutter.

(b) Torsional oscillations have decrease of resonant frequency with airspeed and are less highly damped than the flexural oscillations.

The curves for the coupled system, Figures 36 to 49, are also similar to the corresponding curves for Case A and bear out the same conclusions that vibrations in the range of 30 rad./sec. are highly damped while those around 60 rad./sec. are not.

A curious phenomenon arises in this case, in which the exciting forces are not applied to correspond to the elastic forces. The torsional divergence for the coupled system occurs when the coefficient of $\bar{\varphi}_c$ in equation (2:152) equals zero at zero frequency. However, when $\bar{y}_{.422c} = 0$ by restraint, torsional divergence occurs when the coefficient of $\bar{\ }_c$ in equation (2:158) equals zero at zero frequency, which is at v = 494 ft./sec. (337 m.p.h.). Also, at this speed, which is lower than the critical flutter speed, the phase relation between $\bar{y}_{.422c}$ and $\bar{F}_{.422c}$ for the coupled system at zero frequency jumps 180° and indicates a form of instability. It may be noted in Figure 36 that at v = 332 m.p.h. the response of $\bar{y}_{.422c}$ is very small at zero frequency. At speeds higher than v = 337 m.p.h., the application of a force $\bar{F}_{.422c}$ in one direction requires for equilibrium a response $\bar{y}$ in the opposite.

Figure 50 shows for Case B the same general phenonema as were discussed above for Case A, namely, that the curve for the bending

frequency for maximum amplitude at low airspeeds has little or no relation to the frequency at flutter.

2:11. Determination of Critical Speed for Flexural-Torsional Flutter

It was mentioned above in Section 2:07 that the mathematical condition for flutter is that the determinant $\bar{\Delta}$ of the coefficients of the displacements in the dynamical equations equals zero. It is seen in equations (2:119) and (2:122) that for a given wing, in which ν_1, ε, σ_F, μ, η, and i_F are fixed quantities and known from the structure and weight distribution, the coefficients are functions only of ν, v/c, and $\bar{P}$, in which $\bar{P}$ is a function of $V = v/c\nu$. Consequently, the determinant $\bar{\Delta}$ is a function only of ν and v/c and the problem is essentially to find what combination of ν and v/c makes both the real and imaginary parts of $\bar{\Delta}$ equal zero simultaneously.

The most naive method for the solution of this problem is that presented by Theodorsen[34], which is applicable to any flutter problem with two or three degrees of freedom. In using this method, the dynamical equations may be put in the form of equations (2:121) and (2:122), in which ν and V may be considered the independent variables. It is significant that with the equations in this form the two variables have been separated in the coefficients so that the equations may be written:

$$\frac{\bar{F}}{m_L \nu^2} = \bar{y}_e \left[\frac{\nu_1^2}{\nu^2} + \bar{B}_{11}(V) \right] + \bar{\varphi} c \cdot \bar{B}_{12}(V) \qquad (2:167)$$

$$\frac{\bar{M}_e}{c m_L \nu^2} = \bar{y}_e \cdot \bar{B}_{21}(V) + \bar{\varphi} c \left[\frac{\eta^2 \nu_1^2}{\nu^2} + \bar{B}_{22}(V) \right] \qquad (2:163)$$

In the above equations, $\bar{B}_{11}$, $\bar{B}_{12}$, $\bar{B}_{21}$, and $\bar{B}_{22}$ are functions only of V.

Hence the determinant is

$$\bar{\Delta} = \frac{\eta^2 \nu_1^4 \mu^2}{\nu^4} + \left[\bar{B}_{22} + \eta^2 \bar{B}_{11} \right] \frac{\mu \nu_1^2}{\nu^2} + \left[\bar{B}_{11}\bar{B}_{22} - B_{12}B_{21} \right] \tag{2:169}$$

This determinant is a complex function which can be separated into its real and imaginary parts:

$$\bar{\Delta} = \Delta_R + i\Delta_I \tag{2:170}$$

in which:

$$\Delta_R = \frac{\eta^2 \nu_1^4 \mu^2}{\nu^4} + \mathrm{Re}\left[\bar{B}_{22} + \eta^2 \bar{B}_{11} \right] \frac{\mu \nu_1^2}{\nu^2} + \mathrm{Re}\left[\bar{B}_{11}\bar{B}_{22} - \bar{B}_{12}\bar{B}_{21} \right] \tag{2:171}$$

$$\Delta_I = \mathrm{Im}\left[\bar{B}_{22} + \eta^2 \bar{B}_{11} \right] \frac{\mu \nu_1^2}{\nu^2} + \mathrm{Im}\left[\bar{B}_{11}\bar{B}_{22} - \bar{B}_{12}\bar{B}_{21} \right] \tag{2:172}$$

in which:

Re [ ] means "real part of"

Im [ ] means "imaginary part of."

Setting Δ_R and Δ_I zero yields two equations in real variables only, namely,

for $\Delta_R = 0$

$$\frac{\nu^4}{\nu_1^4} + \frac{\nu^2}{\nu_1^2} \mu \frac{\mathrm{Re}\left[\bar{B}_{22} + \eta^2 \bar{B}_{11} \right]}{\mathrm{Re}\left[\bar{B}_{11}\bar{B}_{22} - \bar{B}_{12}\bar{B}_{21} \right]} + \frac{\mu \eta^2}{\mathrm{Re}\left[\bar{B}_{11}\bar{B}_{22} - \bar{B}_{12}\bar{B}_{21} \right]} = 0 \tag{2:173}$$

which is of the form

$$\frac{\nu^4}{\nu_1^4} + \frac{\nu^2}{\nu_1^2} E(V) + F(V) = 0 \qquad (2:174)$$

where E(V) and F(V) are real functions of V. Therefore, by assigning a range of values to V, a two-valued curve is obtained for ν^2 as a function of V.

For $\Delta_I = 0$

$$\frac{\nu^2}{\nu_1^2} + \mu \frac{\mathrm{Im}\left[\bar{B}_{22} + \eta^2 \bar{B}_{11}\right]}{\mathrm{Im}\left[\bar{B}_{11}\bar{B}_{22} - \bar{B}_{12}\bar{B}_{21}\right]} = 0 \qquad (2:175)$$

which is of the form

$$\frac{\nu^2}{\nu_1^2} + \mu G(V) = 0 \qquad (2:176)$$

in which G(V) is a real function of V. By assigning a range of values to V in this case, a single valued curve is obtained for ν^2 as a function of V.

The critical condition for flutter instability is given by the intersection of the curve defined by (2:174) for $\Delta_R = 0$ with that defined by (2:176) for $\Delta_I = 0$. This is illustrated in Figure 32 for Case A in which flutter occurs at $\nu/\nu_1 = 2.24$; $V = 1.28$; $v/c\nu_1 = 2.87$.

It is apparent that the principle outlined above is applicable to the solution of the determinant equation in general. There is,

however, for the particular case of flexural-torsional flutter another method of determining the values of ν and V such that the determinant is zero, which was developed by Kassner and Fingado[20].

Kassner and Fingado[20] start with dynamical equations using $\bar{y}_h$, the vertical displacement of the three-quarter chord point, the "hinterpunkt," as one coordinate inasmuch as the main lift force is a function of $\bar{\alpha}_h$. (See equation (2:098). Furthermore, since the only lift force containing $\bar{P}$ acts through the quarter-chord point, the moment equation is independent of $\bar{P}$ if moments are taken about the quarter-chord point.

Upon the substitution of

$$\bar{y}_e = \bar{y}_h + (\tfrac{1}{2} - \varepsilon)\bar{\varphi}c$$

and

$$\bar{M}_{.25c} = \bar{M}_e - \bar{F}\varepsilon c$$

equations (2:121) and (2:122) are transformed into

$$\frac{\bar{F}}{m_L\nu^2} = \bar{y}_h\left[-\mu(1 - \frac{\nu_1^2}{\nu^2}) - (1 - 4iV\bar{P})\right]$$

$$+ \bar{\varphi}c\left[-\mu(1 - \frac{\nu_1^2}{\nu^2})(\tfrac{1}{2} - \varepsilon) + \mu\sigma_F - \tfrac{1}{4} - iV(1 - 4iV\bar{P})\right] \qquad (2:177)$$

$$\frac{\bar{M}_{.25c}}{cm_L^2} = \bar{y}_h\left[\mu(1 - \frac{\nu_1^2}{\nu^2})\varepsilon + \mu\sigma_F + \tfrac{1}{4}\right]$$

$$+ \bar{\varphi}c\left[\mu\left\{(\frac{\nu_1^2}{\nu^2})(\eta^2 + \varepsilon^2 - \tfrac{\xi}{2}) - i_F^2 - (\varepsilon + \sigma_F)^2 + (\frac{\varepsilon + \sigma_F}{2})\right\} + \tfrac{1}{32} + \tfrac{iV}{2}\right]$$

(2:178)

In the equations in the form above the coefficients of $\bar{y}_h$ and $\bar{\phi}c$ are functions that are separated into two groups:

(a) functions of the dimensions, weight distribution, and frequency ratio ν_1^2/ν^2;

(b) functions of the reduced velocity V.

Kassner and Fingado[20] therefore propose the following parameters to represent the functions in group (a):

$$\mu' = \mu\left(1 - \frac{\nu_1^2}{\nu^2}\right) \tag{2:179}$$

$$z = \frac{\mu\left(1 - \frac{\nu_1^2}{\nu^2}\right)\varepsilon + \mu\sigma_F - \frac{1}{4}}{\mu\left(1 - \frac{\nu_1^2}{\nu^2}\right)} \tag{2:180}$$

$$w = \frac{\mu\left\{\left(\frac{\nu_1^2}{\nu^2}\right)\left(\eta^2 + \varepsilon^2 - \frac{\varepsilon}{2}\right) - i_F^2 - \left(\varepsilon + \sigma_F\right)^2 + \left(\frac{\varepsilon+\sigma_F}{2}\right)\right\} + \frac{1}{32}}{\mu\left(1 - \frac{\nu_1^2}{\nu^2}\right)} \tag{2:181}$$

With the substitution of the three parameters μ', z, w, into the dynamical equations (2:177) and (2:178), the equations become, changing the signs in the force equation,

$$-\frac{\bar{F}}{m_L\nu^2} = \bar{y}_h\left[\mu' + (1 - 4i\bar{V}\bar{P})\right] + \bar{\phi}c\left[\mu'\left(\tfrac{1}{2} - z\right) + iV(1 - 4i\bar{V}\bar{P})\right] \tag{2:182}$$

$$\frac{\bar{M}_{.25c}}{cm_L^2} = \bar{y}_h\left[\mu' z + \frac{1}{2}\right] + \bar{\phi}c\left[\mu' w + i\,\frac{V}{2}\right] \tag{2:183}$$

The determinant of the coefficients in (2:182) and (2:183) is therefore

$$\bar{\Delta} = \mu' \left[(1 - 4iV\bar{P})(w - iVz) + \mu'(w + z^2 - \frac{z}{2}) + \frac{z}{2} - \frac{1}{4} + \frac{iV}{2} \right] \qquad (2:184)$$

The complex lift vector factor $\bar{P}$ may be written as defined by equation (2:093)

$$\bar{P} = A - iB$$

where A and B are positive real quantities, functions only of V. The determinant may then be separated into its real and imaginary parts

$$\Delta_R = \mu' \left[w(1 - 4VB) - 4V^2Az + \mu'(w + z^2 - \frac{z}{2}) + \frac{z}{2} - \frac{1}{4} \right] \qquad (2:185)$$

$$\Delta_I = \mu' \left[- 4VAw - Vz(1 - 4VB) + \frac{V}{2} \right] \qquad (2:186)$$

The stability limit is defined mathematically by the condition that $\Delta_R = \Delta_I = 0$. Taken together, the two equations above define a curved surface in the μ', z, w space such that each point on the surface corresponds to a unique value of the reduced velocity V. The air velocity computed from this reduced velocity and frequency gives the critical speed of the wing.

It is necessary, then, to determine first for a particular design the values of the parameters μ', z, and w. It is to be noted that the parameters $1/\mu'$, z, and w can be expressed as lineal functions of the quantity $\left[\frac{1}{1 - \nu_1^2/\nu^2} \right]$. Hence, if everything except ν^2 is held

constant, $1/\mu'$, z, and w will lie on a straight line in the $1/\mu'$, z, w space. Two points on this line can be located by setting first $\nu = 0$ and then $\nu = \infty$. These points are designated A and B although it should be noted that there is no connection between points A and B and the values A and B of the complex vector $\bar{\bar{P}} = A - iB$. The coordinates of the points are tabulated below.

	2	$\frac{1}{\mu'}$	z	w
Point A	0	0	ε	$-\varepsilon^2 + \frac{\varepsilon}{2} - \eta^2$
Point B	∞	$\frac{1}{\mu}$	$\varepsilon + \sigma_F - \frac{1}{4\mu}$	$-(\varepsilon + \sigma_F)^2 + \frac{\varepsilon + \sigma_F}{2} - i_F^2 + \frac{1}{32\mu}$

Inasmuch as the points A and B lie on a straight line the value of $1/\mu'$ at any point C is given by

$$\left(\frac{1}{\mu'}\right)_C = \frac{\overrightarrow{AC}}{\overrightarrow{AB}} \left(\frac{1}{\mu}\right) \qquad (2:187)$$

The designation $\overrightarrow{AC}$ means the distance from A to C, considered vectorially. By plotting the horizontal projection of this line AC on the wz plane on which are also plotted contours corresponsing to constant values of μ' on the surface defined by (2:185) and (2:186), one can determine on the two-dimensional chart, Figure 51a, reproduced from Kassner and Fingado[20], the point C at which the line and surface

intersect in space such that

$$\mu' = \frac{\overrightarrow{AB}}{\overrightarrow{AC}} \mu \tag{2:188}$$

When the value of μ' is thus obtained, one can determine the frequency of oscillation by returning to the definition of μ', equation (2:179) from which

$$1 - \frac{\nu_1^2}{\nu^2} = \frac{\mu'}{\mu} = \frac{\overrightarrow{AB}}{\overrightarrow{AC}} \tag{2:189}$$

so that

$$\frac{\nu^2}{\nu_1^2} = \frac{\overrightarrow{AC}}{\overrightarrow{BC}} \tag{2:190}$$

The value of V for the point C is obtained from the set of supplementary curves, Figure 51b. Using this value of V and the frequency ν from equation (2:190), the critical velocity for flutter is given as

$$v = V\nu c \tag{2:191}$$

A detailed explanation of the procedure of using this method is given in Section 7:04, and in Figure 52 is given a representative use of Figure 51, in the Case B.

It is instructive to note the general difference in the two methods of attack, one using the dynamical equations (2:167) and (2:168) and the other the dynamical equations (2:182) and (2:183).

Both methods recognize the fact that each coefficient of $\bar{y}$ and $\bar{\varphi}$ can be separated into independent functions of ν and V, the two variables which remain after the parameters of the wing are given fixed values.

The first method combines the wing parameters with the functions of V to obtain $\bar{B}_{11}$, $\bar{B}_{12}$, $\bar{B}_{21}$, and $\bar{B}_{22}$, which then become complicated functions of the wing parameters and V but leave the function of ν extremely simple.

The second method combines the wing parameters with the functions of ν to obtain μ', z, and w, which are real functions that remain lineal in the quantity $\frac{1}{1 - \nu_1^2/\nu^2}$. The functions of V, which are complex and complicated, are independent of the wing parameters and thus may be plotted on a chart to use for all wings. The direct and naive attack by the second method would be to write equations (2:121) and (2:122) in the form below.

$$\frac{\bar{F}}{m_L \nu^2} = \bar{y}_e \left[C_{11}(\nu) + 4iV\bar{P} \right] + \bar{\varphi}c \left[C_{12} - iV\bar{Q}(V) + 4iV\bar{P}(\varepsilon - \tfrac{1}{2}) \right] \qquad (2:192)$$

$$\frac{M_e}{m_L \nu^2} = \bar{y}_e \left[C_{12} + 4iV\bar{P}\varepsilon \right] + \bar{\varphi}c \left[C_{22}(\nu) - iV\bar{Q}(V)\varepsilon + 4iV\bar{P}(\varepsilon^2 - \tfrac{\varepsilon}{2}) + \tfrac{iV}{2} \right] \qquad (2:193)$$

The functions $C_{11}(\nu)$ and $C_{22}(\nu)$ are real functions of the frequency and the wing parameters. The function C_{12} is a function only of the wing parameters, not of ν or V. The functions $\bar{P}$ and $\bar{Q}$ are complex

functions of V alone. $\bar{Q} = (1 - 4iV\bar{P})$.

The determinant of the coefficients of the above equations can be written

$$\bar{\Delta} = \begin{vmatrix} \left[C_{11} + 4iV\bar{P}\right] & \left[C_{12} - iV\bar{Q} + 4iV\bar{P}(\varepsilon - \frac{1}{2})\right] \\ \left[C_{12} + 4iV\bar{P}\varepsilon\right] & \left[C_{22} - iVQ\varepsilon + 4iV\bar{P}(\varepsilon - \frac{1}{2})\varepsilon + \frac{iV}{2}\right] \end{vmatrix} \qquad (2:194)$$

Multiplying the first rwo by ε and subtracting it from the second row does not change the value of the determinant, which becomes

$$\bar{\Delta} = \begin{vmatrix} \left[C_{11} + 4iV\bar{P}\right] & \left[C_{12} - iV\bar{Q} + 4iV\bar{P}(\varepsilon - \frac{1}{2})\right] \\ \left[C_{12} - C_{11}\varepsilon\right] & \left[C_{22} - C_{12}\varepsilon + \frac{iV}{2}\right] \end{vmatrix} \qquad (2:195)$$

Multiplying the first column by $(\varepsilon - \frac{1}{2})$ and subtracting it from the second does not change the value of the determinant, which becomes

$$\bar{\Delta} = \begin{vmatrix} \left[C_{11} + 1 - \bar{Q}\right] & \left[C_{12} + C_{11}(\frac{1}{2} - \varepsilon) - iV\bar{Q}\right] \\ \left[C_{12} - C_{11}\varepsilon\right] & \left[C_{22} + \frac{1}{2}C_{12} + C_{11}(\frac{\varepsilon^2 - \varepsilon}{2}) - \frac{iV}{2}\right] \end{vmatrix} \qquad (2:196)$$

Expanding:

$$\bar{\Delta} = i\bar{V}\bar{Q}\left[\frac{1}{2} - C_{12} + C_{11}\varepsilon\right] - \bar{Q}\left[C_{22} + \frac{1}{2}C_{12} + C_{11}\left(\frac{\varepsilon^2 - \varepsilon}{2}\right)\right] - iV\left[C_{11} + 1\right] + \begin{vmatrix} \left[C_{11} + 1\right] & \left[C_{12} + C_{11}\left(\frac{1}{2} - \varepsilon\right)\right] \\ \left[C_{12} - \varepsilon C_{11}\right] & \left[C_{22} + \frac{1}{2}C_{12} - C_{11}\left(\frac{\varepsilon^2 - \varepsilon}{2}\right)\right] \end{vmatrix} \qquad (2:197)$$

The Kassner-Fingado functions μ', z, and w are in such a form that the above equation for the determinant transforms to equation (2:184), which lends itself nicely to solution.

Figure 33 contains the polar diagrams in the complex plane for the equilibrium of forces and moments for Case A at the stability limit. At the stability limit y reaches its maximum value 35° ahead of φ and the magnitude of y is 0.505 times that of φc. The diagram of the equilibrium of forces shows that the elastic force, El(y) is relatively small in this case. The inertia force of the wing $In(\ddot{y})$ and the aerodynamic force due to angle $Ae(\varphi)$ are the largest forces. The largest moments come from the elastic moment $El(\varphi)$, the inertia moment, $In(\ddot{\varphi})$, and the aerodynamic moment due to φ, $Ae(\varphi)$. The apparent mass contribution to the moments $Ae(\ddot{\varphi})$ is negligible.

2:12. The Treatment of Structural Damping

In the previous sections, it has been assumed that the wing structure is purely elastic and that there is no structural damping. In the case of flexural-torsional flutter of metal wings, the structural damping is small. However, in cases where structural damping is important, it may be accounted for in a relatively simple manner. Several investigators have found that magnitude of the structural damping force is a function only of the displacement and not of the velocity, while the phase of the damping is the same as that of velocity. Inasmuch as the elastic force is also a function of displacement, the structural forces may be written in the form

$$\text{Elastic force} = -k\bar{y}$$

$$\text{Structural friction} = -ihk\bar{y}$$

or

$$\text{Total structural force} = -k\bar{y}(1 + ih)$$

The friction coefficient h is identical in notation and meaning with the "damping number" h used by Kassner[21], and with the coefficient g used by Theodorsen and Garrick[35]. The dynamical equations (2:119) and (2:122) will remain the same except for the substitution of $\nu_1^2(1 + ih_1)$ for ν_1^2 in the force equation, and of $\eta^2\ \nu_1^2(1 + ih_2)$ for $\eta^2\ \nu_1^2$ in the moment equation. The whole method of analysis is then the same as before. Kassner[21] has presented a graphical method for determining the stability limit for this case. However, the work involved in Kassner's method to account

for damping is more complicated than that in the Kassner-Fingado[20] method without damping. It is believed to be easier to calculate this case by the first method of Section 2:11 rather than by Kassner's inasmuch as the dynamical equation may be written:

$$\frac{F}{m_L \nu^2 (1 + ih_1)} = \bar{y}_e \left[\frac{\nu_1^2 \mu}{\nu^2} + \frac{\bar{B}_{11}(V)}{1 + ih_1} \right] + \bar{\varphi}c \cdot \frac{\bar{B}_{12}(V)}{1 + ih_1} \qquad (2:198)$$

$$\frac{M_e M_e}{cm_L \nu^2 (1 + ih_2)} = \bar{y}_e \cdot \frac{\bar{B}_{21}(V)}{1 + ih_2} + \bar{\varphi}c \left[\frac{\eta^2 \nu_1^2 \mu}{\nu^2} + \frac{\bar{B}_{22}(V)}{1 + ih_2} \right] \qquad (2:199)$$

Consequently, equations (2:167) through 2:176) will all apply in the case of structural damping if one

$$\text{replaces } \bar{B}_{11} \text{ by } \frac{\bar{B}_{11}}{1 + ih_1}$$

$$\text{replaces } \bar{B}_{12} \text{ by } \frac{\bar{B}_{12}}{1 + ih_1}$$

$$\text{replaces } \bar{B}_{21} \text{ by } \frac{\bar{B}_{21}}{1 + ih_2}$$

$$\text{replaces } \bar{B}_{22} \text{ by } \frac{\bar{B}_{22}}{1 + ih_2}$$

CHAPTER III. FLEXURAL-AILERON FLUTTER (TWO-DIMENSIONAL)

The aerodynamic forces and moments on a two-dimensional airfoil in a perfect fluid have been determined by both Theodorsen[34] and Küssner[23] for the case of steady state oscillations of the airfoil vertically combined with the aileron torsionally. In this chapter, the results of both of these investigators will be presented, converted to a common basis of notation which is consistent with that of Chapter II.

The dynamical equations will then be set up for the case of steady state forced oscillation which may be solved by the methods explained in Chapter II.

The complex vector notation which was explained in detail in Section 2:04, equations (2:078) to (2:083), will be continued throughout this chapter.

3:01. Aerodynamic Forces and Moments in Steady State Oscillations

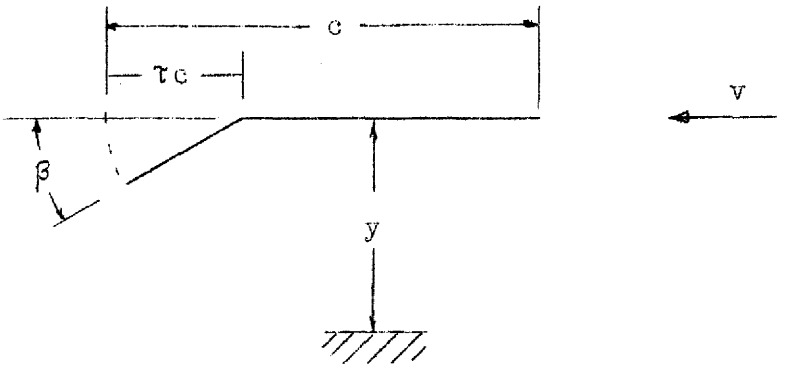

Making the substitutions noted in Appendix II into equation XVIII of Theodorsen[34], or equations (41) and (42) of Küssner[23], gives the following for the total aerodynamic forces per unit span:

$$\frac{\bar{L}}{m_L} = \bar{y}\left[-4i\nu\frac{v}{c}\bar{P} + \nu^2\right] + \bar{\beta}c\left[R_1\frac{v^2}{c^2}\bar{P} + i\nu\frac{v}{c}(R_2\bar{P} + R_3) - \nu^2 R_4\right] \qquad (3:01)$$

From equation XIX of Theodorsen[34], or equations (41) and (42) of Küssner[23], the total hinge moment due to air forces per unit span is

$$\frac{\bar{M}_{\beta air}}{cm_L} = \bar{y}\left[i\nu\frac{v}{c}R_8\bar{P} - R_4\nu^2\right] + \bar{\beta}c\left[-\frac{v^2}{c^2}\frac{R_1R_8}{4}\bar{P} - i\nu\frac{v}{c}\left\{\frac{R_2R_8}{4}\bar{P} + R_{11}\right\} - \frac{v^2}{c^2}R_{10} + R_{12}\nu^2\right] \qquad (2:02)$$

The factors R_1, R_2, R_2, etc., are functions only of the ratio of aileron chord to wing chord and are tabulated in Appendix III.

3:02. Dynamical Equations for Steady State Forced Oscillations

Notation:

m_F	mass of wing plus aileron per unit span
m_1	aileron mass per unit span
$\sigma_1 c$	distance from aileron c.g. to hinge line
$i_1 c$	radius of gyration of aileron about c.g.
$\eta_1^2 c^2 k$	torsional stiffness-aileron control.

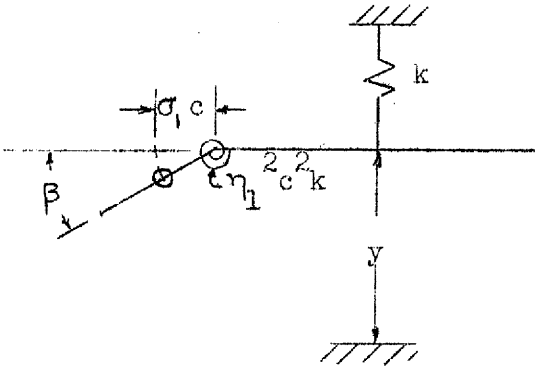

If $\bar{F}$ represents the vertical exciting force applied to the wing proper, and $\bar{M}_\beta$ the exciting moment applied to the aileron, the dynamical equations become

$$\sum F = 0 = \bar{F} + \bar{L} - k\bar{y} - \ddot{\bar{y}} m_F + m_1 \ddot{\bar{\beta}} \sigma_1 c \qquad (3:03)$$

and

$$\sum M_\beta = 0 = \bar{M}_\beta + \bar{M}_{\beta_{air}} - \eta_1^2 c^2 k\bar{\beta} + \ddot{\bar{y}} m_1 \sigma_1 c - \ddot{\bar{\beta}} m_1 (\sigma_1^2 + i_1^2) c^2 \qquad (3:04)$$

Putting in the values of $\bar{L}$ and $\bar{M}_{\beta_{air}}$ from equations (3:01) and (3:02) yields the following equations, with some rearrangement, noting that $\nu_1^2 = \frac{k}{m_F}$:

$$\frac{\bar{F}}{m_L \nu^2} = \bar{y}\left[\frac{\nu_1^2 \mu}{\nu^2} + 4i\bar{V}\bar{P} - (1+\mu)\right] + \bar{\beta}c\left[- R_1 V^2\bar{P} - R_3 iV - R_2 i\bar{V}\bar{P} + (\mu_1\sigma_1 + R_4)\right] \qquad (3:05)$$

$$\frac{\bar{M}_\beta}{cm_L \nu^2} = \bar{y}\left[- R_8 i\bar{V}\bar{P} + (\mu_1\sigma_1 + R_4)\right] + \bar{\beta}c\left[\frac{\eta_1^2 \nu_1^2 \mu}{\nu^2} + R_{10}V^2 + \frac{R_1 R_8}{4} V^2\bar{P} + R_{11} iV + \frac{R_2 R_8}{4} i\bar{V}\bar{P} - \left\{\mu_1(\sigma_1^2 + i_1^2) + R_{12}\right\}\right] \qquad (3:06)$$

3:03. Example of Flexural-Aileron Flutter

Case C-1. $\tau = 0.20$; $\mu = 10$; $\mu_1 = 1.0$; $\sigma_1 = 0.08$;
$i_1 = 0.06$; $\sigma_1^2 + i_1^2 = 0.010$; $\eta_1^2 = 0.001$.

This case has been chosen with parameters that are fairly representative of present day construction except that the aileron is not mass balanced. In terms familiar to engineering practice, the characteristics of the ailerons are as follows:

$\frac{\text{Aileron chord}}{\text{Wing chord}}$	=	0.20
$\frac{\text{Aileron weight per sq.ft.}}{\text{Wing weight per sq.ft.}}$	=	0.5
$\frac{\text{Aileron c.g. aft of hinge}}{\text{Aileron chord}}$	=	0.40
C_{db} (assuming rectangular aileron)	=	0.20
$\frac{\text{Aileron radius of gyration about c.g.}}{\text{Aileron chord}}$	=	0.30
$\frac{\text{Aileron natural frequency}}{\text{Wing natural frequency}}$	=	1.00 (in vacuum)

The dynamical equations are for this case:

$$\frac{\bar{F}}{m_L \nu^2} = \bar{y}\left[10\frac{\nu_1^2}{\nu^2} + 4iV\bar{P} - 11\right]$$

$$+ \bar{\beta}c\left[-2.199\,V^2\bar{P} - 0.1424\,iV - 0.2975\,iV\bar{P} + 0.09161\right] \qquad (3:07)$$

$$\frac{\bar{M}_\beta}{cm_L \nu^2} = \bar{y}\left[+ 0.09161 - 0.01272\, i\bar{V}\bar{P}\right] + \bar{\beta}c\left[0.01\frac{\nu_1^2}{\nu^2} + 0.01651\, V^2 + 0.00699\, V^2\bar{P} + 0.01059\, iV + 0.000946\, i\bar{V}\bar{P} - 0.01056\right] \quad (3:08)$$

The presence of the terms $(+ 0.01651\, V^2 + 0.00699\, V^2\bar{P})$ in the coefficient of $\bar{\beta}c$ in equation (3:08) shows that the natural frequency of the aileron increases with airspeed, whereas in Chapter II it was found that the natural frequency of the wing torsion decreased with airspeed.

The above equations may be written in the form:

$$\frac{\bar{F}}{m_L \nu^2} = \bar{y}\left[10\frac{\nu_1^2}{\nu^2} + \bar{B}_{11}(V)\right] + \bar{\beta}c \cdot \bar{B}_{13}(V) \quad (3:09)$$

$$\frac{\bar{M}_\beta}{cm_L \nu^2} = \bar{y} \cdot \bar{B}_{31}(V) + \bar{\beta}c\left[0.01\frac{\nu_1^2}{\nu^2} + \bar{B}_{33}(V)\right] \quad (3:10)$$

The procedure to calculate the critical speed for flutter is identical to that given in Section 2:11, equations (2:167) through (2:176). In Figure 53 are plotted the curves corresponding to $\Delta_R = 0$ and $\Delta_I = 0$. Instability for this case occurs between $\nu^2/\nu_1^2 = 1.135$; $V = 0.322$; $v/c\,\nu_1 = 0.343$ and $\nu^2/\nu_1^2 = 1.432$; $V = 1.063$; $v/c\,\nu_1 = 1.27$. It is noteworthy that this flutter instability occurs at a substantially lower speed than in Case A for flexural-torsional flutter in which $v/c\,\nu_1 = 2.87$.

Case C-2. (Parameters same as Case C-1 except $\eta_1 = 0$, i.e., no elastic support on aileron.)

In general, ailerons can oscillate in one of two ways, either symmetrically or anti-symmetrically. In the anti-symmetrical oscillations the elasticity of the control system does not enter and the aileron may be considered as having no elastic support.

Figure 54 gives a plot of the curves for $\Delta_R = 0$ and $\Delta_I = 0$ for this case. Flutter instability occurs between $\nu / \nu_1^2 = 0.955$; $V = 0.20$; $v/c\,\nu_1 = 0.196$ and $\nu / \nu_1^2 = 2.62$; $V = 1.66$; $v/c\,\nu_1 = 2.69$. The lower limit for flutter is lower for Case C-2 than for C-1, indicating that the more critical condition is that for anti-symmetrical flutter.

Figures 55 and 56 contain the polar diagrams in the complex plane for the equilibrium of forces and moments for Cases C-1 and C-2 at the lower stability limit. In Case C-1, the aileron angle $\bar{\beta}$ is approximately 90° ahead of $\bar{y}$ in phase and of considerably greater magnitude so that the vertical motion of the aileron trailing edge is eight times that of the main wing. In Case C-2, the aileron angle $\bar{\beta}$ is approximately in phase with $\bar{y}$ and of such magnitude that the mid-point of the aileron is essentially stationary.

In Case C-2, it seems of particular significance that the inertia moment of force due to $\ddot{\bar{\beta}}$ approximately equals that of $\ddot{\bar{y}}$. The moment of force due to $\ddot{\bar{\beta}}$ arises from the mass moment of inertia about the hinge line. The moment of force due to $\ddot{\bar{y}}$ arises from the mass unbalance of the aileron. A criterion of flutter of this type might be,

therefore, for the two-dimensional problem

$$\frac{\text{Mass eccentricity in per cent of chord}}{\text{Aileron radius of gyration in per cent of chord}} = \frac{\sigma_1}{\sqrt{i_1^2 + \sigma_1^2}}$$

This criterion can be approximated in the three-dimensional case for surfaces geometrically similar in shape by

$$\text{Ratio } \frac{\text{Product of Inertia}}{\text{Moment of Inertia}}$$

This criterion has in fact been suggested by Smilg[32] who found it significant in considering the flutter of rudders.

CHAPTER IV. TORSIONAL-AILERON FLUTTER (TWO DIMENSIONAL)

4:01. Aerodynamic Forces and Moments due to Steady State Oscillations

Theodorsen[34] and Küssner[23] have derived independently these forces and moments based on the theory of airfoils in perfect fluids, and are in agreement on the results. It seems appropriate here only to present the results in a form consistent with the remainder of this thesis.

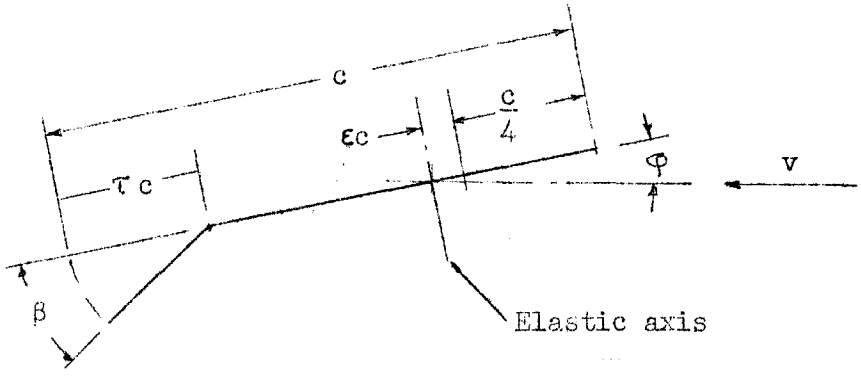

Making the substitution of the notation listed in Appendix II into equation XX of Theodorsen[34], or equations (41) and (42) of Küssner[23], the following moment about the wing elastic axis is obtained of all the air forces acting on the wing and aileron per unit span:

$$\frac{\bar{M}_{\varphi air}}{cm_L} = \bar{\varphi}c\left[i\nu\frac{v}{c}(\varepsilon - \tfrac{1}{2}) + \nu^2(\varepsilon^2 - \frac{\varepsilon}{2} + \frac{3}{32}) + 4\frac{v^2}{c^2}\bar{P} + 4i\nu\frac{v}{c}\bar{P}\varepsilon(\tfrac{1}{2} - \varepsilon)\right]$$

$$+ \bar{\beta}c\left[- R_5\frac{v^2}{c^2} - i\nu\frac{v}{c}(R_6 - R_3\varepsilon) + {}^2(R_7 + R_4\varepsilon)\right.$$

$$\left. + R_1\frac{v^2}{c^2}\bar{P}\varepsilon - R_2 i\nu\frac{v}{c}\bar{P}\varepsilon\right] \qquad (4:01)$$

From equation XIX of Theodorsen[34], or equations (41) and (42) of Küssner[23], the total hinge moment due to air forces per unit span is:

$$\frac{\bar{M}_{\beta air}}{cm_L} = \bar{\varphi}c\left[- R_8\frac{v^2}{c^2} - i\nu\frac{v}{c}\left\{ + R_9 + R_8\bar{P}(\tfrac{1}{2} - \varepsilon)\right\} + (R_7 + R_4\varepsilon)\nu^2\right]$$

$$+ \bar{\beta}c\left[- R_{10}\frac{v^2}{c^2} - i\nu\frac{v}{c}\left\{ R_{11} + (\frac{R_2R_8}{4})\bar{P}\right\} - \frac{R_1R_8}{4}\frac{v^2}{c^2}\bar{P} + R_{12}\nu^2\right]$$

(4:02)

The values of the R functions are given in Appendix III.

4:02. Dynamical Equations for Steady State Forced Oscillations

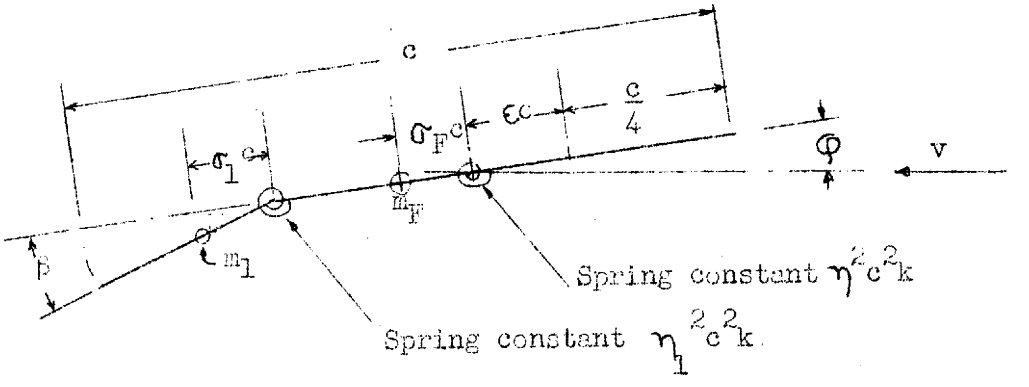

These equations can be set up easily by writing the expression for the potential and kinetic energy and applying Lagrange's Equation as explained in Byerly[4]. The result is in exact agreement, of course, with that which would be obtained from the accelerations and forces. Note that m_F and i_F apply to complete wing, including aileron.

The potential energy is

$$V = \frac{kc^2}{2}\left[\eta^2\varphi^2 + \eta_1^2\beta^2\right] \qquad (4:03)$$

The kinetic energy is

$$T = \frac{c^2}{2}\left[m_F(i_F^2 + \sigma_F^2) - m_1\left\{ i_1^2 + (\tfrac{3}{4} - \tau - \varepsilon + \sigma_1)^2\right\}\right]\dot{\varphi}^2$$

$$+ \frac{c^2}{2}\left[m_1\left\{ (\tfrac{3}{4} - \tau - \varepsilon + \sigma_1)\dot{\varphi} + \sigma_1\dot{\beta}\right\}^2 + m_1 i_1^2(\dot{\varphi} + \dot{\beta})^2\right] \qquad (4:04)$$

Or

$$T = \frac{c^2}{2}\left[m_F(i_T^2 + \sigma_F^2)\dot{\varphi}^2 + 2m_1 \left\{\sigma_1(\tfrac{3}{4} - \tau - \varepsilon + \sigma_1) + i_1^2 \right\}\dot{\varphi}\dot{\beta} \right.$$

$$\left. m_1(i_1^2 + \sigma_1^2)\dot{\beta}^2 \right] \qquad (4:05)$$

Lagrange's Equation is

$$\frac{d}{dt}\left[\frac{\partial(T-V)}{\partial \dot{q}_k}\right] + \frac{\partial V}{\partial q_k} = Q_k \equiv \text{external generalized force corresponding to } q_k \qquad (4:06)$$

The external generalized force corresponding to φ is the sum of the air force $\bar{M}_{\varphi_{air}}$ and the exciting force $\bar{M}_e$.

$$\frac{\partial T}{\partial \dot{\varphi}} = c^2 m_F(i_F^2 + \sigma_F^2)\dot{\varphi} + c^2 m_1 \left\{ i_1^2 + \sigma_1(\tfrac{3}{4} - \tau - \varepsilon + \sigma_1) \right\} \dot{\beta} \qquad (4:07)$$

$$\frac{\partial V}{\partial \varphi} = kc^2\eta^2\varphi \qquad (4:08)$$

whence

$$\frac{\bar{M}_e}{c^2 m_L} + \frac{\bar{M}_{\varphi_{air}}}{c^2 m_L} = \mu(i_F^2 + \sigma_F^2)\ddot{\bar{\varphi}} + \mu\, v_1^2 c^2 \eta^2 \bar{\varphi}$$

$$+ \mu_1 \left\{ i_1^2 + \sigma_1(\tfrac{3}{4} - \tau - \varepsilon + \sigma_1) \right\} \ddot{\bar{\beta}} \qquad (4:09)$$

The external generalized force corresponding to β is the sum of the air force $\bar{M}_{\beta_{air}}$ and the exciting force $\bar{M}_{\beta}$.

$$\frac{\partial T}{\partial \dot{\beta}} = c^2 m_1^2 \left[\left\{ i_1^2 + \sigma_1 \left(\frac{3}{4} - \tau - \varepsilon + \sigma_1 \right) \right\} \dot{\varphi} + \left(i_1^2 + \sigma_1^2 \right) \dot{\beta} \right] \tag{4:10}$$

$$\frac{\partial V}{\partial \beta} = k c^2 \eta_1^2 \beta \tag{4:11}$$

whence

$$\frac{\bar{M}_{\beta_{air}}}{c^2 m_L} + \frac{\bar{M}_{\beta}}{c^2 m_L} = \mu_1 \left[i_1^2 + \sigma_1 \left(\frac{3}{4} - \tau - \varepsilon + \sigma_1 \right) \ddot{\varphi} + i_1^2 \ddot{\beta} \right] + \mu \nu_1^2 c^2 \eta_1^2 \beta \tag{4:12}$$

Combining equations (4:01) and (4:02) with (4:09) and (4:12), at the same time writing $\dot{\bar{\varphi}} = i\nu\bar{\varphi}$, $\ddot{\bar{\varphi}} = -\nu^2\bar{\varphi}$, etc., the equilibrium equations for steady state forced oscillations become:

$$\frac{\bar{M}_e}{c m_L} = \bar{\varphi} c \left[\mu \nu_1^2 c^2 \eta^2 - 4 \frac{\nu^2}{c^2} \bar{P} \varepsilon + i\nu \frac{v}{c} \left(\frac{1}{2} - \varepsilon \right) - 4 i \nu \frac{v}{c} \bar{P} \varepsilon \left(\frac{1}{2} - \varepsilon \right) \right.$$

$$\left. - \nu^2 \left\{ \varepsilon^2 - \frac{\varepsilon}{2} + \frac{3}{32} + \mu \left(i_F^2 + \sigma_F^2 \right) \right\} \right]$$

$$+ \bar{\beta} c \left[-\nu^2 \mu_1 \left\{ i_1^2 + \sigma_1 \left(\frac{3}{4} - \tau - \varepsilon + \sigma_1 \right) \right\} - \nu^2 \left(R_7 + R_4 \varepsilon \right) \right.$$

$$\left. + \frac{\nu^2}{c^2} \left\{ R_5 - R_1 \bar{P} \varepsilon \right\} + i\nu \frac{v}{c} \left\{ R_6 - R_3 \varepsilon + R_2 \bar{P} \varepsilon \right\} \right] \tag{4:13}$$

$$\frac{\bar{M}_\beta}{cm_L} = \bar{\varphi}c\left[-\nu^2\mu_1\left\{i_1^2+\sigma_1\left(\frac{3}{4}-\tau-\varepsilon+\sigma_1\right)\right\}-\nu^2\left(R_7+R_4\varepsilon\right)\right.$$

$$\left.+R_8\frac{v^2}{c^2}\bar{P}+i\nu\frac{v}{c}\left\{R_9+R_8\bar{P}\left(\frac{1}{2}-\varepsilon\right)\right\}\right]$$

$$+\bar{\beta}c\left[\nu_1^2\eta_1^2\mu+R_{10}\frac{v^2}{c^2}+\frac{R_1R_8}{4}\frac{v^2}{c^2}\bar{P}+i\nu\frac{v}{c}\left\{R_{11}+\frac{R_2R_8}{4}\bar{P}\right\}\right.$$

$$\left.-\nu^2\left\{\mu_1\left(i_1^2+\sigma_1^2\right)+R_{12}\right\}\right] \qquad (4:14)$$

The solution of the above equations is carried out by the method explained in Section 2:07.

CHAPTER V. FLEXURAL-TORSIONAL-AILERON FLUTTER (TWO-DIMENSIONAL)

5:01. Dynamical Equation for Steady State Forced Oscillation

The dynamical equations for this mode of flutter with three degrees of freedom can be written by collecting suitable terms from the two-degrees-of-freedom cases, equations (2:119), (2:120), (3:05), (3:06), (4:13), (4:14), in which $\bar{F}$, $\bar{M}_e$, $\bar{M}_\beta$ are the external exciting forces and moments.

Force Equation:

$$\frac{\bar{F}}{m_L} = \bar{A}_{11}\bar{y}_e + \bar{A}_{12}\bar{\varphi}c + \bar{A}_{13}\bar{\beta}c \qquad (5:01)$$

Moment about elastic axis:

$$\frac{\bar{M}_e}{cm_L} = \bar{A}_{21}\bar{y}_e + \bar{A}_{22}\bar{\varphi}c + \bar{A}_{23}\bar{\beta}c \qquad (5:02)$$

Moment of aileron about hinge:

$$\frac{\bar{M}_\beta}{cm_L} = \bar{A}_{31}\bar{y}_e + \bar{A}_{32}\bar{\varphi}c + \bar{A}_{33}\bar{\beta}c \qquad (5:03)$$

The coefficients $\bar{A}_{11}$, $\bar{A}_{12}$, ... $\bar{A}_{33}$ are all complex in nature and are functions of ν and v/c, and of the elastic and weight distribution of the wing, as follows:

$$\bar{A}_{11} = \nu_1^2\mu + 4i\nu\frac{v}{c}\bar{P} - (1+\mu)\nu^2 \tag{5:04}$$

$$\bar{A}_{12} = \left\{\mu\sigma_F + \left(\frac{1}{4} - \varepsilon\right)\right\}\nu^2 - 4\frac{v^2}{c^2}\bar{P} - 4i\nu\frac{v}{c}\bar{P}\left(\frac{1}{2} - \varepsilon\right) - \frac{i\nu v}{c} \tag{5:05}$$

$$\bar{A}_{13} = (\sigma_1\mu_1 + R_4)\nu^2 - R_1\frac{v^2}{c^2}\bar{P} - i\nu\frac{v}{c}(R_2\bar{P} + R_3) \tag{5:06}$$

$$\bar{A}_{21} = \left\{\mu\sigma_F + \left(\frac{1}{4} - \varepsilon\right)\right\}\nu^2 + 4i\nu\frac{v}{c}\bar{P}\varepsilon \tag{5:07}$$

$$\bar{A}_{22} = \eta^2\nu_1^2\mu - \left\{\mu(i_F^2 + \sigma_F^2) + \varepsilon^2 - \frac{\xi}{2} + \frac{3}{32}\right\}\nu^2$$

$$+ i\nu\frac{v}{c}\left(\frac{1}{2} - \varepsilon\right) + 4i\nu\frac{v}{c}\bar{P}\left(\varepsilon^2 - \frac{\xi}{2}\right) - 4\frac{v^2}{c^2}\bar{P}\varepsilon \tag{5:08}$$

$$\bar{A}_{23} = -\nu^2\left[\mu_1\left\{i_1^2 + \sigma_1\left(\frac{3}{4} - \tau - \varepsilon + \sigma_1\right)\right\} + R_7 + R_4\varepsilon\right]$$

$$+ \frac{v^2}{c^2}(R_5 - R_1\bar{P}\varepsilon) + i\nu\frac{v}{c}(R_6 - R_3\varepsilon - R_2\bar{P}\varepsilon) \tag{5:09}$$

$$\bar{A}_{31} = (\sigma_1\mu_1 + R_4)\nu^2 - R_8 i\nu\frac{v}{c}\bar{P} \tag{5:10}$$

$$\bar{A}_{32} = -\nu^2\left[\mu_1\left\{i_1^2 + \sigma_1\left(\frac{3}{4} - \tau - \varepsilon + \sigma_1\right)\right\} + R_7 + R_4\varepsilon\right]$$

$$+ R_8\frac{v^2}{c^2}\bar{P} + i\nu\frac{v}{c}\left\{R_9 + R_8\bar{P}\left(\frac{1}{2} - \varepsilon\right)\right\} \tag{5:11}$$

$$\bar{A}_{33} = \eta_1^2\nu_1^2\mu + \frac{v^2}{c^2}\left(R_{10} + \frac{R_1R_8}{4}\bar{P}\right) + i\nu\frac{v}{c}\left\{R_{11} + \frac{R_2R_8}{4}\bar{P}\right\}$$

$$- \nu^2\left\{\mu_1(i_1^2 + \sigma_1^2) + R_{12}\right\} \tag{5:12}$$

The functions R_1, R_2, ... R_{12}, are functions only of the ratio of aileron chord to wing chord and are tabulated in Appendix III.

The dynamical equations in the above form are well suited to the calculation of responses under forced oscillations. However, if it is desired to determine only the critical flutter speed which is defined by the condition that the determinant of the coefficients vanishes, it is more convenient to use the equations in the form below.

Force Equation:

$$\frac{\bar{F}}{m_L \nu^2} = \left[\bar{B}_{11} + \frac{\nu_1^2 \mu}{\nu^2 + \mu}\right] \bar{y}_e + \bar{B}_{12}\bar{\varphi}c + \bar{B}_{13}\bar{\beta}c \qquad (5:13)$$

Moment about elastic axis:

$$\frac{\bar{M}_e}{cm_L \nu^2} = \bar{B}_{21}\bar{y}_e + \left[\bar{B}_{22} + \frac{\eta^2 \nu_1^2 \mu}{\nu^2}\right] \bar{\varphi}c + \bar{B}_{23}\bar{\beta}c \qquad (5:14)$$

Moment of aileron about hinge:

$$\frac{\bar{M}_\beta}{cm_L \nu^2} = \bar{B}_{31}\bar{y}_e + \bar{B}_{32}\bar{\varphi}c + \left[\bar{B}_{33} + \frac{\eta_1^2 \nu_1^2 \mu}{\nu^2}\right]\bar{\beta}c \qquad (5:15)$$

The coefficients $\bar{B}_{11}$, $\bar{B}_{12}$, ... $\bar{B}_{33}$ are functions only of the reduced velocity V and of the weight characteristics of the wing, as follows:

$$\bar{B}_{11} = -(1+\mu) + 4i\bar{V}\bar{P} \tag{5:16}$$

$$\bar{B}_{12} = \sigma_F\mu + (\tfrac{1}{4} - \varepsilon) - 4\bar{V}^2\bar{P} - 4i\bar{V}\bar{P}(\tfrac{1}{2} - \varepsilon) - i\bar{V} \tag{5:17}$$

$$\bar{B}_{13} = \sigma_1\mu_1 + R_4 - R_1\bar{V}^2\bar{P} - i\bar{V}(R_2\bar{P} + R_3) \tag{5:18}$$

$$\bar{B}_{21} = \sigma_F\mu + (\tfrac{1}{4} - \varepsilon) + 4i\bar{V}\bar{P}\varepsilon \tag{5:19}$$

$$\bar{B}_{22} = -\left\{\mu(i_F^2 + \quad_F^2) + \varepsilon^2 - \frac{\varepsilon}{2} + \frac{3}{32}\right\} + i\bar{V}(\tfrac{1}{2} - \varepsilon)$$

$$+ 4i\bar{V}\bar{P}(\varepsilon^2 - \frac{\varepsilon}{2}) - 4\bar{V}^2\bar{P}\varepsilon \tag{5:20}$$

$$\bar{B}_{23} = -\left[\mu_1\left\{i_1^2 + \sigma_1(\tfrac{3}{4} - \tau - \varepsilon + \sigma_1)\right\} + R_7 + R_4\varepsilon\right]$$

$$+ \bar{V}^2(R_5 - R_1\bar{P}\varepsilon) + i\bar{V}(R_6 - R_3\varepsilon - R_2\bar{P}\varepsilon) \tag{5:21}$$

$$\bar{B}_{31} = \sigma_1\mu_1 + R_4 - R_8 i\bar{V}\bar{P} \tag{5:22}$$

$$\bar{B}_{32} = -\left[\mu_1\left\{i_1^2 + \sigma_1(\tfrac{3}{4} - \tau - \varepsilon + \sigma_1)\right\} + R_7 + R_4\varepsilon\right]$$

$$+ R_8\bar{V}^2\bar{P} + i\bar{V}\left\{R_9 + R_8\bar{P}(\tfrac{1}{2} - \varepsilon)\right\} \tag{5:23}$$

$$\bar{B}_{33} = -\left\{\mu_1(i_1^2 + \sigma_1^2) + R_{12}\right\} + \bar{V}^2(R_{10} + \frac{R_1R_8}{4}\bar{P})$$

$$+ i\bar{V}(R_{11} + \frac{R_2R_8}{4}\bar{P}) \tag{5:24}$$

The determinant of the coefficients of y_e, $\bar{c}$, and $\bar{\beta}c$ in equations (4:13) to (4:15) is then

$$\bar{\Delta} = \left\{\frac{\nu_1^2 \mu}{\nu^2}\right\}^3 \left[\bar{\eta}^2 \eta_1^2\right]$$

$$+ \left\{\frac{\nu_1^2 \mu}{\nu^2}\right\}^2 \left[\bar{B}_{11}\eta^2 \eta_1^2 + \bar{B}_{22}\eta_1^2 + \bar{B}_{33}\eta^2\right]$$

$$+ \left\{\frac{\nu_1^2 \mu}{\nu^2}\right\} \left[\eta_1^2 \bar{B}_{11}\bar{B}_{22} + \bar{B}_{22}\bar{B}_{33} + \eta^2 \bar{B}_{33}\bar{B}_{11}\right.$$

$$\left. - \bar{B}_{23}\bar{B}_{32} - \eta_1^2 \bar{B}_{12}\bar{B}_{21} - \eta^2 \bar{B}_{13}\bar{B}_{33}\right]$$

$$+ \begin{vmatrix} \bar{B}_{11} & \bar{B}_{12} & \bar{B}_{13} \\ \bar{B}_{21} & \bar{B}_{22} & \bar{B}_{23} \\ \bar{B}_{31} & \bar{B}_{32} & \bar{B}_{33} \end{vmatrix} \qquad (5:25)$$

When this equation for $\bar{\Delta}$ is broken up into its real and imaginary parts, the real part will be a cubic equation in $(\nu_1^2 \mu/\nu^2)$ and the imaginary part a quadratic equation in $(\nu_1^2 \mu/\nu^2)$. Flutter occurs when the curves for $\Delta_R = 0$ cross those for $\Delta_I = 0$. The theory of the determination of the roots is straightforward although the calculations involved are tedious.

5:02. Aileron Reversal Speed

The speed at which there is reversal of aileron control can be determined from the dynamical equations derived in this section and in previous sections. The frequency is taken as zero for these calculations and $\bar{P} = 1$. For the condition of three degrees of freedom, without external exciting forces $\bar{F}$ or $\bar{M}_e$,

$$\frac{\bar{F}}{m_L} = 0 = \bar{y}_e \left[\mu\nu_1^2\right] + \bar{\varphi}c \left[-4\frac{v^2}{c^2}\right] + \bar{\beta}c \left[-R_1\frac{v^2}{c^2}\right] \qquad (5:26)$$

$$\frac{\bar{M}_e}{cm_L} = 0 = \bar{y}_e \cdot 0 + \bar{\varphi}c \left[\mu\nu_1^2\eta^2 - 4\frac{v^2}{c^2}\varepsilon\right] + \bar{\beta}c \left[\frac{v^2}{c^2}(R_5 - R_1\varepsilon)\right] \qquad (5:27)$$

(5:27)

$$\frac{\bar{M}_\beta}{cm_L} = \bar{y}_e \cdot 0 + \bar{\varphi}c \left[R_8\frac{v^2}{c^2}\right] + \bar{\beta}c \left[\mu\nu_1^2\eta_1^2 + \left\{R_{10} + \left(\frac{R_1R_8}{4}\right)\right\}\frac{v^2}{c^2}\right] \qquad (5:28)$$

By equation (5:27), if the aileron is given a definite displacement β, then the wing will twist to

$$\frac{\varphi}{\beta} = -\frac{\frac{v^2}{c^2}(R_5 - R_1\varepsilon)}{\mu\nu_1^2\eta^2 - 4\frac{v^2}{c^2}\varepsilon} = \frac{R_5 - R_1\varepsilon}{4\varepsilon - \frac{\mu\nu_1^2\eta^2c^2}{v^2}} \qquad (5:29)$$

Note that the divergence speed is defined by equation (2:135) as

$$v_d^2 = \frac{\eta^2 \nu_1^2 c^2 \mu}{4\varepsilon}$$

so that

$$\frac{}{\beta} = \frac{\frac{R_5}{\varepsilon} - R_1}{4(1 - \frac{v_d^2}{v^2})} \tag{5:30}$$

Substituting equation (5:30 into equation (5:26)

$$\frac{y_e}{\beta} = \left[\frac{\frac{R_5}{\varepsilon} - R_1}{1 - \frac{v_d^2}{v^2}} + R_1 \right] \frac{v^2}{c^2} \cdot \frac{1}{\mu \nu_1^2} \tag{5:31}$$

or

$$\frac{y_e}{\beta} = \left[\frac{\frac{R_5}{\varepsilon} - R_1 \frac{v_d^2}{v^2}}{1 - \frac{v_d^2}{v^2}} \right] \frac{v^2}{c^2} \quad \frac{1}{\mu \nu_1^2} \tag{5:32}$$

The critical speed of aileron reversal may be defined as that speed at which $y_e = 0$, or

$$v_r^2 = \frac{v_d^2 R_1 \varepsilon}{R_5} \tag{5:33}$$

or

$$v_r = \frac{\eta \nu_1 c}{2} \sqrt{\frac{R_1 \mu}{R_5}} \qquad (5:34)$$

It is interesting and significant that the reversal speed is independent of the position of the elastic axis.

CHAPTER VI. EXTENSION OF METHOD OF ANALYSIS TO THREE-DIMENSIONAL CASE OF FLEXURAL-TORSIONAL FLUTTER

The development of the stability criteria for the three-dimensional case will be carried out here in a manner similar to that for the two-dimensional case in Chapter II. Certain of the basic conceptions of the reports of Frazer and Duncan[14], Duncan and Collar[10], and Duncan and Lyon[11] will be used, but a distinct difference exists in the aerodynamic forces used in this thesis from those used by the above earlier investigators. In many respects, this section parallels the work of Theodorsen and Garrick[35].

It is believed by the author that the tail surfaces with the vertical surfaces at the tips of the horizontal are relatively susceptible to flutter in the flexural-torsional mode. Consequently this chapter will include the effects of the mass of the tip surface.

6:01. Dynamical Equations for Free Oscillations at Stability Limit

It is explicitly assumed in this section that at the stability limit the wing oscillates

(a) with a constant circular frequency ν in all portions;

(b) with constant amplitudes (i.e., no damping);

(c) with all portions of the wing in phase in bending along the elastic axis;

(d) with all portions of the wing in phase in torsion; but the phase for the bending and torsion may differ.

Under the above conditions, it is possible to choose two generalized coordinates

z_{e_t} = vertical displacement (upward of the elastic axis at the tip

φ_t = angular displacement of the tip section.

The complex vector notation will be used in the same manner as was done in Section 2:04 in which, for example, the actual displacement z_e at any instant is the real part of the complex quantity $\bar{z}_e$.

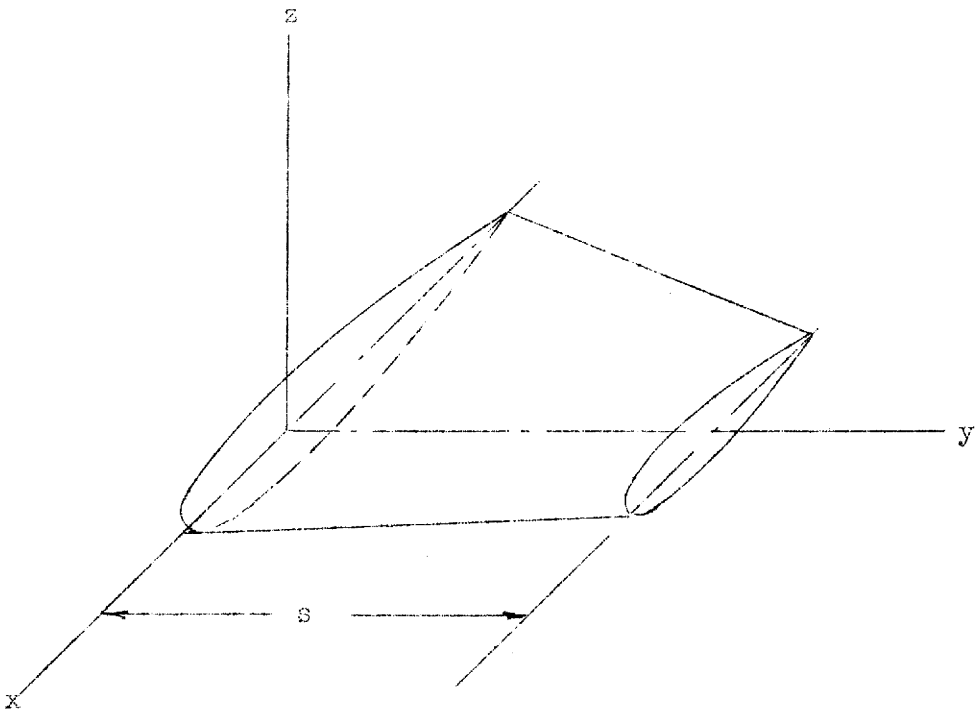

The spanwise distribution of deflection of the elastic axis is taken as

$$\overline{z}_e = \overline{z}_{e_t} f\left(\frac{y}{s}\right) \qquad (6:01)$$

and the variation of twist along the span as

$$\overline{\varphi} = \overline{\varphi}_t F\left(\frac{y}{s}\right) \qquad (6:02)$$

in which

s = semi span

It is assumed in this section that the aerodynamic forces per length of span of a wing are identical to those of the two-dimensional case. This is definitely an assumption, but its validity is essentially substantiated by recent work by Dr. William R. Sears (unpublished) on the wake effects in the three-dimensional oscillating wing. The total aerodynamic force per unit span is the following, from Section 2:05:

$$\frac{d\bar{L}}{dy} = \bar{z}_e \cdot \frac{\pi\rho c^2}{4}\left[\nu^2 - 4i\nu\frac{v}{c}\bar{P}\right]$$

$$+ \bar{\varphi}c \cdot \frac{\pi\rho c^2}{4}\left[-\nu^2\left(\frac{1}{4}-\varepsilon\right) + 4\frac{v^2}{c^2}\bar{P} + 4i\nu\frac{v}{c}\bar{P}\left(\frac{1}{2}-\varepsilon\right) + i\nu\frac{v}{c}\right] \qquad (6:03)$$

The total aerodynamic moment per unit span about the elastic axis is

$$\frac{d\bar{M}_{e_{air}}}{dy} = \bar{z}_e c \cdot \frac{\pi\rho c^2}{4}\left[-4i\nu\frac{v}{c}\bar{P}\varepsilon - {}^2\left(\frac{1}{4}-\varepsilon\right)\right]$$

$$+ \bar{\varphi}c^2 \cdot \frac{\pi\rho c^2}{4}\left[4\frac{v^2}{c^2}\bar{P}\varepsilon + 4i\nu\frac{v}{c}\bar{P}\left(\frac{1}{2}-\varepsilon\right)\varepsilon - i\nu\frac{v}{c}\left(\frac{1}{2}-\varepsilon\right)\right.$$

$$\left. + \frac{\nu^2}{32} + \left(\frac{1}{4}-\varepsilon\right)^2\nu^2\right] \qquad (6:04)$$

Inasmuch as it has been postulated that the oscillation is considered to be a steady state oscillation, it is possible to replace the lift and moment along the span by an equivalent lift and moment applied at the tip such that

$$\bar{L}_t \cdot \bar{z}_{e_t} = \int \bar{z}_e \left[\frac{d\bar{L}}{dy}\right] dy \qquad (6:05)$$

$$\bar{M}_{e_t} \cdot \bar{\varphi}_t = \int \bar{\varphi} \left[\frac{d\bar{M}_e}{dy}\right] dy \qquad (6:06)$$

The function $\bar{F}$ is rigorously a function of $v/c\nu$ at each point on the span. However, inasmuch as this function is a relative constant, it will be taken as a constant along the span and having a value corresponding to $v/c_o\nu$ at the effective chord.

In the substitution of equations (6:01) to (6:04) into (6:05) and (6:06), a number of integrals are involved which shall be defined as follows:

$$I_1 = \int \frac{c}{c_o} f^2 \frac{dy}{s} \qquad I_5 = \int \left(\frac{c}{c_o}\right)^3 fF \frac{dy}{s}$$

$$I_2 = \int \left(\frac{c}{c_o}\right)^2 f^2 \frac{dy}{s} \qquad I_6 = \int \left(\frac{c}{c_o}\right)^2 F^2 \frac{dy}{s}$$

$$I_3 = \int \frac{c}{c_o} fF \frac{dy}{s} \qquad I_7 = \int \left(\frac{c}{c_o}\right)^3 F^2 \frac{dy}{s}$$

$$I_4 = \int \left(\frac{c}{c_o}\right)^2 fF \frac{dy}{s} \qquad I_8 = \int \left(\frac{c}{c_o}\right)^4 F^2 \frac{dy}{s}$$

c_o may be taken as any reference chord. It is desirable to take it as the chord at the mid-point of the aileron, or at the 75% span station.

In taking care of the inertia and elastic forces, additional integrals arise

$$I_9 = \int m_F f^2 \frac{dy}{s}$$

$$I_{10} = \int (\frac{c}{c_o}) m_F \sigma_F f F \frac{dy}{s}$$

$$I_{11} = \int (\frac{c}{c_o})^2 m_F (\sigma_F^2 + i_F^2) F^2 \frac{dy}{s}$$

The effective tip forces due to inertia are then

$$\frac{\bar{F}_{t_{inertia}}}{s} = I_9 \nu^2 \bar{z}_{e_t} - I_{10} \nu^2 \bar{\varphi} c_o \qquad (6:07)$$

$$\frac{\bar{M}_{t_{inertia}}}{c_o s} = - I_{10} \nu^2 \bar{z}_{e_t} + I_{11} \nu^2 \bar{\varphi} c_o \qquad (6:08)$$

To account for the elastic forces rigorously it would be necessary to set up an integral expression in which the effective elastic force at the tip would be

$$\bar{F}_t \cdot \bar{z}_{e_t} = \int EI (\frac{d^4 \bar{z}_e}{dy^4}) \bar{z}_e dy \qquad (6:09)$$

and

$$\bar{M}_{e_t} \cdot \bar{\varphi}_t = \int GI_p \left(\frac{d^2\bar{\varphi}}{dy^2}\right) \bar{\varphi} dy \tag{6:10}$$

or

$$\frac{\bar{F}_{t_{elastic}}}{s} = \bar{z}_{e_t} \int \frac{EI}{s^4} \left[\frac{d^4 f}{d(\frac{y}{s})^4}\right] f \frac{dy}{s} \tag{6:11}$$

and

$$\frac{\bar{M}_{e_{t_{elastic}}}}{s} = \bar{\varphi}_t \int \frac{GI_p}{s^2} \left[\frac{d^2 F}{d(\frac{y}{s})^2}\right] F \frac{dy}{s} \tag{6:12}$$

However, if the assumption is made further that the functions f(y/s) and F(y/s) in the vibration at the critical speed are the same as at the normal modes without air forces present, a simplification is possible and the elastic forces may be written

$$\frac{\bar{F}_{elastic}}{s} = - I_9 \nu_1^2 \bar{z}_{e_t} \tag{6:13}$$

$$\frac{\bar{M}_{elastic}}{c_o s} = - I_{11} \nu_2^2 \bar{\varphi} c_o \tag{6:14}$$

in which:

ν_1 = frequency of primary bending mode (in vacuum)

ν_2 = frequency of primary torsional mode with elastic axis restrained (in vacuum)

With these assumptions the dynamical equations become:

Force Equation:

$$0 = \bar{z}_{e_t}\left[I_9(\nu^2 - \nu_1^2) + m_{L_o}\nu^2 \left\{ I_2 - 4i\nu\bar{P}I_1 \right\} \right]$$

$$+ \bar{\varphi}_t c_o \left[- I_{10}\nu^2 + m_{L_o}\nu^2 \left\{ - I_5(\tfrac{1}{4} - \varepsilon) + 4i\nu I_4 \left[\bar{P}(\tfrac{1}{2} - \varepsilon) + \tfrac{1}{4} \right] \right.\right.$$

$$\left.\left. + 4\nu^2\bar{P}I_3 \right\}\right] \qquad (6:13)$$

Moment Equation:

$$0 = \bar{z}_{e_t}\left[- I_{10}\nu^2 + m_{L_o}\nu^2 \left\{ - I_5(\tfrac{1}{4} - \varepsilon) - 4i\nu\bar{P}I_4\varepsilon \right\}\right]$$

$$+ \bar{\varphi} c_o \left[I_{11}(\nu^2 - \nu_2^2) + m_{L_o}\nu^2 \left\{ 4I_6\nu^2\bar{P}\varepsilon + 4i\nu I_7(\bar{P}\varepsilon - \tfrac{1}{4})(\tfrac{1}{2} - \varepsilon) \right.\right.$$

$$\left.\left. + I_8(\varepsilon^2 - \tfrac{\varepsilon}{2} + \tfrac{3}{32}) \right\}\right] \qquad (6:14)$$

The method of solution in the general case would involve the evaluation of all the integrals, I_1 to I_{11}, after which equations (6:13) and (6:14) could be solved by the general method outlined in Section 2:11.

6:02. Special Case - Constant Chord-Constant Weight per Unit Span-Concentrated Tip Weight

The integrals of the previous section simplify considerably under the assumption that c = const., and m_F = const., plus a concentrated mass at the tip M_v. In this section, the functions f(y/s) and F(y/s) are taken as

$$f(\frac{y}{s}) = \frac{3}{2}(\frac{y}{s})^2 - \frac{1}{2}(\frac{y}{s})^3 \tag{6:15}$$

which corresponds to the deflection curve of a uniform cantilever beam with a concentrated force at tip, and

$$F(\frac{y}{s}) = \frac{y}{s} \tag{6:16}$$

which corresponds to the angular deflection curve of a uniform rod with a concentrated moment at the tip. The integrals of Section 6:01 become

$$I_1 = I_2 = \int_{\xi=0}^{1} (\frac{3}{2}\xi^2 - \frac{\xi^3}{2})^2 \, d\xi$$

$$= \int_0^1 \frac{1}{4}(9\xi^4 - 6\xi^5 + \xi^6) \, d\xi$$

$$I_1 = I_2 = \frac{29}{120} = 0.242 \tag{6:17}$$

$$I_3 = I_4 = I_5 = \int_0^1 (3\xi^2 - \xi^3)\,\frac{\xi}{2}\,d = \frac{11}{40} = 0.275 \qquad (6:13)$$

$$I_6 = I_7 = I_8 = \int_0^1 \xi^2 d\xi = \frac{1}{3} = 0.333 \qquad (6:19)$$

$$I_9 = I_1 m_F + \frac{M_V}{s} \qquad (6:20)$$

$$I_{10} = I_3 m_F \sigma_F + \frac{M_V \sigma_V}{s} \qquad (6:21)$$

$$I_{11} = I_6 m_F (i_F^2 + \sigma_F^2) + \frac{M\,(i_V^2 + \sigma_V^2)}{s} \qquad (6:22)$$

in which:

M_V = total mass of vertical surface fastened to tip of wing

$\sigma_V c$ = distance of c.g. of vertical surface aft of elastic axis

$i_V c$ = radius of gyration of vertical surface about c.g. of surface.

An interesting result is obtained if the approximation is made that

$$I_1 = I_2 = I_3 = I_4 = I_5 = I_6 = I_7 = I_8 = 0.3 \qquad (6:23)$$

and the substitution is made into equations (6:13) and (6:14), multiplying the equations through by s/v^2 at the same time. The equations become:

Force Equation:

$$0 = \bar{z}_e \left[(0.3\, m_F s + M_V)\left(1 - \frac{\nu_1^2}{\nu^2}\right) + 0.3\, m_L s(1 - 4i\nu\bar{P}) \right]$$

$$+ \bar{\varphi}c \left[- (0.3\, m_F \sigma_F s + M_V \sigma_V) \right.$$

$$\left. + 0.3\, m_L s \left\{ - \left(\frac{1}{4} - \varepsilon\right) + 4\nu^2\bar{P} + 4i\nu\bar{P}\left(\frac{1}{2} - \varepsilon\right) + i\nu \right\} \right] \qquad (6:24)$$

Moment Equation:

$$0 = \bar{z}_e \left[- (0.3\, m_F \sigma_F s + M_V \sigma_V) + 0.3\, m_L s \left\{ - \left(\frac{1}{4} - \varepsilon\right) - 4i\nu\bar{P}\varepsilon \right\} \right]$$

$$+ \bar{\varphi}c \left[\left(1 - \frac{\nu_2^2}{\nu^2}\right) \left\{ 0.3\, m_F (i_F^2 + \sigma_F^2) s + M_V (i_V^2 + \sigma_V^2) \right\} \right.$$

$$\left. + 0.3\, m_L s \left\{ 4\nu^2\bar{P}\varepsilon + 4i\nu(\bar{P}\varepsilon - \frac{1}{4})\left(\frac{1}{2} - \varepsilon\right) + \varepsilon^2 - \frac{\varepsilon}{2} \quad \frac{3}{32} \right\} \right]$$

(6:25)

The following parameters will be used for the three-dimensional case, which are analogous to those of the two-dimensional case in Chapter II:

$$\mu = \frac{0.3\, m_F s + M_V}{0.3\, m_L s} \qquad (6:26)$$

$$\sigma_o = \frac{0.3\, m_F \sigma_F s + M_V \sigma_V}{0.3\, m_F s + M_V} \qquad (6:27)$$

$$i_o^2 + \sigma_o^2 = \frac{0.3\, m_F s(i_F^{\,2} + \sigma_F^{\,2}) + M_V(i_V^{\,2} + \sigma_V^{\,2})}{0.3\, m_F s + M_V} \tag{6:28}$$

$$\nu_2^2 = \frac{\eta^2 \nu_1^2}{(i_o^2 + \sigma_o^2)} \tag{6:29}$$

Equations (6:24) and (6:25) reduce to:

Force Equation:

$$0 = \bar{z}_e \left[-\frac{\nu_1^2}{\nu^2} - 4iV\bar{P} + (1+\mu) \right]$$

$$+ \bar{\varphi}c \left[-\mu\sigma_o - (\tfrac{1}{4} - \varepsilon) + 4V^2\bar{P} + 4iV\bar{P}(\tfrac{1}{2} - \varepsilon) + iV \right] \tag{6:30}$$

Moment Equation:

$$0 = \bar{\bar{z}}_e \left[-\mu\sigma_o - (\tfrac{1}{4} - \varepsilon) - 4iV\bar{P}\varepsilon \right]$$

$$+ \bar{\varphi}c \left[-\eta^2 \frac{\nu_1^2 \mu}{\nu^2} + \mu(i_o^2 + \sigma_o^2) + \varepsilon^2 - \frac{\varepsilon}{2} + \frac{3}{32} + 4V^2\bar{P}\varepsilon \right.$$

$$\left. + 4iV\bar{P}\varepsilon(\tfrac{1}{2} - \varepsilon) - iV(\tfrac{1}{2} - \varepsilon) \right] \tag{6:31}$$

It is seen that equations (6:30) and (6:31) are identical to (2:121) and (2:122) with signs changed and with $\bar{F} = \bar{\bar{M}} = 0$. Therefore, a good first approximation can be had for the critical flutter speed by using Kassner-Fingado[20] charts and the values of μ, σ_o, i_o, η as defined in (6:29), in which the wing mass is

taken as the mass of the outer 0.3 of the wing plus the vertical surface, and the air mass as the enclosing air mass around the outer 0.3 of the wing. This is in agreement with Theodorsen and Garrick[35] who indicate that, in general, the chord and section properties of the 3/4 span point may be used in estimating flutter speed.

CHAPTER VII. PROCEDURE FOR THE PRELIMINARY PREDICTION OF FLUTTER SPEEDS

7:01. Introduction

This chapter has been prepared to serve as a guide in the carrying out of calculations and tests to determine the critical flutter speeds of a typical transport airplane.

It is anticipated that the ailerons of the airplane will be mass balanced by elements to provide complete static balance. The elevators, with no leading edge aerodynamic balance, will be dynamically balanced by a weight moving inside the fin to the extent that the product of inertia is zero about the hinge line and centerline of the airplane. Each rudder will be dynamically balanced for the upper and lower portions independently to the extent that each portion will have the product of inertia zero about the hinge line and stabilizer chord plane. With the above procedures for static balance, the mass couplings of the movable control surfaces will be eliminated so that the possibilities of flutter are excluded in the modes of aileron-wing flexure, aileron-wing torsion, elevator-stabilizer flexure, elevator-stabilizer torsion, elevator-fuselage torsion, rudder-fin flexure, rudder-stabilizer flexure, rudder-fuselage torsion.

The modes of flutter which require special investigation are primarily wing flexure-torsion and stabilizer flexure-torsion. Further attention must also be given to the possible occurrence of rudder-fuselage side bending when the vibration characteristics have been

measured. This latter mode of vibration can be investigated by the methods of Chapter III.

The principal body of this chapter deals with the method of calculation of the flexural and torsional characteristics of the wings and tail to use in estimating the flexural-torsional flutter speeds by the method of Kassner-Fingado[20].

Statistical data published by Smilg[32] and Stitz[33], together with other data from several sources, are presented in Figures 57 to 66 of the measured vibration frequencies of a number of airplanes. It is anticipated that these data will afford a check of the characteristics of the new airplanes in comparison to the trend of design.

7:02. Method of Calculation of Primary Flexural Mode of Vibration of Wings and Tails

The rigorous solution of the problem of the vibration of a wing in flexure at zero airspeed involves the determination of a deflection curve of vibration such that at every point on the beam,

$$EI \frac{\partial^4 z}{\partial y^4} = - \frac{w}{g} \frac{\partial^2 z}{\partial t^2} \qquad (7:01)$$

in which:

E = Young's modulus of elasticity

I = moment of inertia of cross-sectional area

w = weight per unit span

g = acceleration of gravity

z = deflection (upward)

y = measure of distances along span

t = time

The solution of equation (7:01) explicitly is possible in general only by methods of successive approximation which are tedious and difficult. However, a method is available which lends itself nicely to solution of problems such as this, known as Rayleigh's Method. A complete discussion of this method is given by Den Hartog[7], (pages 167 to 182), and Timoshenko[36], (Chapter III). The essence of this method is the fact that the kinetic energy of the beam at the instant of zero deflection is equal to the potential energy of bending at the instant of maximum deflection to which must be added the assumption

that all points on the beam are vibrating at one frequency, and in phase. It should be noted that, when the true deflection curve for the normal mode is used, the above assumption is rigorously true. Rayleigh's contribution was the fact that the above assumption is approximately true for any reasonable form of the deflection curve.

Hence, expressing the deflection at any point along the span as

$$z = (z)_{max.} \cos \nu t \tag{7:02}$$

the velocity is

$$\frac{dz}{dt} = \dot{z} = -\nu(z)_{max.} \sin \nu t \tag{7:03}$$

in which:

$(z)_{max.}$ = the maximum deflection of any point,

ν = circular frequency of vibration, in rad./sec.

Hence, considering only maximum values irrespective of time,

$$(\dot{z})_{max.} = \nu(z)_{max.} \tag{7:04}$$

Inasmuch as Rayleigh's method is concerned only with the maximum values of $\dot{z}$ and z, henceforth the notation $\dot{z}$ and z is used without the designation "max." which is implied in all cases, it being noted further that the maximum values of $\dot{z}$ and of z do not occur at the same instant of time, but rather are displaced at 90^{o} in time to each other.

The total kinetic energy of the beam is

$$\text{Kin} = \frac{1}{2g} \int \dot{wz}^2 \, dy \qquad (7:05)$$

Or, using the relation of equation (7:04)

$$\text{Kin} = \frac{V^2}{2g} \int wz^2 \, dy \qquad (7:06)$$

The total potential energy of bending is,

$$\text{Pot} = \frac{1}{2} \int EI\left(\frac{d^2z}{dy^2}\right)^2 dy \qquad (7:07)$$

Equation these energies of equations (7:06) and (7:07), the frequency is given by

$$V^2 = g \frac{\int EI\left(\frac{d^2z}{dy^2}\right)^2 dy}{\int wz^2 \, dy} \qquad (7:08)$$

in which the integration is carried out along the span.

A reasonable assumption for the deflection curve is given by:

$$z = z_o \left[1 - \frac{4y}{3L} + \frac{1}{3}\left(\frac{y}{L}\right)^4 \right] \qquad (7:09)$$

in which:

y = distance from tip in feet

L = semi-span in feet (from root to tip).

Differentiation equation (7:09)

$$\frac{d^2z}{dy^2} = \frac{4z_o}{L^2}\left(\frac{y}{L}\right)^2 \qquad (7:10)$$

so that the circular frequency in radians per second is given by,

$$\nu_1^2 = \frac{16g}{L^2} \frac{\int EI\left(\frac{y}{L}\right)^4 dy}{\int w \left[1 - \frac{4y}{3L} + \frac{1}{3}\left(\frac{y}{L}\right)^4 \right]^2 dy} \qquad (7:11)$$

The evaluation of the integrals of equation (7:11) can be performed graphically by plotting and planimetering the curves

(a) $EI\left(\frac{y}{L}\right)^4$ as a function of y

and

(b) $w \left[1 - \frac{4y}{3L} + \frac{1}{3}\left(\frac{y}{L}\right)^4 \right]^2$ as a function of y.

It is believed that the evaluation of the above quantities at five stations along the wing will provide a frequency of reasonable accuracy.

In the case of a tail configuration with the vertical surfaces at the tips of the horizontal, a modification must be made to take into account the effects of vertical surfaces.

It is reasonable to use equation (7:09) as the deflection curve for the stabilizer and further to assume that the fin remains stiff during the vibration. The kinetic energy of the vertical surface is,

$$Kin_v = 2\,\frac{W_v}{g}\cdot\frac{z_o^2}{2} + \frac{V^2}{2g}\int w\left(\frac{dz}{dy}\right)_o^2 y'^2\,dy' \qquad (7:12)$$

or,

$$Kin_v = \frac{V^2 z_o^2}{2g}\left[W_v + \frac{16}{9L^2}\int wy'^2\,dy'\right] \qquad (7:13)$$

in which:

z_o = deflection of stabilizer tip

$\left(\frac{dz}{dy}\right)_o$ = slope of stabilizer at tip

W_v = total weight of fin and rudder

w = weight per unit height of fin and rudder

L = stabilizer semi-span

y' = vertical distance to station on fin from centerline stabilizer.

The bending frequency of the tail is then given by,

$$\nu_1^2 = \frac{\frac{16g}{L^2}\int_{\text{Stab.}} EI\left(\frac{y}{L}\right)^4 dy}{\int_{\text{Stab.}} w\left[1 - \frac{4y}{3L} + \frac{1}{3}\left(\frac{y}{L}\right)^4\right]^2 dy + W_v + \frac{16}{9L^2}\int_{\text{Fin}} w\, y'^2\, dy'} \qquad (7:14)$$

The integrals can be evaluated by planimetering the areas under the following curves:

(a) $EI\left(\frac{y}{L}\right)^4$ for stabilizer as a function of y, the distance from stabilizer tip.

(b) $w\left[1 - \frac{4y}{L} \quad \frac{1}{3}\left(\frac{y}{L}\right)^4\right]^2$ for stabilizer as a function of y.

(c) wy'^2 for fin as a function of y', the vertical distance from stabilizer centerline.

It is believed that the evaluation of functions (a) and (b) at four stations on the stabilizer and of function (c) at three stations on the fin is satisfactory. The weight of the elevator should be included in the running weight w of the horizontal tail. The weight of the rudder should be similarly included in the vertical tail. The weight of the elevator dynamic balance should be included in the weight of the vertical tail W_v.

The frequencies calculated here are the frequencies that would be observed vibrating the wing or tail in a vacuum. The bending frequency

that would be observed in practice would be

$$\nu_{\text{bending}} = \frac{\nu_1}{\sqrt{1 + \frac{1}{\mu}}}$$

The value of μ ranges from 5 to 10 so that the bending frequency is generally 5% to 10% lower than ν_1.

7:03. Method of Calculation of Primary Torsional Mode of Wing or Tail

These calculations can best be made using Rayleigh's Method which was described in principle in Section 7:02.

It has been found that the normal torsional mode of vibration of a wing is such that the inertia axis of the wing is also the nodal axis (see Theodorsen and Garrick[35]). It is therefore necessary to determine first the inertia axis along the span at several points and then to choose a nodal axis which is straight and coincides with the average of the inertia axis.

The kinetic energy is,

$$\text{Kin} = \frac{1}{2g} \int w(\dot{\varphi})^2 \, i_F{}^2 c^2 \, dy \qquad (7:15)$$

in which:

$\dot{\varphi} = \frac{d\varphi}{dt}$

φ = angular displacement at any station along span

w = weight per unit span

i_F = radius of gyration of wing mass about nodal axis in fraction of chord

c = wing chord

y = distance from wing tip

g = acceleration of gravity.

In a manner analogous to that of equation (7:04) one can write,

$$\dot{\varphi} = \nu \varphi \tag{7:16}$$

so that

$$\text{Kin} = \frac{\nu^2}{2g} \int w \varphi^2 i_F^2 c^2 \, dy \tag{7:17}$$

To obtain the potential energy it is necessary to use the equation for the twist of a sheet metal shell, namely,

$$\frac{d\varphi}{dy} = \frac{QP}{4A^2 tG} \tag{7:18}$$

in which:

Q = torque

P = perimeter

A = enclosed area of shell

t = thickness of shell

G = shear modulus of elasticity

In cases where the sheet thickness is not constant around the perimeter, the value of P/t should be obtained by,

$$\frac{P}{t} = \frac{P_1}{t_1} + \frac{P_2}{t_2} + \frac{P_3}{t_3} + \ldots + \frac{P_n}{t_n} \tag{7:19}$$

in which P_n is the amount of the perimeter which corresponds to t_n.

The element of potential energy due to an element of span dy is,

$$d\ Pot = \frac{1}{2} Q \frac{d\varphi}{dy} dy \tag{7:20}$$

whence,

$$Pot = \frac{1}{2} \int Q \frac{d\varphi}{dy} dy \tag{7:21}$$

Eliminating Q from equation (7:21) by using (7:18), there results

$$Pot = \frac{1}{2} \int (\frac{d\varphi}{dy})^2 \frac{4A^2G}{P/t} dy \tag{7:22}$$

Equating (7:22) to (7:17), gives an expression which determines the frequency,

$$\nu^2 = g \frac{\int (\frac{d\varphi}{dy})^2 \frac{4A^2G}{P/t} dy}{\int w\varphi^2 i_P{}^2 c^2 dy} \tag{7:23}$$

A reasonable equation for the torsional deflection under vibrations is,

$$\varphi = \varphi_o (\frac{L-y}{L}) \tag{7:24}$$

in which:

y = distance from wing tip

L = semi-span from root to tip.

Substituting equation (7:24) in (7:23) gives,

$$V_2^2 = g \frac{\int \frac{4A^2G}{P/t}\,dy}{\int w(L-y)^2 i_F{}^2 c^2 dy} \qquad (7:25)$$

The integrals of equation (7:25) can be evaluated by planimetering the area under the curves of,

(a) $\frac{4A^2G}{P/t}$ plotted as a function of y

(b) $w(L-y)^2 i_F{}^2 c^2$ plotted as a function of y.

In the case of a tail configuration with the vertical surfaces at the tips of the horizontal the calculations can be made in a manner identical to that above, modified for the effect of the vertical surfaces. Equation (7:25) then becomes:

$$V_2^2 = g \frac{\int \frac{4A^2G}{P/t}\,dy}{\left[\int w(L-y)^2 i_F{}^2 c^2 dy\right] + \left[W_v i_v{}^2 c^2 L^2\right]} \qquad (7:26)$$

in which the integrals are evaluated along the stabilizer only and,

W_v = total weight of fin and rudder

$(i_v c)$ = radius of gyration of fin and rudder about the nodal axis of the stabilizer

L = semi-span of stabilizer (from root to tip).

The nodal axis of the stabilizer at the root may be taken to pass through the center of gravity of the root section. The nodal axis at the tip should be taken through the center of gravity of the combined weights of the vertical tail surface and of the outer 30% of the horizontal tail.

In calculating the inertia axis (c.g.) of the horizontal tail the weight of the elevator should be assumed to be distributed along the elevator hinge line. The weight of the elevator dynamic balance at the end of the elevator should be included in the weight of the fin and should be assumed to be concentrated at the elevator hinge line for all calculation.

In calculating the radius of gyration of the mass of the horizontal tail, the mass of the elements of the elevator should be taken in their true chordwise positions.

7:04. Method of Calculation of Critical Speed of Torsional-Flexural Flutter

The method recommended for this calculation is that developed by Kassner and Fingado[20]. The parameters needed for this investigation are:

ν_1 = primary flexural frequency obtained in Section 7:02. (rad./sec.).

ν_2 = primary torsional frequency obtained in Section 7:03 (rad./sec.).

The following characteristics of the wing are needed for the station at 75% of the distance from the centerline of the airplane to the tip:

c = wing chord (ft.)

εc = distance of elastic axis back of 25% point (ft.)

$\sigma_F c$ = distance of inertia axis back of elastic axis (ft.)

$i_F c$ = radius of gyration of mass of wing about inertia axis (ft.)

w = wing weight per unit span (lb./ft.)

From the above parameters, the following additional parameters can be calculated:

$$\mu = \frac{m_F}{m_L} = \frac{\frac{W}{g}}{\pi \frac{\rho c^2}{4}}$$

$$\mu = \frac{W}{c^2} \cdot \frac{4}{\pi \; 0.002378 \cdot 32.2}$$

$$\mu = 16.641 \frac{W}{c^2} \text{ (at sea level)} \qquad (7:27)$$

$$\mu = 16.641 \frac{W}{c^2} \frac{1}{\frac{\rho}{\rho_o}} \text{ (at altitude)} \qquad (7:27a)$$

in which:

$\frac{\rho}{\rho_o}$ = density ratio

Further, the "elastic radius of gyration" is determined by the relation:

$$\eta = \frac{\nu_2}{\nu_1} i_F \qquad (7:28)$$

The critical speed can now be determined, using Figure 51. A typical determination is illustrated in Figure 52.

Point A is located by going vertically a distance ε on the parabolic curve, and measuring horizontally from this point a distance η^2 to the left. In many cases, it will be found that the point A lies off the sheet a substantial distance but this has no adverse effect.

Point (B) is located in a manner similar to that for A, by going vertically a distance $(\varepsilon + \sigma_F)$ to the parabola and then to the left a distance $i_F{}^2$.

Point B is located from point (B) by drawing a line through (B) parallel to the sloping line designated at the ends P_h and P_m.

$$\overrightarrow{(B)B} = \frac{1}{\mu} \overrightarrow{P_h P_m} \tag{7:29}$$

A line is now drawn through points A and B and extended to the right. The point C is located in the figure on the right by successive approximations such that the value of μ' corresponding to the point C is equal to,

$$\mu' = \mu \frac{\overrightarrow{AB}}{\overrightarrow{AC}} \tag{7:30}$$

By $\overrightarrow{AB}$ is meant the distance from A to B, and by $\overrightarrow{AC}$ the distance from A to C. It should be noted that $\overrightarrow{AB}$ and $\overrightarrow{AC}$ have vector characteristics so that the ratio becomes negative whenever $\overrightarrow{AB}$ is in the direction opposite to $\overrightarrow{AC}$.

Point (C) is located in the figure on the left by going horizontally from point C to the curve having the value of μ' calculated by equation (7:30). The value of the "reduced velocity" V is obtained from the point (C) by the construction shown.

The frequency of the vibration at the critical speed is obtained from the ratio of lengths AC and BC by the expression:

$$\nu = \nu_1 \sqrt{\frac{AC}{BC}} \quad \text{(rad./sec.)} \tag{7:31}$$

The critical speed of flutter is given by:

$$v_{cr} = Vc\nu \quad \text{(ft./sec.)} \tag{7:32}$$

in which ν is the frequency obtained by equation (7:31).

In the case of a tail configuration with the vertical surfaces at the tips of the horizontal, the method above must be expanded to take into account the effects of the vertical tail. The development of the method outlined below is presented in Chapter VI, Section 6:02.

The following frequencies are needed:

ν_1 = primary flexural frequency obtained in Section 7:02 (rad./sec.)

ν_2 = primary torsional frequency obtained in Section 7:03 (rad./sec.)

The following characteristics of the stabilizer are needed for the station at 85% of the distance from the centerline of the airplane to the centerline of the fin:

c = horizontal tail chord (ft.) on trapezoidal planform without reduction for cut-out.

εc = distance of elastic axis back of 25% point (ft.).

w_h = weight of horizontal tail per unit span (lb./ft.).

W_v = total weight of vertical tail per side (lb.) (including elevator balance weight)

$\sigma_h c$ = distance of inertia axis of horizontal tail back of elastic axis of stabilizer (ft.)*

$\sigma_v c$ = horizontal distance of c.g. of vertical tail (including elevator balance) back of elastic axis of stabilizer (ft.)

$$\sigma_F = \frac{0.30\ w_h s \sigma_h + W_v \sigma_v}{0.30\ w_h s + W_v} \tag{7:33}$$

s = semi-span of tail from centerline of fuselage to tip (ft.)

$i_h c$ = radius of gyration of mass of horizontal tail about nodal axis of horizontal (ft.)**

$i_v c$ = radius of gyration of vertical tail, including elevator balance weights about nodal axis of stabilizer (ft.)

$$i_F^2 = \frac{0.30\ w_h s i_h^2 + W_v i_v^2}{0.30\ w_h s + W_v} \tag{7:34}$$

$$\mu = 16.641 \left[\frac{w_h + 3.33 \frac{W_v}{s}}{c^2} \right] \tag{7:35}$$

$$\eta = \frac{\nu_2}{\nu_1} \cdot i_F \tag{7:36}$$

---

*In calculating the inertia axis of horizontal tail the weight of the elevator should be assumed to be distributed along the elevator hinge line. The weight of the dynamic balance weight at the end of the elevator should be included in the weight of the vertical tail. The elevator dynamic balance weight should be considered to be concentrated at the elevator hinge line.

**In calculating the radius of gyration the weights of the elements of the elevator should be taken in their true chordwise positions.

The critical speed can be determined for the tail by the Kassner-Fingado[20] chart, Figure 51, using the parameters ν_1, c, ε, σ_F, i_F, μ and η as defined above, in the manner described above.

The divergence speed of the wing or tail can be obtained directly from the parameters of Section 7:04 by equation (2:135).

$$v_d = \frac{\eta \nu_1 c}{2} \sqrt{\frac{\mu}{\varepsilon}} \quad \text{(ft./sec.)} \tag{7:37}$$

Inasmuch as the torsional frequency may be written

$$\nu_t = \frac{\eta \nu_1}{i_F} \tag{7:38}$$

the divergence speed is also

$$v_d = \frac{\nu_t i_F c}{2} \sqrt{\frac{\mu}{\varepsilon}} \tag{7:39}$$

The aileron reversal speed can be obtained by equation (5:33)

$$v_r = v_d \sqrt{\frac{R_1 \varepsilon}{R_5}} \tag{7:40}$$

Values of R_1 and R_5 are tabulated in Appendix III.

7:05. Statistical Data of Vibration Frequencies

Data published by Smilg[32] and Stitz[33] on the measured natural frequencies of various airplanes are plotted in Figures 57 to 66, together with other data available to the author from various sources. In many cases the span was considered the most important parameter against which to plot the frequency.

The variation of frequency with span of a cantilever beam can be determined from the equation for the bending frequency of a uniform beam given by Den Hartog[7], (page 172),

$$V = 3.52 \sqrt{\frac{EI}{m_F L^4}} \qquad (7:40)$$

in which:

m_F = mass per unit span

L = span of cantilever

E = modulus of elasticity

I = moment of inertia of area

If a family of beams of the same material are taken in which geometric similarity is maintained, the following relations will apply:

$$I = I_o \left(\frac{L}{L_o}\right)^4 \qquad (7:41)$$

$$m_F = m_{F_o} \left(\frac{L}{L_o}\right)^2 \qquad (7:42)$$

Substituting into equation (7:38), considering E invariant, there results:

$$\frac{\nu}{\nu_0'} = \frac{L_0}{L} \tag{7:43}$$

Hence the frequency varies inversely as the span. This same relation holds for all the frequencies throughout the airplane, assuming geometric similarity. The deviations of the points are a measure of the deviations of the airplanes from a single base of geometric similarity.

When the vibration characteristics of an airplane have been determined experimentally, these characteristics should be used in preference to those calculated by the methods of Sections 7:02 and 7:03. If the bending frequency f_b is known in cycles per minute, it should be converted to radians per second as follows:

$$\nu_b \text{ (rad./sec.)} = f_b \text{ (cy./min.)} \cdot \frac{2\pi}{60} \tag{7:44}$$

The frequency, ν_1 used throughout the calculations is obtained from ν_b, taking into account the apparent mass

$$\nu_1 = \nu_b \sqrt{1 + \frac{1}{\mu}} \tag{7:45}$$

or, approximately

$$\nu_1 = \nu_b\left(1 + \frac{1}{2\mu}\right) \tag{7:46}$$

If we write f_t = torsional frequency observed (cy./min.)

then

$$\nu_t \text{ (rad./sec.)} = f_t \cdot \frac{2\pi}{60} \tag{7:47}$$

It has been found, generally, that wings oscillate in the torsional mode at zero airspeed with the nodal point close to the inertia axis. Where this is the case the quantity η can be estimated with reasonable accuracy by the expression*

$$\nu_t = \frac{\eta \nu_1}{i_F} \tag{7:48}$$

or

$$\eta = \frac{\nu_t}{\nu_b}\left(1 + \frac{1}{2\mu}\right) i_F \tag{7:49}$$

in which:

i_F = mass radius of gyration of wing section in fraction of chord.

*It was found that the effect of the apparent mass on the torsional moment of inertia is small in general so that equation (7:48) may be written without the inclusion of the apparent mass term.

CHAPTER VIII. CONCLUSIONS AND RECOMMENDATIONS

The art of the dynamics of airplane structures has now reached the stage where it is possible to determine from the dimensions and characteristics of the aircraft components a qualitative critical speed at which flutter is likely to occur. This critical speed may represent only an approximation, but even an approximation is a great advance over the condition which has maintained until very recently when certain precautions have been followed blindly and without specific knowledge of their effectiveness to prevent flutter at a given speed. The anarchy of this ignorance should and can be eliminated now.

The question has often been put, "How close to the critical speed is it safe to fly?" The author feels that the answer is that no airplane should be flown at speeds higher than two-thirds of the critical speed for any mode of flutter, divergence, or aileron reversal.

The response curves calculated in this thesis show that, at speeds lower than two-thirds of the flutter speed, the responses are highly damped throughout. (Note the response curves for $v/c\,\nu_1 = 2.0$ of Case A, and for v = 256 m.p.h. for Case B.) In that realm there is great safety. However, at speeds greater than two-thirds of the critical speeds, large responses begin to appear. These responses may easily cause structural failures even at speeds substantially below the so-called critical speed of flutter instability.

Cox and Pugsley[6] show that the maximum aileron rolling moment occurs at a speed 0.73 times the speed of aileron reversal. At speeds above this point, the aileron control diminishes rapidly.

reaching zero at the reversal speed. Inasmuch as the aileron control force per unit of aileron deflection increases as the square of the airspeed, the aileron response in terms of rolling moment for a given pilot exertion is already rapidly diminishing at speeds as high as 0.73 times reversal speed. For this reason, it is believed that airplane speeds should not exceed two-thirds of the reversal speeds.

It is noteworthy that it is now common practice to restrict accelerations in maneuvers to two-thirds of the design load factors of airplanes. These accelerations are the extremes, the average acceleration will seldom exceed one-fourth of the design load factor. Similarly, speeds should be restricted to two-thirds of the critical speeds of flutter and related phenomena.

The author foresees that research and progress must be made in three distinct fields in order that this dynamical technology may keep abreast of the advances in the speeds of aircraft:

1. Research should be carried out with three-dimensional models in wind tunnels (a) to further check the aerodynamic forces acting, (b) to determine the effects of spanwise differences in vibration characteristics, and (c) to determine the effects of structural damping. It is believed that this research should be done by the method of steady-state forced oscillations, measuring the amplitudes and phases at speeds below the critical speed;

2. The technique of determining vibration characteristics should be improved. In particular, mechanical vibrators should be developed capable of exciting pure torsional vibrations in wings and tails on the ground. Also, vibration pick-up equipment should be

developed to determine pure torsional vibrations of small angular amplitudes. It is believed that this can be accomplished with electrical lineal pick-ups connected in opposition.

3. Structural research should be carried out to develop new methods of construction that will provide, (a) greater torsional rigidity, (b) more forward positions of the inertia axis, and (c) reduced moments of inertia of the wing and tail masses about the inertia axis.

APPENDIX I. REFERENCES

1. von Baumhauer, A. G., and C. Koning: On the Stability of Oscillations of an Airplane Wing. N.A.C.A. T.M. No. 223 (1923). Translated from Verslagen en verhandelingen vaan den rijksstudiedienst voor de Luchtvaart, Rep. A 48, Amsterdam, Vol. II, 1923.

2. Birnbaum, W.: Das ebene Problem des schlagenden Flügels. Zeit. Angew. Math. Mech., Vol. IV, No. 4, p. 277 (1924).

3. Birnbaum, W.: Der Schlagflügelpropeller und die kleinen Schwingungen elastic befestigter Tragflügel. Z.F.M., Vol. 15, nos. 11-12, p. 128 (1924).

4. Byerly, W.E.: Generalized Coordinates. Ginn and Co. (1916).

5. Cox, H. Roxbee: Statistical Method of Investigating Relations between Elastic Stiffnesses of Acroplane Wings and Wing-Aileron Flutter. R. & M. No. 1505 (1933).

6. Cox, H. Roxbee, and A. G. Pugsley: Theory of Loss of Lateral Control due to Wing Twisting. R. & M. No. 1506

7. Den Hartog, J.P.: Mechanical Vibrations. McGraw-Hill Book Company (1934).

8. Dietze, F.: Die Luftkräfte der harmonisch schwingenden, in sich verformbaren Platte (Ebenes Problem). Luftfarhtforschung, Vol. 16, No. 2, p. 84 (1939).

9. Duncan, W. J., and G. A. McMillan: Reversal of Aileron Control due to Wing Twist. R. & M. No. 1499 (1932).

10. Duncan, W. J., and A. R. Collar: Present Investigations of Airscrew Flutter. R. & M. No. 1518 (1933).

11. Duncan, W. J., and H. M. Lyon: Calculated Flexural-Torsional Flutter of some Typical Cantilever Wings. R. & M. No. 1782 (1937).

12. Durand, W. F.: Aerodynamic Theory, Vol. I. Julius Springer (1935).

13. Ellenberger, G.: Berechnung der kritischen Geswindigkeit für das ebene Problem eines Tragflügels mit Querruder. Luftfahrtforschung, Vol. 15, No. 8, p. 395 (1938).

14. Frazer, R. A., and W. J. Duncan: The Flutter of Aeroplane Wings. R. & M. No. 1155 (1929).

REFERENCES (continued)

15. Frazer, R. A., and W. J. Duncan: The Flutter of Monoplanes, Biplanes, and Tail Units. R. & M. No. 1255 (1931).

16. Frazer, R. A., and W. P. Jones: Forced Oscillations of Aeroplanes, with special reference to von Schlippe's Method of predicting Critical Speeds for Flutter. R. & M. No. 1795 (1937).

17. Hanson, J.: Critical Speeds of Monoplanes. Journ. Roy. Ae. Soc., Aug. 1937.

18. von Karman, Th., and J. M. Burgers: Aerodynamic Theory, Vol. II. Edited by W. F. Durand. Julius Springer (1935).

19. von Karman, Th., and W. R. Sears: Airfoil Theory for Non-Uniform Motion. Journ. Ae. Sci., Vol. 5, No. 10, p. 379 (1938).

20. Kassner, R., and H. Fingado: Das ebene Problem der Flügelschwingung. Journ. Roy. Ae. Soc., Vol. 41, pp. 921-944, Oct. 1937. Translated from Luftfahrtforschung, Vol. 13, No. 11, 1936.

21. Kassner, R.: Die Berucksichtigung der inneren Dampfung beim ebenen Problem der Flügelschwingung. Journ. Roy. Ae. Soc., Vol. 41, pp. 945-952 (1937). Translated from Luftfahrtforschung, Vol. 13, No. 11, 1936.

22. Küssner, H. G.: Status of Wing Flutter. N.A.C.A. T.M. No. 782 (1936). Translated from Luftfahrtforschung, Oct. 3, 1935, pp. 193-209.

23. Küssner, H. G.: Zusammenfassender Bericht über den instationären Auftrieb von Flügeln. Luftfahrtforschung, Vol. 13, No. 12 (1936).

24. Lamb, H.: Hydrodynamics. Cambridge University Press, Sixth Edition (1932).

25. Millikan, C. B.: Theoretical Aerodynamics of Perfect Fluids. Lecture Notes for AE 266 at Calif. Inst. of Technology.

26. Parish, E. W., Jr., and A. M. Jackson, Jr.: An Investigation of Forced Flexural-Torsional Oscillations of a Wing and the Phenomenon of Flutter. Thesis at Calif. Inst. of Technology, 1939.

27. Pugsley, A. G., and A. W. Clegg: Wing Stiffness of Monoplanes. R. & M. No. 1742.

REFERENCES (continued)

28. Pugsley, A. G.: Control Surface and Wing Stability Problems. Journ. Roy. Ae. Soc., Nov. 1937. Also in Aircraft Engineering, Oct. 1937, p. 268.

29. Roche, J. A.: Airplane Vibrations and Flutter Controllable by Design. S.A.E. Journ., p. 305, Sept. 1933.

30. von Schlippe, B.: Die innere Dampfung, Berechnungsansatze. Ing.-Archiv., Vol. VI, p. 127 (1935).

31. von Schlippe, B.: The Question of Spontaneous Wing Oscillations. N.A.C.A. T.M. No. 806. Translated from Luftfahrtforschung, Vol. 13, No. 2, pp. 41-45, 1936.

32. Smilg, B.: Tests of a Wind Tunnel Flutter Model, Phase I. Air Corps Tech. Rep. No. 4429 (1938).

33. Stitz, W. E.: Vibration Characteristics of Twenty Air Corps Airplanes. Air Corps Information Circular No. 702 (1935).

34. Theodorsen, Theodore: General Theory of Aerodynamic Instability and the Mechanism of Flutter. N.A.C.A. T.R. No. 496 (1935).

35. Theodorsen, Theodore, and I. E. Garrick: Mechanism of Flutter-- A Theoretical and Experimental Investigation on the Flutter Problem. N.A.C.A. Confidential Memorandum, Nov. 1938.

36. Timoshenko, S.: Vibration Problems in Engineering. D. Van Nostrand Co., Inc. (1928).

37. Voigt, H.: Untersuchungen von angefachten Dreh-Biege-Tragflugel-schwingungen im Windkanal. N.A.C.A. T.M. No. 877 (1938). Translated from Luftfahrtforschung, Vol. 14, No. 9, pp. 427-433 (1937).

38. Voigt, H.: Windkanalversuche zum obene Problem der Tragflügelschwing-ungen. Lilienthal-Jahrbuch, pp. 216-226 (1936).

39. Voigt, H.: Weitere Versuche über Tragflügelschwingungen. D.V.L. Yearbook, p. 71 (1938).

40. Webster, A.G.: The Dynamics of Particles and of Rigid, Elastic, and Fluid Bodies. G. E. Stechert & Co. (1912).

41. Hirst, D. M.: Calculation of Critical Reversal Speeds of Wings. R. & M. No. 1568 (1933).

ADDITIONAL BIBLIOGRAPHY

Ackeret, and Studer: Bemerkungen uber Tragflugelschwingungen, Helvetica Physica Acta, p. 501 (1934).

Bairstow, L.: The Theory of Wing Flutter. R. & M. No. 1041 (1927).

Birnbaum, W.: Die tragende Wirbelfäche als Hilfsmittel sur Behandlung des ebenen Problems der Tragflügeltheorie. Z. Angew. Math. Mech., Vol. 3, p. 290 (1923).

Blasius, H.: Über Schwingungserscheinungen an einholmigen Unterflügeln. Z.F.M., Vol. 16, No. 3, p. 39 (1925).

Blenk, H.: Der Eindecker als tragende Wirbelfläche. Z. Angew. Math. Mech., Vol. 5, p. 36 (1925).

Blenk, H., and F. Liebers: Gekoppelte Torsionschwingungen von Tragflügeln. Z.F.M., Vol. 16, No. 23, p. 479 (1925).

Blenk, H., and F. Liebers: Flügelschwingungen freitragender Eindecker. D.V.L. Yearbook, p. 63 (1928).

Blenk, H., and F. Liebers: Gekoppelte Biegungs-Torsions- und Querruderschwingungen von freitragenden und halbfreitragenden Flügeln. D.V.L. Yearbook, p. 257 (1929). Also in Luftfahrtforschung, Vol. 4, No. 3 (1929).

Borbely, S.V.: Mathematischer Beitrag zur Theorie der Flügelschwingungen. Z. Angew. Math. Mech., Vol. 16, No. 1 (1936).

Cicala, P.: Le oscilazioni flesso-torsionali di un'ala in corrente uniforme. L'Aerotecnica, Vol. 16, p. 735 (1936).

Cicala, P.: Le azioni aerodinamiche sui profili di ala oscillanti in presenza di corrente uniforme. Mem. R. Accad. Sci. Torini, II, Vol. 68, p. 73.

Cicala, P.: Ricerche sperimental sulle azione aerodynamiche sopra l'ala oscillante. Aerotechnica 17, pp. 405-414 (1937). Summarized in Zentralblatt für Mechanic, 6 Band, Heft 3, Sept. 8, 1937.

Cicala, P.: Le azioni aerodinamiche sul profilo oscillante. L'Aerotecnica, Vol. 16, p. 653 (1936).

Cicala, P.: Comparison of Theory with Experiment in the Phenomenon of Wing Flutter. N.A.C.A. T.M. No. 887 (1939). Translated from L'Aerotecnica, Vol. XVIII, No. 4, April 1938.

ADDITIONAL BIBLIOGRAPHY (continued)

Cox, H. Roxbee: Problems involving the Stiffness of Aeroplane Wings. Journ. Roy. Ae. Soc., Vol. 38, No. 278 (1934).

Cox, H. Roxbee, and A. G. Pugsley: Stability of Static Equilibrium of Elastic and Aerodynamic Actions on a Wing. R. & M. No. 1509.

Dietze, F.: Zur Berechnung der Auftriebskraft am schwingenden Ruder. Luftfahrtforschung, Vol. 14, No. 7, pp. 361-362 (1937).

Duncan, W. J.: The Wing Flutter of Biplanes. R. & M. No. 1227 (1930).

Duncan, W. J.: Calculation of the Resistance Derivatives of Flutter Theory. Part I. R. & M. No. 1500 (1933).

Duncan, W. J., and A. R. Collar: Calculation of the Resistance Derivatives of Flutter Theory. R. & M. No. 1500 (1932).

Duncan, W. J., and A. R. Collar: A Theory of Binary Servo-Rudder Flutter, with Applications to a Particular Aircraft. R. & M. No. 1527 (1933).

Duncan, W. J., and H. M. Lyon: Torsional Oscillation of a Cantilever when the Stiffness is of Composite Origin. R. & M. No. 1809 (1937).

Ellenberger, G.: Bestimmung der Luftkräfte auf einen ebenen Tragflügel mit Querruder. Zeit. Angew. Math. Mech., Vol. 16, No. 4 (1936).

Essers, J.: Untersuchung von Flügelschwingungen im Windkanal. D.V.L. Yearbook, p. 345 (1929).

Frazer, R.A., and W. J. Duncan: A Brief Survey of Wing Flutter with an Abstract of Design Recommendations. R. & M. No. 1177 (1928).

Frazer, R.A.: The Influence of Differential Aileron Control on Wing Flutter. R. & M. No. 1723 (1936).

Frazer, R.A.: An Investigation of Wing Flutter. R. & M. No. 1042 (1926).

Frazer, R.A., and W. J. Duncan: Wing Flutter as Influenced by the Mobility of the Fuselage. R. & M. 1207 (1929).

Frazer, R.A., and W. J. Duncan: Conditions for the Prevention of Flexural-Torsional Flutter of an Elastic Wing. R. & M. No. 1217 (1930).

ADDITIONAL BIBLIOGRAPHY (continued)

Garrick, I.E.: Propulsion of a Flapping and Oscillating Airfoil. N.A.C.A. T.R. No. 567 (1936).

Glauert, H.: The Lift and Pitching Moment of an Aerofoil due to a Uniform Angular Velocity of Pitch. R. & M. No. 1216 (1929).

Glauert, H.: The Accelerated Motion of a Cylindrical Body through a Fluid. R. & M. No. 1215 (1929).

Glauert, H.: The Force and Moment on an Oscillating Airfoil. R. & M. No. 1242 (1933).

Hesselbach, B.: Über die gekoppelten Schwingungen von Tragflugel und Verwindungsklappe. Z.F.M., Vol. 18, No. 20, p. 465 (1927).

Hull, E. H.: Modern Aids in Vibration Study. Journ. Appl. Mech., Vol. 4, No. 4, Dec. 1937.

Kinner, W.: Die kreisförmige Tragfläche auf potentialtheoretischer Grundlage. Ing.-Arch. VIII, p. 47 (1937).

Kinner, W.: Über Tragflügel mit kreisförmigem Grundriss. Zeit. Angew. Math. Mech., Vol. 16, p. 349 (1936).

Klemin, Alexander: Bibliography of Vibration and Flutter of Aircraft Wings and Control Surfaces. Compiled by U. S. Works Progress Administration (1937).

Koning, C.: Einige Bemerkungen über nichtstationäre Strömungen an Tragflügeln. Proc. 1st Int. Congr. Appl. Mech., Delft, p. 414 (1924).

Küssner, H. G.: Schwingungen von Flugzeugflügeln. D.V.L. Yearbook, p. 313, (1929). Also in Luftfahrtforschung, Vol. 4, No. 2, 1929.

Küssner, H. G.: Untersuchung der Bewegung einer Platte beim Eintritt in eine Strahlgrenze. Luftfahrtforschung, Vol. 13, p. 425 (1936).

Leiss, K.: Einfluss der einzelnen Baugrössen auf das Flattern und das aperiodische Auskippen von Tragflächen mit und ohne Ruder. D.V.L. Yearbook, p. 276 (1938).

Lyon, H.M.: A Review of Theoretical Investigations of the Aerodynamic Forces on a Wing in Non-uniform Motion. R. & M. No. 1786 (1937).

Morris, J.: Approximate Methods for Finding Frequencies of Vibration, p. 815 Journ. Roy. Ae. Soc., Nov. 1936.

ADDITIONAL BIBLIOGRAPHY (continued)

Nagel, F.: Flügelschwingungen im stationären Luftstrom. Luftfahrtforschung, Vol. 4, p. 69 (1929).

Prandtl, L.: Beitrag zur Theorie der tragende Fläche. Zeit. Angew. Math. Mech., Vol. 16, p. 360 (1936).

Prandtl, L.: Über die Entstehung von Wirbeln in der idealen Flussigheit, Vorträge aus dem Gebiete der Hydro- und Aerodynamik, p. 18, (Innsbruck, 1922).

Prandtl, L.: Theorie des Flugzeugtragflügels in zusammendruckbaren Medium. Luftfahrtforschung, Vol. 13, p. 313 (1936(.

Pugsley, A. G.: A Simplified Theory of Wing Flutter. R. & M. No. 1839 (1933).

Pugsley, A. G., and Brooke: Critical Reversal Speed for an Elastic Wing. R. & M. No. 1508.

Pugsley, A. G.: Aerodynamic Characteristics of a Semi-rigid Wing. R. & M. No. 1490.

Pugsley, A. G., and H. Roxbee Cox: The Aerodynamic Power of a Monoplane. R. & M. No. 1640.

Pugsley, A. G.: The Influence of Wing Elasticity upon the Longitudinal Stability of an Aeroplane. R. & M. No. 1548.

Raab, A.: Flugelschwingungen an freitragenden Eindeckern. Z.F.M., vol. 17, no. 7, p. 146 (1926).

Rühl, K. H.: Forschungsaufgaben über der Sicherheitsgrad und die Schwingungssicherhiet von Flugzeugen. Lilienthal Jb. (1936).

Schlichting, H.: Tragflügeltheorie bei Überschallgeschwindigkeit. Luftfahrtforschung, Vol. 13, p. 320 (1936).

Schmeiden, C.: Die Strömung um einen ebenen Tragflügel mit Querruder. Zeit. Angew. Math. Mech., Vol. 16, p. 193 (1936).

Sezawa, K., and S. Kubo: The Nature of the Torsion-Aileron Flutter of a Wing as Revealed by Analytical Experiments. Tokyo Report No. 136, Vol. 11, p. 107 (1936).

Sezawa, K., S. Kubo, and H. Miyazaki: Vibration Phenomena in Ternary Wing Flutter. Tokyo Report, Vol. 12, pp. 131-162 (1937).

Sezawa, K., and S. Kubo: The Nature of Deflection Aileron Flutter of a Wing as Revealed through its Vibrational Frequencies. Tokyo Reports, Vol. 11, pp. 303-338 (1936).

ADDITIONAL BIBLIOGRAPHY (continued)

Sezawa, K.: The Nature of Wing Flutter as Revealed through its Vibrational Frequencies. Journ. Ae. Sci., Vol. 4, No. 1, pp. 30-34 (1936).

Shishkin, S.: The Strength of Bird's Wings. Trans. Central Aero-Hydrodynamical Inst., Moscow, No. 258.

Studer, H. L.: Experimentelle Untersuchungen über Flügelschwingungen. Mitteilungen aus dem Institut für Aerodynamik der Eidegenössischen Technische Hochschule Zurich, Nr. 4.

Wagner, Herbert: Dynamischer Auftrieb von Tragflügeln. Zeit. Angew. Math. Mech., Vol. 5, p. 17 (1925).

Walker, P. B.: Growth of Circulation about a Wing and an Apparatus for Measuring Fluid Motion. R. & M. No. 1402 (1931-32).

Williams, and Fairbanks: A Study of the Flexural Axis of Certain Box Sections. R. & M. No. 1751.

von Wolff, R.: Dynamischer Ruderausgleich. Forsch.-Ing.-Wes., Vol. 8, pp. 184-191 (1937).

Younger, J. E.: Wing Flutter Investigation on Brady's Wind Tunnel Model. A.C.I.C. No. 608 (1928).

APPENDIX II. NOMENCLATURE

The author has endeavored to choose a nomenclature in this thesis which would have a direct meaning to the practicing aeronautical engineer, insofar as such is possible. For this reason, he has used the wing chord as the fundamental measure of length, as is doen by Kassner-Fingado[20], rather than the semi-chord as is done by von Karman-Sears[19], Küssner[23], and Theodorsen[34]. The author has therefore adhered to the nomenclature of Kassner-Fingado[20] insofar as it applies, with the exception that he has used c for wing chord, t for time, k for the elastic constant of vertical support, whereas Kassner-Fingado use t for chord, τ for time, and c for the elastic constant. The nomenclature generally used in Chapter II to Chapter VII is as follows:

c = wing chord (ft.)

ε = distance of elastic axis back of 0.25c point, as fraction of chord.

σ_F = distance of inertia axis back of elastic axis, as fraction of chord.

i_F = radius of gyration of wing mass about inertia axis, as fraction of chord.

m_F = mass of wing per ft. span (including aileron).

m_L = mass of enclosing air cylinder per ft. span.

$\mu = \frac{m_F}{m_L}$

NOMENCLATURE (continued)

τ = ratio: $\frac{\text{aileron chord}}{\text{wing chord}}$

σ_1 = distance of c.g. of aileron mass back of hinge line, as fraction of wing chord.

i_1 = radius of gyration of aileron mass about aileron c.g., as fraction of wing chord.

m_1 = aileron mass per ft. span.

$\mu_1 = \frac{m_1}{m_L}$

k = bending stiffness (lb./ft.)

M_φ = torsional stiffness (ft.lb./rad.)

η = "elastic radius" = $\frac{1}{c}\sqrt{\frac{M_\varphi}{k}}$

v = true airspeed (ft./sec.)

ν = circular frequency of oscillation (rad./sec.)

$\nu_1 = \sqrt{\frac{k}{m_F}}$

ν_b = natural bending frequency as measured at zero airspeed (rad./sec.)

ν_t = natural torsional frequency as measured at zero airspeed (rad./sec.)

V = reduced velocity = $\frac{v}{c\nu}$

$\bar{P}$ = complex lift vector, see Figures 11 - 13.

$i = \sqrt{-1}$

NOMENCLATURE (continued)

In Chapters II to V only:

y = vertical displacement (up) (ft.)

ϕ = angular displacement of wing.

β = angular displacement of aileron relative to wing.

y_e = vertical displacement of elastic axis.

$y_{.422c}$ = vertical displacement of 0.422c point.

F = force (up).

M_o = moment about elastic axis.

M_β = aileron moment about hinge axis.

In Chapters VI and VII only:

x = distance fore and aft (ft.)

y = distance spanwise (ft.)

z = vertical displacement (up) (ft.)

φ = angular displacement.

Throughout this thesis, all complex quantities are barred, such as $\bar{P}$, $\bar{y}$, $\bar{\varphi}$, $\bar{L}$, $\bar{F}$, $\bar{M}$, $\bar{A}_{11}$, etc., in order to attract particular attention to their complex character. Furthermore, all variables which are performing sinusoidal variations such as forces and displacements in steady state oscillations are represented by complex vectors rotating in the complex plane with frequency ν such that the real part of the

NOMENCLATURE (continued)

complex vector at any instant of time represents the actual force or displacement at that instant. (See Den Hartog[7], page 3.)

All derivatives with respect to time are represented by the Newtonian notation thus,

$$\frac{dq}{dt} = \dot{q}$$

$$\frac{d^2q}{dt^2} = \ddot{q}$$

NOMENCLATURE (continued)

A table of equivalents comparing the notation used by the author with that of Theodorsen and Küssner is given below.

	The Author	Theodorsen[34]	Küssner[23]
Wing chord	c	$2b$	$2l$
Aileron chord	τc	$(1-c)b$	$2\tau l$
Velocity	V	v	v
Frequency (circular)	ν	ω	ν
Upward displacement	$\bar{y}$	$-h$	$Ale^{i\nu t}$
Wing angle	$\bar{\varphi}$	α	$-Be^{i\nu t}$
Aileron angle to wing	$\bar{\beta}$	β	$-Ce^{i\nu t}$
Lift (up)	$\bar{L}$	$-P$	$+K$
Moment about elastic axis	$\bar{M}_e$	M_α	--
Moment about 0.25c	$\bar{M}_{0.25c}$	--	M_o
Aileron hinge moment	$\bar{M}_\beta$	M_β	N
Complex lift vector	$\bar{P}$	C	$(1+T)/2$
Reduced frequency	$1/2V$	$k = \omega b/v$ *	$= i\nu l/v$ *

*Note: Theodorsen's k is not equivalent to Küssner's ω but rather $\omega = ik = i/2V$.

NOMENCLATURE (continued)

Table of Equivalents (continued)

	The Author	Theodorsen[34]	Küssner[23]
Reduced velocity	$V = v/c\nu$	$1/2k$	$i/2\omega$
Mass of wing per unit span	m_F	M	--
Mass of air cylinder	$m_L = \pi\rho c^2/4$	$\pi\rho b^2$	--
Ratio m_F/m_L	μ	$1/\kappa$	--
Aileron mass per unit span	m_1	--	--
	$2(\varepsilon - 1/4)$	a	--
	$c/2$	b	--
	$2(1/2 - \tau)$	c	--
	$2\sigma_F$	x_α	--
	$2\sigma_1 m_1/m_F$	x_β	--
	$2\sqrt{i_F^2 + \sigma_F^2}$	r_α	--
	$2\sqrt{(i_1^2 + \sigma_1^2)m_1/m_F}$	r_β	--
	ν_1	ω_h	--
	$\eta\nu_1/\sqrt{i_F^2 + \sigma_F^2}$	ω_α	--
	$\dfrac{\eta_1 \nu_1}{\sqrt{(i_1^2 + \sigma_1^2)m_1/m_F}}$	ω_β	--

NOMENCLATURE (continued)

Table of Equivalents (continued)

The Author	Theodorsen[34,35]	Küssner[23]
R_1	$4T_{10}/\pi$	$4\Phi_1/\pi$
R_2	T_{11}/π	Φ_2/π
R_3	$-T_4/\pi$	Φ_3/π
R_4	$-T_1/2\pi$	$\Phi_4/4\pi$
R_5	$(T_4 + T_{10})/\pi$	Φ_5/π
R_6	$\left[2T_1 - 2T_8 + T_{11} + 4T_4(\tau - 3/4)\right]/4\pi$	$\Phi_6/4\pi$
R_7	$\left[-T_7 + 2T_1(\tau - 3/4)\right]/4\pi$	$\Phi_7/16\pi$
R_8	T_{12}/π	Φ_8/π
R_9	$+ (2p - 2T_1 - T_4)/4\pi$	$\Phi_9/4\pi$
R_{10}	$(T_5 - T_4T_{10})/\pi^2$	Φ_{10}/π^2
R_{11}	$-T_4T_{11}/4\pi^2$	$\Phi_{11}/4\pi^2$
R_{12}	$-T_3/4\pi^2$	$\Phi_{12}/16\pi^2$
$(R_7 + R_4\varepsilon)$	$T_{13}/2\pi$	--

APPENDIX III. VALUES OF R FUNCTIONS*

	Aileron Chord / Wing Chord = τ					
	0	0.15	0.20	0.25	0.30	0.50
R_1	0	1.92200	2.19928	2.43600	2.64300	3.27324
R_2	0	0.19424	0.29748	0.41350	0.54058	1.13662
R_3	0	0.09406	0.14238	0.19550	0.25231	0.5000
R_4	0	0.005725	0.01161	0.02004	0.03119	0.10610
R_5	0	0.38644	0.40744	0.41350	0.40844	0.31831
R_6	0	0.08567	0.12552	0.16667	0.20784	0.35610
R_7	0	0.002680	0.005315	0.008966	0.013648	0.04215
R_8	0	0.00612	0.01272	0.02250	0.03596	0.13662
R_9	0	0.00992	0.02004	0.03446	0.05343	0.17805
R_{10}	0	0.00999	0.01651	0.02384	0.03156	0.05783
R_{11}	0	0.00457	0.01059	0.02021	0.03410	0.14208
R_{12}	0	0.000178	0.000558	0.001348	0.00277	0.02048
$R_1R_8/4$	0	0.00294	0.00699	0.01370	0.02376	0.11180
$R_2R_8/4$	0	0.000297	0.000946	0.002325	0.004860	0.07764

*Calculated from the values of the T functions of Theodorsen and Garrick[35] and Φ functions of Küssner[23].

Lombard_ae_1939

APPENDIX IV. TYPICAL CALCULATION OF RESPONSE IN STEADY STATE OSCILLATION

Case A. $\frac{V}{v_1 c} = 2.0 \qquad v_1 = 10$

Dynamical Equations:

$$\frac{\bar{F}}{m_F} = \bar{y}_{0.5c}\underbrace{\left[100 + 8.0\, i\nu\bar{P} - 1.10\nu^2\right]}_{\bar{A}_{11}} + \bar{\varphi}_c\underbrace{\left[-2\, i\nu(1+\bar{P}) - 160\,\bar{P}\right]}_{\bar{A}_{12}}$$

$$\frac{\bar{M}}{m_F} = \bar{y}_{0.5c}\underbrace{\left[+2.0\, i\nu\bar{P}\right]}_{\bar{A}_{21}} + \bar{\varphi}_c\underbrace{\left[100 + 0.5\, i\nu(1-\bar{P}) - 40\,\bar{P} - 0.1031\nu^2\right]}_{\bar{A}_{22}}$$

ν			0	4	8	12	16	20	24	28	30	32	36	40	48
$\bar{P}$ *	$1/V = \nu/20$	(1)	0	0.2	0.4	0.6	0.8	1.0	1.2	1.4	1.5	1.6	1.8	2.0	2.4
	A	(2)	1.000	0.832	0.728	0.665	0.625	0.598	0.579	0.565	0.560	0.554	0.546	0.539	0.530
	B	(3)	0	0.1723	0.1886	0.1793	0.1650	0.1507	0.1378	0.1264	0.121	0.1165	0.1078	0.1002	0.0877
	$1 + A$	(4)	2.000	1.832	1.728	1.665	1.625	1.598	1.579	1.565	1.560	1.554	1.546	1.539	1.532
	$1 - A$	(5)	0	0.168	0.272	0.335	0.375	0.402	0.421	0.435	0.440	0.446	0.454	0.461	0.470
$\bar{A}_{11}$	$100 - 1.1\nu^2$	(6)	+100	+82.4	+29.6	-58.4	-181.6	-340	-534	-762	-890	-1026	-1326	-1660	-2434
	$+ 8\nu B$	(7)	0	5.5	12.1	17.2	21.1	24	26.4	28	29	30	31	32	34
	Re $A_{11} = (6) + (7)$	(8)	100	87.9	41.7	-41.2	-160.5	-316	-508	-734	-861	-996	-1295	-1628	-2400
	Im $A_{11} = 8\nu A$	(9)	0	26.6	46.6	63.8	80.0	96	111	127	134	142	157	173	203
	$\theta = \tan^{-1}(9)/(8)$	(10)	0°	16.9°	41.9°	123.2°	153.5°	163.1°	167.7°	170.4°	171.1°	171.9°	173.1°	174.0°	175.1°
	$r = \sqrt{(8)^2 + (9)^2}$	(11)	100	91.9	62.5	76.3	179.3	330	520	744	872	1006	1305	1637	2410
$\bar{A}_{12}$	$- 2\nu B$	(12)	0	- 1.4	-3.0	-4.3	-5.3	-6.0	-6.6	-7.1	-7.2	-7.5	-7.8	-8.0	-8.4
	$- 160\ A$	(13)	-160.0	-133.0	-116.4	-106.3	-100.0	-95.6	-92.6	-90.4	-89.6	-88.4	-87.3	-86.2	-84.9
	Re A_{12}	(14)	-160.0	-144.4	-119.4	-110.6	-105.3	-101.6	-99.2	-97.5	-96.8	-95.9	-95.1	-94.2	-93.1
	$- 2\nu(1 + A)$	(15)	0	- 14.6	- 27.6	- 40.0	- 52.0	- 64.0	- 75.8	- 87.6	- 93.6	- 99.9	-111.2	-123.1	-147.0
	$+ 160\ B$	(16)	0	27.6	30.2	28.7	26.4	24.1	22.1	20.2	19.3	18.6	17.1	16.0	14.0
	Im A_{12}	(17)	0	13.0	2.6	- 11.3	- 25.6	- 39.9	- 53.7	- 67.4	- 74.3	- 81.3	- 94.1	-107.1	-133.0
	$\theta = \tan^{-1}(17)/(14)$	(18)	180°	174.9°	178.4°	185.8°	193.6°	201.4°	208.4°	214.6°	217.5°	220.3°	224.8°	-131.2°	-125.0°
	$r = \sqrt{(14)^2 + (17)^2}$	(19)	160	145	119.4	111.1	118.4	109.2	113.0	118.5	122.1	125.8	133.8	142.6	162.4
$\bar{A}_{21}$	Re $A_{21} = + 2\nu B$	(20)	0	1.4	3.0	4.3	5.3	6.0	6.6	7.1	7.2	7.5	7.8	8.0	8.4
	Im $A_{21} = + 2\nu A$	(21)	0	6.7	11.7	16.0	20.0	23.9	27.8	31.6	33.6	35.4	39.3	43.1	50.9
	$\theta = \tan^{-1}(21)/(20)$	(22)	90°	78.2°	75.6°	75.0°	75.2°	75.9°	76.6°	77.3°	77.9°	78.0°	78.8°	79.5°	80.6°
	$r = \sqrt{(20)^2 + (21)^2}$	(23)	0	6.8	12.1	16.6	20.3	24.6	28.6	32.4	34.4	36.2	40.1	43.9	51.6
$\bar{A}_{22}$	$100 - 0.1031\nu^2$	(24)	100.0	98.4	93.4	85.2	73.6	58.8	40.6	19.2	7.3	- 5.6	- 33.7	- 65.0	-137.6
	$- 0.5\nu B$	(25)	0	- 0.3	- 0.8	- 1.1	- 1.3	- 1.5	- 1.7	- 1.8	- 1.8	- 1.9	- 1.9	- 2.0	- 2.1
	$- 40\ A$	(26)	- 40.0	- 33.3	- 29.1	- 26.6	- 25.0	- 23.9	- 23.2	- 22.6	- 22.6	- 22.2	- 21.8	- 21.6	- 21.2
	Re A_{22}	(27)	60.0	64.8	63.5	57.5	47.3	33.4	15.7	- 5.2	- 17.1	- 29.7	- 57.4	- 88.6	-160.9
	$+ 0.5\nu(1 - A)$	(28)	0	0.3	1.1	2.0	3.0	4.0	5.1	6.1	6.6	7.1	8.2	9.2	11.3
	$+ 40\ B$	(29)	0	6.9	7.5	7.2	6.6	6.0	5.5	5.1	4.8	4.7	4.3	4.0	3.5
	Im A_{22}	(30)	0	7.2	8.6	9.2	9.6	10.0	10.6	11.1	11.4	11.8	12.5	13.2	14.8
	$\theta = \tan^{-1}(30)/(27)$	(31)	0°	6.3°	7.7°	9.1°	11.5°	16.6°	33.8°	115.2°	146.4°	158.4°	167.7°	171.5°	174.8°
	$r = \sqrt{(27)^2 + (30)^2}$	(32)	60.0	65.2	64.1	58.2	48.3	34.9	18.9	12.3	20.6	32.0	58.4	89.6	161.6
$\bar{\Delta}$	$(8) \cdot (27)/100$	(33)	60.0	57.0	26.5	- 23.7	- 75.9	-105.5	- 79.8	38.2	147.1	296.0	744.0	1442.0	3862.0
	$-(9) \cdot (30)/100$	(34)	0	- 1.9	- 4.0	- 5.9	- 7.7	- 9.6	- 11.7	- 14.1	- 15.3	- 16.8	- 20.0	- 23.0	- 30.0
	$-(14) \cdot (20)/100$	(35)	0	2.0	3.6	4.8	5.6	6.1	6.5	6.9	7.0	7.2	7.4	7.0	8.0
	$+(17) \cdot (21)/100$	(36)	0	0.9	0.3	1.8	- 1.8	- 5.1	- 14.9	- 21.3	- 25.0	- 28.8	- 37.0	- 46.0	- 68.0
	$\Delta_R/100$	(37)	60.0	58.0	26.4	- 26.6	- 83.1	-118.5	- 99.9	- 9.7	113.8	257.6	694.0	1380.0	3772.0
	$(8) \cdot (30)/100$	(38)	0	6.3	3.6	- 3.8	- 15.4	- 31.6	- 53.4	- 81.5	- 98.1	-117.5	-161.9	-214.9	-351.0
	$(9) \cdot (27)/100$	(39)	0	17.2	29.6	36.7	37.8	32.1	17.4	- 6.6	- 22.9	- 42.2	- 90.0	-153.2	-326.0
	$-(14) \cdot (21)/100$	(40)	0	9.7	14.0	17.7	21.0	24.3	27.6	30.8	32.5	34.0	37.4	40.6	47.0
	$-(17) \cdot (20)/100$	(41)	0	- 0.2	0	0.5	1.4	2.4	3.5	4.8	5.3	6.1	7.3	8.6	11.0
	$\Delta_I/100$	(42)	0	33.0	47.2	51.1	44.8	27.2	- 4.9	- 52.5	- 83.2	-119.6	-207.2	-318.9	-619.0
	$\theta = \tan^{-1}(42)/(37)$	(43)	0°	29.6°	60.8°	117.5°	151.7°	167.0°	191.5°	280.5°	- 36.1°	- 24.9°	- 16.6°	- 13.0°	- 9.3°
	$r/100 = \sqrt{(37)^2 + (42)^2}$	(44)	60.0	66.7	54.1	57.3	94.5	121.5	102.0	53.4	141.0	284.0	724.0	1417.0	3821.0
Responses to $\bar{F}$ (Coupled System)															
$\frac{y_{0.5c}}{y_o}$	$r = (32)/(44)$	(45)	1.000	0.978	1.185	1.015	0.511	0.287	0.185	0.230	0.146	0.091	0.081	0.063	0.042
	$\theta = (31) - (43)$	(46)	0°	- 23.3°	- 53.1°	- 98.4°	-140.2°	-150.4°	-157.7°	-165.3°	-177.5°	-176.7°	-175.7°	-175.5°	-175.9°
$\frac{\bar{\varphi}_c}{y_o}$	$r = (23)/(44)$	(47)	0	0.10	0.224	0.289	0.219	0.202	0.280	0.606	0.244	0.127	0.055	0.031	0.013
	$\theta = (22) - (43) + 180°$	(48)	270°	228.6°	194.8°	137.5°	103.5°	88.9°	64.1°	- 23.2°	- 66.0°	- 77.1°	- 84.6°	- 87.5°	- 90.1°
$\frac{\bar{\varphi}_c}{\bar{y}}$	$r = (23)/(32)$	(49)	0	0.104	0.189	0.285	0.420	0.705	1.515	2.638	1.670	1.131	0.684	0.490	0.319
	$\theta = (23) - (31) + 180°$	(50)	270°	251.9°	247.9°	245.9°	243.7°	239.3°	222.8°	142.1°	104.6°	99.6°	91.1°	88.0°	85.2°
Responses to $\bar{M}$ (Coupled System)															
$\frac{\bar{\varphi}}{\varphi_o}$	$r = (11)/(44)$	(51)	1.667	1.378	1.155	1.331	1.902	2.716	5.10	13.93	6.19	3.54	1.803	1.156	0.631
	$\theta = (10) - (43)$	(52)	0°	- 12.7°	- 18.9°	5.7°	1.8°	- 3.9°	- 28.4°	-110.1°	-152.8°	-163.2°	-170.3°	-173.0°	-175.6°
$\frac{\bar{y}_{0.5c}}{\varphi_o^c}$	$r = (19)/(44)$	(53)	2.67	2.17	2.20	1.94	1.25	0.90	1.11	2.22	0.865	0.44	0.185	0.100	0.042
	$\theta = (18) - (43) + 180°$	(54)	0°	- 34.7°	- 62.8°	-111.7°	-138.1°	-145.6°	-163.1°	-245.9°	-288.4°	-294.8°	-298.6°	-298.2°	-295.7°
$\frac{\bar{y}_{0.5c}}{\bar{\varphi}_c}$	$r = (19)/(11)$	(55)	1.600	1.577	1.910	1.455	0.662	0.331	0.217	0.159	0.140	0.125	0.102	0.087	0.067
	$\theta = (18) - (10) + 180°$	(56)	0°	- 22.0°	- 43.5°	-117.4°	-139.9°	-141.7°	-139.3°	-135.8°	-133.6°	-131.6°	-128.3°	-125.2°	-120.1°
Response to $\bar{F}$ ($\bar{\varphi} = 0$ by restraint)															
$\frac{\bar{v}}{v_o}$	$r = 100/(11)$	(57)	1.000	1.088	1.600	1.310	0.558	0.303	0.192	0.134	0.105	0.099	0.077	0.061	0.041
	$\theta = - (10)$	(58)	0°	- 16.9°	- 41.9°	-123.2°	-153.5°	-163.1°	-167.7°	-170.4°	-171.1°	-171.9°	-173.1°	-174.0°	-175.1°
Response to $\bar{M}$ ($\bar{y}_{0.5c} = 0$ by restraint)															
$\frac{\bar{\varphi}}{\varphi_o}$	$r = 100/(32)$	(59)	1.667	1.533	1.560	1.718	2.072	2.868	5.29	8.13	4.85	3.125	1.712	1.116	0.619
	$\theta = - (31)$	(60)	0°	- 6.3°	- 7.7°	- 9.1°	- 11.5°	- 16.6°	- 33.8°	-115.2°	-146.4°	-158.4°	-167.7°	-171.5°	-174.8°

* $\bar{P} = A - iB$ (See Figures 11-13).

APPENDIX V

SUMMARY OF CHARACTERISTICS OF SPECIFIC CASES STUDIED

Case	A	B	C-1	C-2
Type of Oscillation	Flex. tors.	Flex. tors.	Flex. ail.	Flex. ail.
c (ft.)	c	7.5	c	c
ε	0.25	0.10	-	-
σ_F	0	0.05	-	-
i_F^2	0.100	0.0625	-	-
η^2	1.00	0.50	-	-
μ	10.0	6.00	10.0	10.0
ν_1 (rad./sec.)	ν_1	31.41	ν_1	ν_1
τ	-	-	0.20	0.20
μ_1	-	-	1.0	1.0
σ_1	-	-	0.08	0.08
i_1	-	-	0.06	0.06
η_1^2	-	-	0.001	0

SUMMARY OF CHARACTERISTICS OF SPECIFIC CASES STUDIED (continued)

Case		A	B	C-1	C-2
Natural frequencies at zero airspeed					
ν "bending"	(rad./sec.)	$0.954\ \nu_1$	28.9	-	-
ν "torsion"	(rad./sec.)	$3.115\ \nu_1$	85.6	-	-
ν (upper)		-	-	$1.13\ \nu_1$	$0.99\ \nu_1$
ν (lower)		-	-	$0.85\ \nu_1$	0
Critical flutter (lower limit)					
v_{cr}	ft./sec.	$2.87\ \nu_1 c$	549	$0.343\ \nu_1 c$	$0.195\ \nu_1 c$
	m.p.h.	-	374	-	-
ν_{cr}	(rad./sec.)	$2.26\ \nu_1$	57.2	$1.07\ \nu_1$	$0.98\ \nu_1$
V		1.27	1.28	0.20	0.322
Critical flutter (upper limit)					
v_{cr}		∞	∞	$1.27\ \nu_1 c$	$2.69\ \nu_1 c$
ν_{cr}				$1.196\ \nu_1$	$1.62\ \nu_1$
V				1.06	1.66
Torsional divergence					
v_d	ft./sec.	$3.16\ \nu_1 c$	645	-	-
	m.p.h.	-	440	-	-

FIG. 1.

FLEXURAL CRITERION FOR MONOPLANES

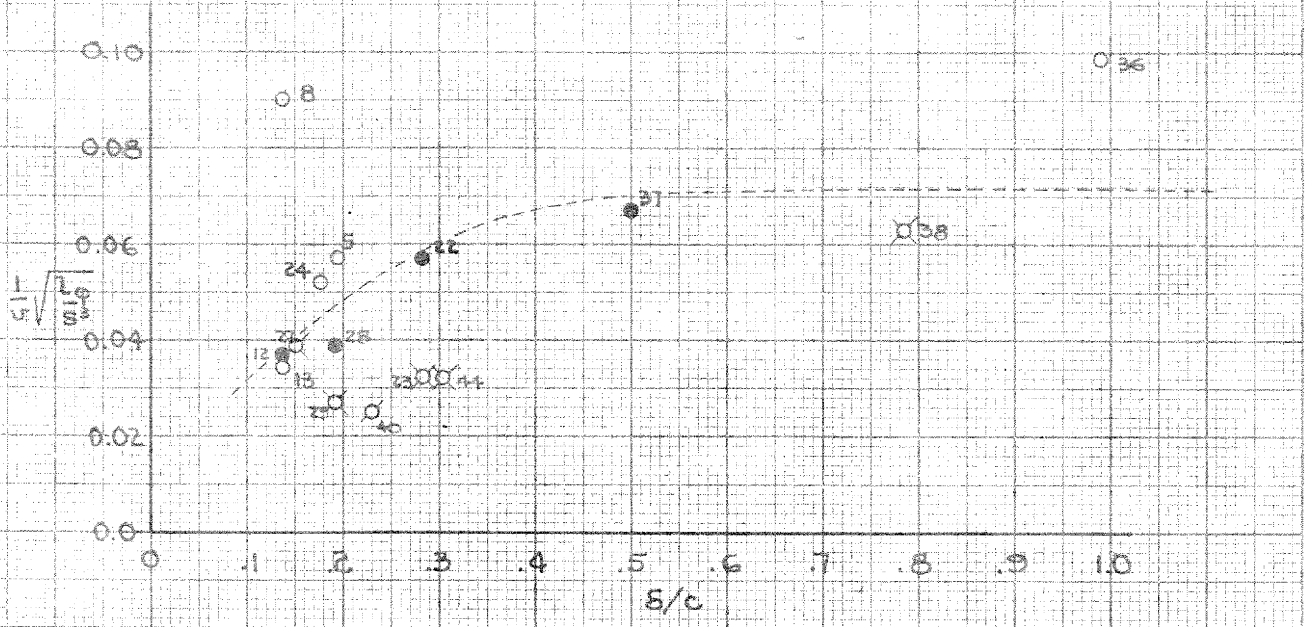

FIG. 2.

TORSIONAL CRITERION FOR MONOPLANES

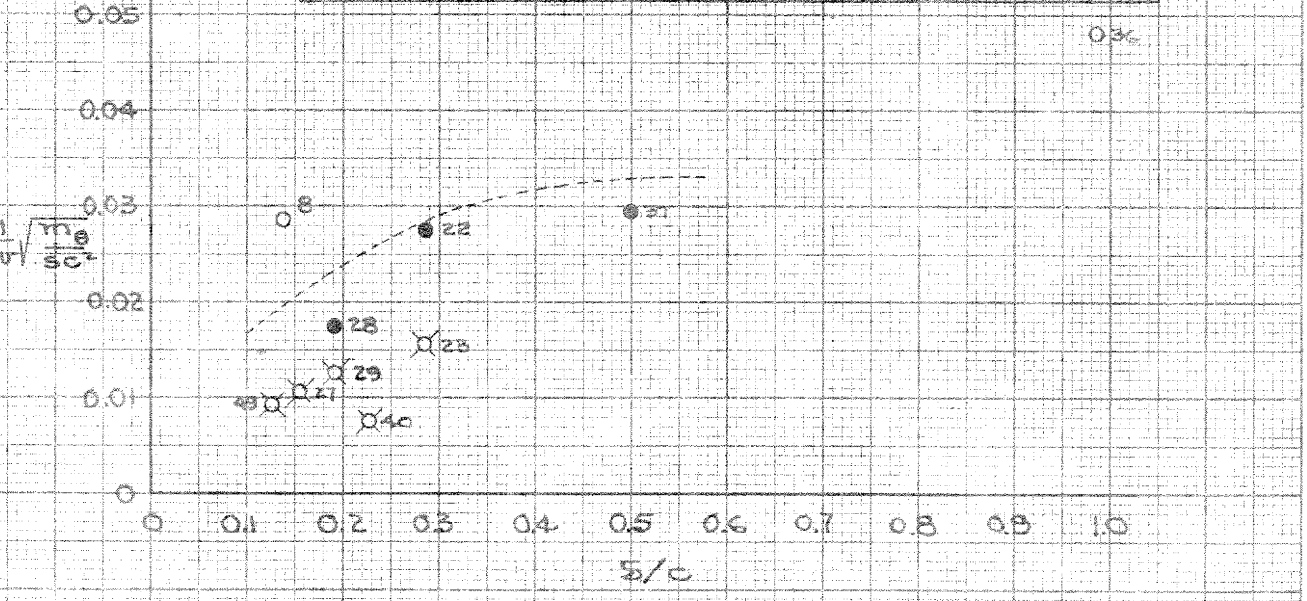

○ AIRCRAFT WHICH HAVE NOT EXPERIENCED FLUTTER.

● AIRCRAFT WHICH HAVE EXPERIENCED FLUTTER.

⊗ AIRCRAFT FITTED WITH MASS BALANCED AILERONS.

ALL DATA FROM COX [5]

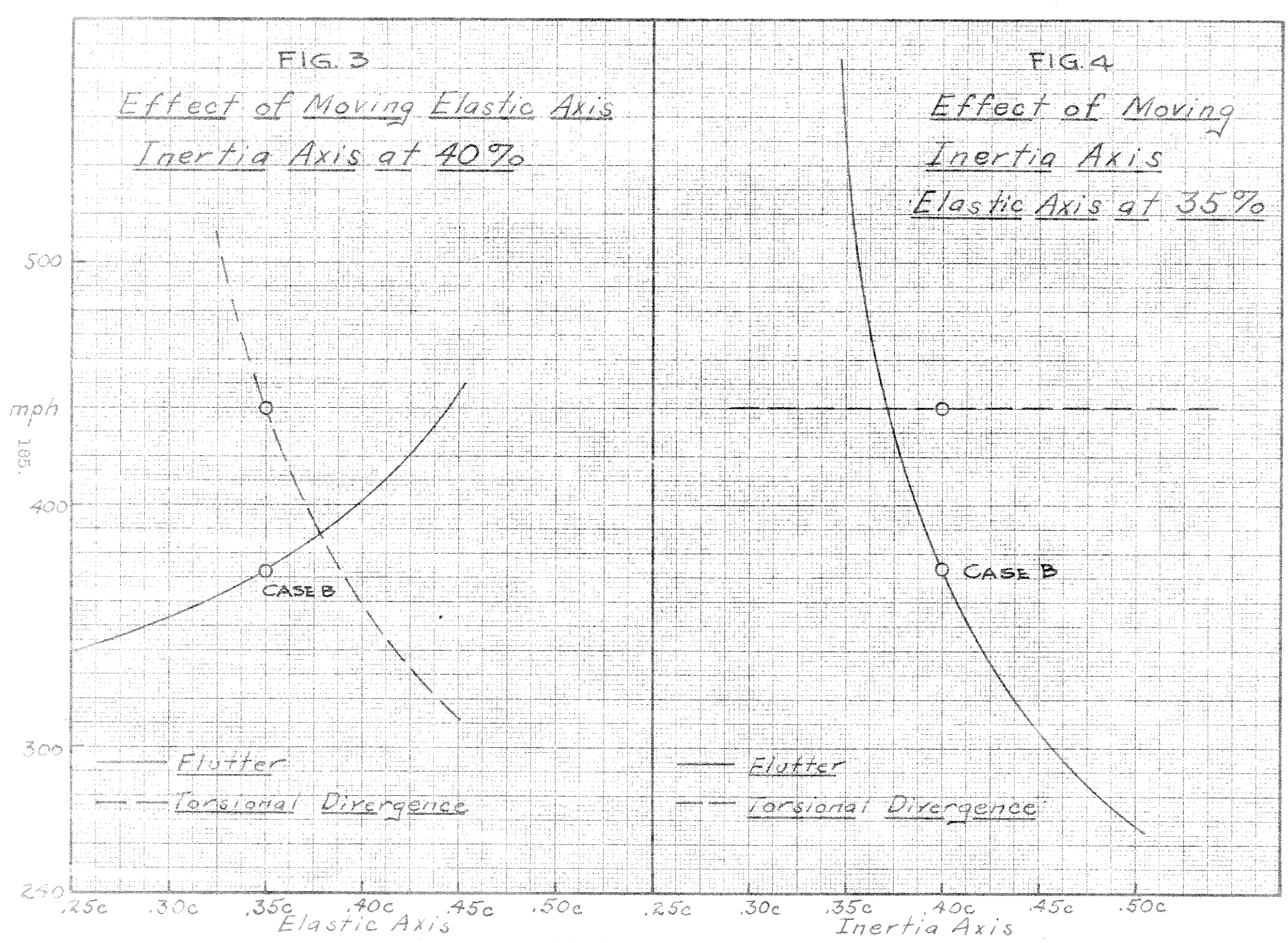
FIG. 3
Effect of Moving Elastic Axis
Inertia Axis at 40%
500
mph
400
300
250
CASE B
Flutter
Torsional Divergence
.25c
.30c
.35c
.40c
.45c
.50c
Elastic Axis
FIG. 4
Effect of Moving
Inertia Axis
Elastic Axis at 35%
CASE B
Flutter
Torsional Divergence
.25c
.30c
.35c
.40c
.45c
.50c
Inertia Axis

FIG. 3, 4

FIG. 5

Effect of Moving Elastic Axis and Inertia Axis Simultaneously

$\sigma = 0.05$

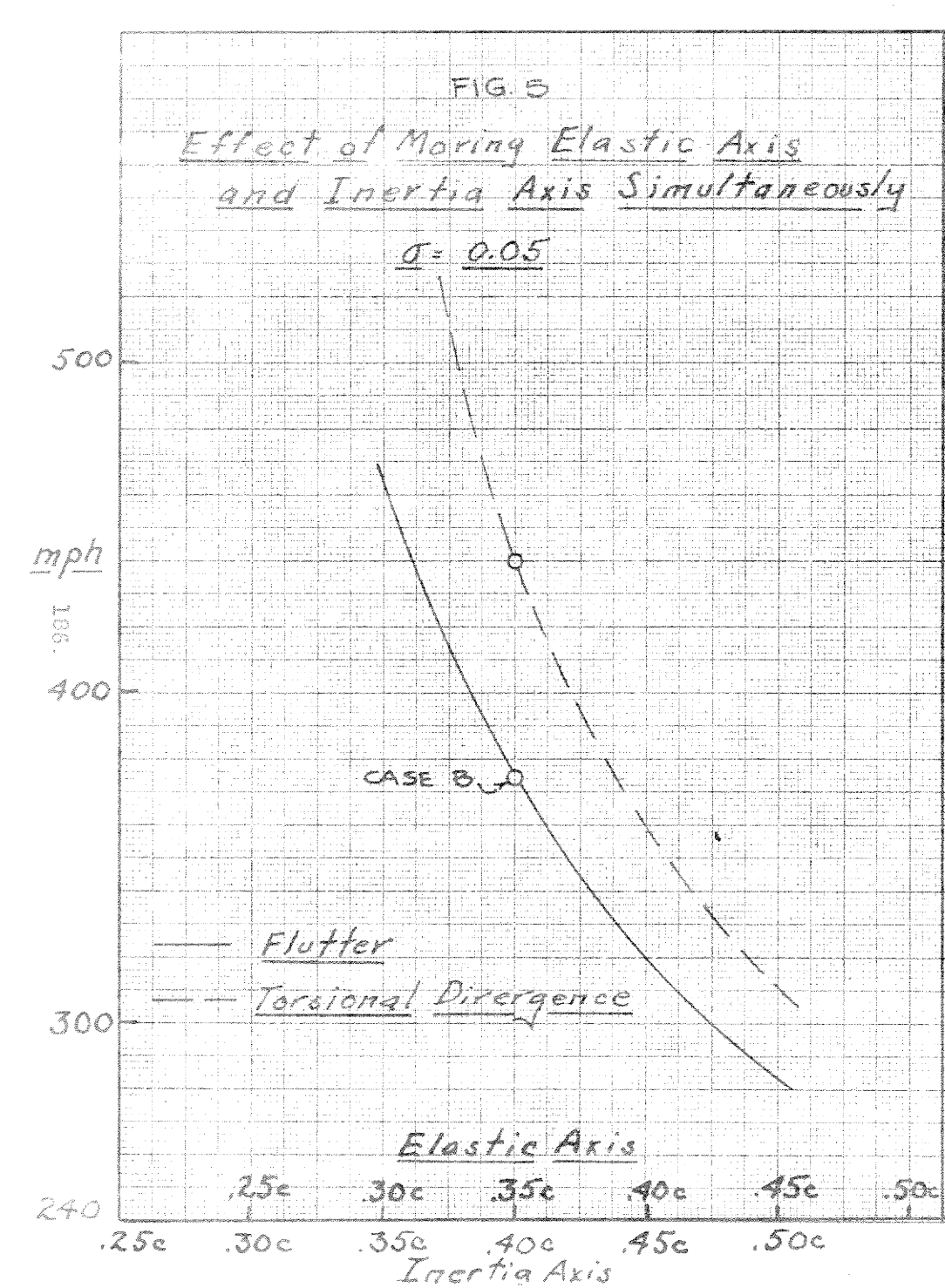

FIG. 6

Effect of Variation of Radius of Gyration Holding Torsional Stiffness Constant

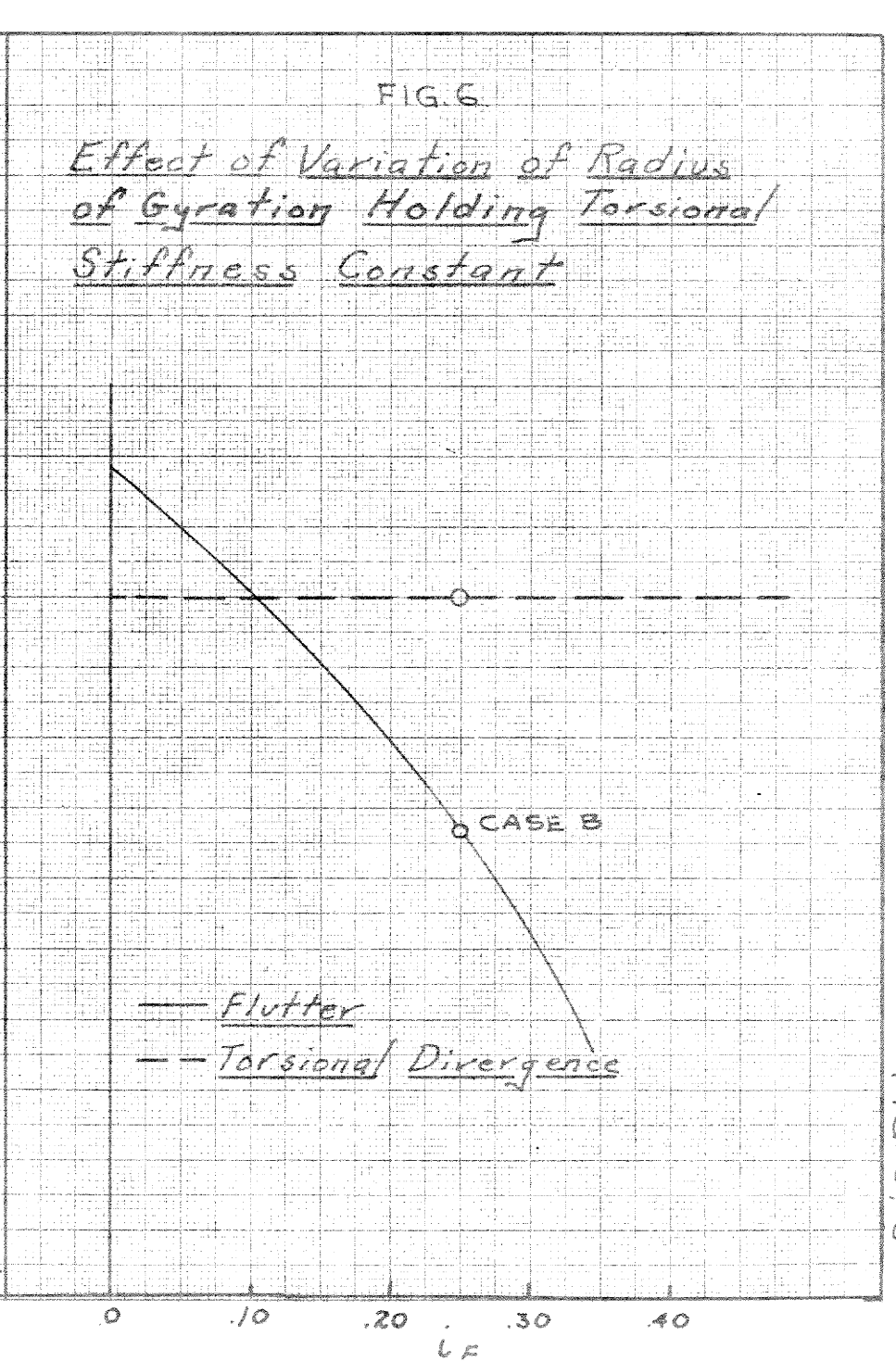

FIG. 5, 6

FIG. 7

Effect of Torsional Frequency

Bending Frequency Constant

(Torsional stiffness varied)

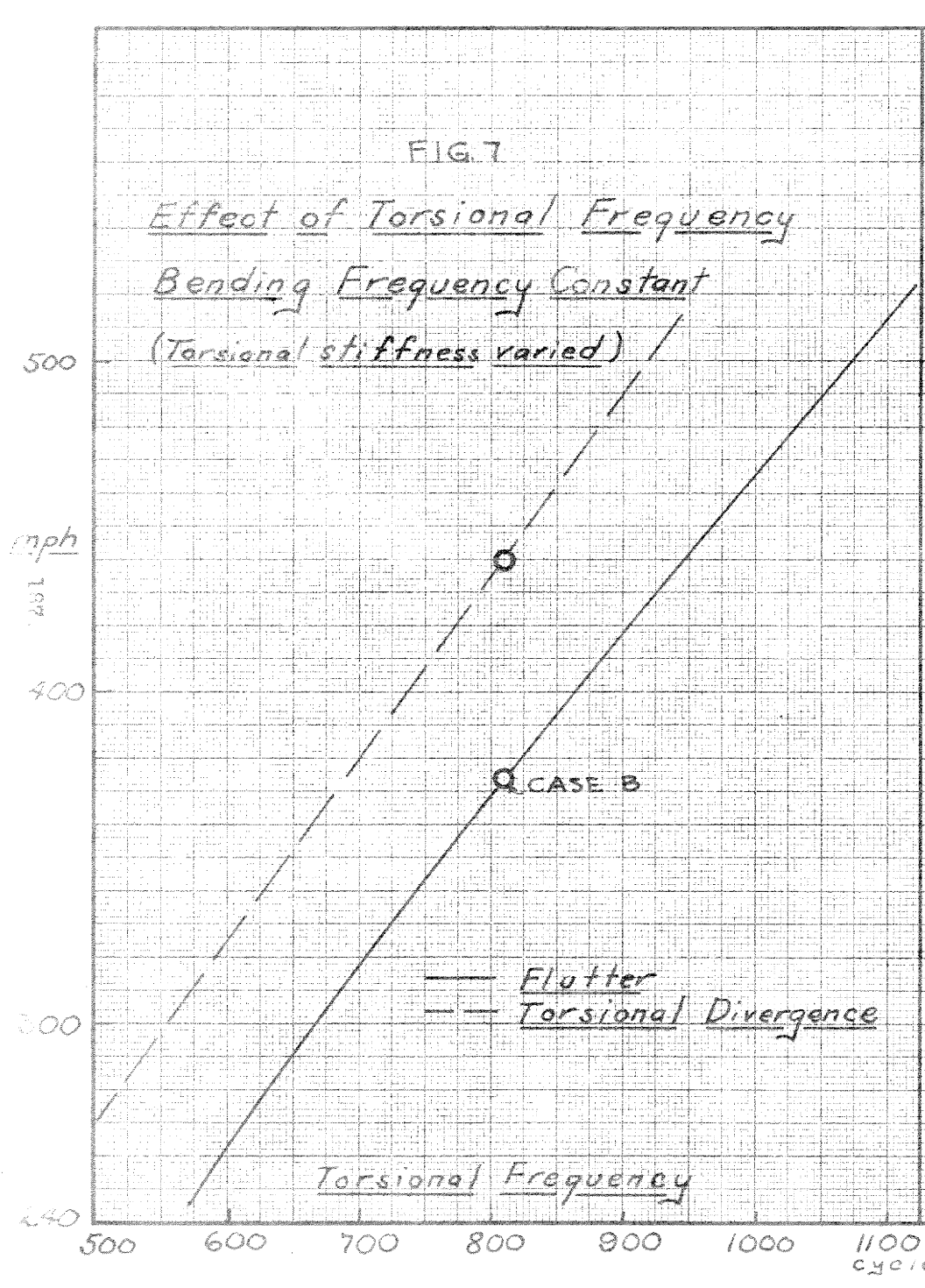

FIG. 8

Effect of Bending Frequency

Torsional Frequency Constant

(Bending stiffness varied)

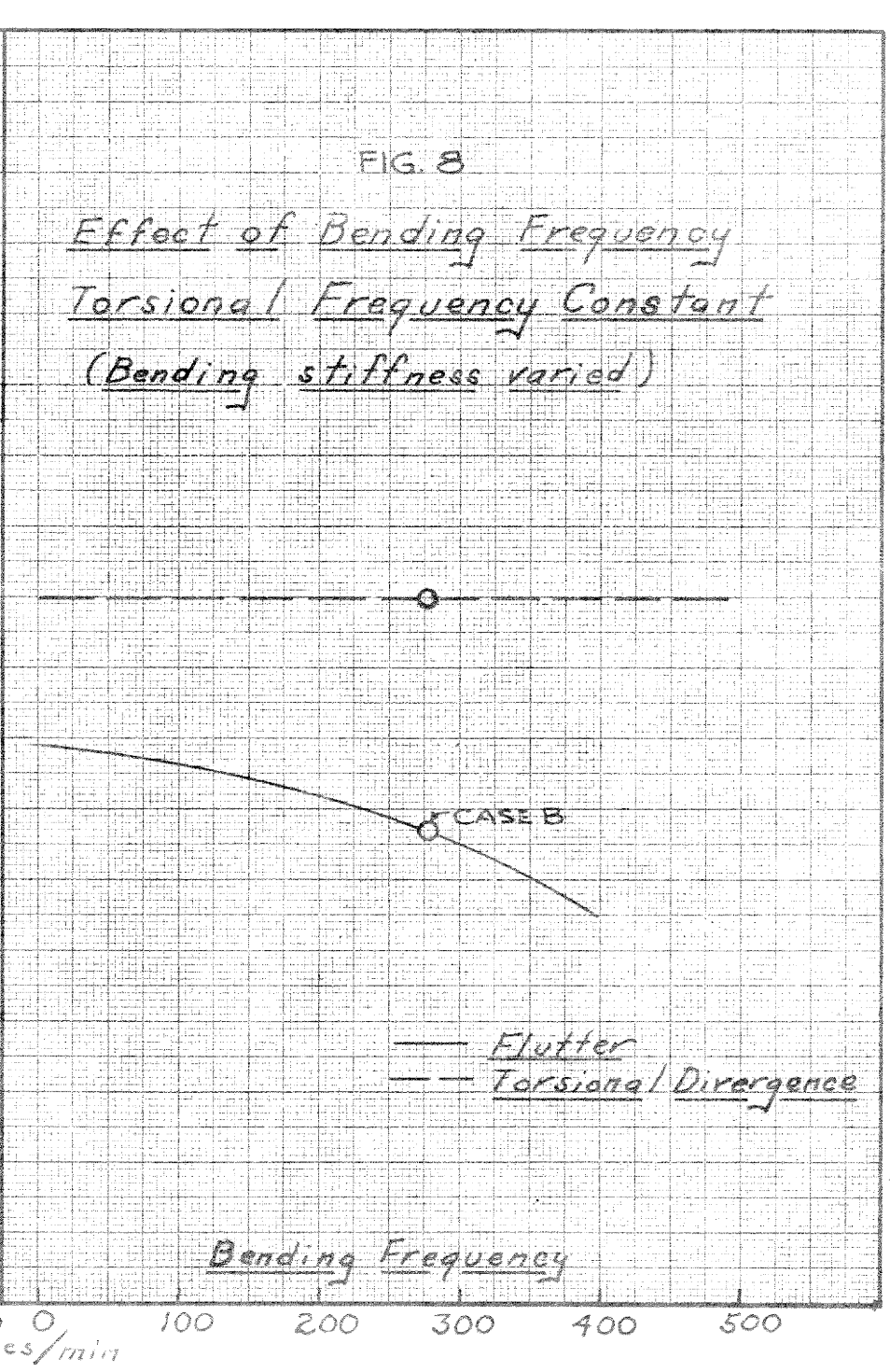

FIG. 7, 8.

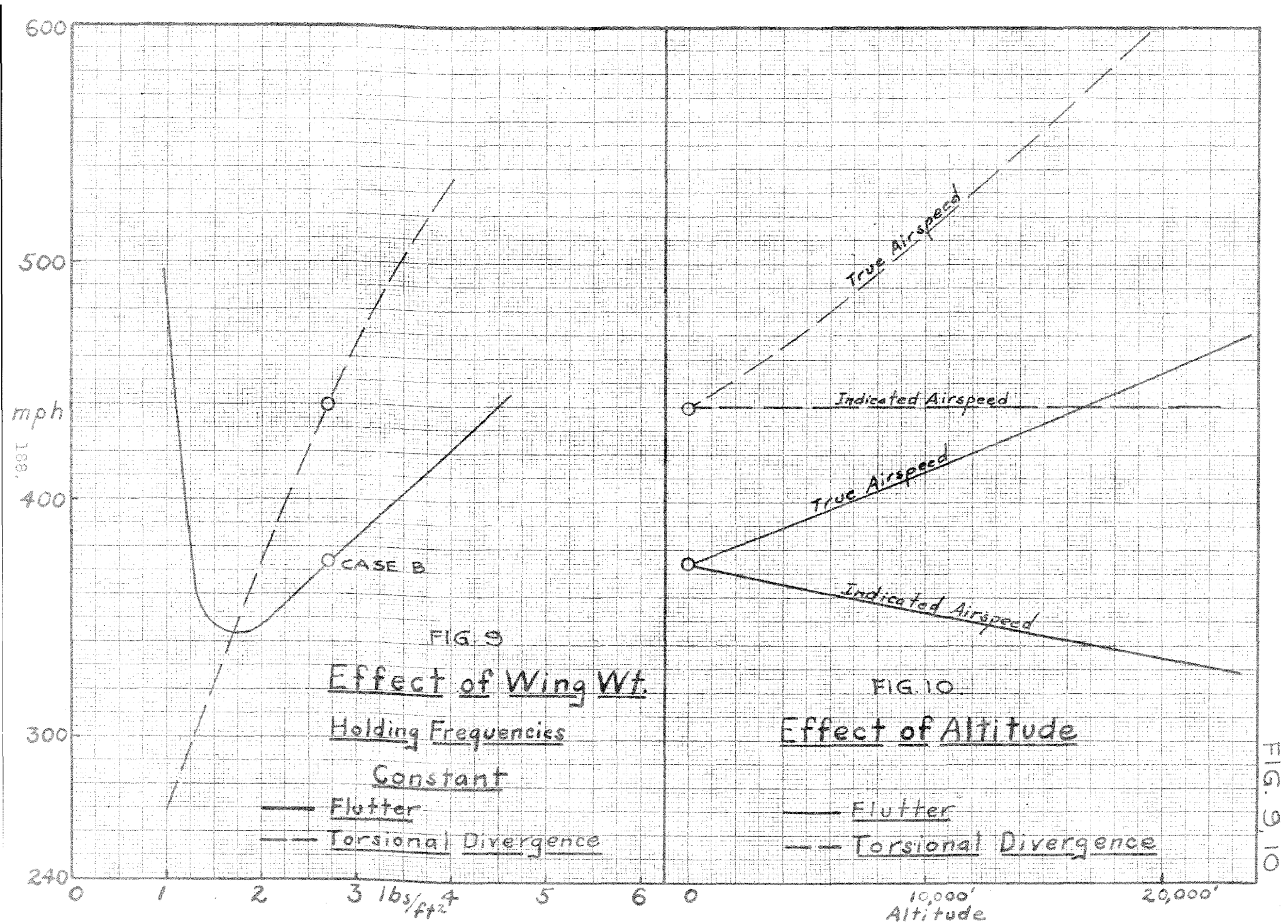

FIG. 9

Effect of Wing Wt.

Holding Frequencies Constant

FIG. 10.

Effect of Altitude

FIG. 9, 10

FIG. 11.

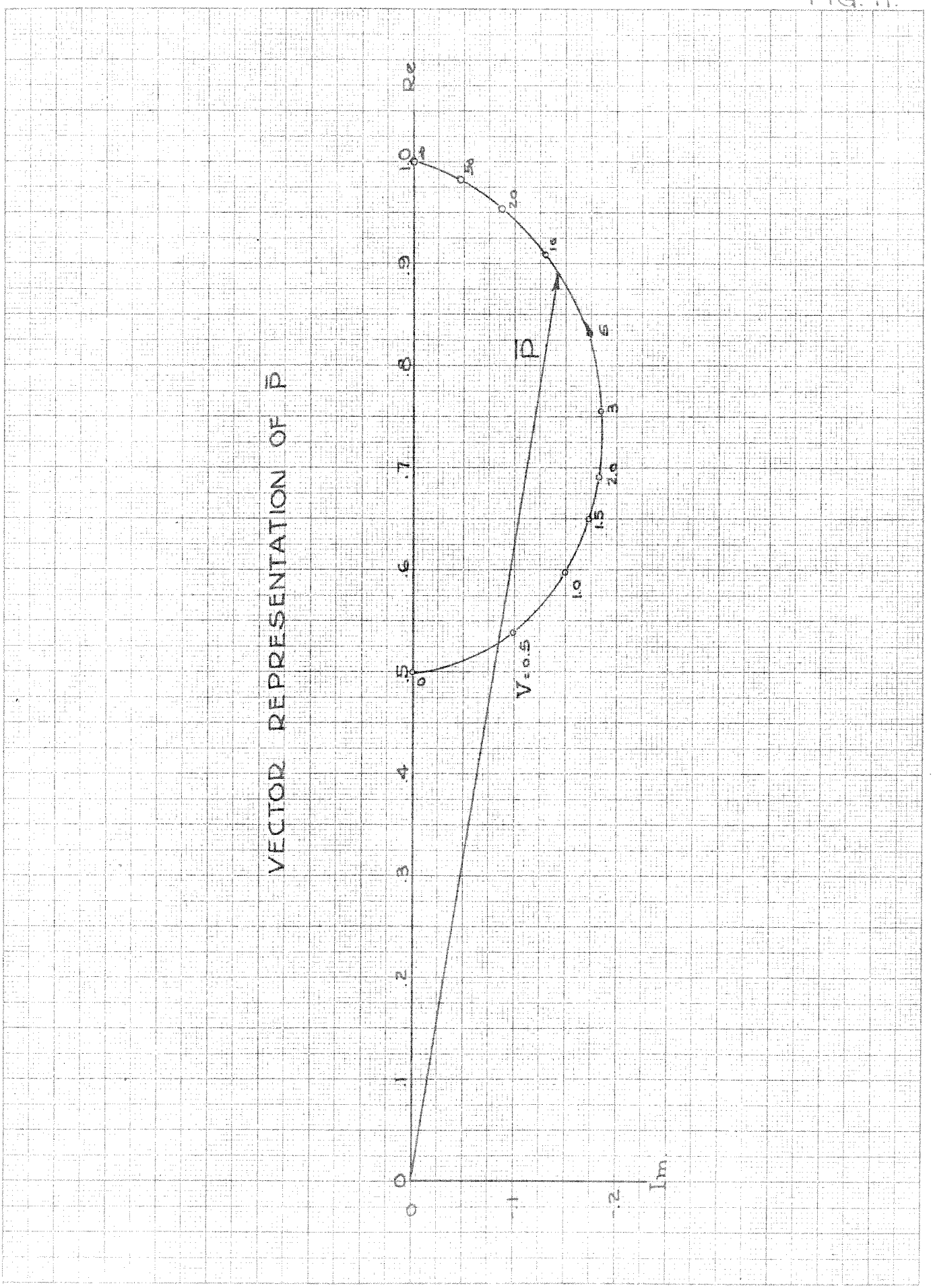
VECTOR REPRESENTATION OF $\bar{P}$
Re
Im
$\bar{P}$
V = 0.5
0
.1
.5
2.0
1.6
.5
3
2.0
1.5
1.0
.5
0
.9
.8
.7
.6
.4
.3
.2
.1
0
-.1
-.2

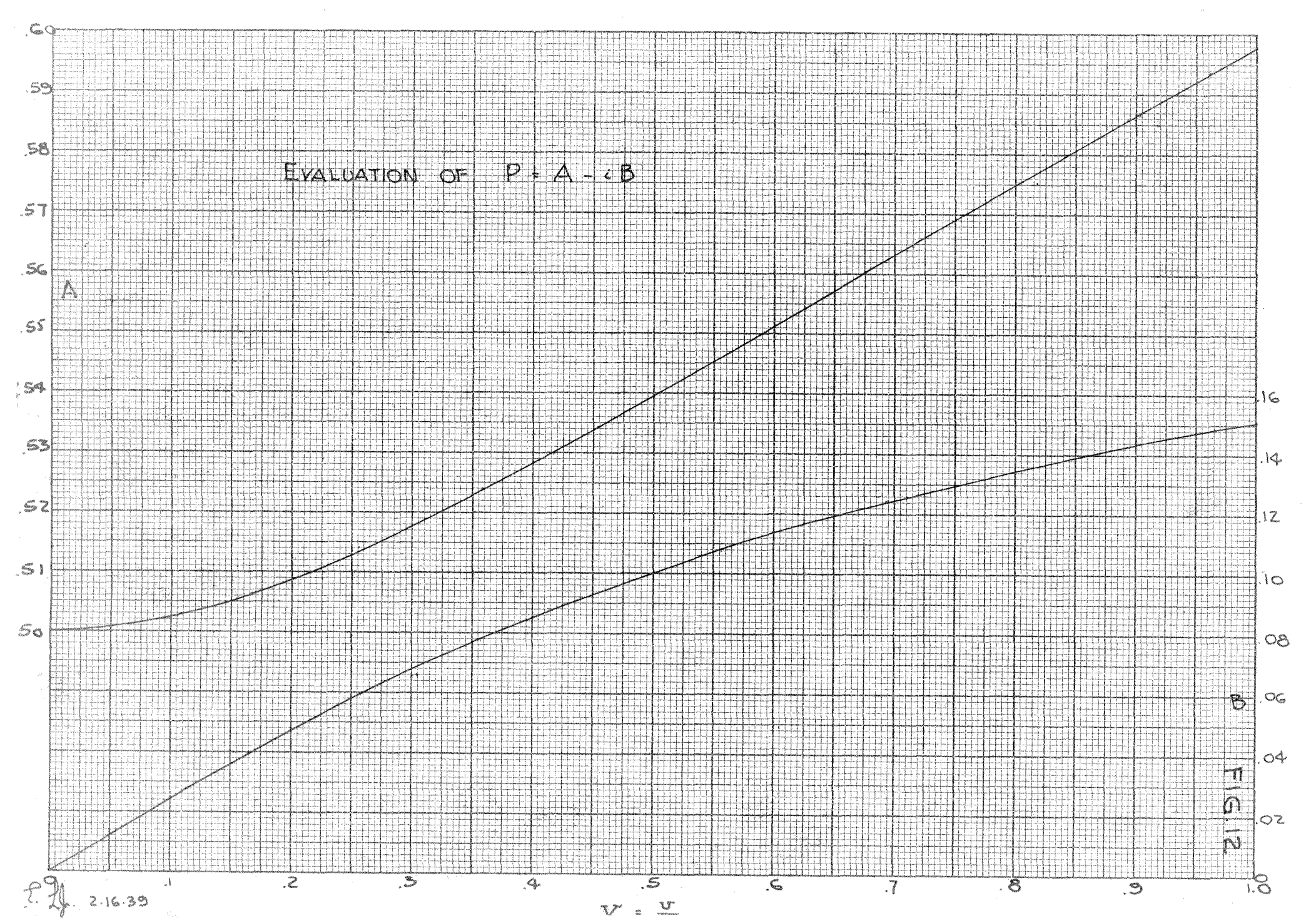
EVALUATION OF P = A - ¿B
A
B
.60
.59
.58
.57
.56
.55
.54
.53
.52
.51
.50
.16
.14
.12
.10
.08
.06
.04
.02
0
.1
.2
.3
.4
.5
.6
.7
.8
.9
1.0
V = v/V
2.16.39

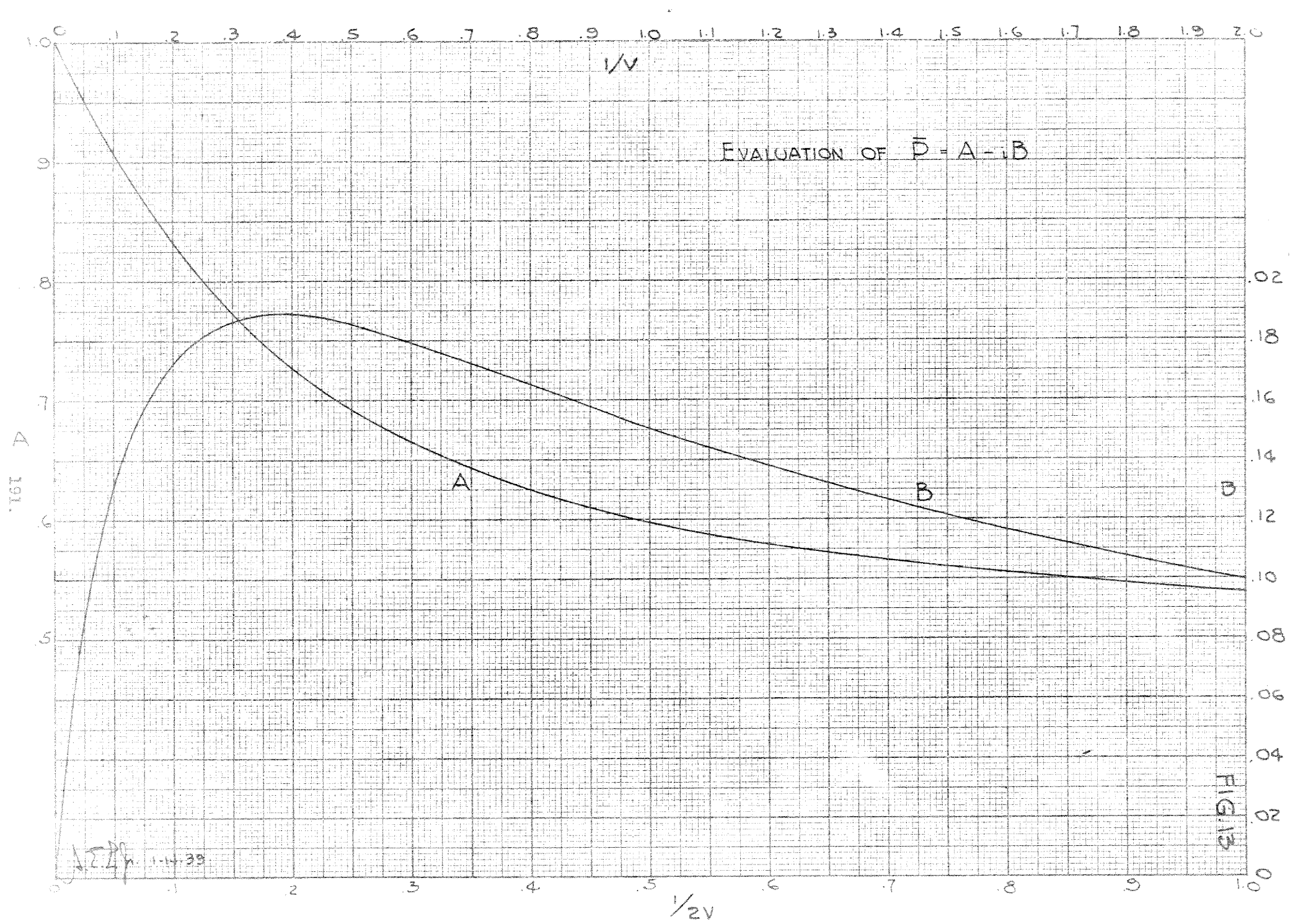
EVALUATION OF $\bar{D} = A - iB$
1/V
1/2V
A
B
D
.02
.18
.16
.14
.12
.10
.08
.06
.04
.02
0
1.0
.9
.8
.7
.6
.5
.1
.2
.3
.4
.5
.6
.7
.8
.9
1.0
1.1
1.2
1.3
1.4
1.5
1.6
1.7
1.8
1.9
2.0

FIG 13

FIG. 14.

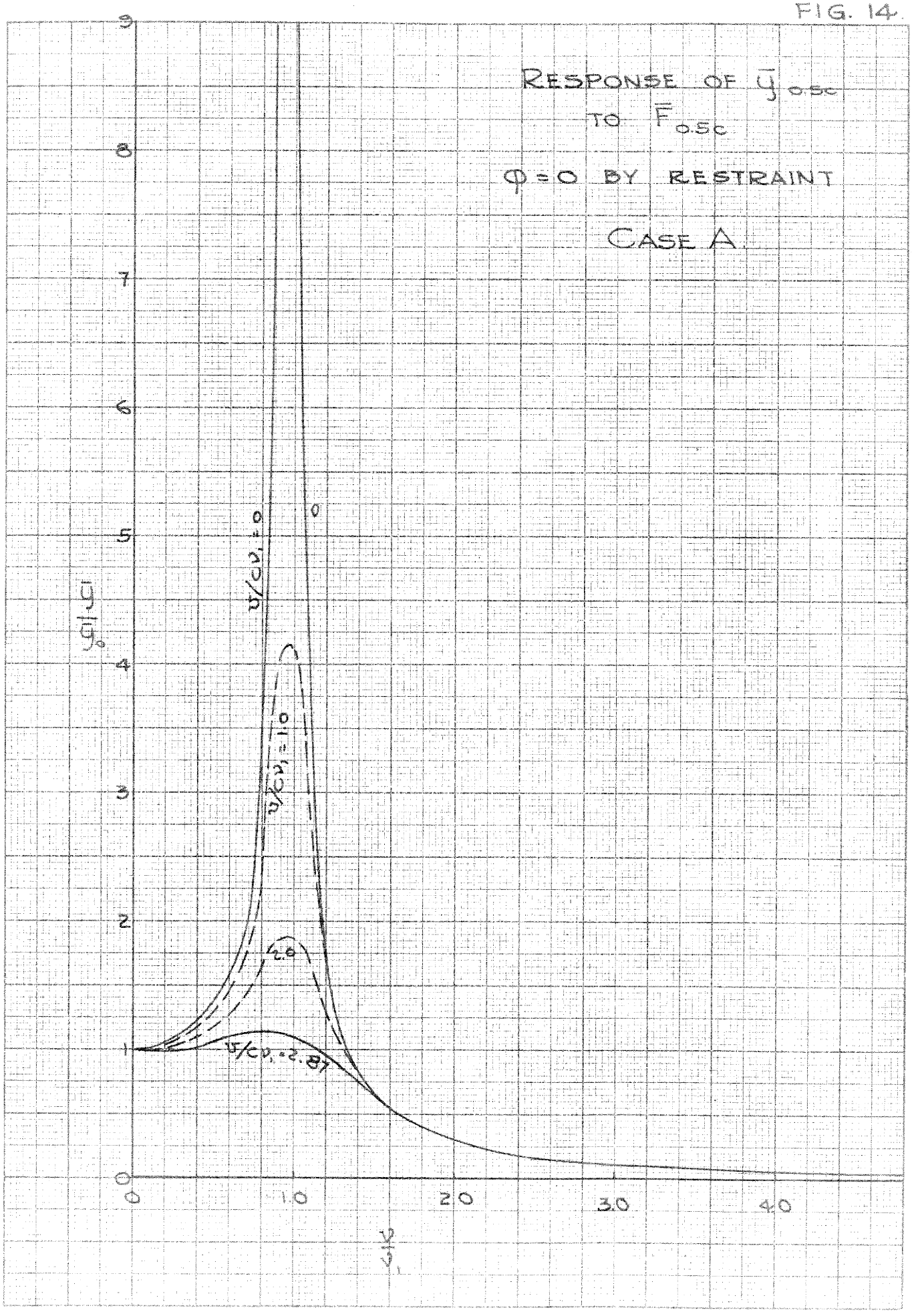
RESPONSE OF $\bar{y}_{o.sc}$
TO $\bar{F}_{o.sc}$
$\varphi = 0$ BY RESTRAINT
CASE A
$y/y_1 = 0$
$y/y_1 = 1.0$
2.0
$y/y_1 = 2.87$
$\bar{y}/y_1$
y_0/y_1
0
1.0
2.0
3.0
4.0
1
2
3
4
5
6
7
8
9

FIG. 15.

PHASE OF $\bar{q}_{0.5c}$ TO $F_{0.5c}$

$\varphi = 0$ BY RESTRAINT

CASE A.

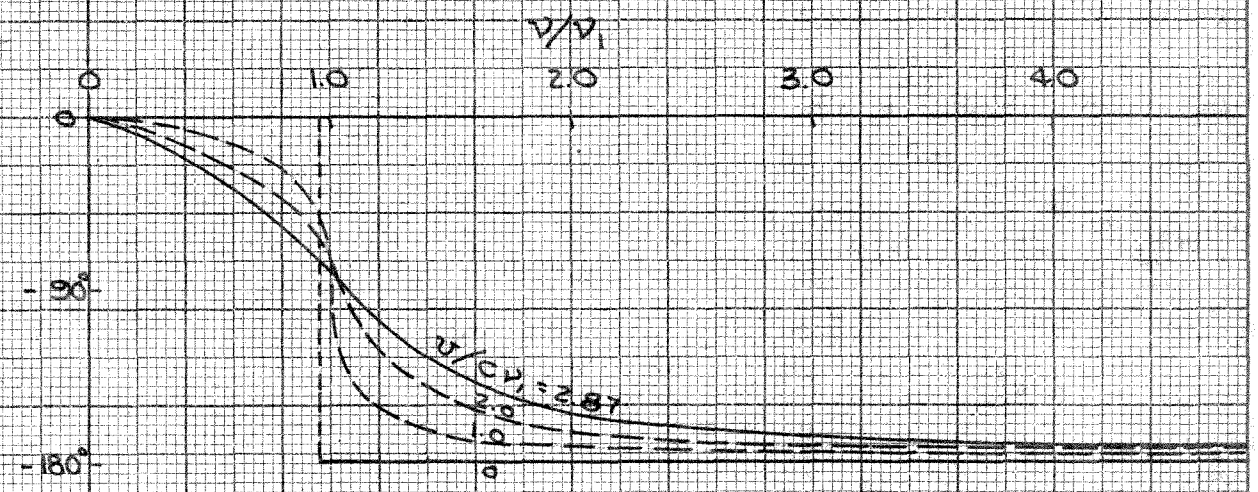

FIG. 16

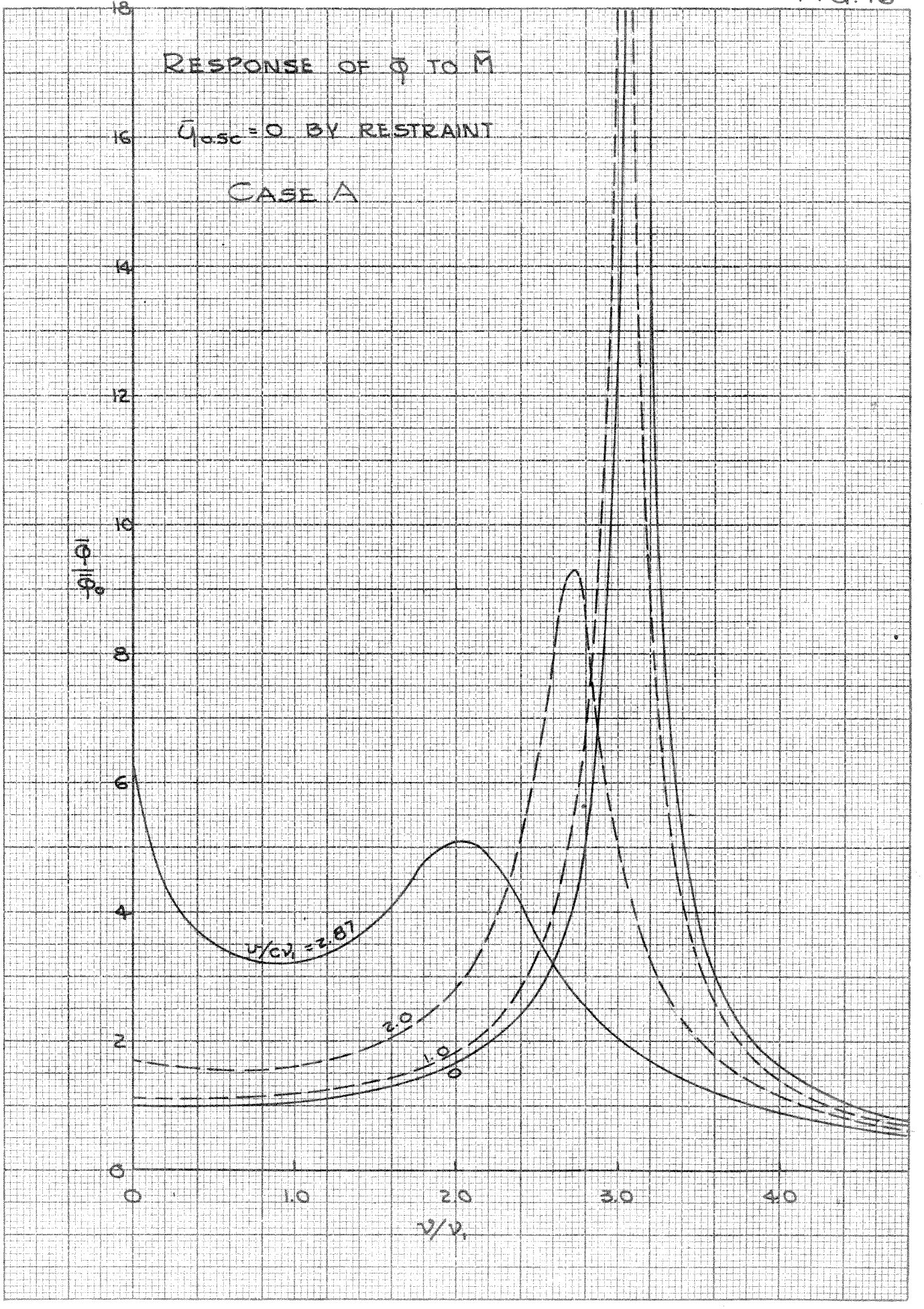
RESPONSE OF $\bar{\phi}$ TO $\bar{M}$
$\bar{Q}_{a.sc} = 0$ BY RESTRAINT
CASE A
$\frac{\theta - \theta_0}{\theta_0}$
$U/cv_1 = 2.87$
2.0
1.0
0
v/v_1
0
1.0
2.0
3.0
4.0
2
4
6
8
10
12
14
16
18

FIG. 17.

PHASE OF $\bar{\Phi}$ TO $\bar{M}$

$\bar{y} = 0$ BY RESTRAINT

CASE A

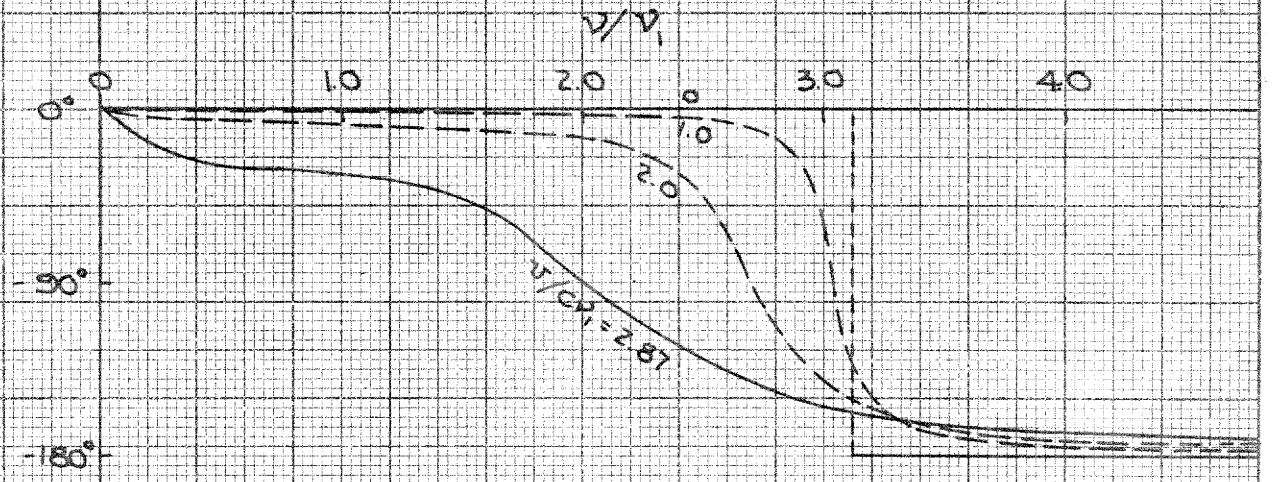

FIG. 18.

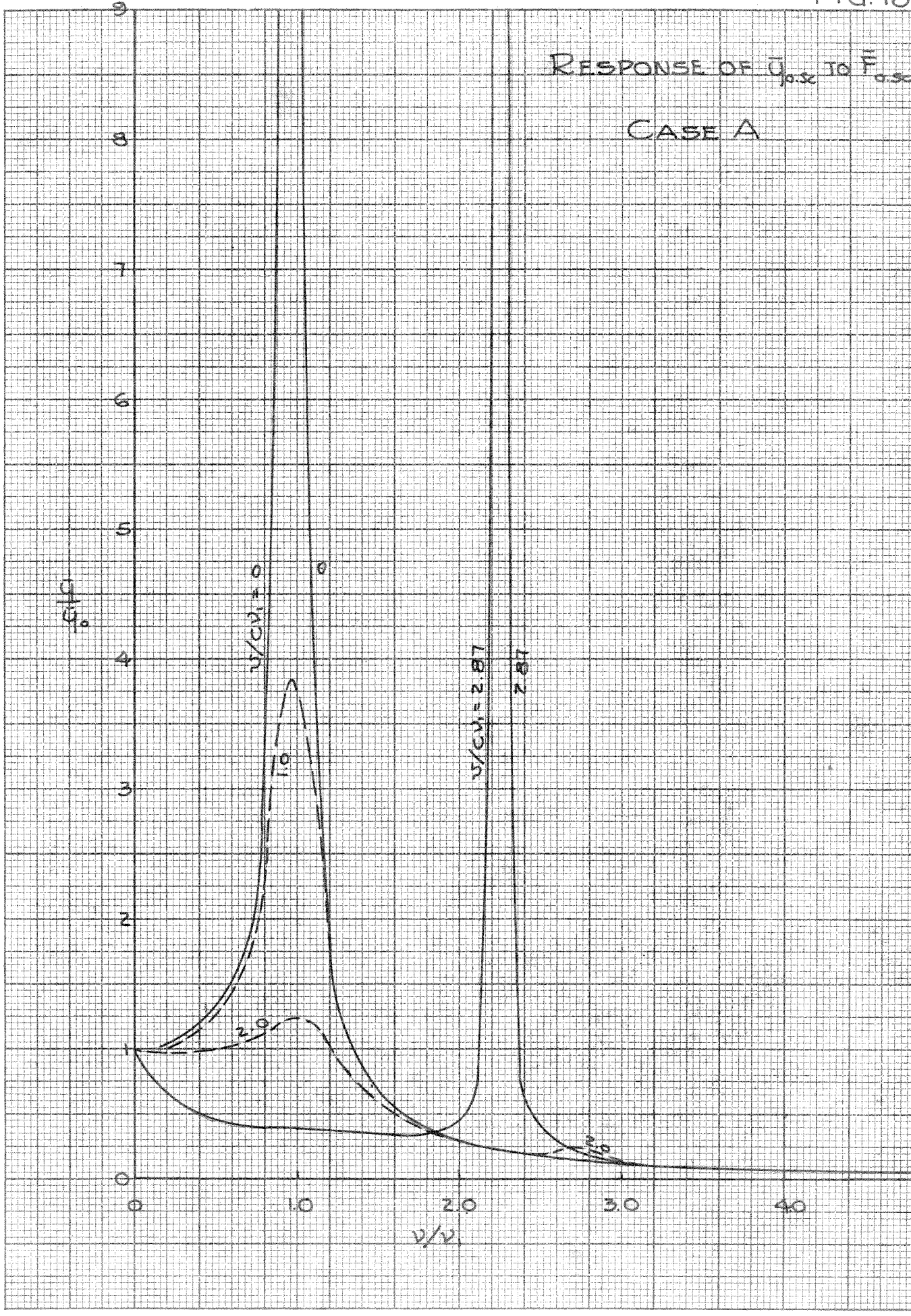
RESPONSE OF $\bar{q}_{o.sc}$ TO $\bar{F}_{o.sc}$
CASE A
$\bar{q}_{o.sc}$
ν/ν_1
$\nu/\nu_1 = 0$
0
0.1
2.0
$\nu/\nu_1 = 2.87$
2.87
2.0
0
1.0
2.0
3.0
4.0
1
2
3
4
5
6
7
8
9

FIG. 19

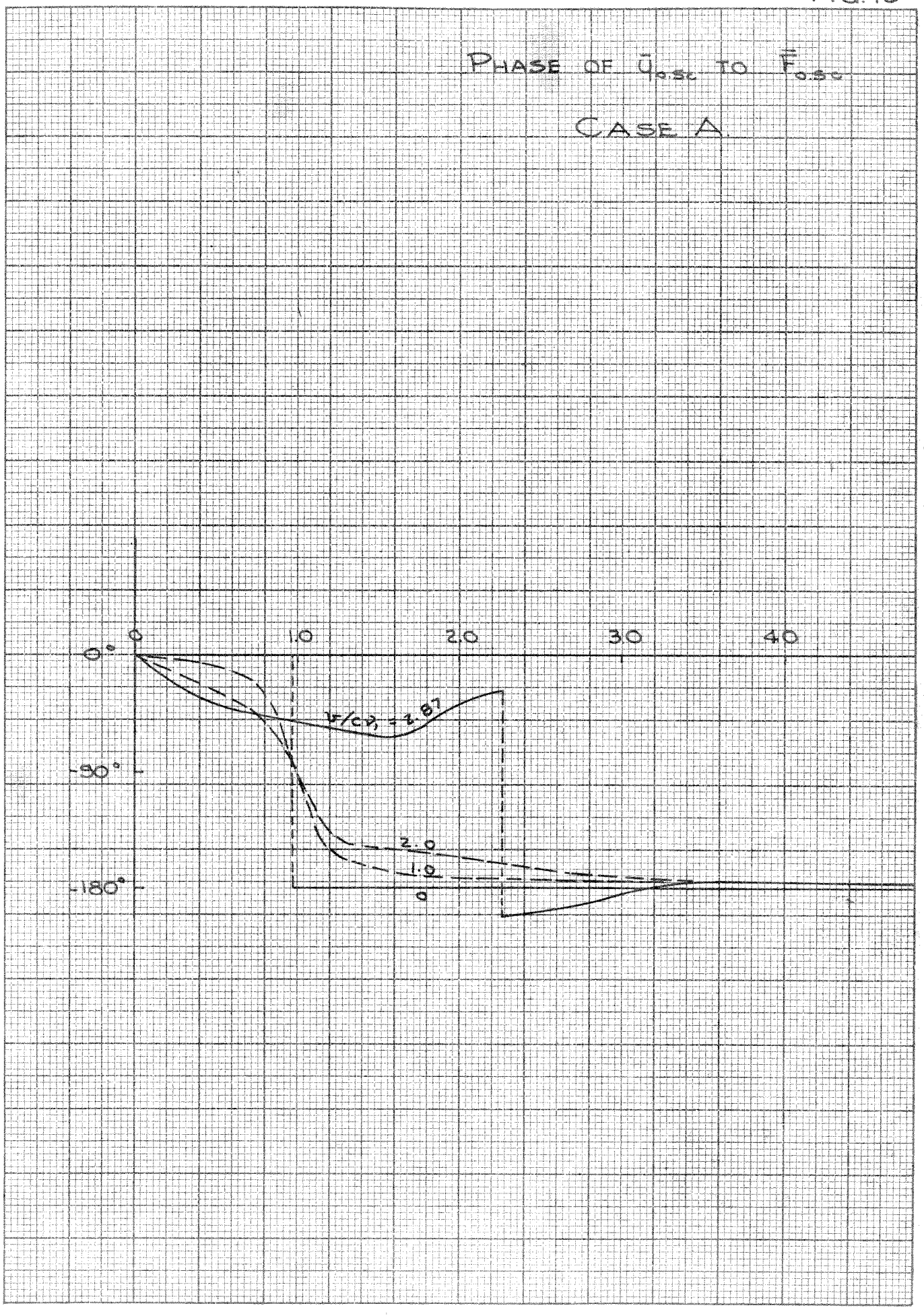
PHASE OF $\ddot{u}_{o.sc}$ TO $\bar{F}_{o.sc}$
CASE A.
0°
-90°
-180°
0
1.0
2.0
3.0
4.0
$\bar{u}/c\bar{v}_1 = 2.87$
2.0
1.0
0

FIG. 20

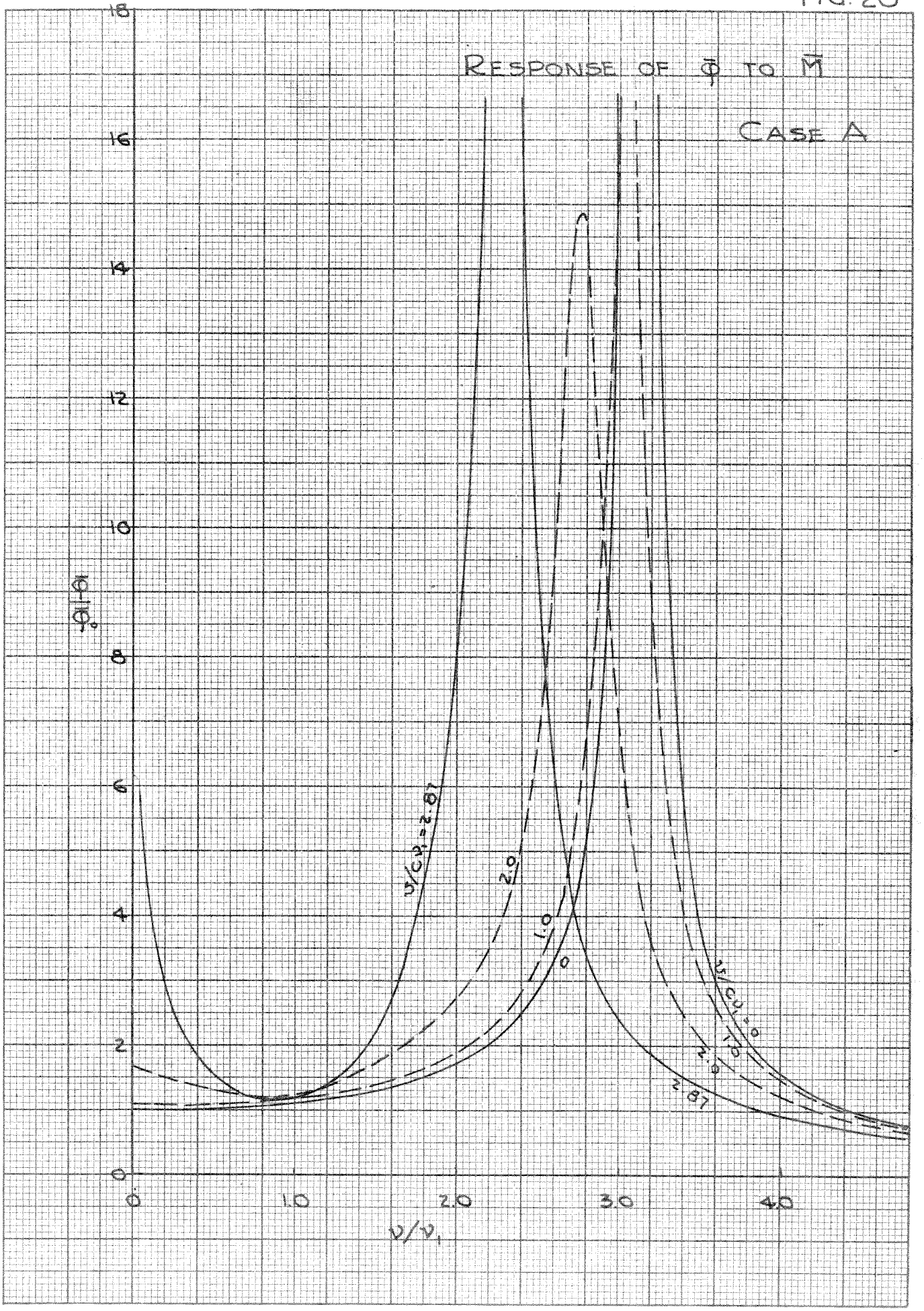
RESPONSE OF Φ TO M̄
CASE A
18
16
14
12
10
8
6
4
2
0
0
1.0
2.0
3.0
4.0
ν/ν₁
|Φ|/Φ₀
ν/ν₁ = 2.87
2.0
1.0
0
ν/ν₁ = 0
1.0
2.0
2.87

FIG. 21

PHASE OF $\bar{\varphi}$ TO $\bar{M}$

CASE A.

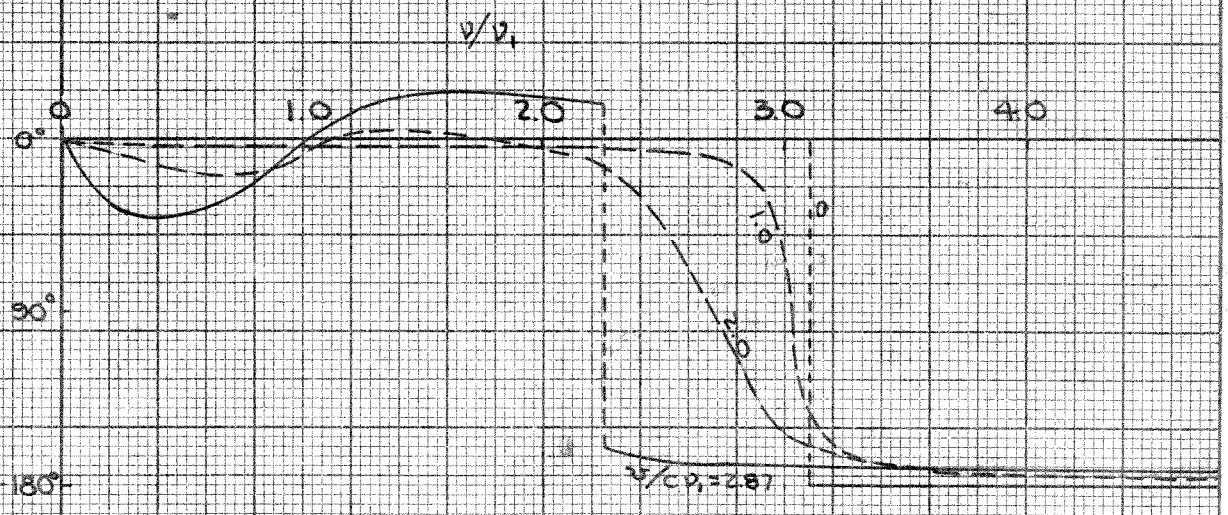

FIG. 22

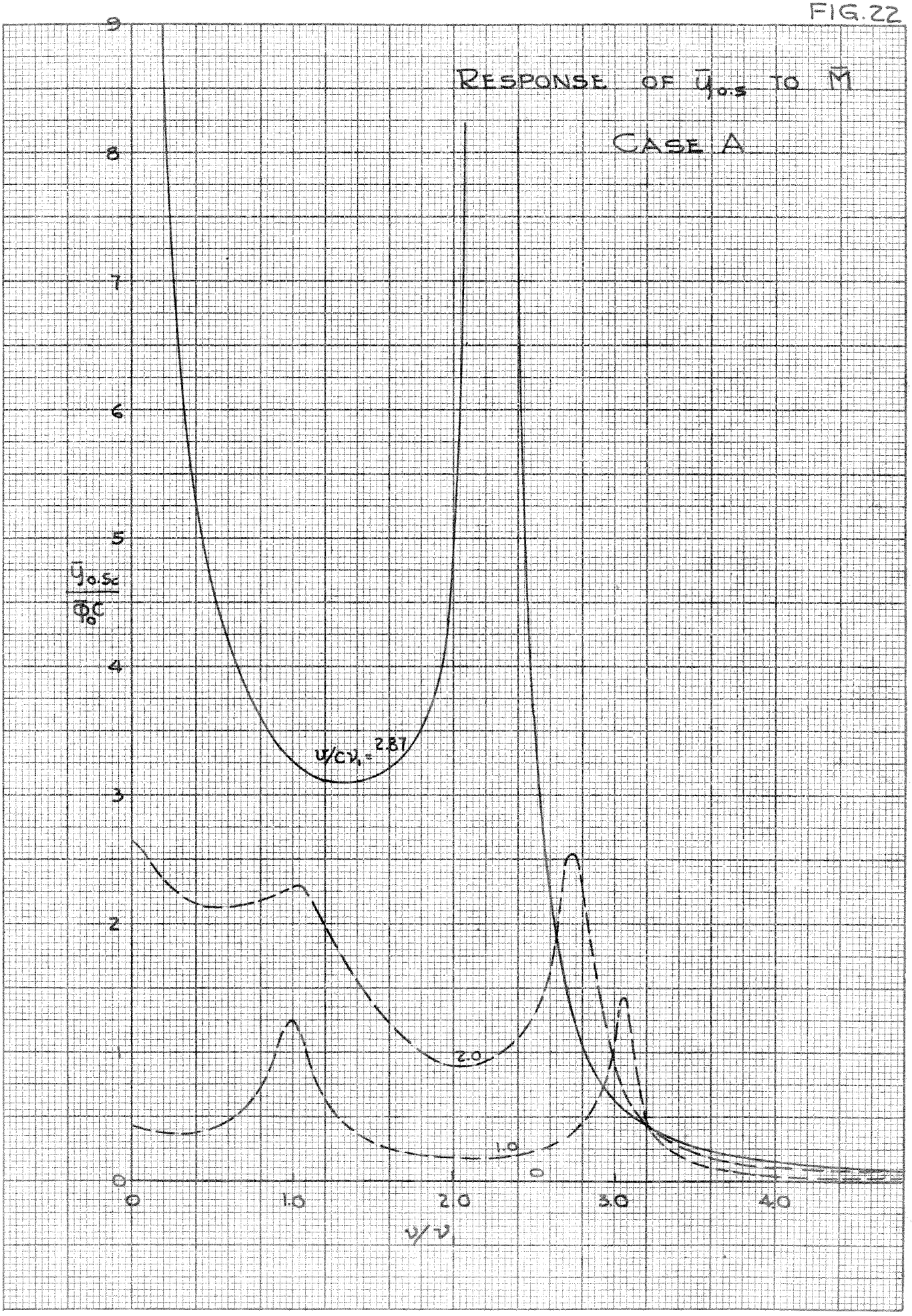
RESPONSE OF $\bar{u}_{0.5}$ TO $\bar{M}$
CASE A
$\frac{\bar{u}_{0.5c}}{\Phi_0 c}$
$u/cv_1 = 2.87$
2.0
1.0
0
0
1.0
2.0
3.0
4.0
v/v_1

FIG. 23

PHASE OF $\bar{y}_{0.5c}$ TO $\bar{M}$

CASE A

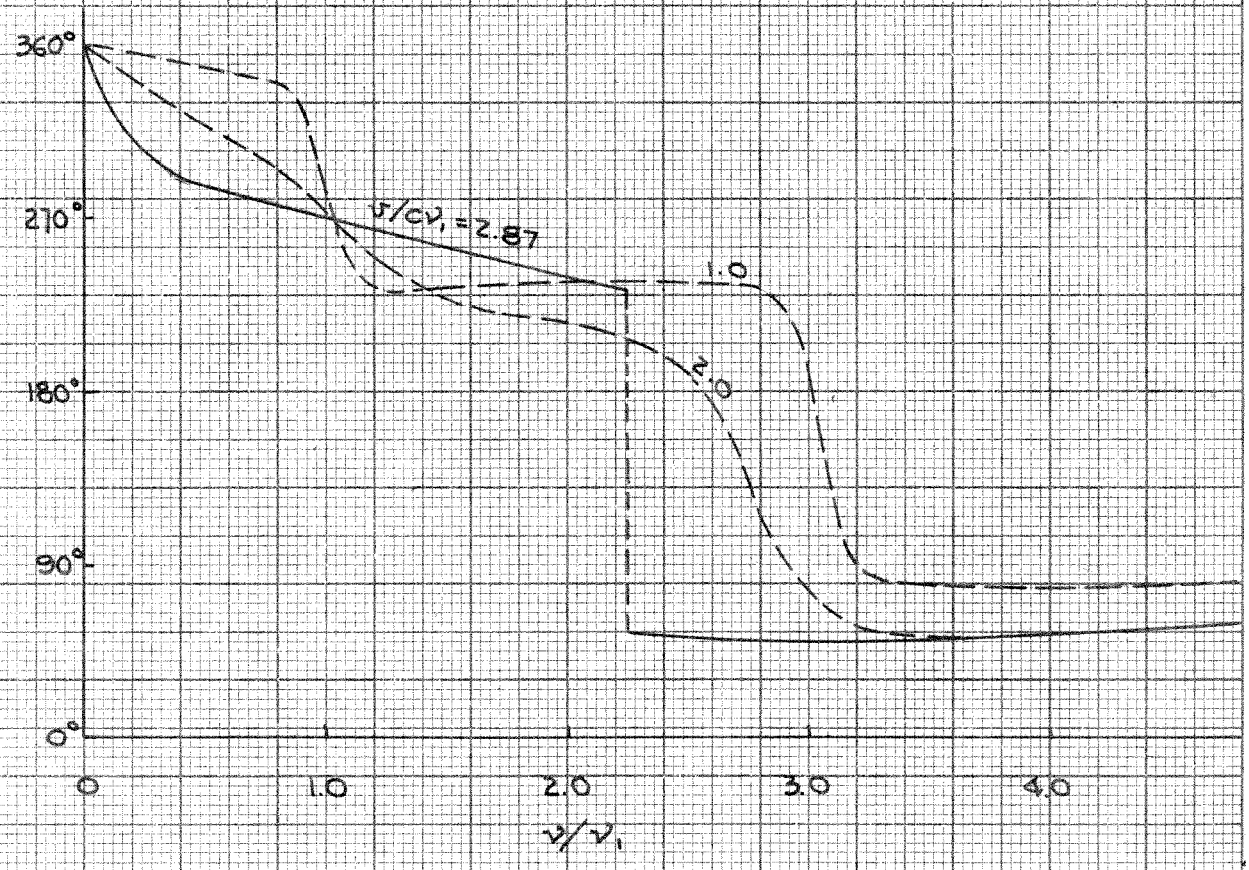

FIG. 24

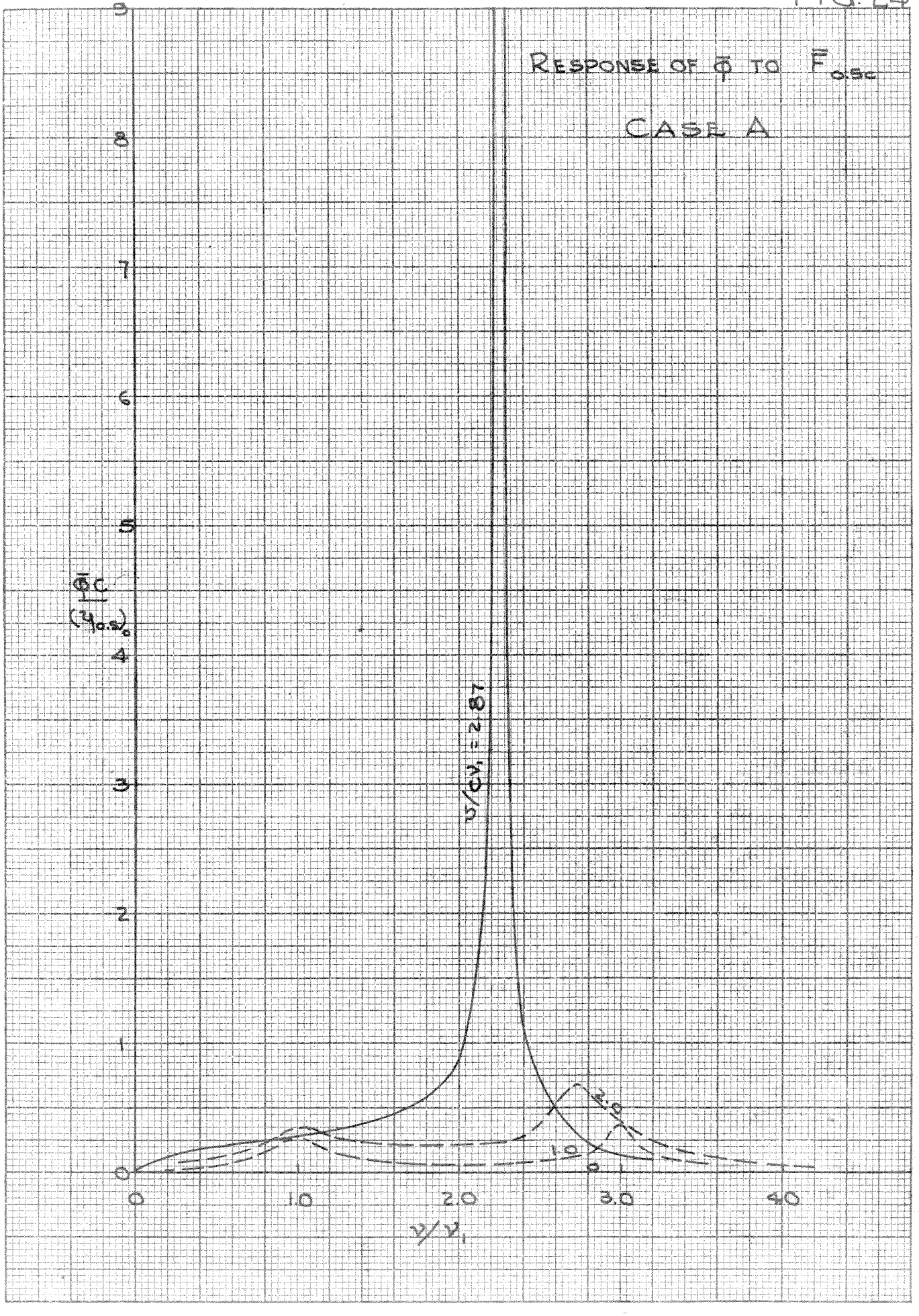
RESPONSE OF $\bar{\phi}$ TO $\bar{F}_{o.sc}$
CASE A
$\frac{\bar{\phi}_c}{(\bar{\gamma}_{o.s})_o}$
$\nu/\nu_1 = 2.87$
2.0
1.0
0
0
1.0
2.0
3.0
4.0
ν/ν_1

FIG. 25

PHASE OF $\bar{\varphi}$ TO $F_{0.5C}$

CASE A

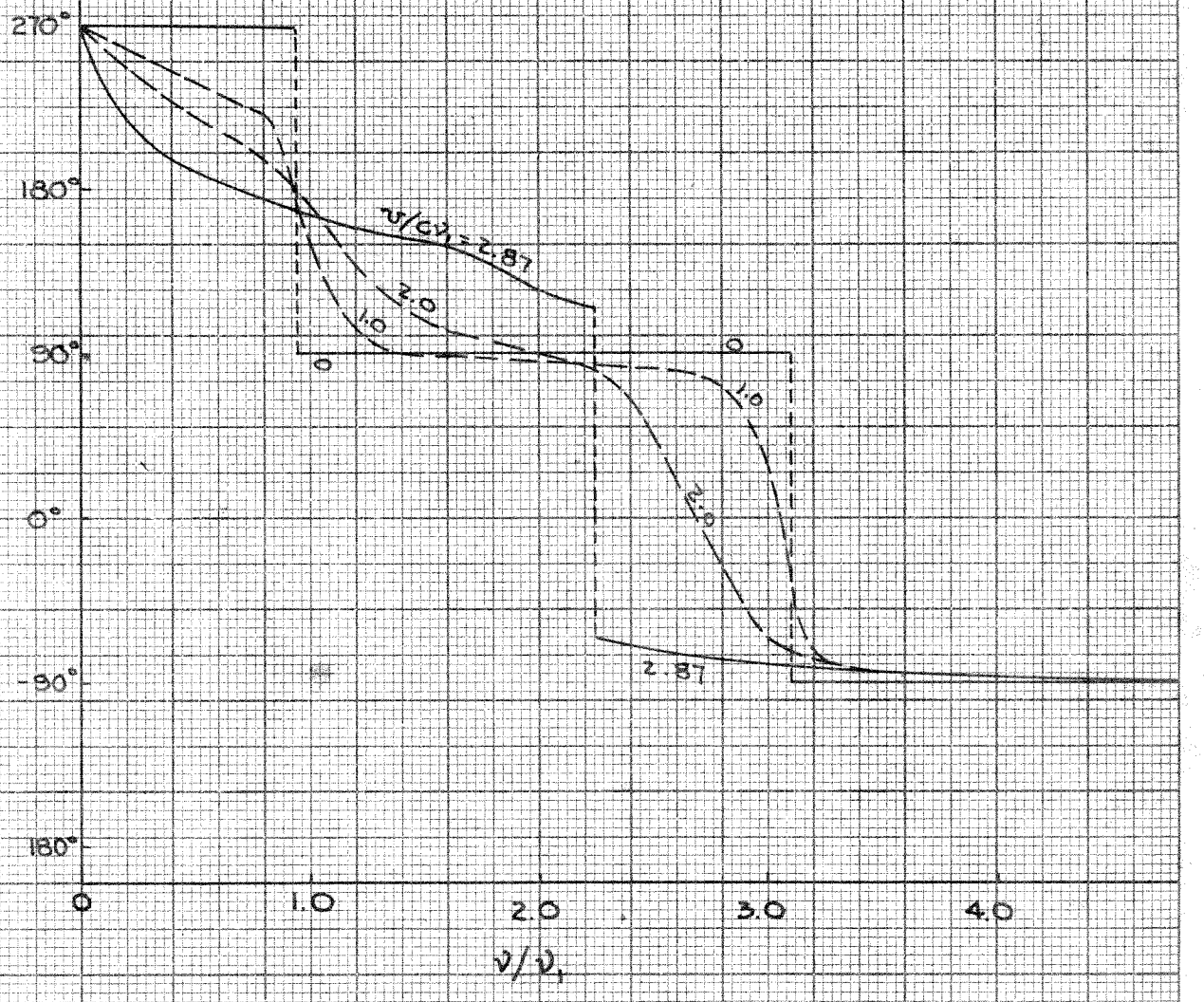

FIG. 26

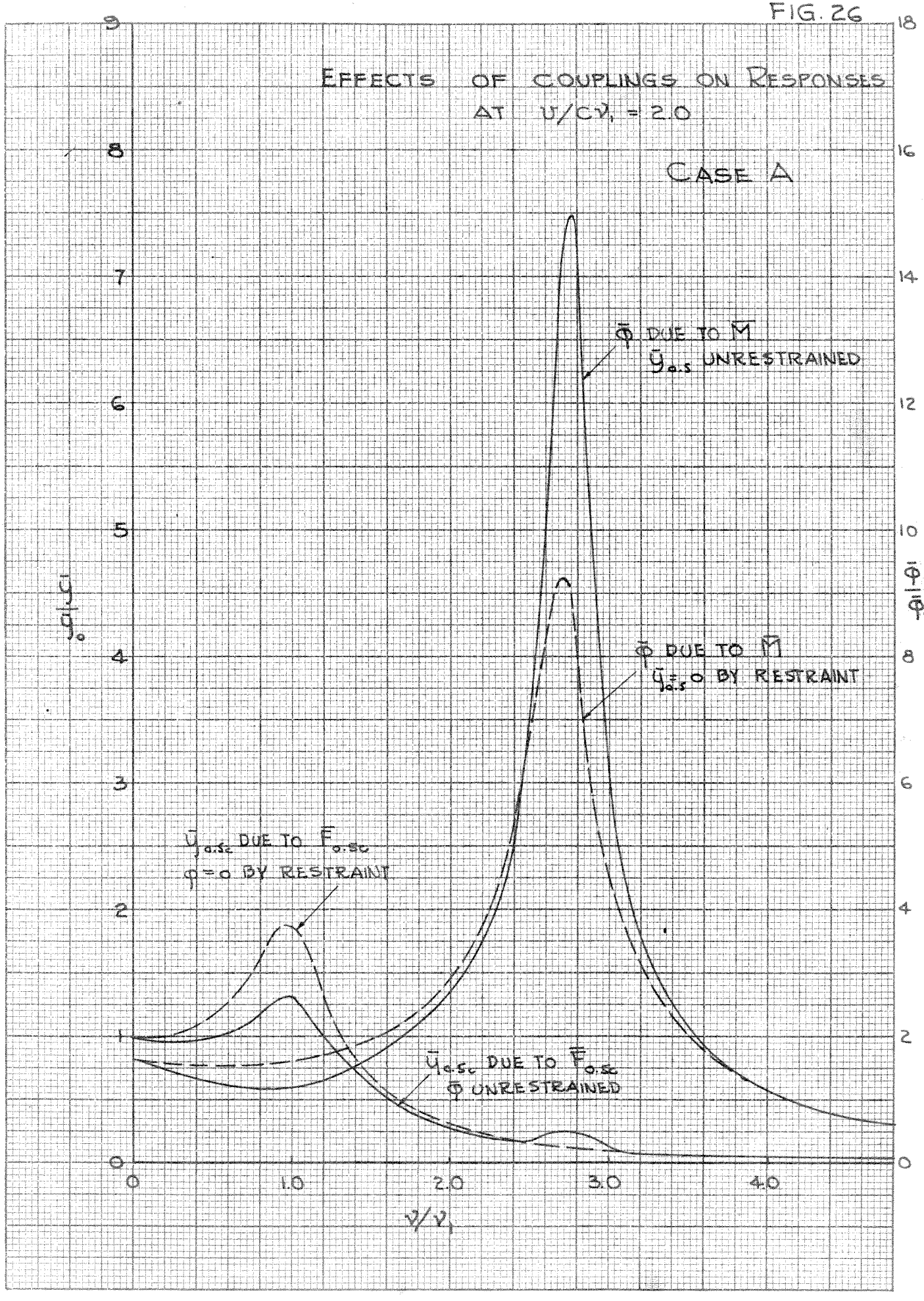
EFFECTS OF COUPLINGS ON RESPONSES
AT U/CV₁ = 2.0
CASE A
φ̄ DUE TO M̄
ȳ₀.s UNRESTRAINED
φ̄ DUE TO M̄
ȳ₀.s = 0 BY RESTRAINT
ȳ₀.s.c DUE TO F̄₀.s.c
φ = 0 BY RESTRAINT
ȳ₀.s.c DUE TO F̄₀.s.c
φ̄ UNRESTRAINED
ȳ/ȳ₀
φ̄/φ̄₀
V/V₁
0
1.0
2.0
3.0
4.0
0
1
2
3
4
5
6
7
8
9
0
2
4
6
8
10
12
14
16
18

FIG. 27

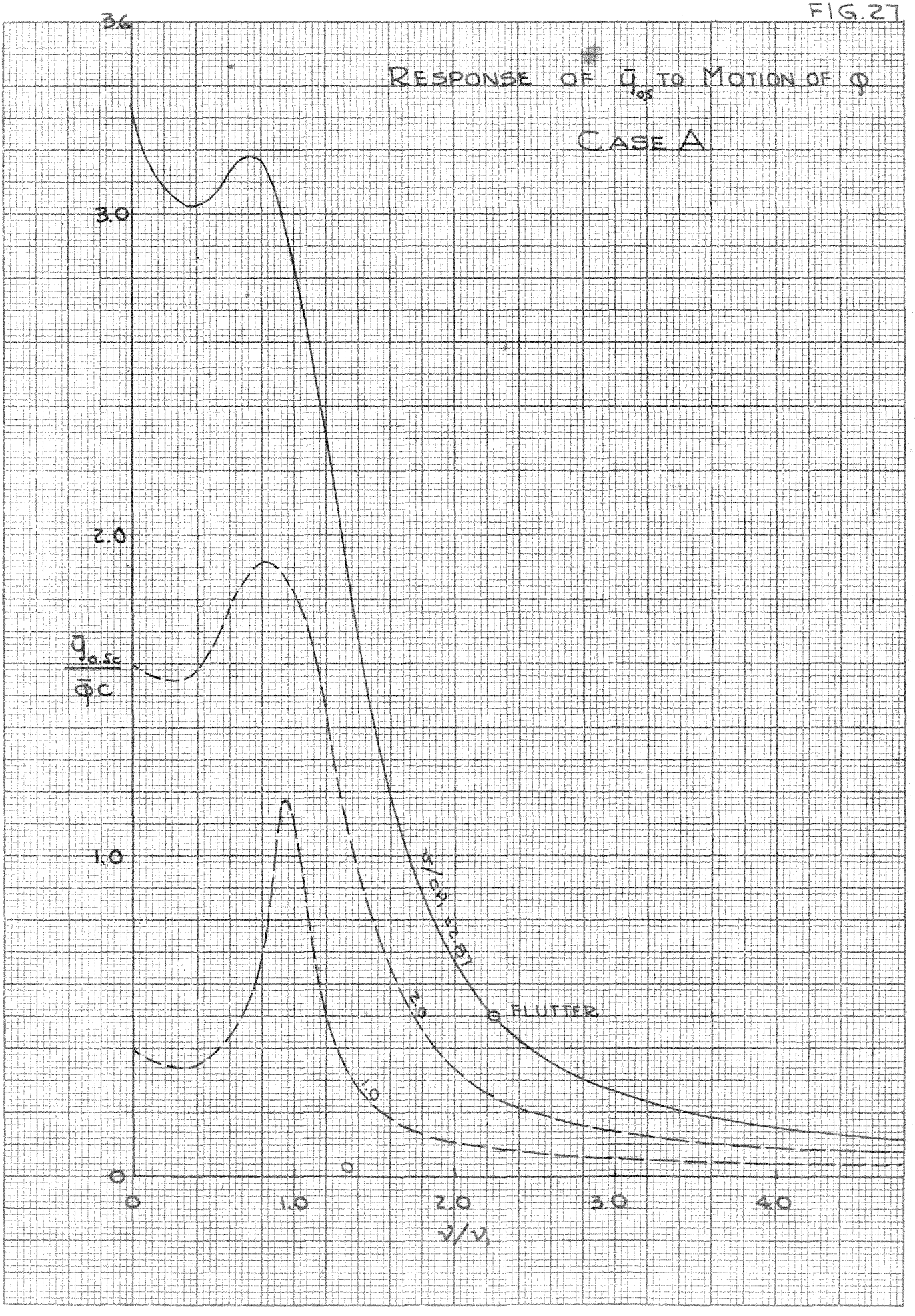
RESPONSE OF $\bar{y}_{0.5}$ TO MOTION OF φ
CASE A
3.6
3.0
2.0
1.0
0
$\frac{\bar{y}_{0.5c}}{\bar{\varphi}c}$
α/c_2 = 2.81
2.0
1.0
FLUTTER
0
1.0
2.0
3.0
4.0
v/v_1

FIG. 28

PHASE OF $\bar{q}_{osc}$ TO MOTION OF $\bar{\phi}$

CASE A.

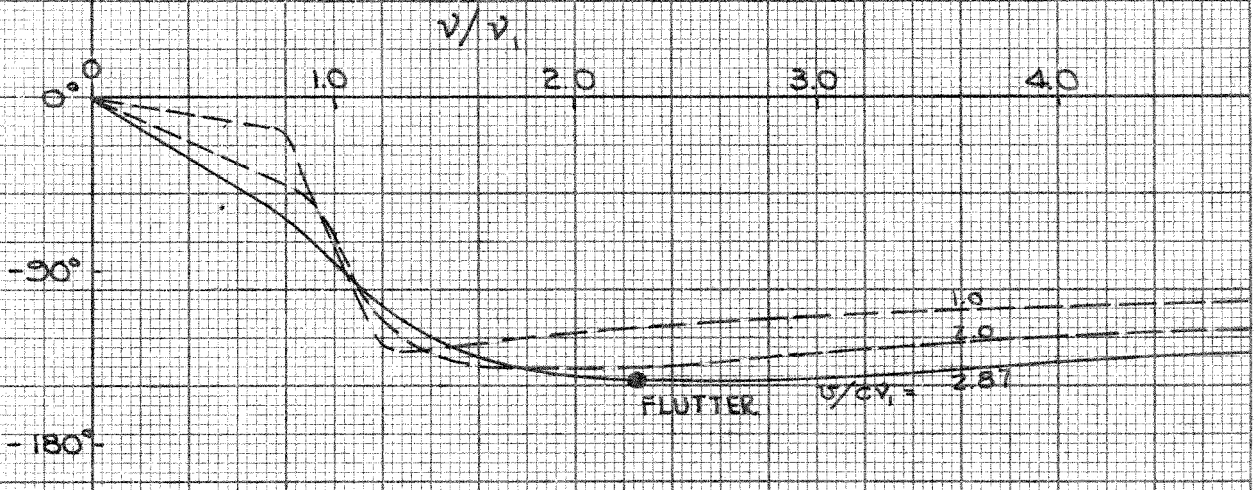

FIG. 29

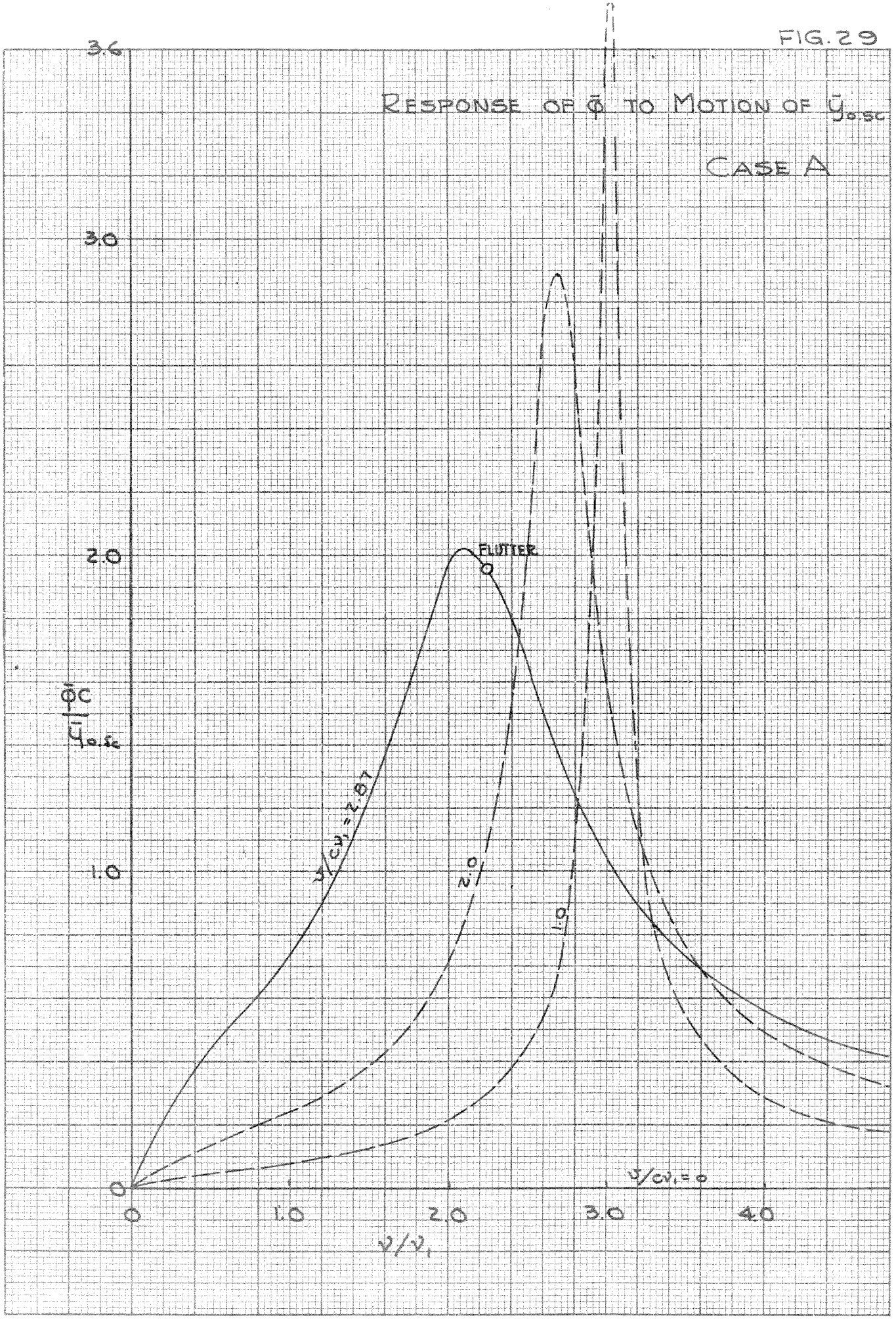
RESPONSE OF $\bar{\phi}$ TO MOTION OF $\bar{y}_{0.5c}$
CASE A
3.6
3.0
2.0
1.0
0
$\frac{\phi c}{\bar{y}_{0.5c}}$
FLUTTER
$y/cv_1 = 2.67$
2.0
1.0
$y/cv_1 = 0$
0
1.0
2.0
3.0
4.0
v/v_1

FIG. 30

PHASE OF $\bar{\phi}$ TO MOTION OF $y_{o.sc}$

CASE A

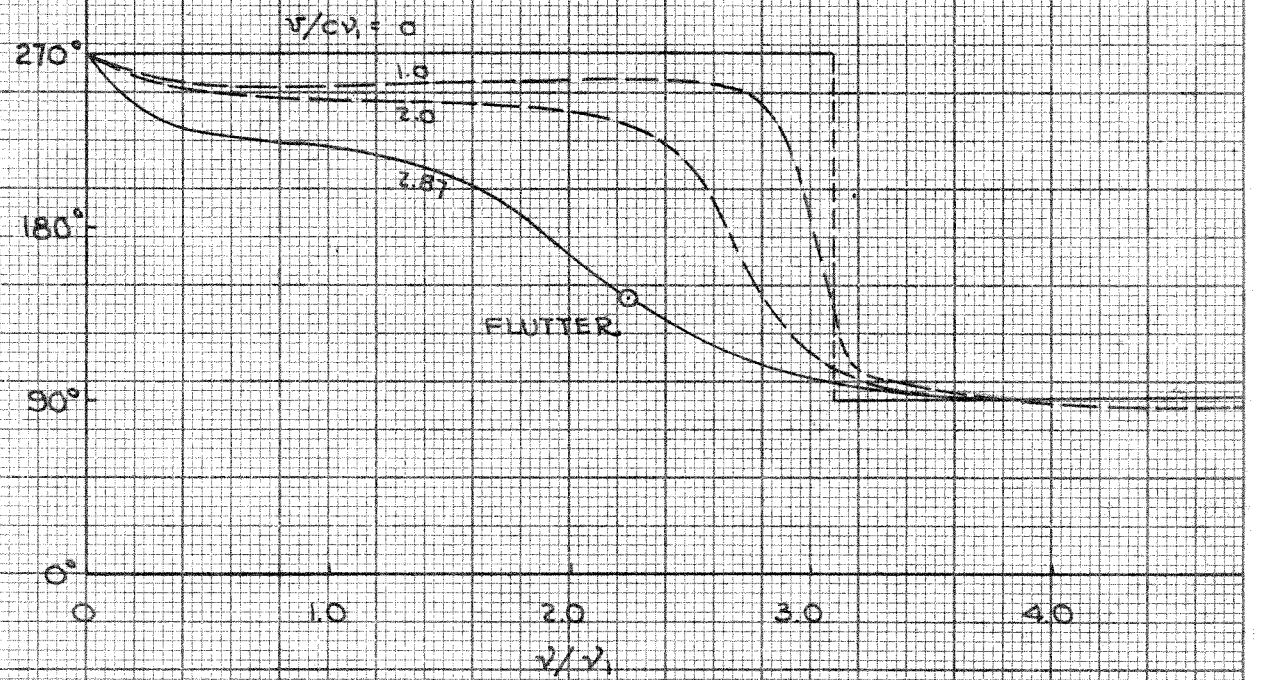

FIG. 31.

FREQUENCY FOR MAXIMUM RESPONSE AS FUNCTION OF AIRSPEED

CASE A.

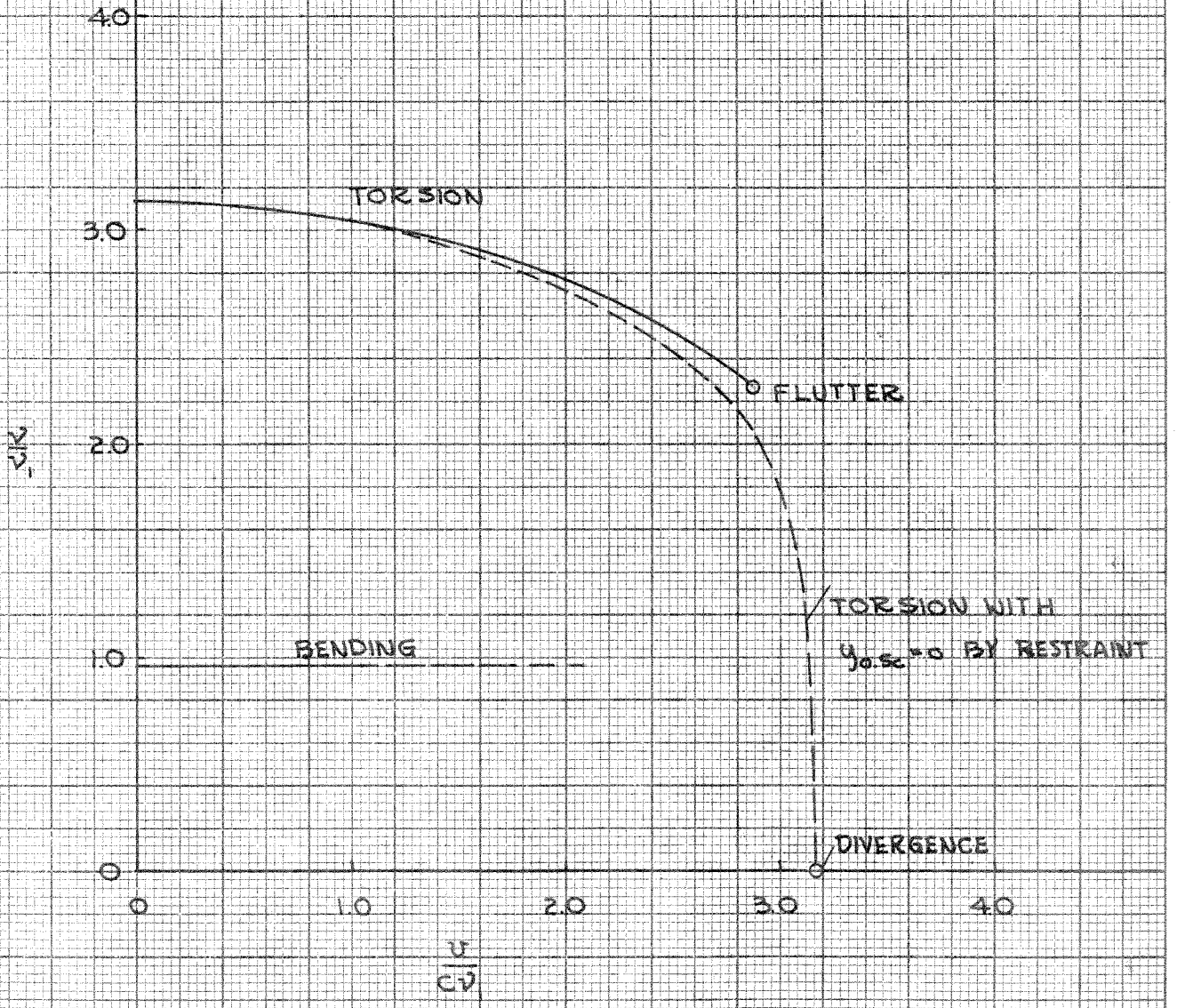

FIG. 32

SOLUTION OF DETERMINANT EQUATIONS FOR STABILITY LIMIT

CASE A

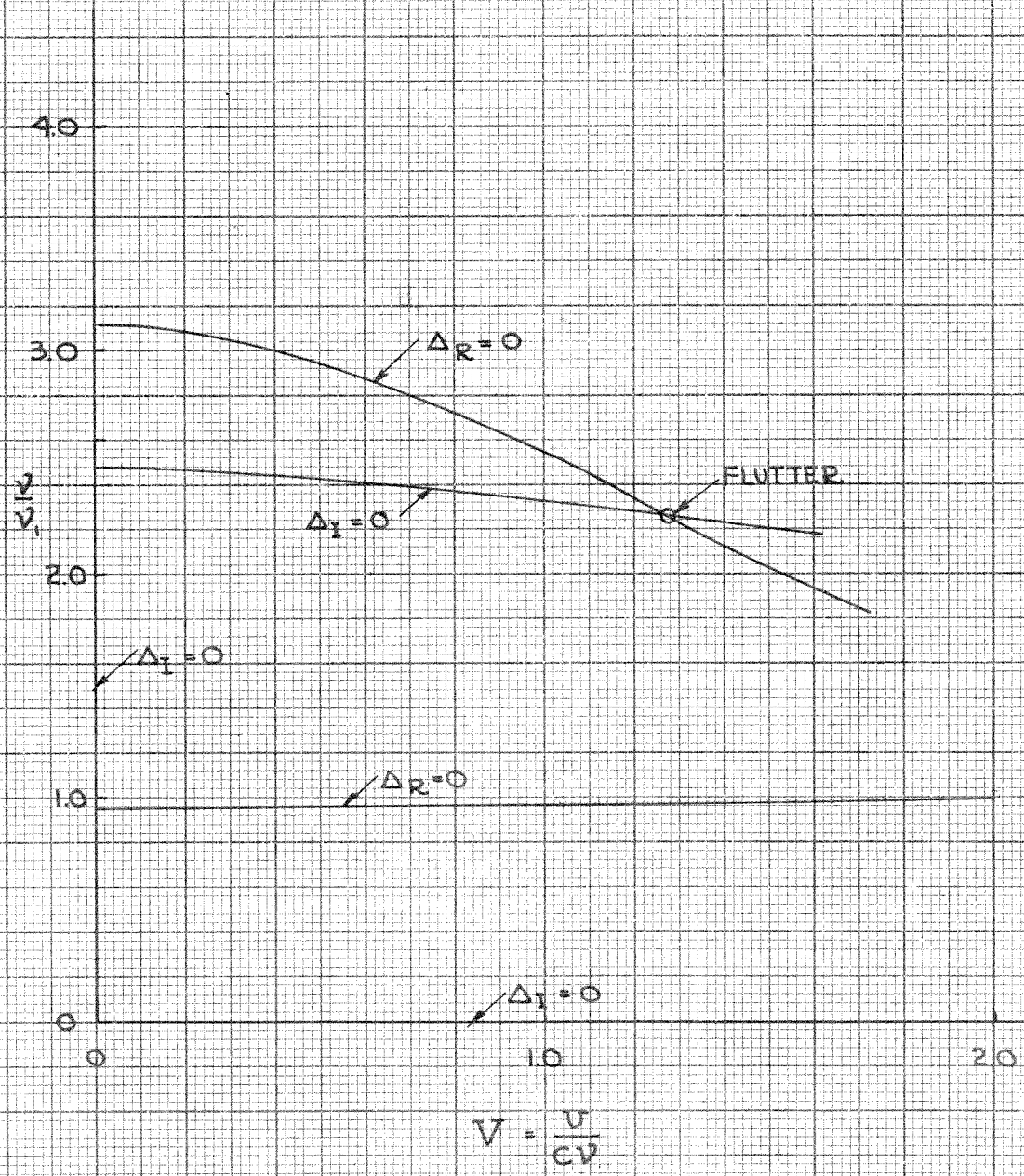

FIG. 33

POLAR DIAGRAM OF CONDITIONS AT STABILITY LIMIT

CASE A

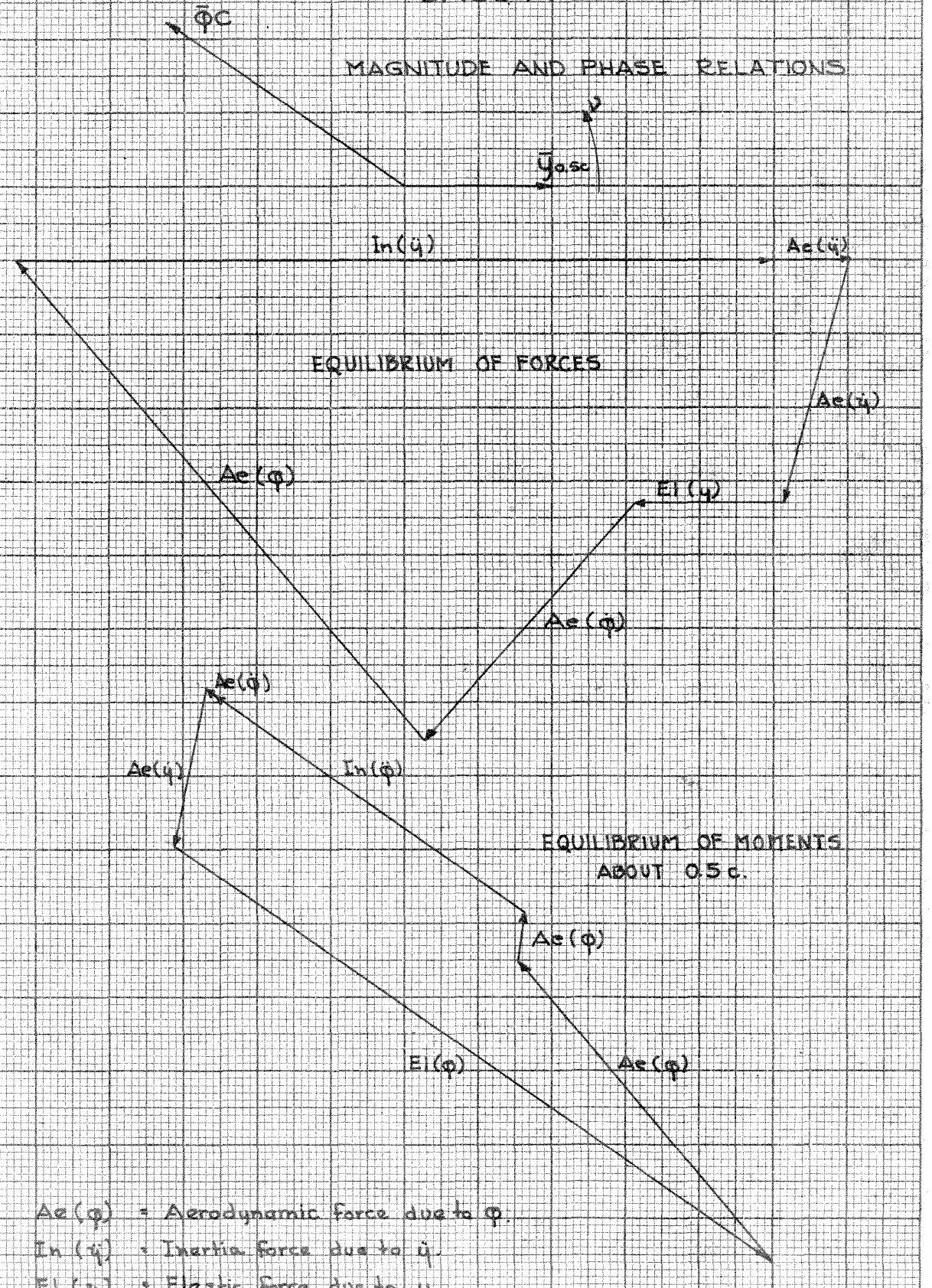

Ae(φ) = Aerodynamic force due to φ.

In(ÿ) = Inertia force due to ÿ.

El(y) = Elastic force due to y.

FIG. 34

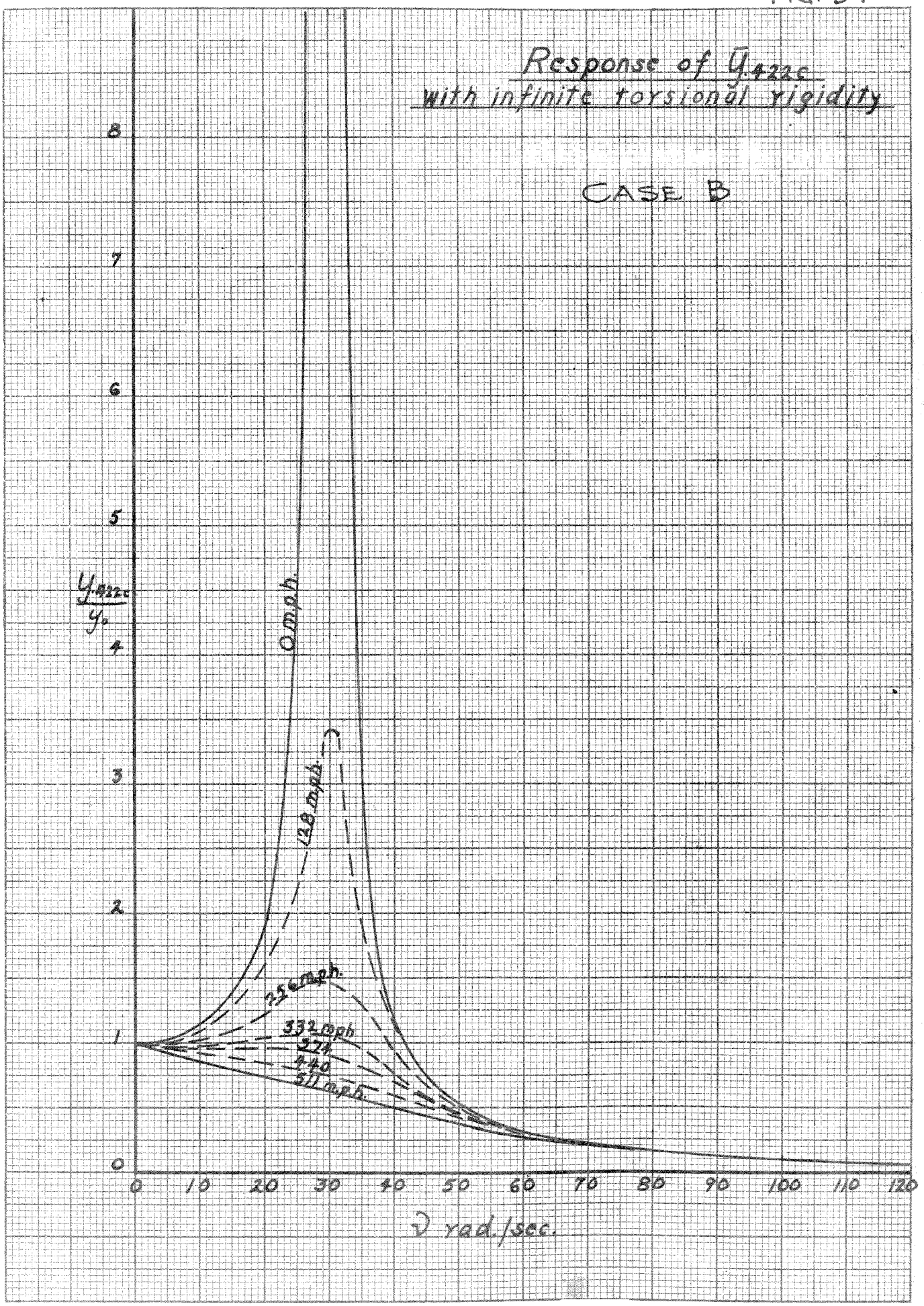
Response of $\bar{y}_{.422c}$
with infinite torsional rigidity
CASE B
$\frac{y_{.422c}}{y_0}$
0 m.p.h.
128 m.p.h.
275 m.p.h.
332 m.p.h.
374
440
511 m.p.h.
0
1
2
3
4
5
6
7
8
0
10
20
30
40
50
60
70
80
90
100
110
120
ν rad./sec.

FIG. 35

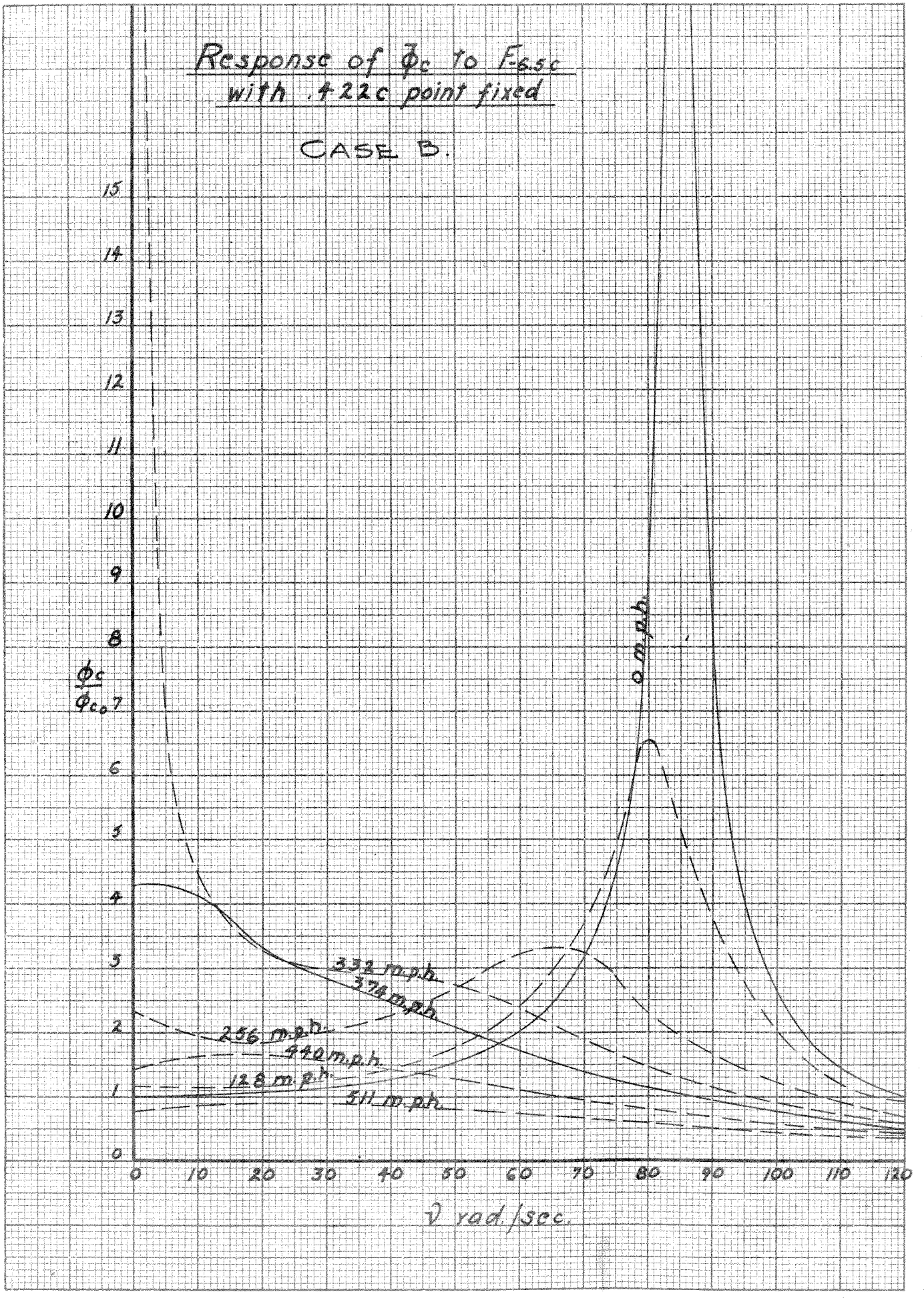
Response of ϕ_c to $F_{6.5c}$
with .422c point fixed
CASE B.
$\frac{\phi_c}{\phi_{c_0}}$
0 m.p.h.
332 m.p.h.
378 m.p.h.
256 m.p.h.
440 m.p.h.
128 m.p.h.
511 m.p.h.
0
1
2
3
4
5
6
7
8
9
10
11
12
13
14
15
0
10
20
30
40
50
60
70
80
90
100
110
120
ν rad./sec.

FIG. 36

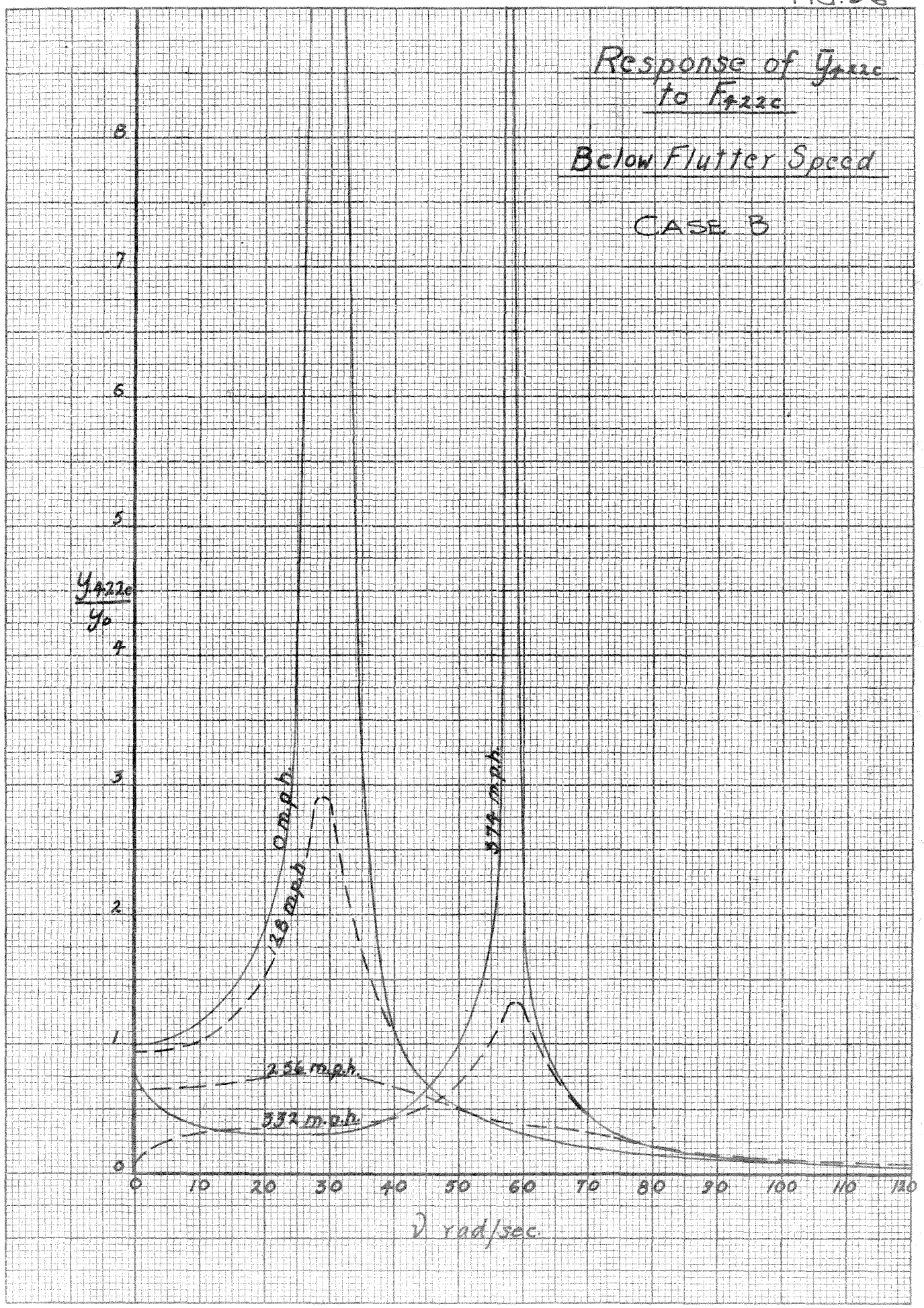
Response of y_{422c} to F_{422c}
Below Flutter Speed
CASE B
$\frac{y_{422c}}{y_0}$
0
1
2
3
4
5
6
7
8
0 m.p.h.
128 m.p.h.
256 m.p.h.
332 m.p.h.
374 m.p.h.
0
10
20
30
40
50
60
70
80
90
100
110
120
ν rad/sec.

FIG. 37

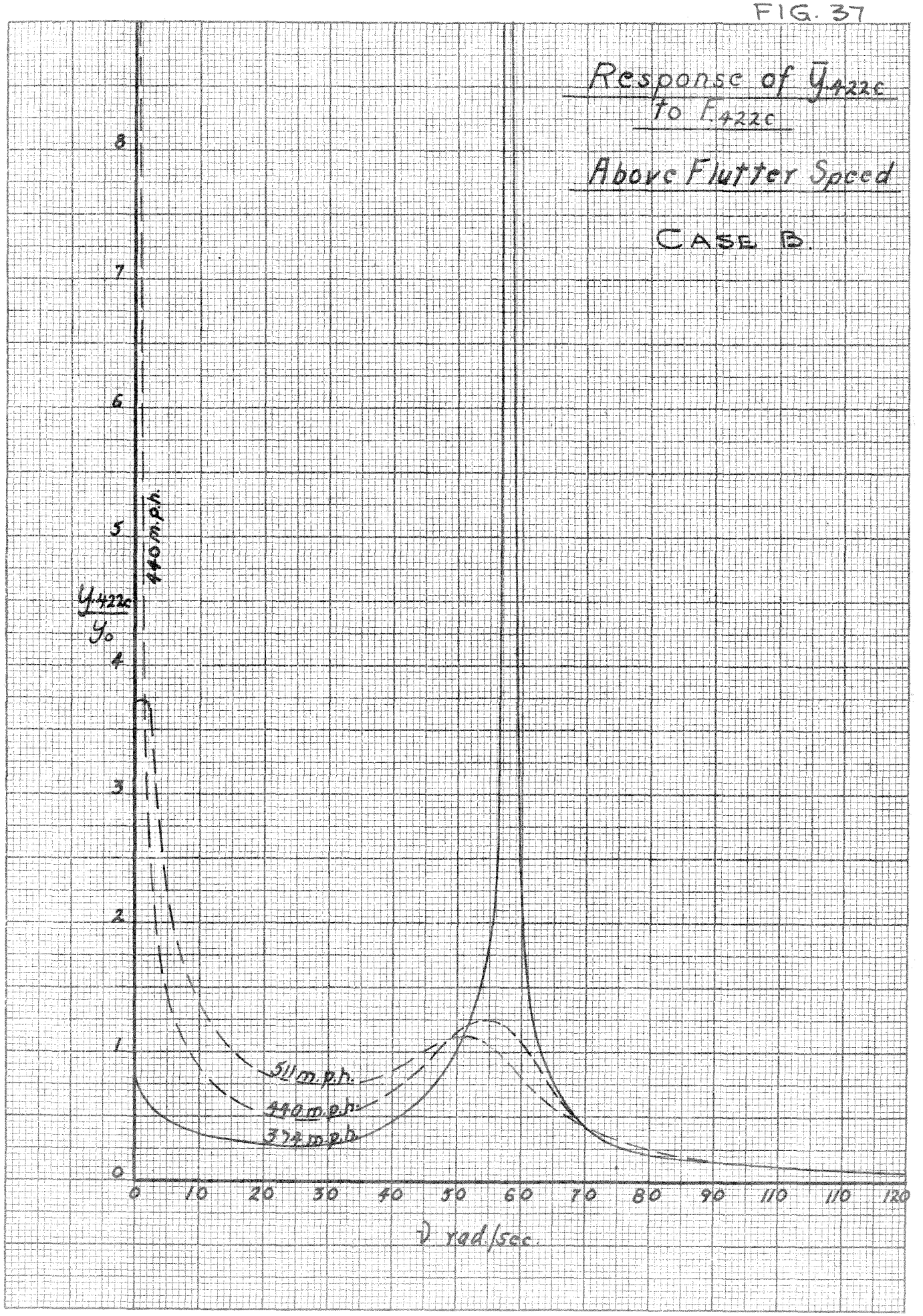
Response of $\bar{y}_{.422c}$ to $F_{.422c}$
Above Flutter Speed
CASE B.
$\frac{y_{.422c}}{y_0}$
440 m.p.h.
511 m.p.h.
440 m.p.h.
374 m.p.h.
0
1
2
3
4
5
6
7
8
0
10
20
30
40
50
60
70
80
90
110
110
120
ν rad/sec.

FIG. 38

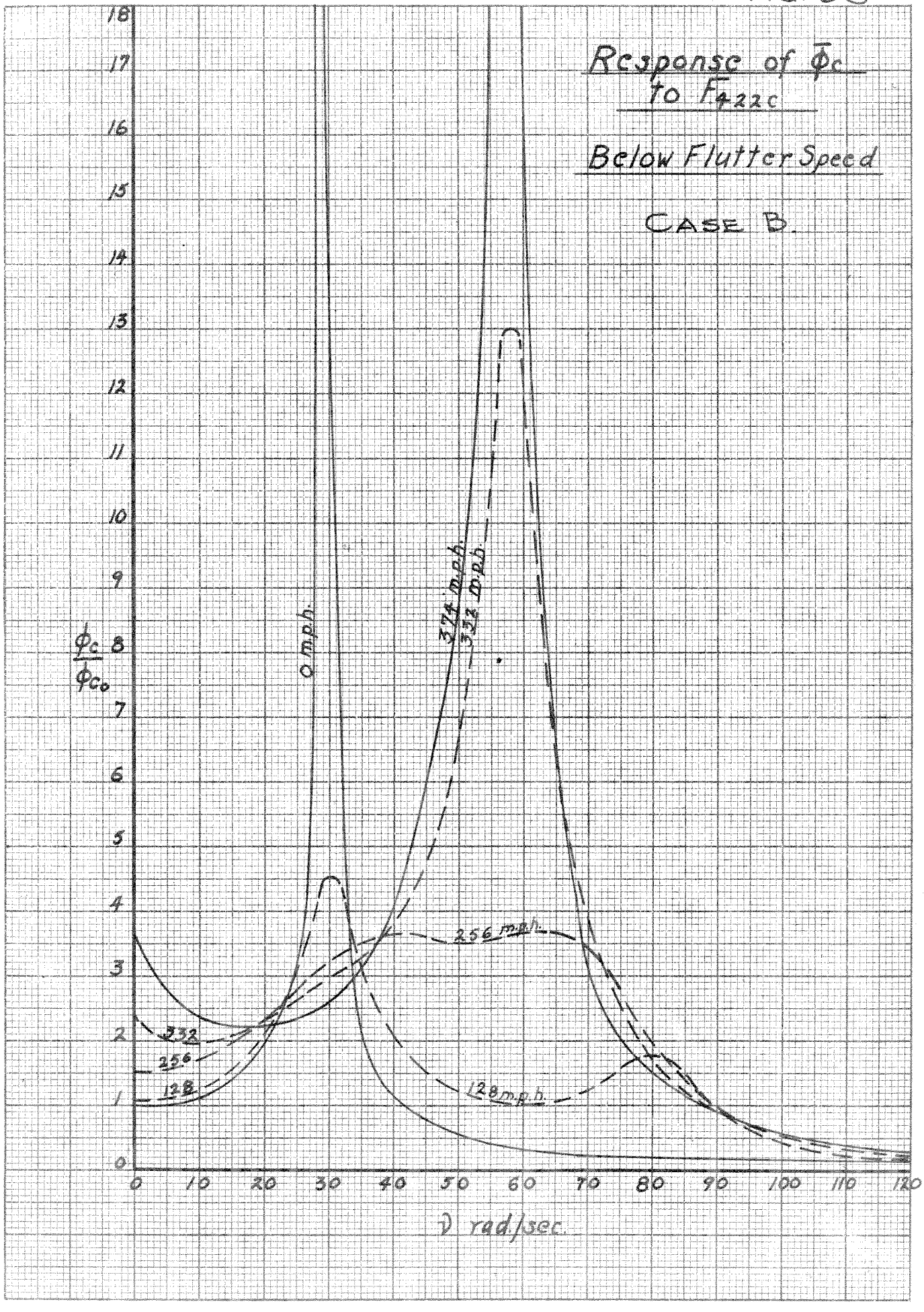
Response of $\bar{\phi}_c$ to $\bar{F}_{422c}$
Below Flutter Speed
CASE B.
$\frac{\phi_c}{\phi_{c_0}}$
0 m.p.h.
374 m.p.h.
352 m.p.h.
256 m.p.h.
128 m.p.h.
232
256
128
0 10 20 30 40 50 60 70 80 90 100 110 120
ν rad/sec.

FIG. 39

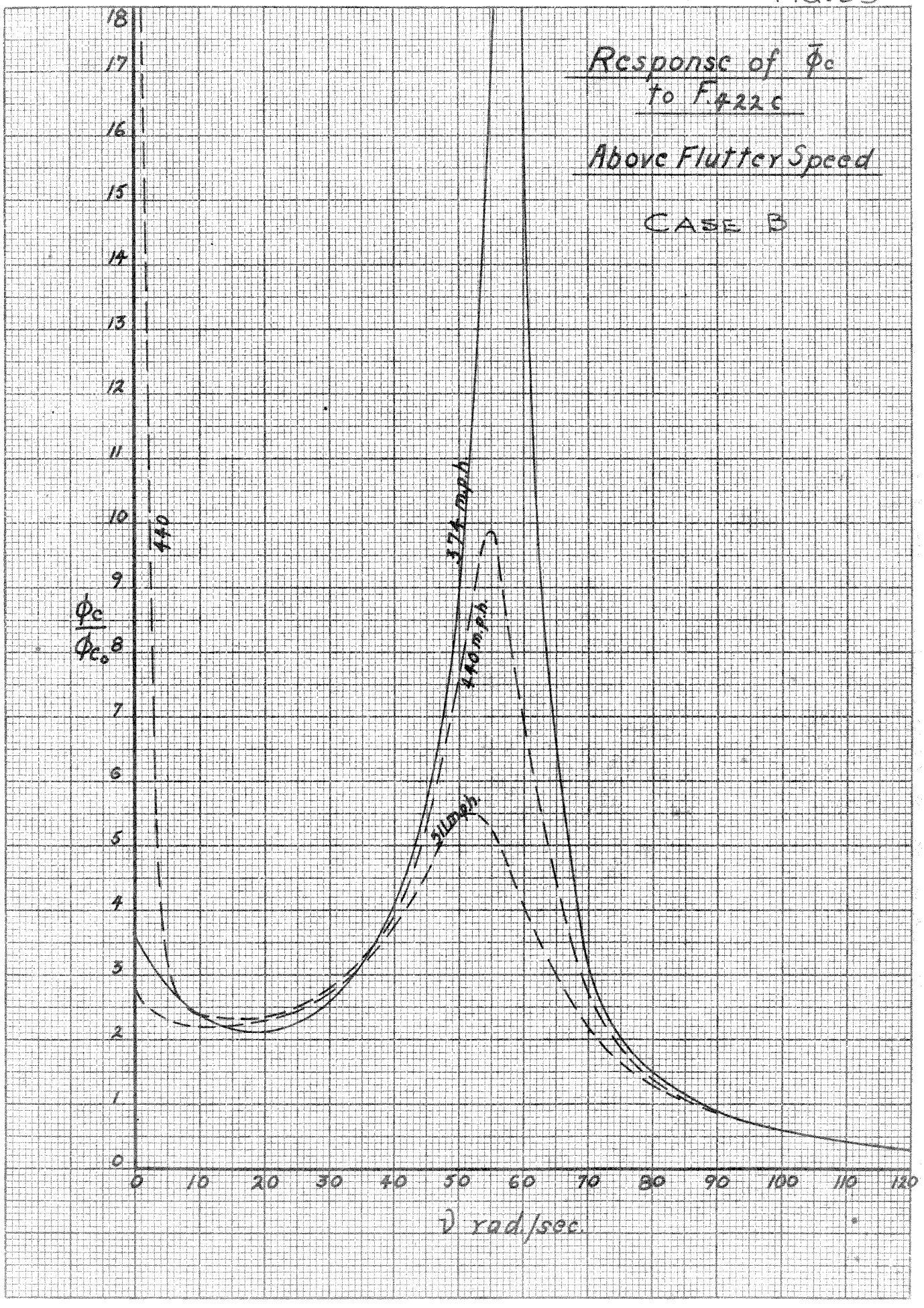
Response of ϕ_c to $F_{\phi 22c}$
Above Flutter Speed
CASE B
$\frac{\phi_c}{\phi_{c_0}}$
440
374 m.p.h.
440 m.p.h.
311 m.p.h.
0 10 20 30 40 50 60 70 80 90 100 110 120
ν rad./sec.

FIG. 40

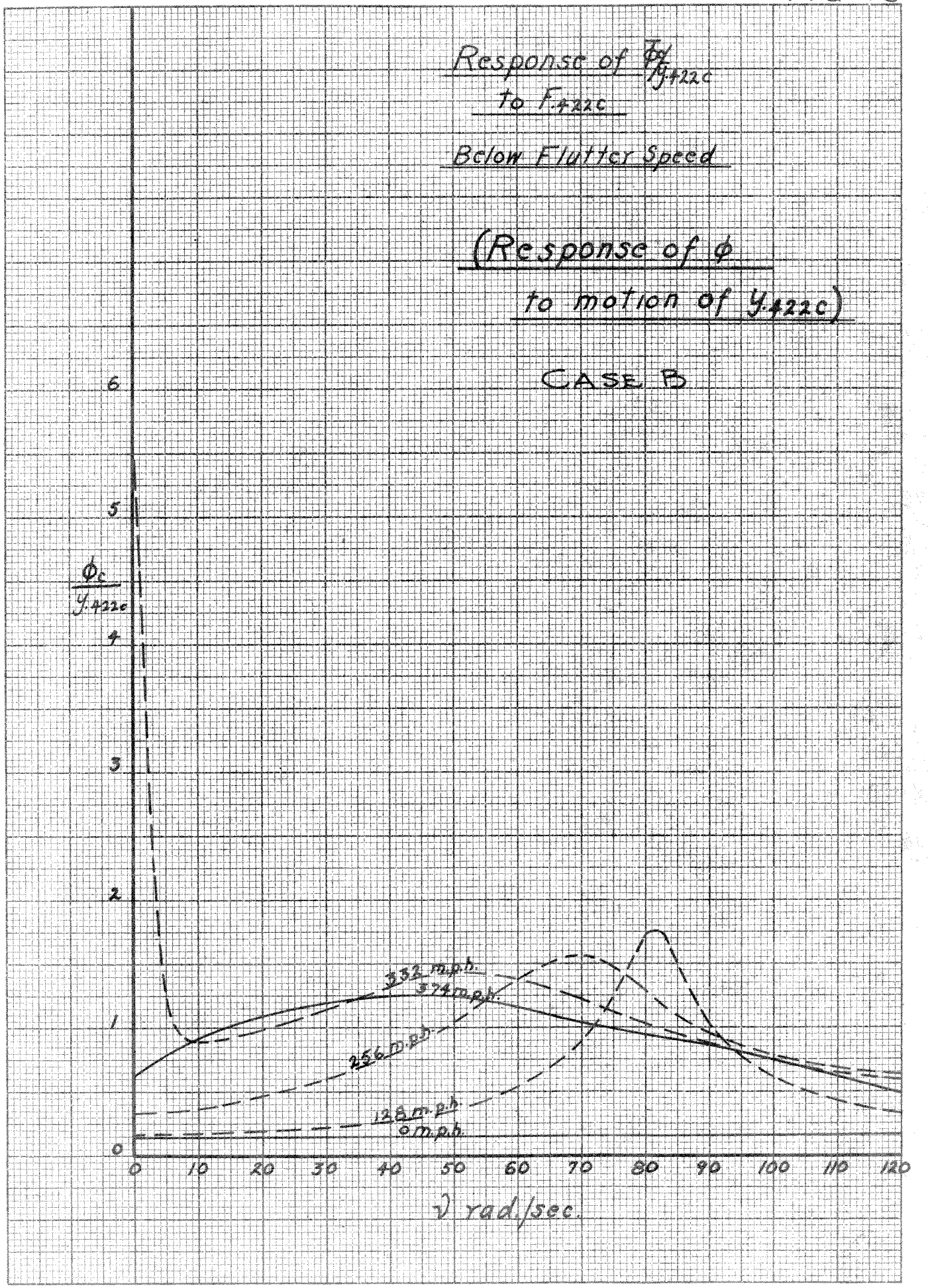
Response of $\frac{\phi}{y_{.422c}}$ to $F_{.422c}$
Below Flutter Speed
(Response of ϕ to motion of $y_{.422c}$)
CASE B
$\frac{\phi_c}{y_{.422c}}$
6
5
4
3
2
1
0
332 m.p.h.
274 m.p.h.
256 m.p.h.
128 m.p.h.
0 m.p.h.
0
10
20
30
40
50
60
70
80
90
100
110
120
ν rad./sec.

FIG. 41

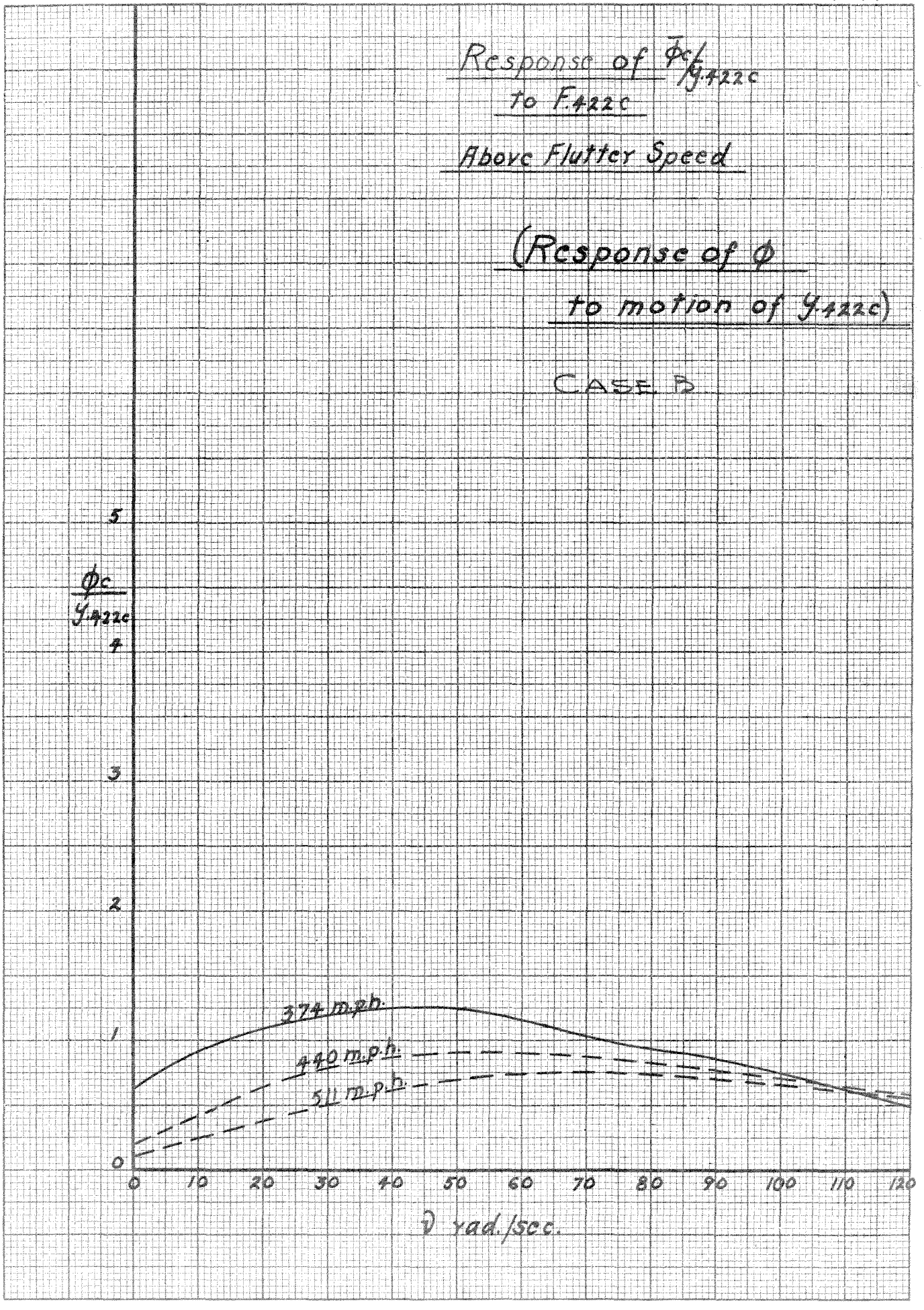
Response of ϕ_c / y_{422c}
to F_{422c}
Above Flutter Speed
(Response of ϕ
to motion of y_{422c})
CASE B
$\frac{\phi_c}{y_{422c}}$
5
4
3
2
1
0
374 m.p.h.
440 m.p.h.
511 m.p.h.
0
10
20
30
40
50
60
70
80
90
100
110
120
ν rad./sec.

CASE B. FIG. 42

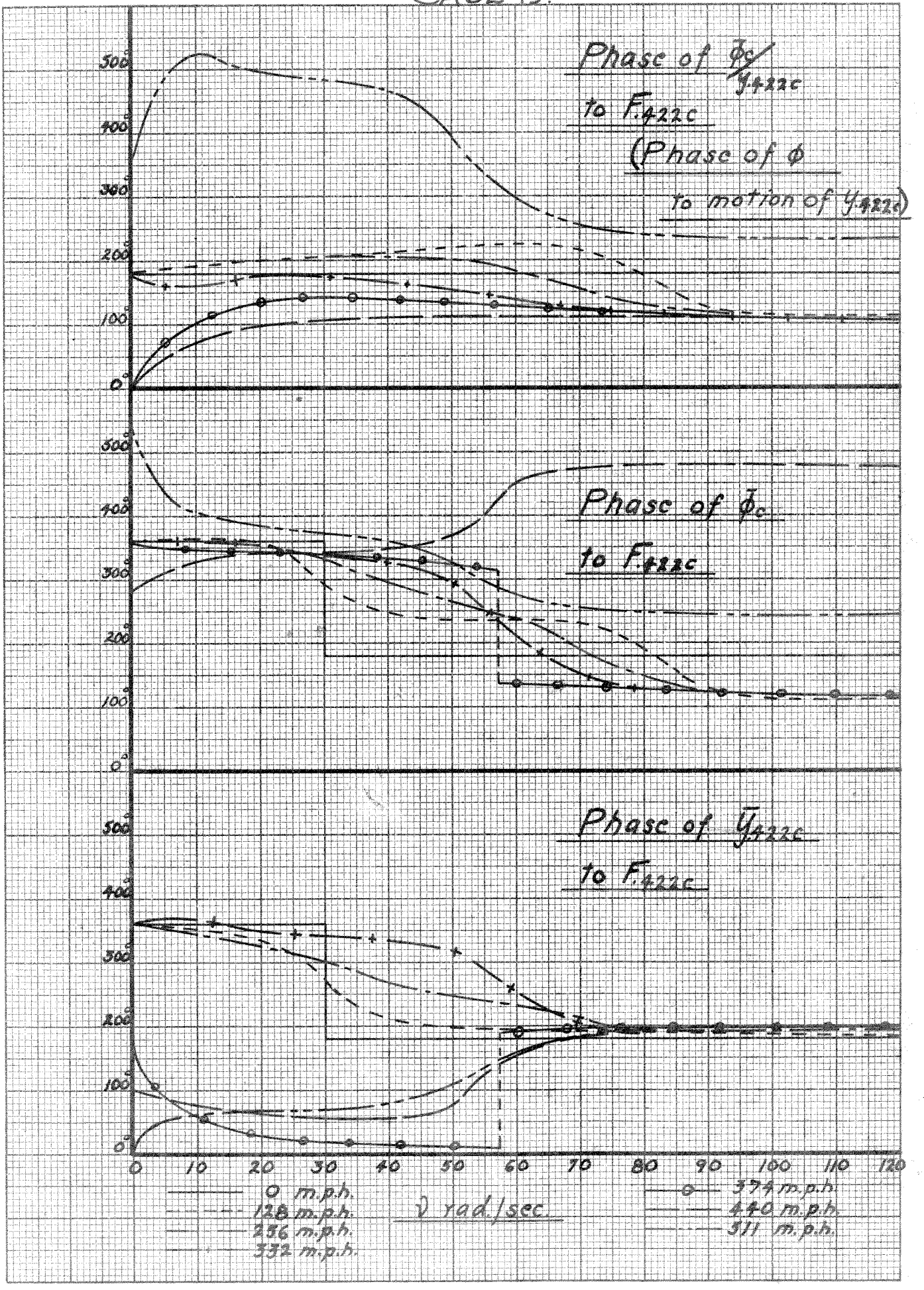
Phase of $\bar{y}_g$ / y_{422c} to F_{422c}
(Phase of ϕ to motion of y_{422c})
Phase of ϕ_c to F_{422c}
Phase of $\bar{y}_{422c}$ to F_{422c}
500°
400°
300°
200°
100°
0°
0 10 20 30 40 50 60 70 80 90 100 110 120
0 m.p.h.
128 m.p.h.
236 m.p.h.
332 m.p.h.
374 m.p.h.
440 m.p.h.
511 m.p.h.
ν rad./sec.

FIG. 43

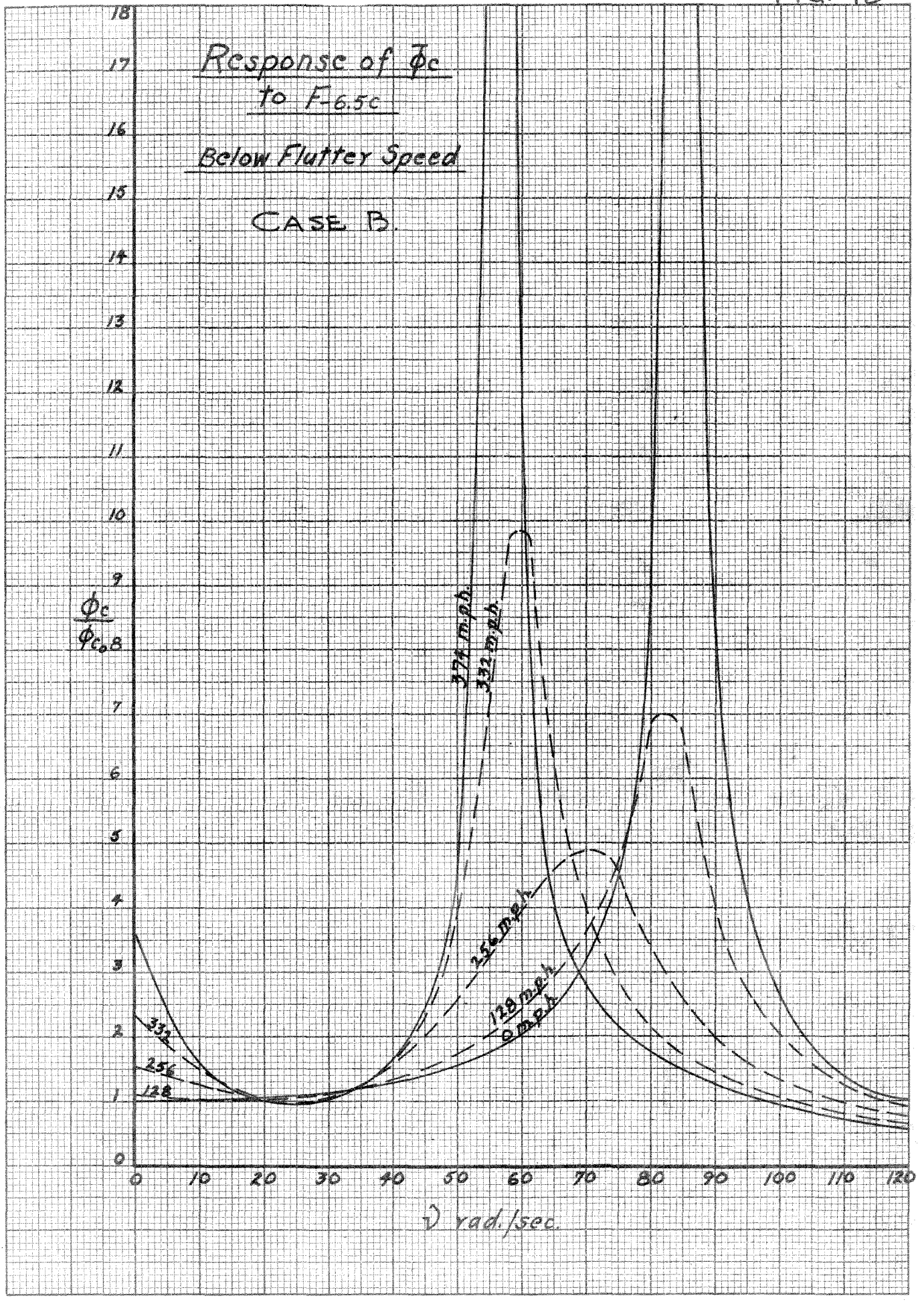
Response of ϕ_c to $F_{6.5c}$
Below Flutter Speed
CASE B.
$\frac{\phi_c}{\phi_{c_{0.8}}}$
374 m.p.h.
332 m.p.h.
256 m.p.h.
128 m.p.h.
0 m.p.h.
332
256
128
0 10 20 30 40 50 60 70 80 90 100 110 120
ν rad./sec.

FIG. 44

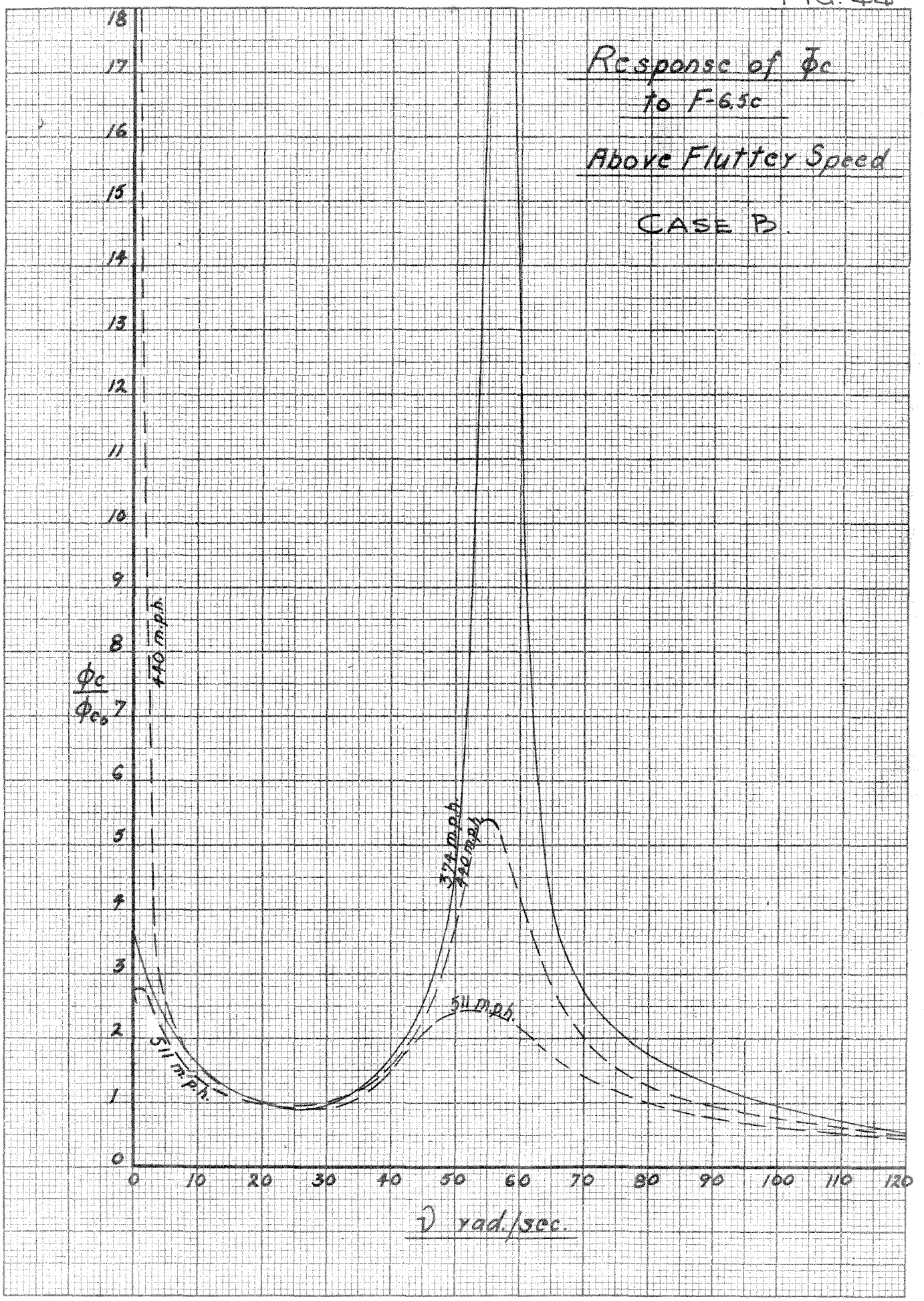
Response of ϕ_c to F-6.5c
Above Flutter Speed
CASE B.
$\frac{\phi_c}{\phi_{c_0}}$
410 m.p.h.
374 m.p.h.
340 m.p.h.
511 m.p.h.
511 m.p.h.
0
1
2
3
4
5
6
7
8
9
10
11
12
13
14
15
16
17
18
0
10
20
30
40
50
60
70
80
90
100
110
120
ν rad./sec.

FIG. 45

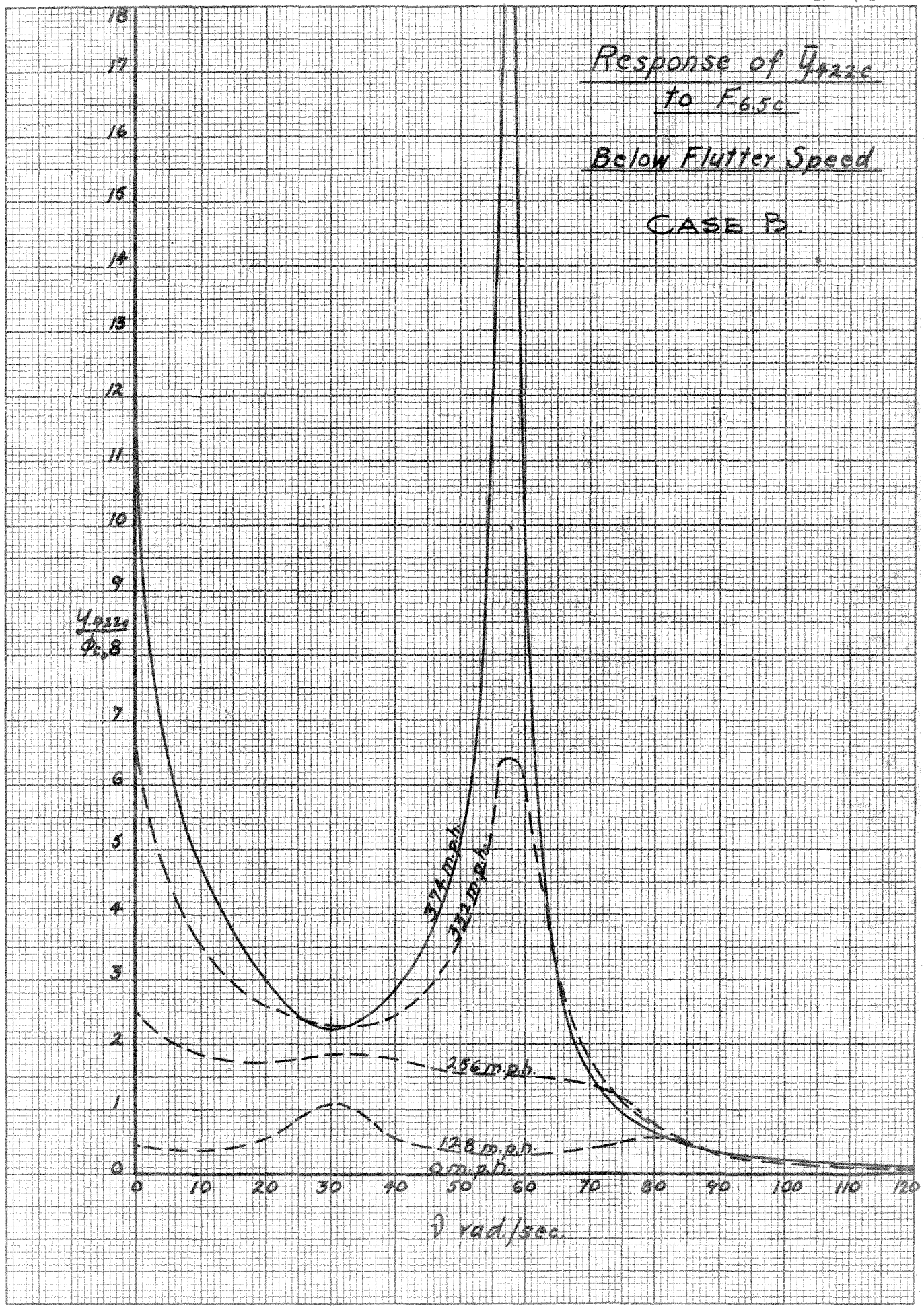
Response of $\bar{y}_{\#22c}$
to $F_{6.5c}$
Below Flutter Speed
CASE B.
$\frac{\bar{y}_{\#22c}}{\phi_{c,8}}$
374 m.p.h.
322 m.p.h.
256 m.p.h.
128 m.p.h.
0 m.p.h.
0 10 20 30 40 50 60 70 80 90 100 110 120
θ rad./sec.

FIG. 46

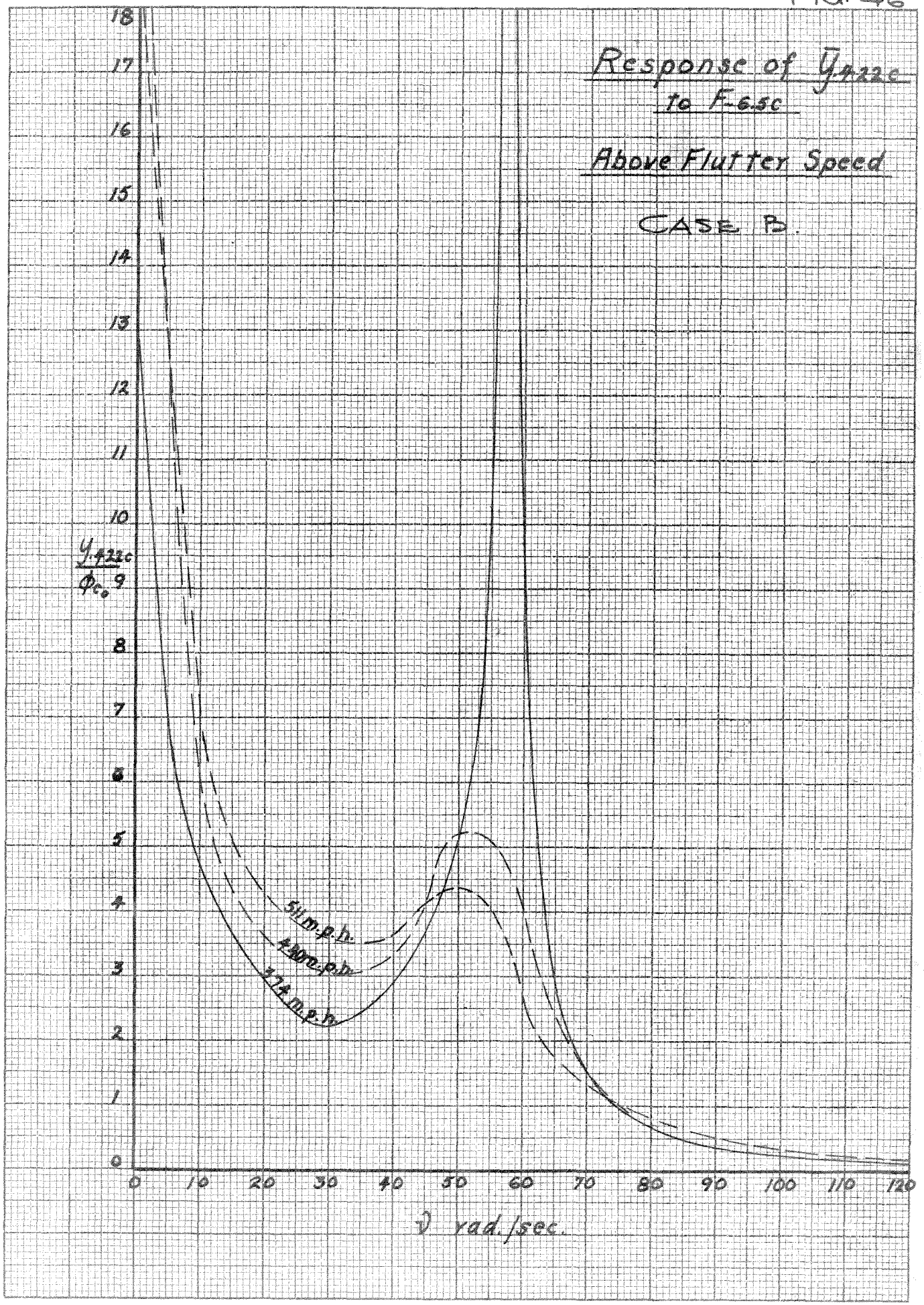
Response of $\bar{y}_{.422c}$
to F-6.5c
Above Flutter Speed
CASE B.
$\frac{\bar{y}_{.422c}}{\phi_{c_0}}$
18
17
16
15
14
13
12
11
10
9
8
7
6
5
4
3
2
1
0
0
10
20
30
40
50
60
70
80
90
100
110
120
ν rad./sec.
5411 M.P.H.
4800 M.P.H.
3774 M.P.H.

FIG. 47

Response of $\frac{y_{4.22c}}{\phi_c}$ to $F_{6.5c}$

(Response of $y_{4.22c}$ to motion of ϕ)

CASE B.

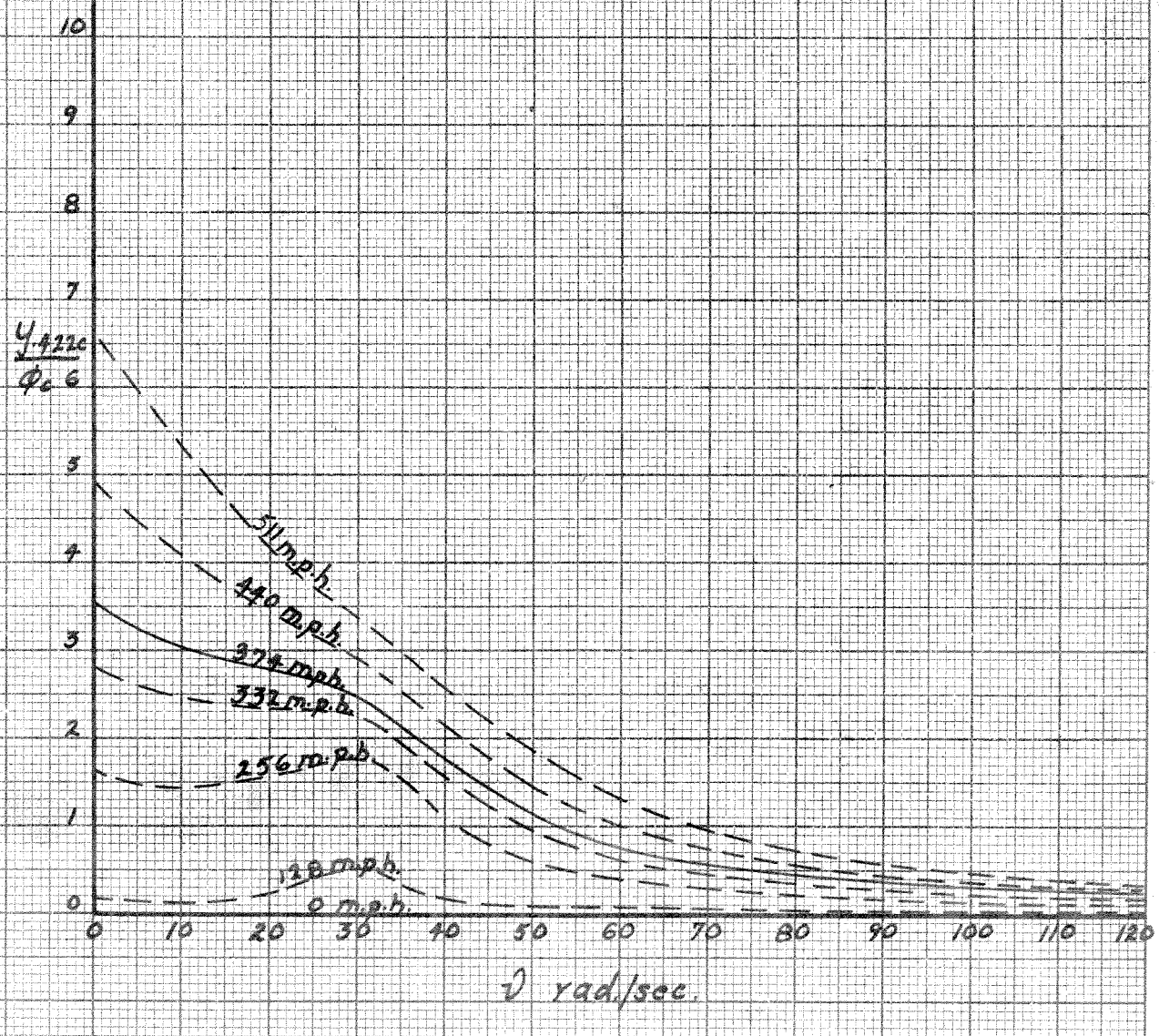

CASE B. FIG. 48

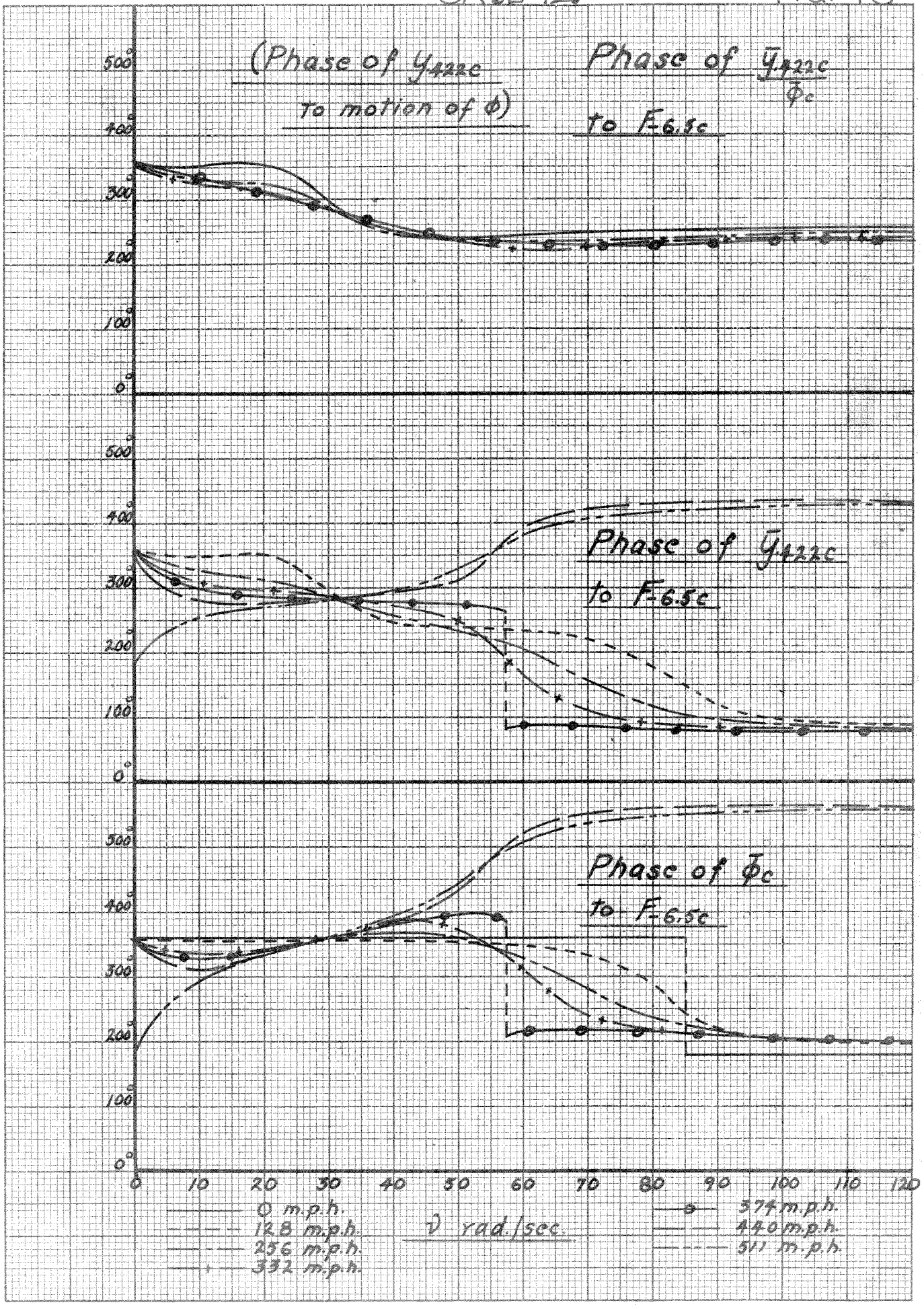
(Phase of y_{422c} to motion of ϕ)
Phase of $\bar{y}_{422c}$ to $F_{6.5c}$
Phase of $\bar{y}_{422c}$ to $F_{6.5c}$
Phase of $\bar{\phi}_c$ to $F_{6.5c}$
500°
400°
300°
200°
100°
0°
0 10 20 30 40 50 60 70 80 90 100 110 120
ν rad./sec.
0 m.p.h.
128 m.p.h.
256 m.p.h.
332 m.p.h.
374 m.p.h.
440 m.p.h.
511 m.p.h.

FIG. 49

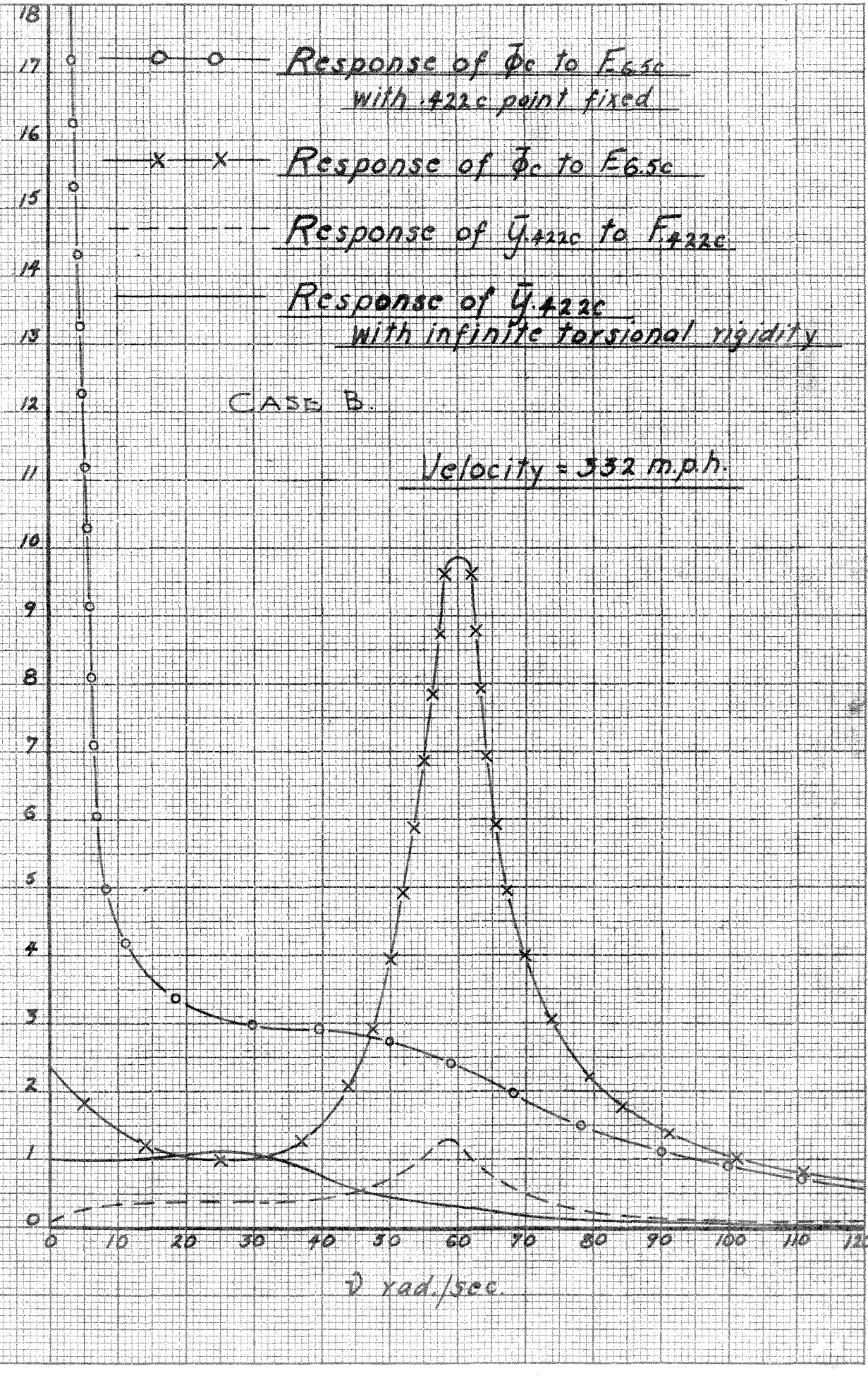
Response of $\bar{\phi}_c$ to $F_{6.5c}$ with .422c point fixed
Response of $\bar{\phi}_c$ to $F_{6.5c}$
Response of $\bar{y}_{.422c}$ to $F_{.422c}$
Response of $\bar{y}_{.422c}$ with infinite torsional rigidity
CASE B.
Velocity = 332 m.p.h.
0 10 20 30 40 50 60 70 80 90 100 110 120
$\bar{\nu}$ rad./sec.

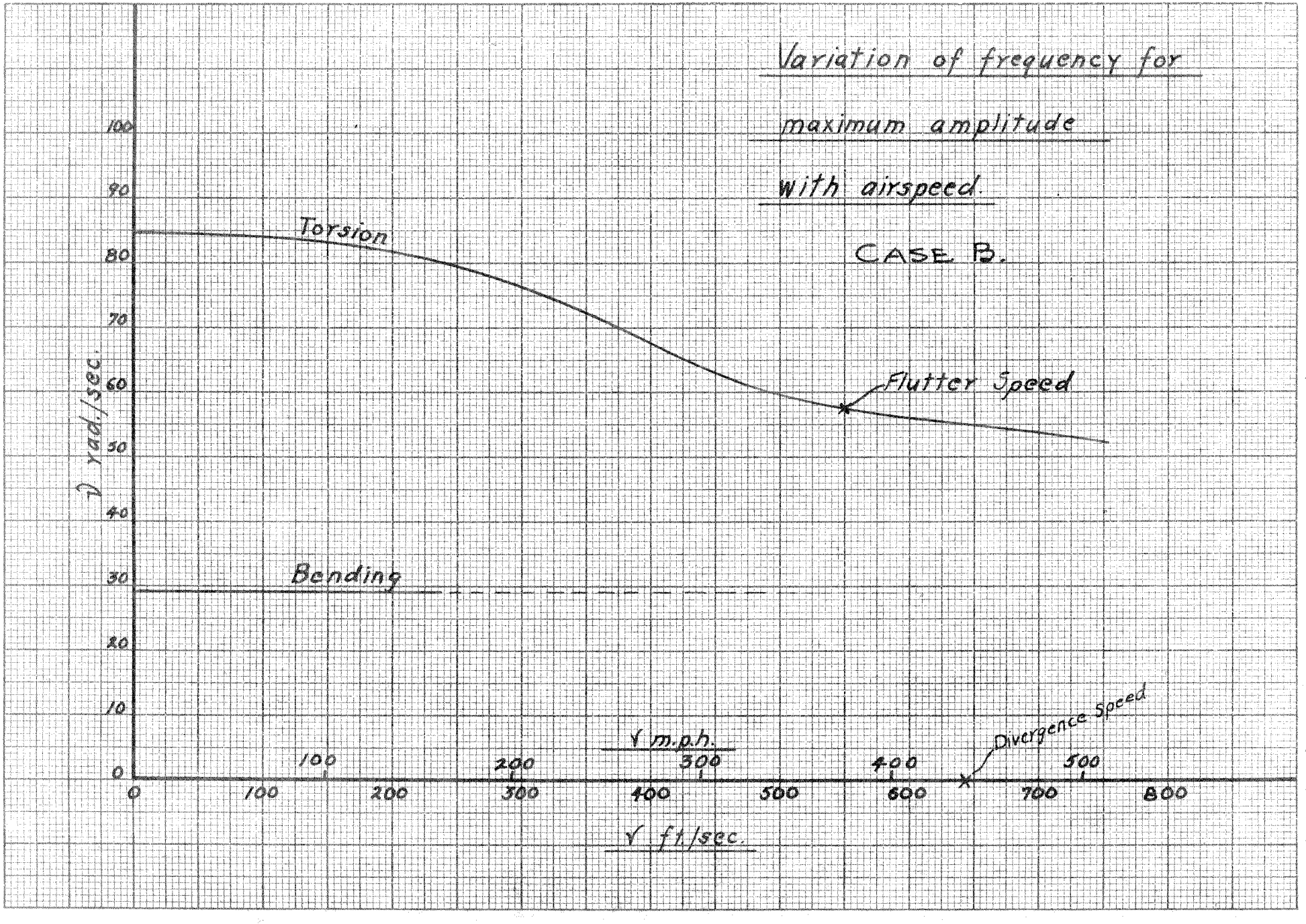
Variation of frequency for maximum amplitude with airspeed.
CASE B.
Torsion
Bending
Flutter Speed
Divergence Speed
n rad./sec.
100
90
80
70
60
50
40
30
20
10
0
V m.p.h.
100
200
300
400
500
600
700
800
V ft/sec.

FIG. 50

FIG. 51.

KASSNER - FINGADO (20) CHART FOR FLEX-TORS. STABILITY LIMIT

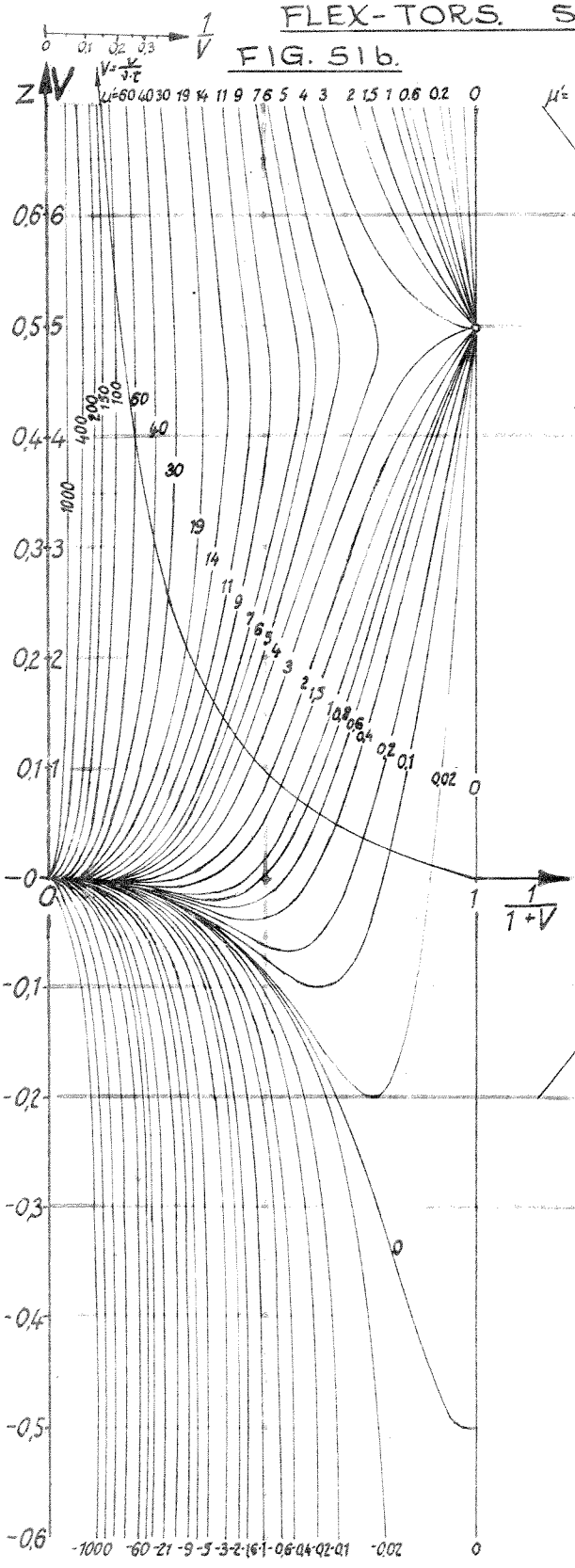

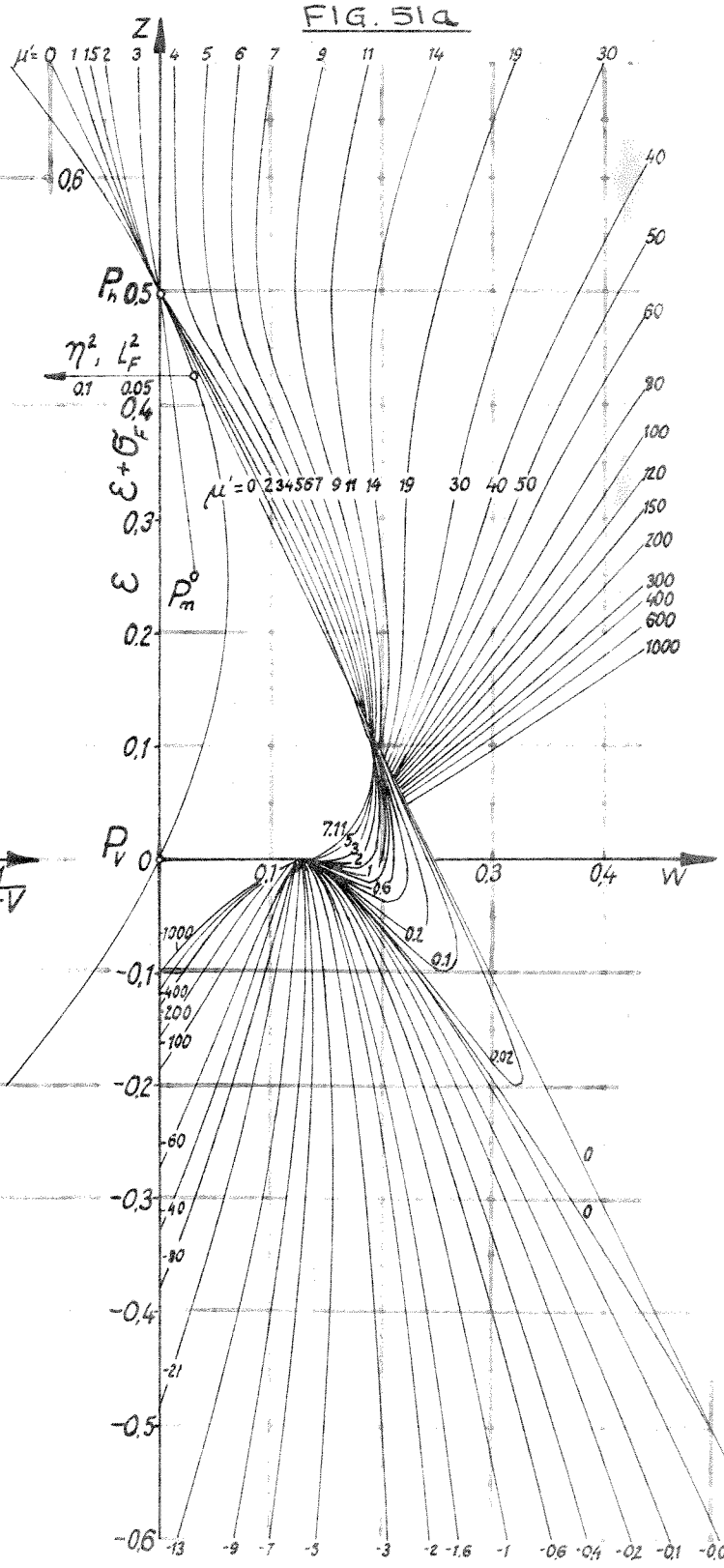

$$\overline{(B)B} = \frac{1}{\mu} \cdot \overline{P_n P_m} \qquad \mu' = \mu \cdot \frac{\overrightarrow{AB}}{\overrightarrow{AC}} \qquad \nu = \nu_1 \sqrt{\frac{AC}{BC}}$$

FIG. 52

REPRESENTATIVE USE OF FIG. 51.

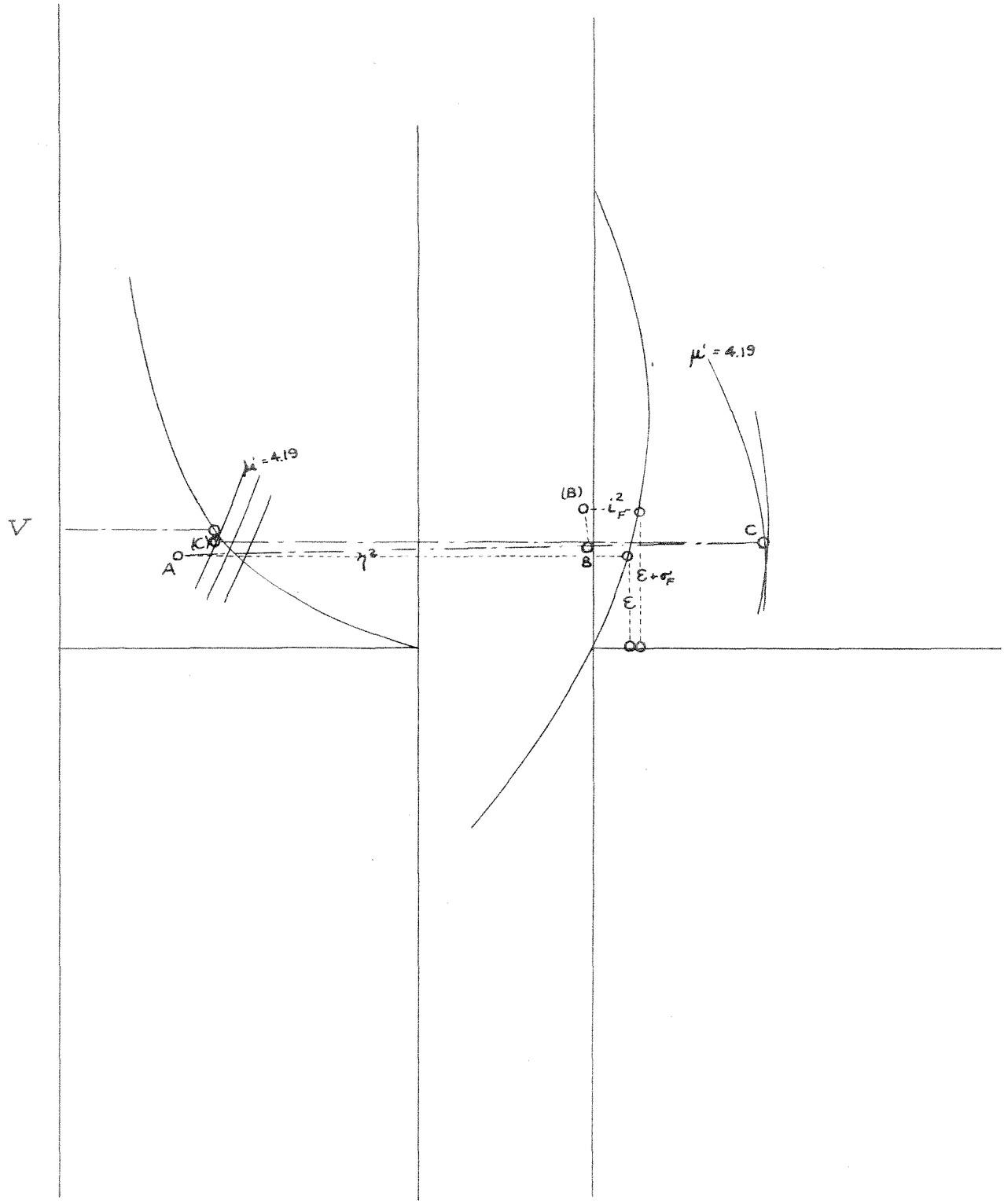

FIG. 53

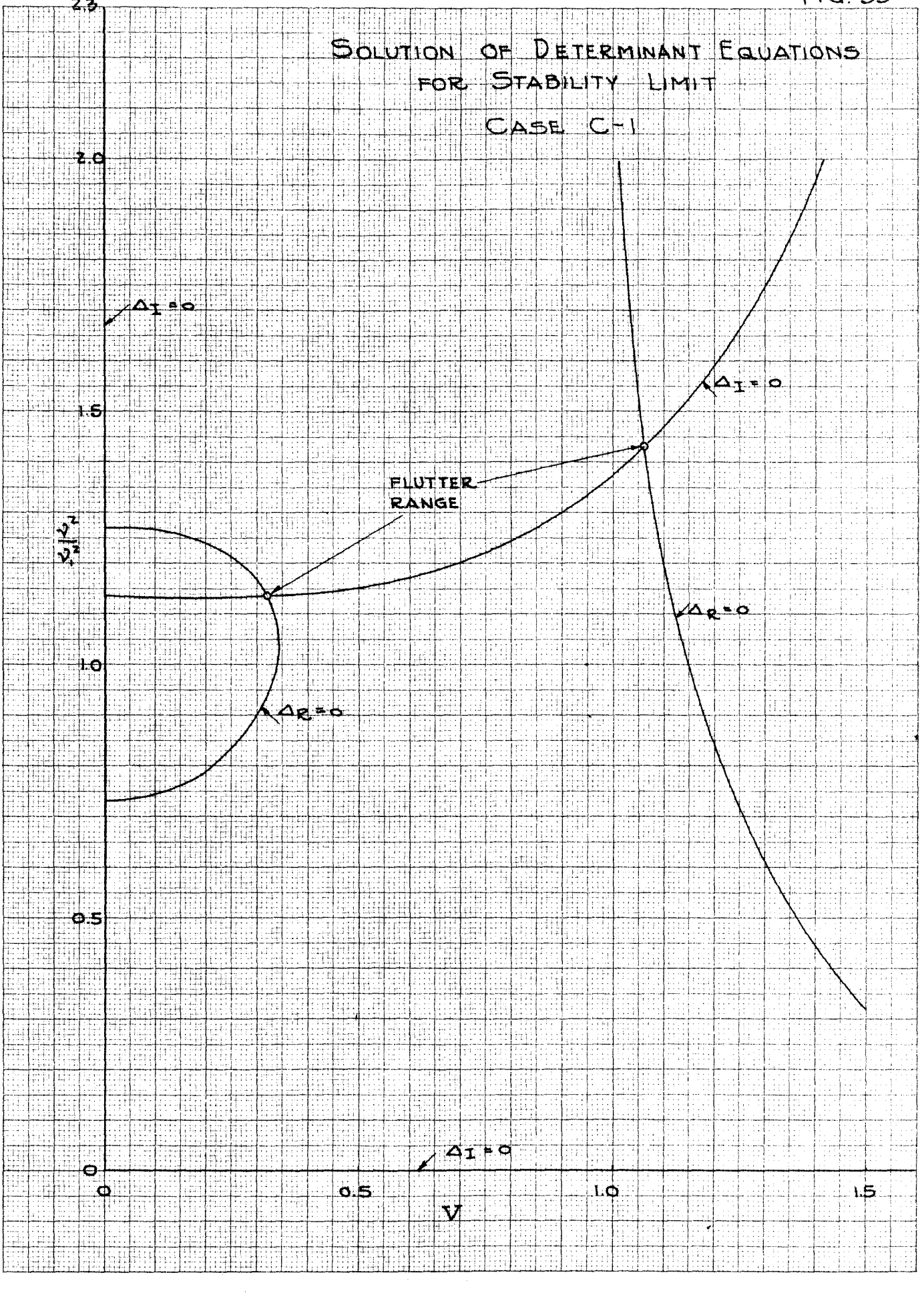
SOLUTION OF DETERMINANT EQUATIONS
FOR STABILITY LIMIT
CASE C-1
2.5
2.0
1.5
1.0
0.5
0
$\frac{\nu_2^2}{\nu_1^2}$
$\Delta_I = 0$
$\Delta_I = 0$
FLUTTER
RANGE
$\Delta_R = 0$
$\Delta_R = 0$
$\Delta_I = 0$
0
0.5
1.0
1.5
V

FIG. 54

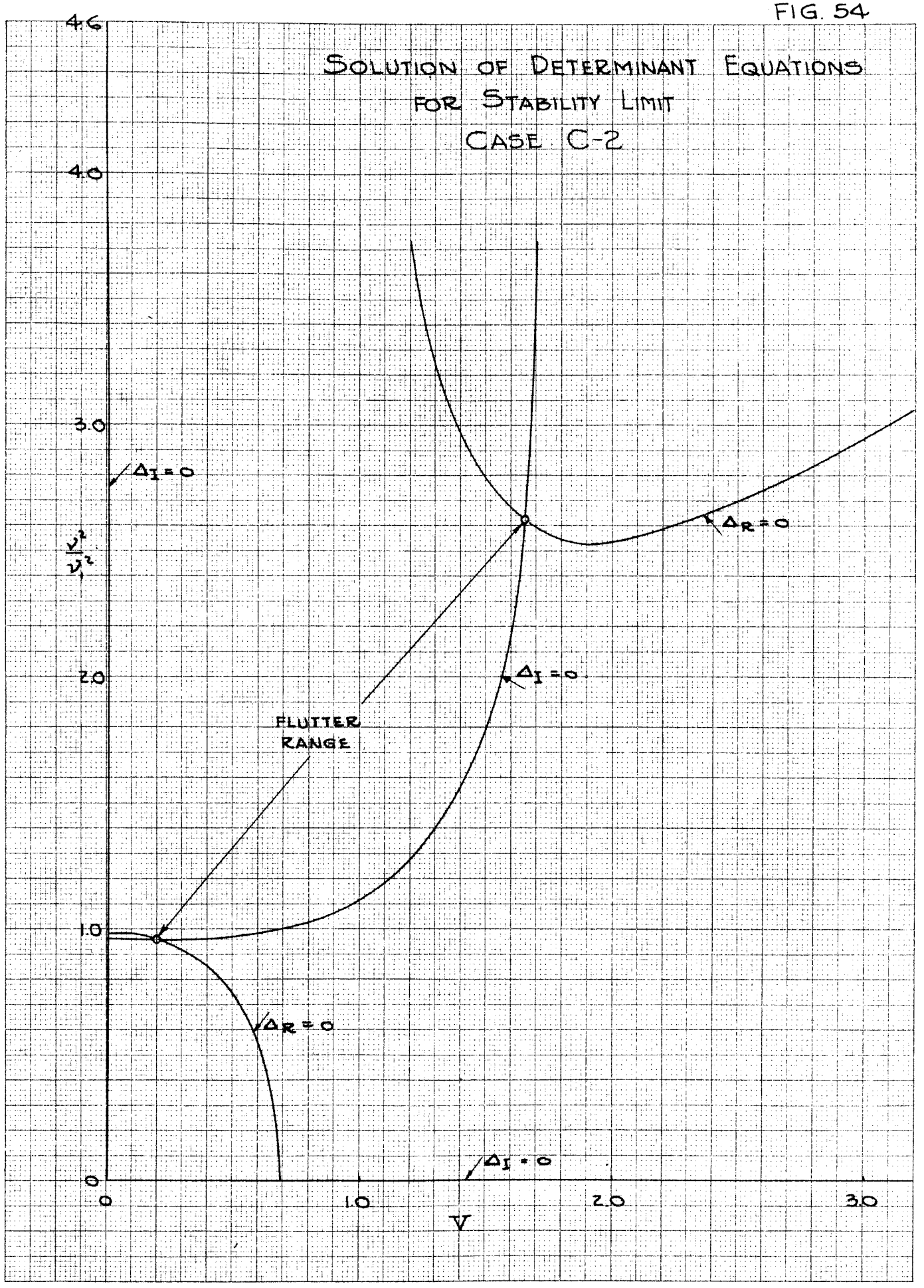
SOLUTION OF DETERMINANT EQUATIONS
FOR STABILITY LIMIT
CASE C-2
4.6
4.0
3.0
2.0
1.0
0
$\frac{\nu^2}{\nu_1^2}$
$\Delta_I = 0$
$\Delta_R = 0$
$\Delta_I = 0$
FLUTTER RANGE
$\Delta_R = 0$
$\Delta_I = 0$
0
1.0
2.0
3.0
V

FIG. 55

POLAR DIAGRAM OF CONDITIONS AT STABILITY LIMIT

CASE C-1 ($V = 0.332$; $(v/v)^2 = 1.135$)

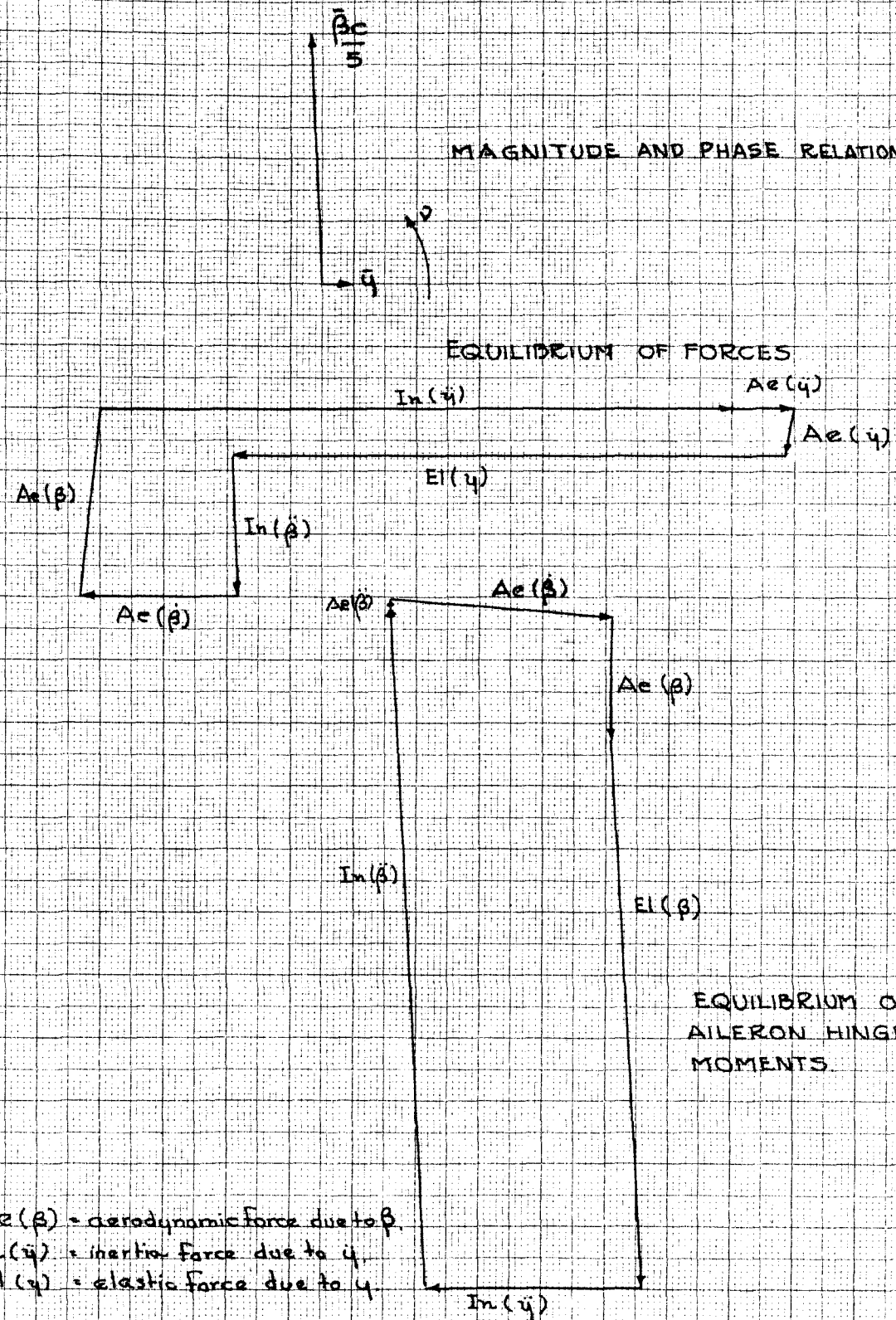

Ae(β) = aerodynamic force due to β.
In(η̈) = inertia force due to η̈.
El(η) = elastic force due to η.

POLAR DIAGRAM OF CONDITIONS AT STABILITY LIMIT.

CASE C-2 $(V = 0.200\ ,\ (v/v)^2 = 0.955)$

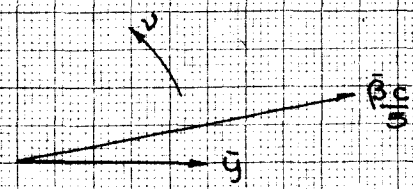

MAGNITUDE AND PHASE RELATIONS

EQUILIBRIUM OF FORCES

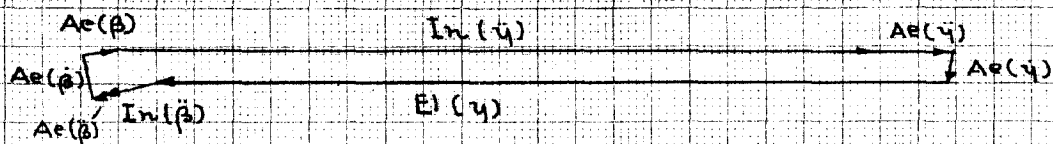

EQUILIBRIUM OF AILERON HINGE MOMENTS

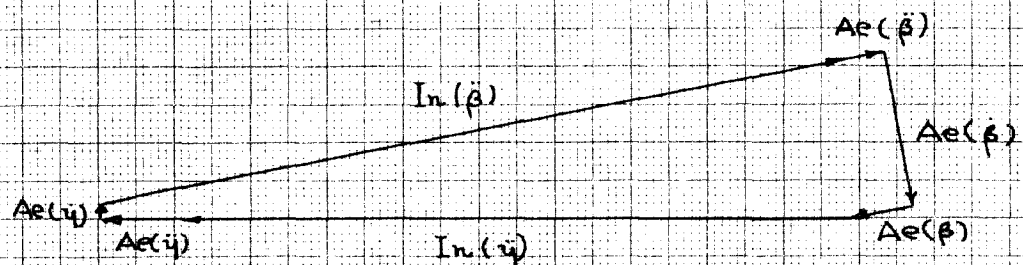

Ae(β) = Aerodynamic force due to β.
In.(ÿ) = Inertia force due to ÿ.
El.(y) = Elastic force due to y.

NATURAL FREQUENCY
WING BENDING

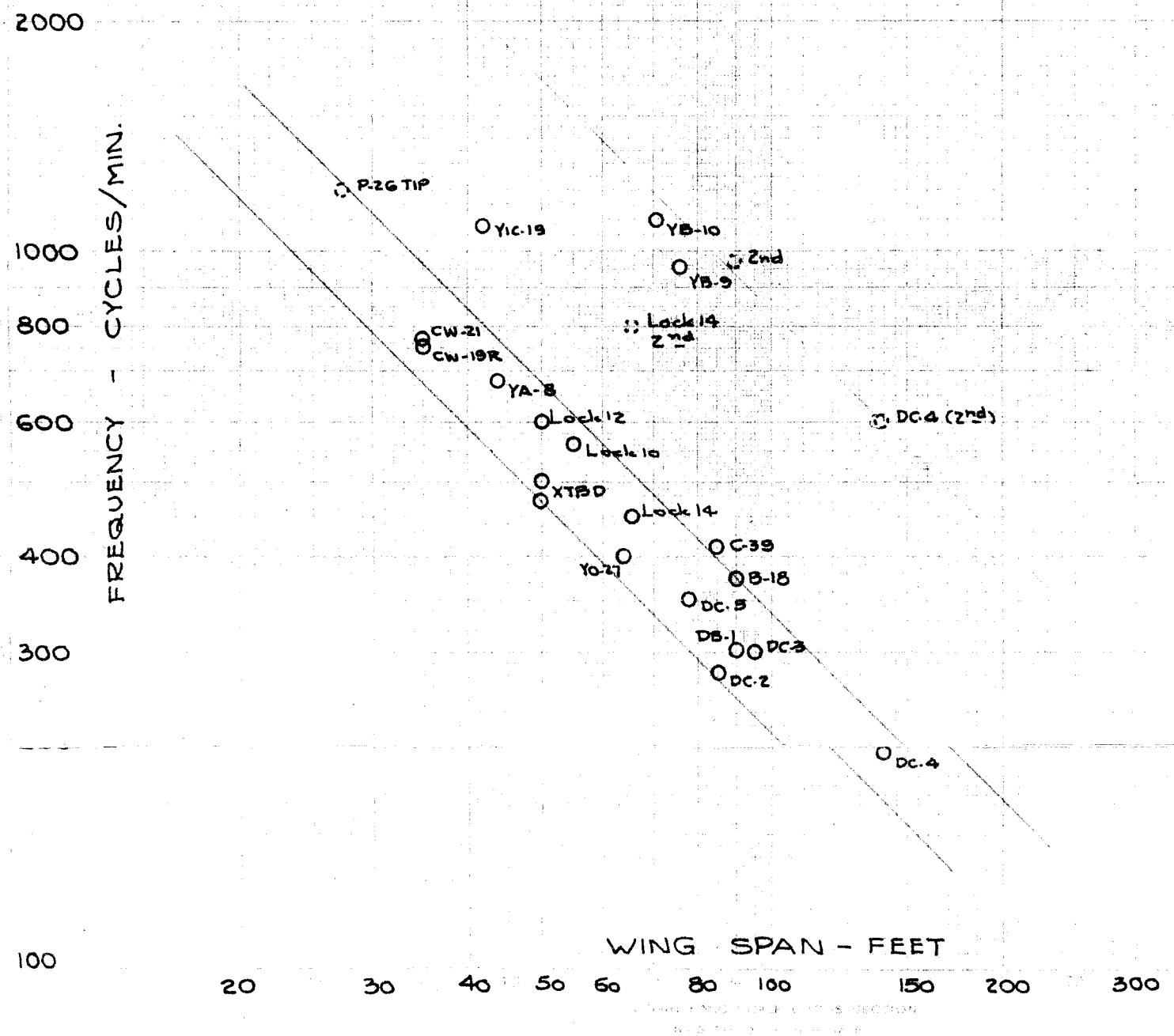

FIG. 51

FIG. 58

NATURAL FREQUENCY
WING TORSION
FREQUENCY - CYCLES/MIN.
3000
2000
1500
1000
800
600
400
300
WING SPAN - FEET
20
30
40
60
80
100
150
200
300
P-26
1192
XTBD
Y1B-9
DB-1 & DC-3 2nd
B18
Y0-27
DC-5
DC-3
DC-4

NATURAL FREQUENCY
AILERON - CONTROL SYSTEM

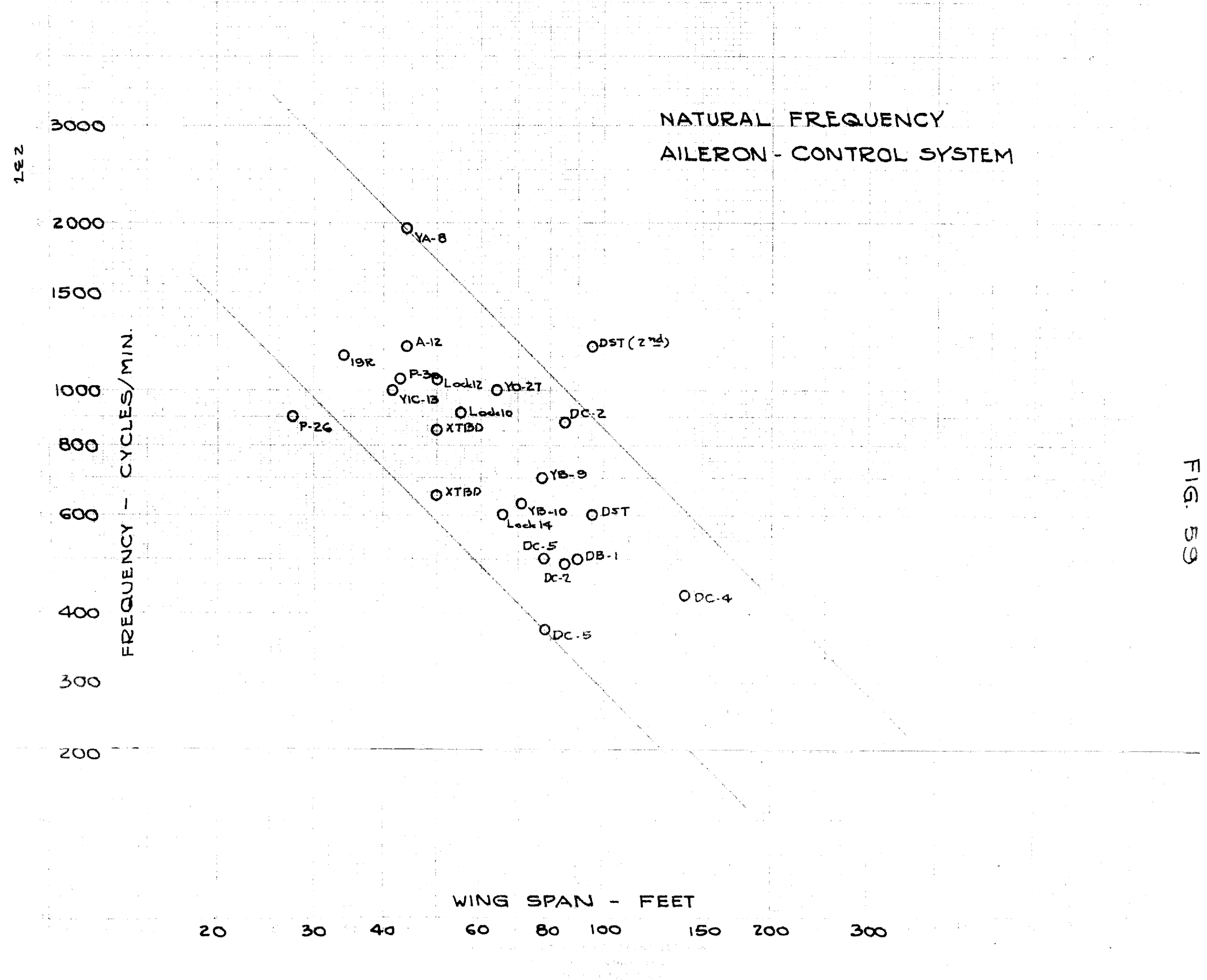

FIG. 59

NATURAL FREQUENCY
FUSELAGE - TORSION

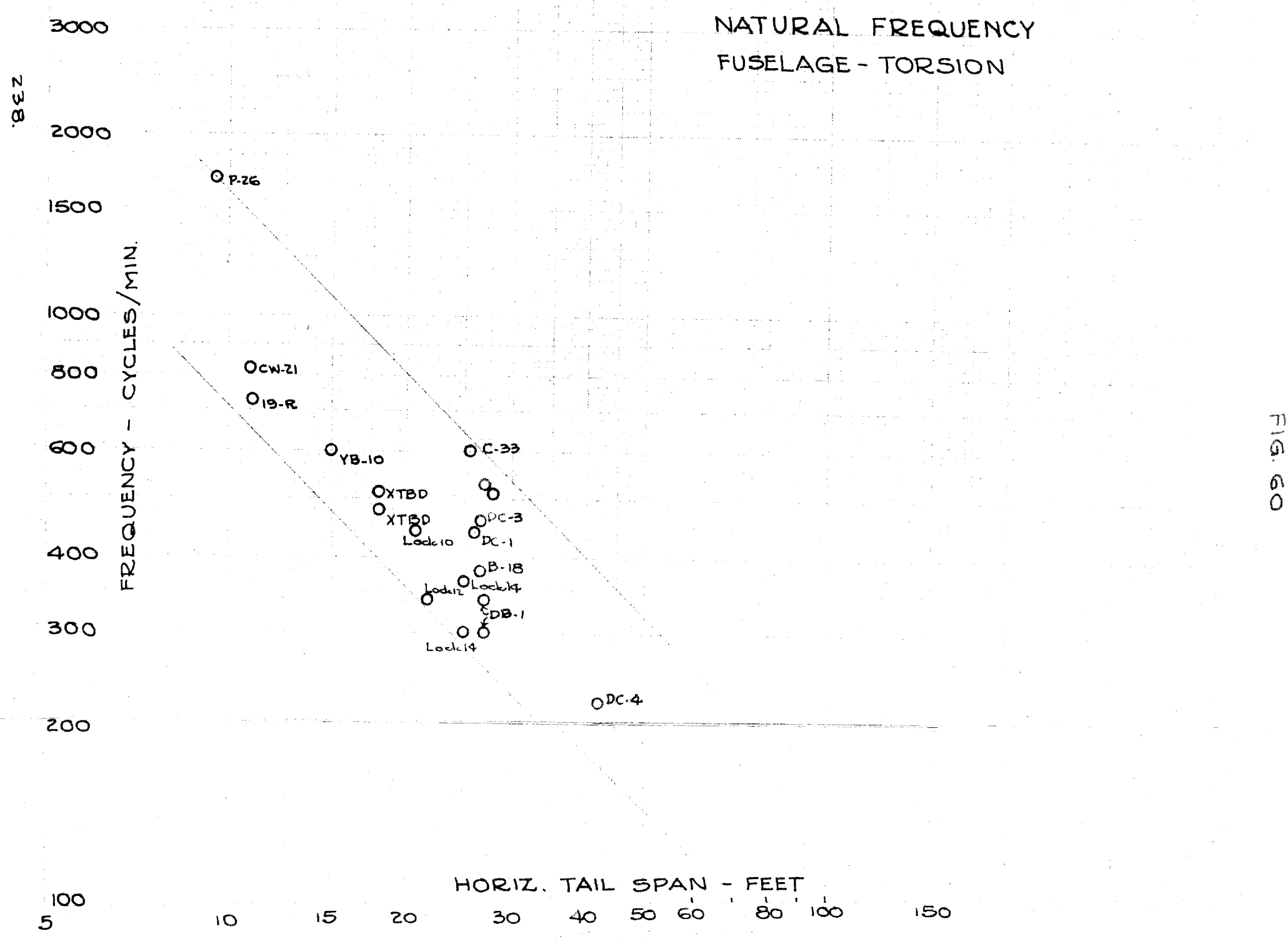

Z38.

FIG. 60

NATURAL FREQUENCY
STABILIZER BENDING

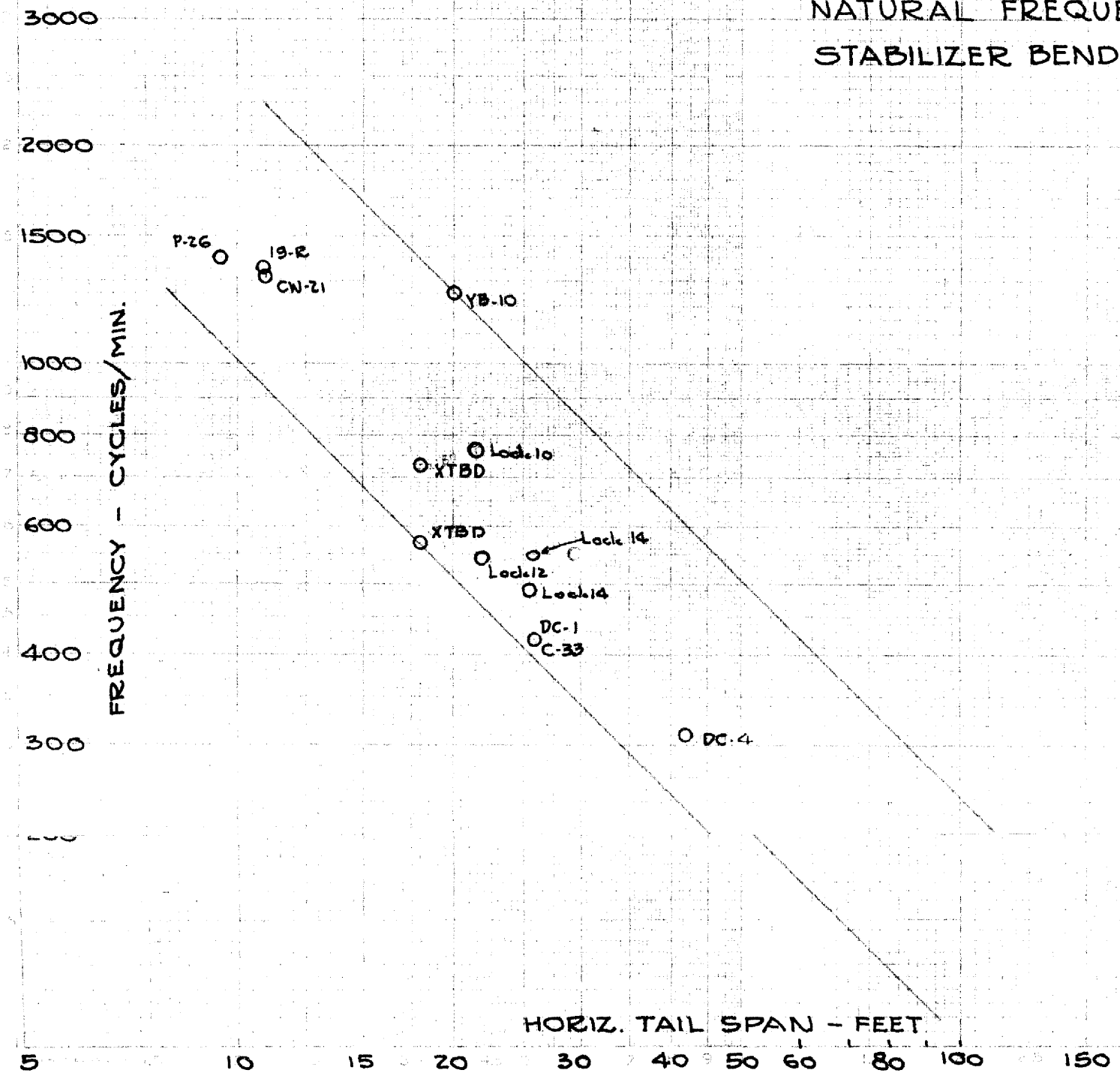

FIG. 61.

FIG. 67

NATURAL FREQUENCY
STABILIZER TORSION
FREQUENCY - CYCLES/MIN.
3000
2000
1500
1000
800
600
400
300
200
HORIZ. TAIL SPAN - FEET
5
10
15
20
30
40
50
60
80
100
150
⊙ 1x4

NATURAL FREQUENCY
FIN BENDING

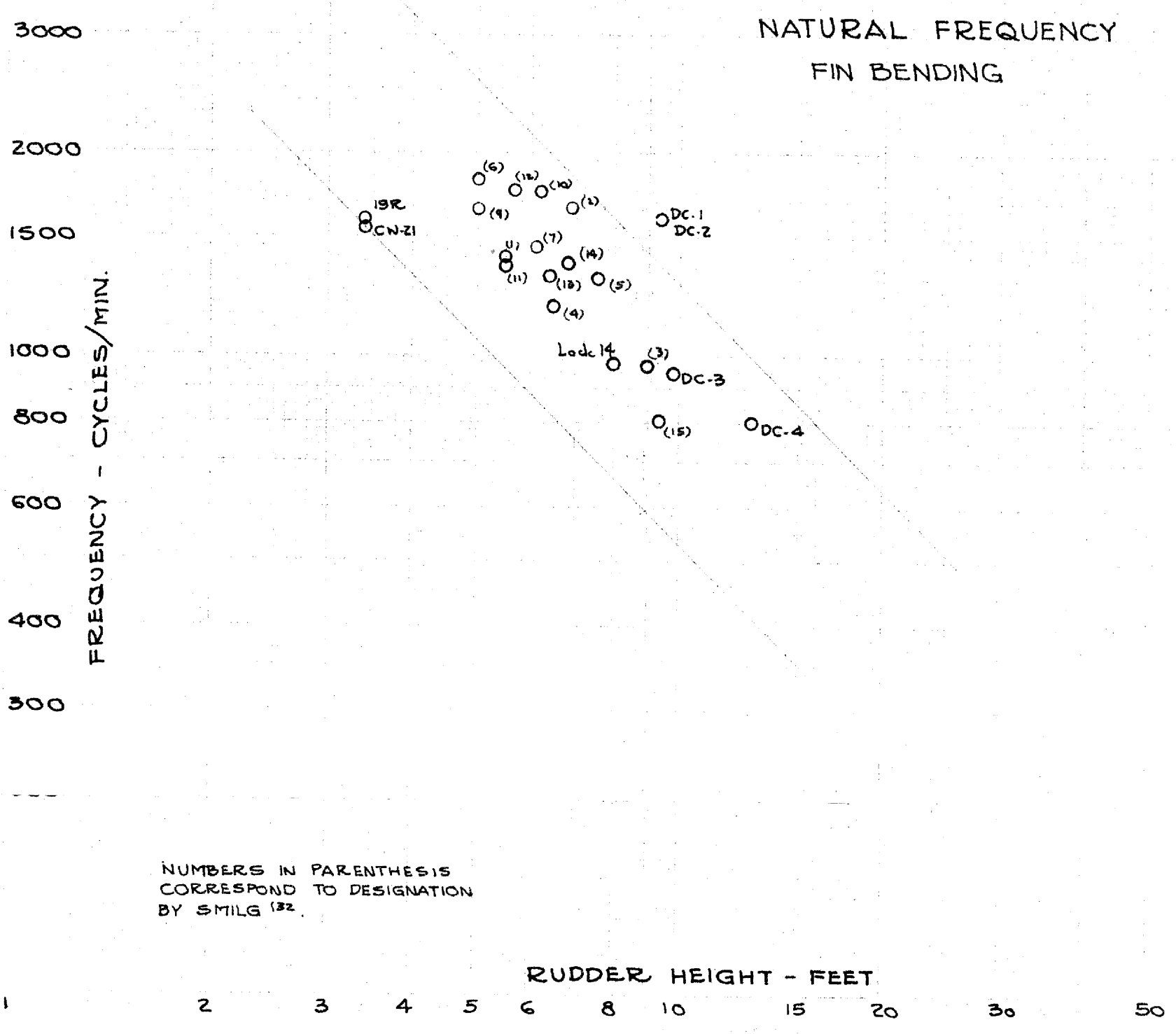

NATURAL FREQUENCY
ELEVATOR CONTROL SYSTEM

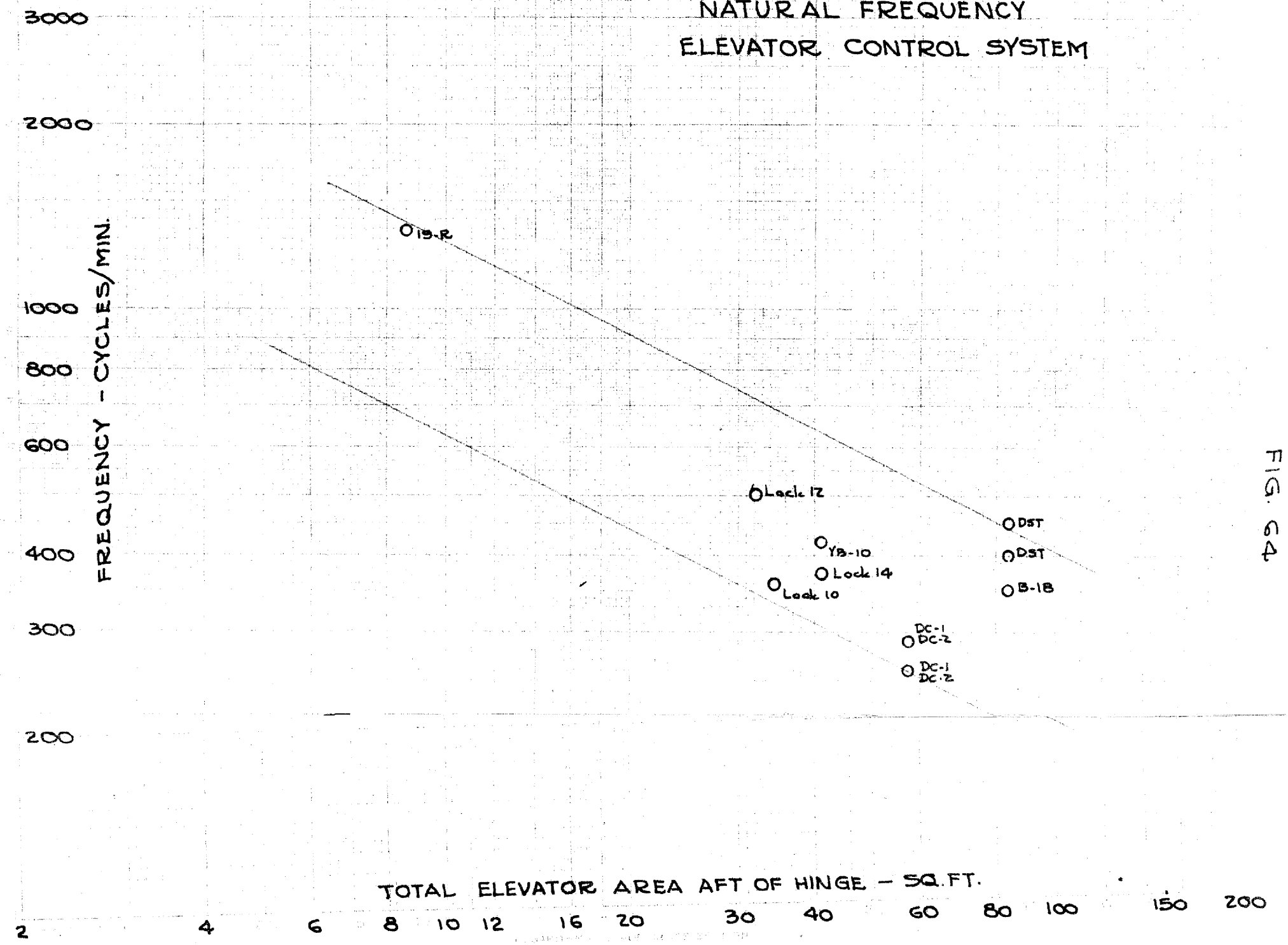

FIG. 64

NATURAL FREQUENCY
ELEVATOR - TORSION OF TORQUE TUBE

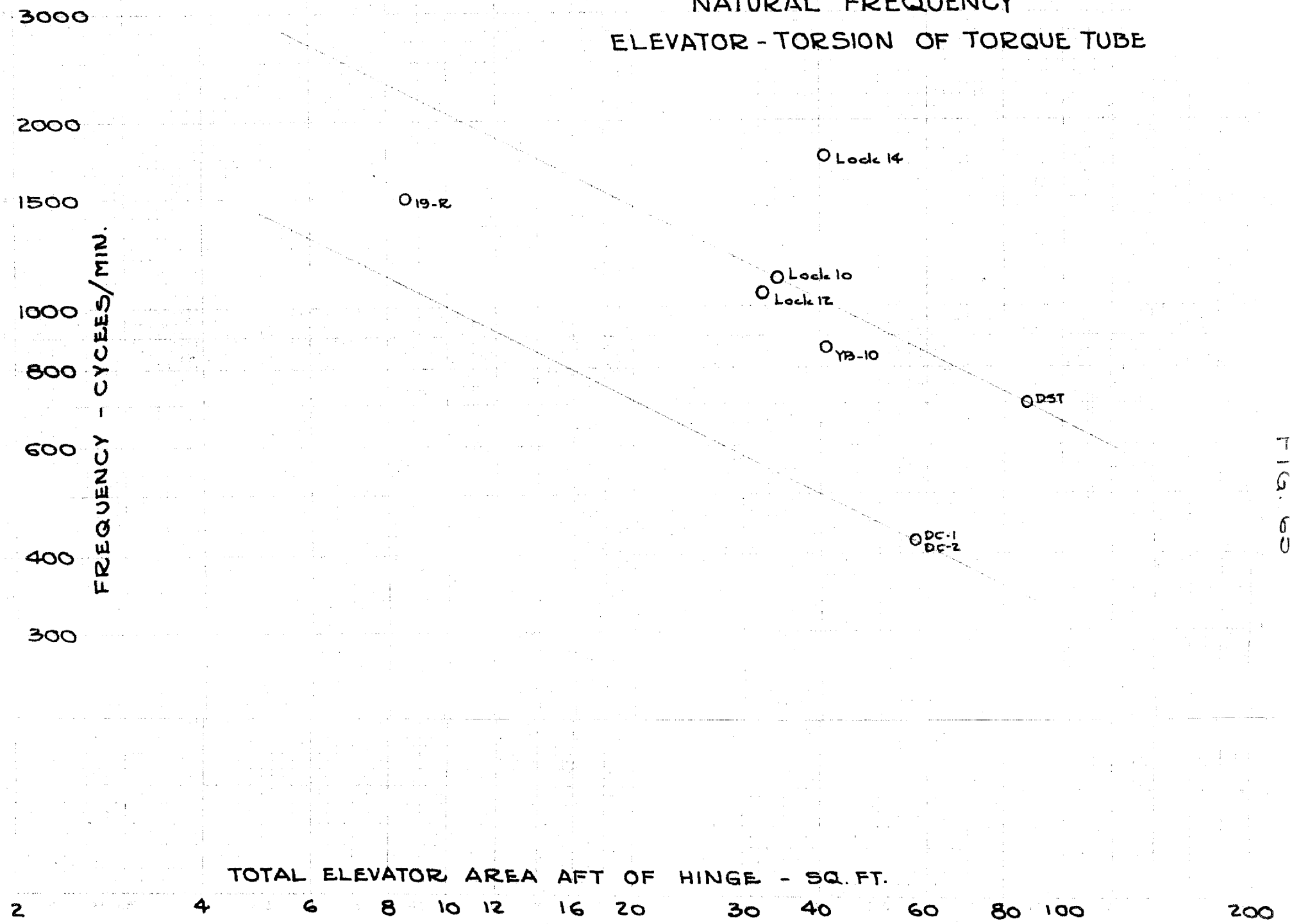

FIG. 93

NATURAL FREQUENCY
RUDDER CONTROL SYSTEM

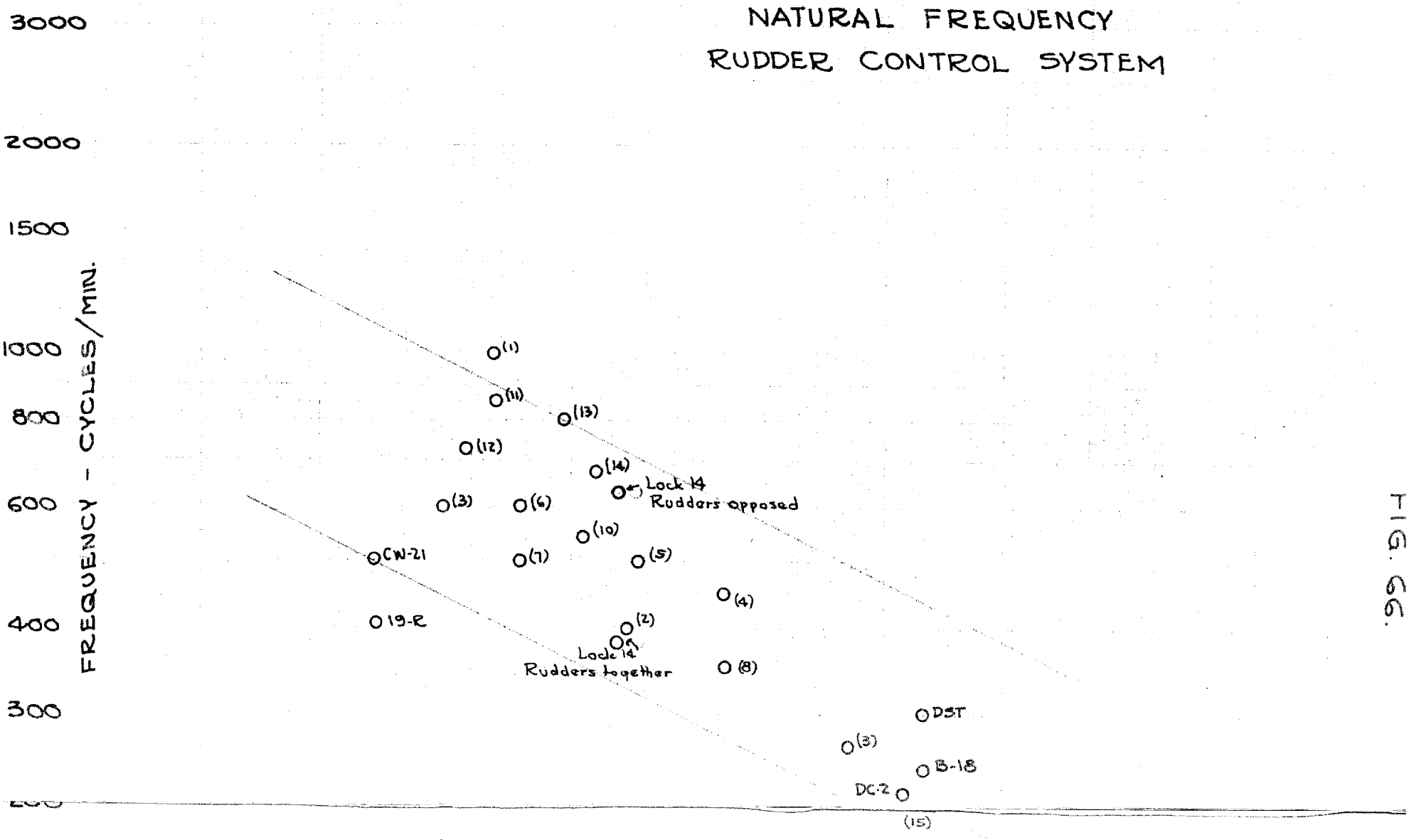

FIG. 66.